Université de Montréal

La végétation aquatique submergée dans les eaux continentales : mieux comprendre sa réponse aux changements environnementaux et ses conséquences sur le fonctionnement des écosystèmes

Par

Morgan Botrel

Département de sciences biologiques, Faculté des arts et sciences

Thèse présentée en vue de l'obtention du grade de Philosophiae Doctor (Ph.D.)

en sciences biologiques

Avril 2022

Université de Montréal

Département de sciences biologiques, Faculté des arts et sciences

---

Cette thèse intitulée

La végétation aquatique submergée dans les eaux continentales : mieux comprendre sa réponse aux changements environnementaux et ses conséquences sur le fonctionnement des écosystèmes

Présenté par

Morgan Botrel

A été évaluée par un jury composé des personnes suivantes

Étienne Laliberté
Président-rapporteur

Roxane Maranger
Directrice de recherche

Pascale M. Biron
Codirectrice

Christiane Hudon
Codirectrice

Lars L. Iversen
Membre du jury

Sabine Hilt
Examinatrice externe

Résumé

La végétation aquatique submergée (VAS) est une composante essentielle qui structure les écosystèmes aquatiques continentaux. Elle soutient plusieurs fonctions et services écosystémiques, dont le soutien d'habitats pour la faune, la stabilisation du rivage, le maintien d'une eau claire et la régulation des cycles des nutriments. Cependant, la VAS est soumise aux activités humaines qui modifient leur habitat, altère leur quantité et menacent le maintien de ces services. L'objectif de cette thèse est de mieux comprendre comment les quantités de la VAS répond aux variations environnementales et quels sont les effets de ces modifications sur les fonctions et services qu'elle soutient. Cet objectif est abordé de différents angles d'attaque et à différentes échelles spatiales et temporelles.

Tout d'abord, une nouvelle méthode permettant des économies de temps et d'argent pour mesurer la biomasse de la VAS est proposée. À l'aide de deux modèles de calibration, la méthode combine trois techniques existantes couramment utilisées pour estimer la biomasse de la VAS : le prélèvement de biomasse dans des quadrats en plongée, le prélèvement à l'aide d'un râteau manié depuis la surface et l'échosondage à partir d'une embarcation. Cette approche offre l'avantage de limiter l'utilisation risquée et fastidieuse du quadrat avec plongeur, mais fournissant la mesure de biomasse la plus fiable. La première calibration avec le quadrat permet d'utiliser le râteau et corrige son biais, alors que la deuxième calibration entre râteau et échosondage convertit les valeurs mesurées par cette dernière en biomasse. L'utilisation de l'échosondage permet ainsi d'estimer plus rapidement la biomasse à grande échelle. La méthode est validée à partir de données d'échosondage qui sont confrontées avec des biomasses par quadrat, démontrant la robustesse de l'approche.

Ensuite, les variations climatiques interannuelles et leurs effets sur la rétention de l'azote ont été évalués pendant six étés dans un herbier aquatique à la confluence de deux tributaires agricoles avec le fleuve Saint-Laurent. Des budgets d'azote journalier ont été estimés par la différence entre les concentrations modélisées de nitrate dans les tributaires et les concentrations sortantes de l'herbier mesurées par une sonde à haute fréquence. La rétention totale a été partitionnée en assimilation autotrophe et en dénitrification à partir de la variation diurne en nitrate. Les budgets ont été confrontés à un indice de biomasse de VAS, la pente de la surface du niveau de l'eau, qui a révélé un portrait détaillé de l'évolution de la biomasse au cours de la saison de croissance. Les résultats montrent que la rétention est influencée par les variations de niveau de l'eau, de température, de

biomasse de la VAS et d'apports en nitrate. De hauts taux de consommation de nitrate sont rapportés, parmi les plus élevés mesurés en rivière, avec une biomasse accrue de plantes accrue favorisant l'élimination permanente par la dénitrification.

Enfin, une synthèse sur les tendances, les facteurs globaux déterminant les quantités de VAS dans les lacs ainsi que comment les quantités y ont été mesurées est présentée. La compilation a été effectuée à l'aide d'une recherche par mot clés réalisée sur une base de données bibliographiques. La synthèse montre un portrait dynamique dans le temps et dans l'espace des quantités de VAS. Bien que les déclins de quantités soient prédominants, plusieurs séries temporelles récentes indiquent une récupération de la VAS, patrons qui varient selon les régions et les activités humaines. Les usages dans les bassins versants liés à l'eutrophisation sont associés aux déclins, particulièrement en Asie, alors que les augmentations sont surtout associées à la gestion de la VAS en Europe. Les tendances plus variables en Amérique du Nord sont associées à l'arrivée d'espèces envahissantes.

Cette thèse innove en fournissant une nouvelle méthode qui facilite la mesure de la biomasse de la VAS à grande échelle. Elle contribue également aux connaissances sur la VAS et le cycle de l'azote en grande rivière en caractérisant la variation de la rétention de nitrate et en soulignant leur important rôle comme site de transformation dans ces écosystèmes. Finalement, elle contribue à la biogéographie de la VAS continentale dans les lacs, indique des lacunes de connaissance, souligne les développements méthodologiques souhaitables et informe sur l'influence de facteurs expliquant la variation de la VAS qui seront utiles pour sa gestion future. Ces informations seront profitables au maintien des fonctions et services soutenus par la VAS et à son utilisation comme une solution fournie par la nature face aux changements globaux.

Mots-clés : végétation aquatique submergée, quantité, biomasse, lac, rivière, azote, rétention, services écosystémiques, spatiotemporel, climat

Résumé vulgarisé

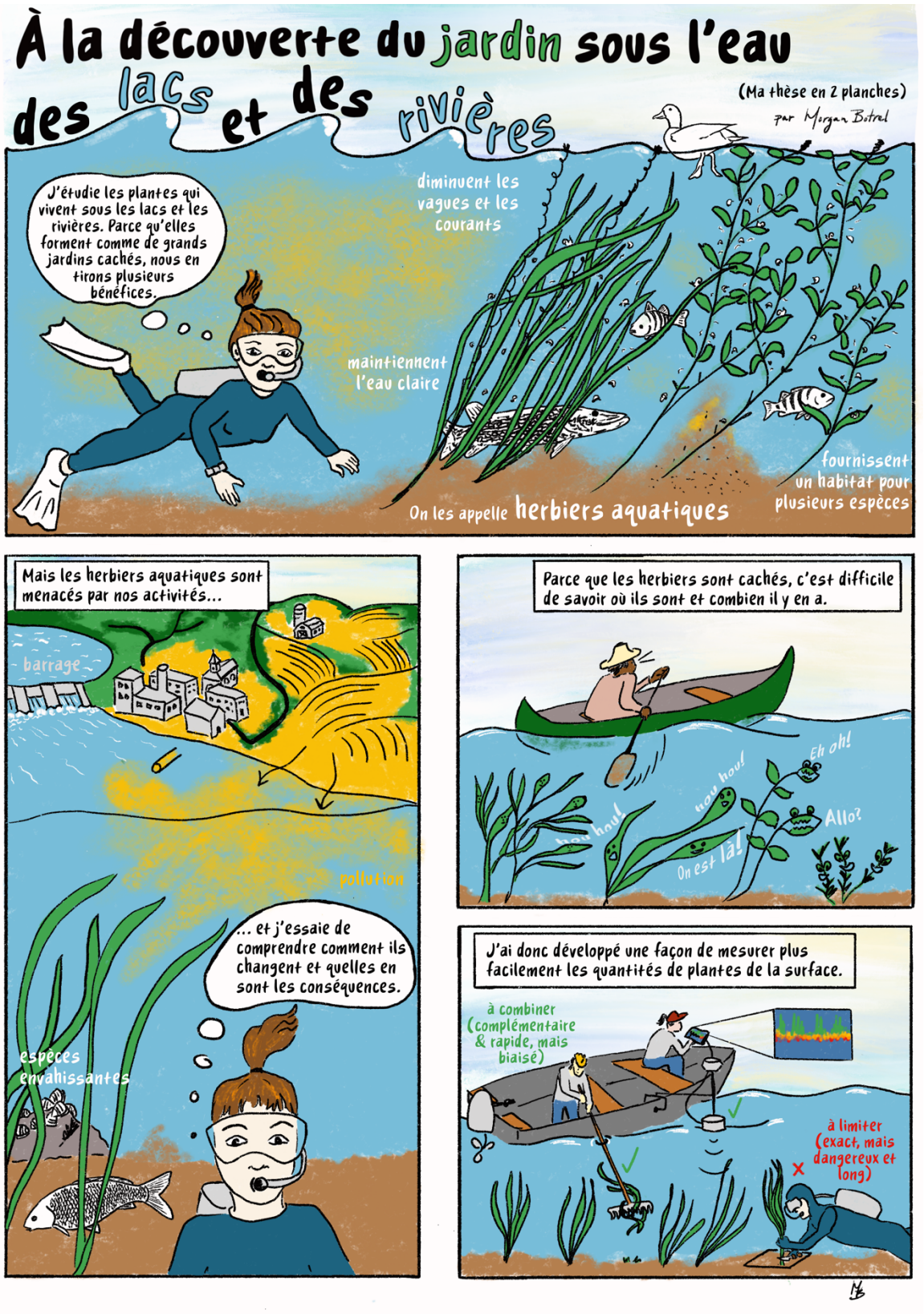

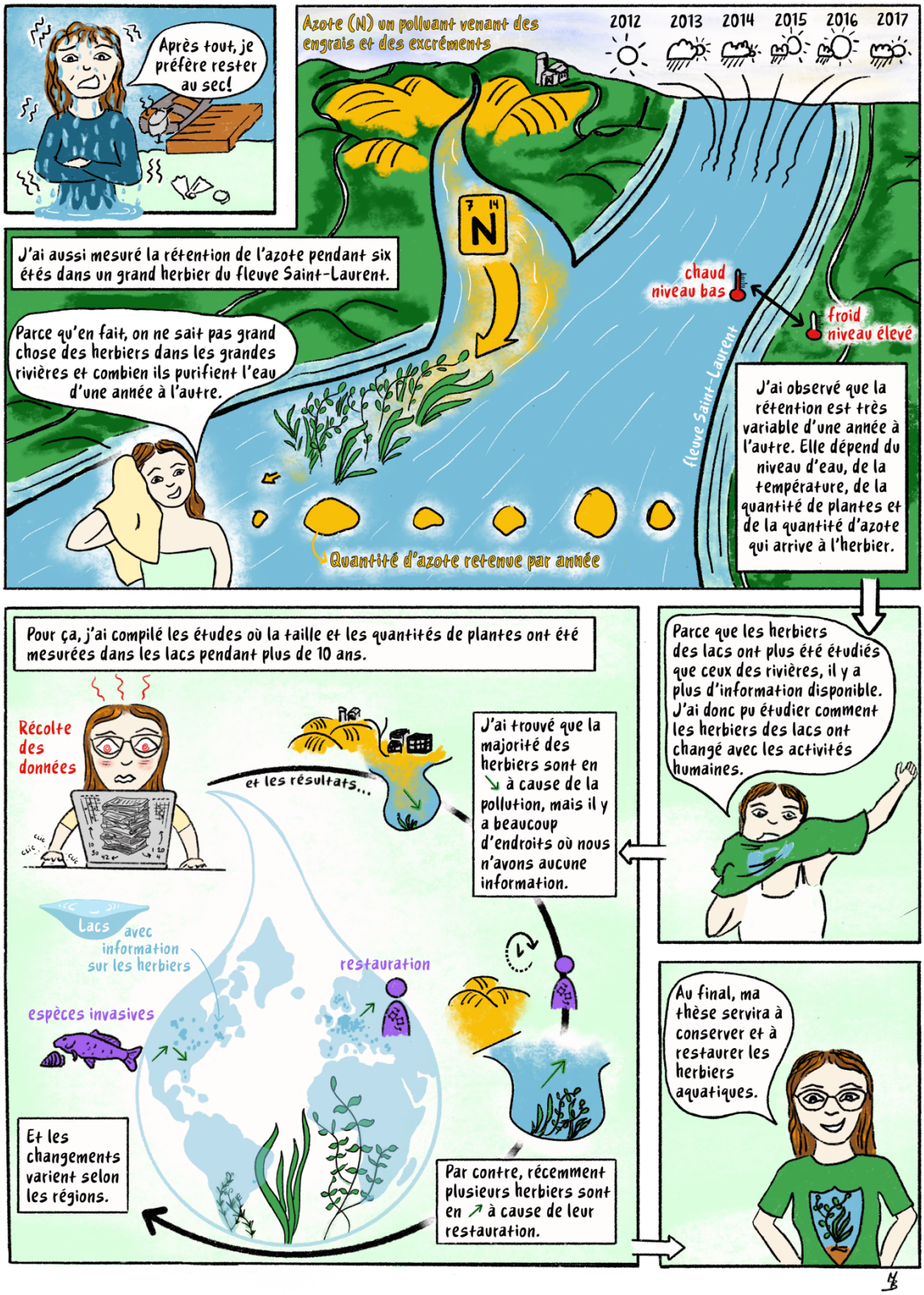
Après tout, je préfère rester au sec!
Azote (N) un polluant venant des engrais et des excréments
2012
2013
2014
2015
2016
2017
J'ai aussi mesuré la rétention de l'azote pendant six étés dans un grand herbier du fleuve Saint-Laurent.
Parce qu'en fait, on ne sait pas grand chose des herbiers dans les grandes rivières et combien ils purifient l'eau d'une année à l'autre.
chaud niveau bas
froid niveau élevé
fleuve Saint-Laurent
J'ai observé que la rétention est très variable d'une année à l'autre. Elle dépend du niveau d'eau, de la température, de la quantité de plantes et de la quantité d'azote qui arrive à l'herbier.
Quantité d'azote retenue par année
Pour ça, j'ai compilé les études où la taille et les quantités de plantes ont été mesurées dans les lacs pendant plus de 10 ans.
Récolte des données
et les résultats...
J'ai trouvé que la majorité des herbiers sont en ↘ à cause de la pollution, mais il y a beaucoup d'endroits où nous n'avons aucune information.
Parce que les herbiers des lacs ont plus été étudiés que ceux des rivières, il y a plus d'information disponible. J'ai donc pu étudier comment les herbiers des lacs ont changé avec les activités humaines.
Lacs avec information sur les herbiers
restauration
espèces invasives
Et les changements varient selon les régions.
Par contre, récemment plusieurs herbiers sont en ↗ à cause de leur restauration.
Au final, ma thèse servira à conserver et à restaurer les herbiers aquatiques.

Abstract

Submerged aquatic vegetation (SAV) is an essential component that structures inland waters. SAV sustains numerous ecosystem services and functions, such as providing habitat for fauna, stabilizing shoreline, maintaining clear water and regulating nutrient cycles. However, SAV is submitted to human activities that modify their habitat, alter their quantities and threaten the ecosystem services they may provide. The objective of this thesis is to better understand how SAV quantities responds to environmental variations, and what are the effect of these modifications on the functions and services they sustain. This objective is approached in different ways and at various spatial and temporal scales.

First, a new cost-effective method to measure SAV biomass is proposed. The method combines three existing techniques by means of two calibration models. This approach has the advantage of reducing the hazardous and cumbersome use of quadrats with divers, whilst providing the most accurate biomass measure. The first calibration with the quadrat allows for the application of the rake and corrects for its bias, while the second calibration between rake and echosounding converts the values measured by the latter into biomass. The use of echosounding thus allows for the estimation of biomass more rapidly at larger scale. The method is validated from echosounding data that are compared to quadrat biomasses, demonstrating the robustness of the approach.

Second, interannual climate variation and their effect on nitrogen retention were evaluated during six summers in a SAV meadow at the confluence zone of two agricultural tributaries with the Saint Lawrence River. Daily nitrogen budgets were estimated as the difference between modelled nitrate concentration in the tributaries and concentration outflowing the SAV meadow measured with a high frequency sensor. Total retention was partitioned into autotrophic assimilation and denitrification from the diel nitrate variation. The budgets were compared to an indicator of SAV biomass, the slope of water level surface, which provided a detailed portrait of biomass changes throughout the growing season. The results show that retention is influenced by variation in water levels, temperature, SAV biomass and nitrate inputs. Among the highest nitrate uptake rates are reported compared to previous measurements in inland waters, with plant biomass favoring permanent removal through denitrification.

Third, a synthesis on trends and drivers of SAV quantities in lakes, as well as on how it was measured is presented. The compilation was conducted from a keyword search on a bibliographic database. The synthesis shows a dynamic depiction in space and time of SAV quantities. Although decreasing quantities are predominant, many recent time series indicate SAV recovery, and these patterns vary with regions and human activities. Direct activities in watersheds leading to eutrophication are associated with decreases, particularly in Asia, while increases are more associated with SAV management in Europe. Trends are more variable in North America due to invasive species.

This thesis innovates by providing a new method facilitating SAV biomass measurement at large scale. The thesis also contributes to knowledge on SAV and on nitrogen cycling in large rivers by characterizing the variation in nitrate retention. Finally, the thesis contributes to inland SAV biogeography, identifies knowledge gaps, indicates desirable methodological developments and informs on drivers of SAV that could inform its future management. This information will be beneficial for the preservation of the ecosystem services and functions provided by SAV and its use as a nature-based solution against global changes.

Keywords : submerged aquatic vegetation, quantity, biomass, lake, river, nitrogen, retention, ecosystem services, spatiotemporal, climate

Plain language summary

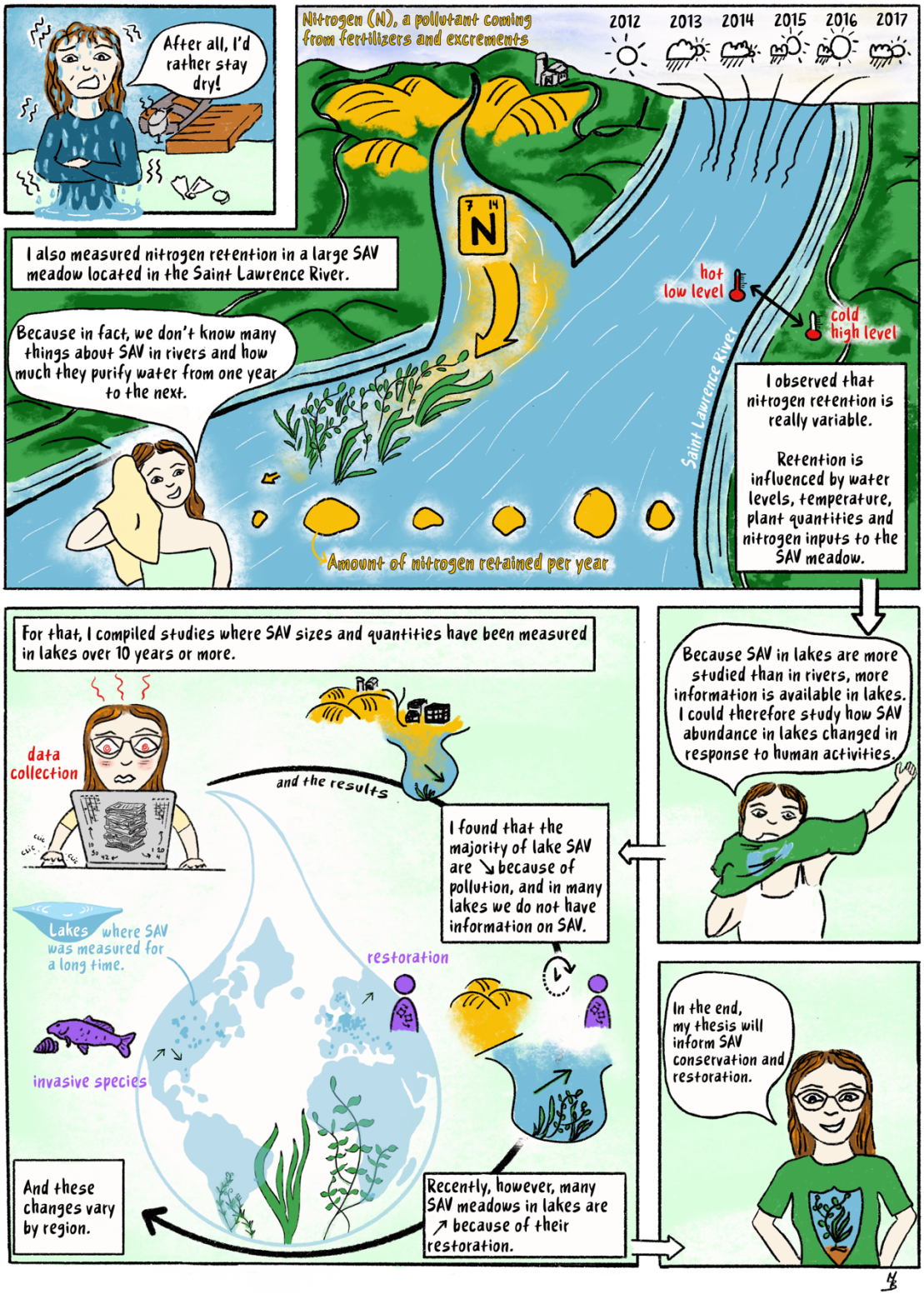
After all, I'd rather stay dry!
Nitrogen (N), a pollutant coming from fertilizers and excrements
2012
2013
2014
2015
2016
2017
I also measured nitrogen retention in a large SAV meadow located in the Saint Lawrence River.
Because in fact, we don't know many things about SAV in rivers and how much they purify water from one year to the next.
hot
low level
cold
high level
Saint Lawrence River
I observed that nitrogen retention is really variable.
Retention is influenced by water levels, temperature, plant quantities and nitrogen inputs to the SAV meadow.
Amount of nitrogen retained per year
For that, I compiled studies where SAV sizes and quantities have been measured in lakes over 10 years or more.
data collection
and the results
Because SAV in lakes are more studied than in rivers, more information is available in lakes. I could therefore study how SAV abundance in lakes changed in response to human activities.
I found that the majority of lake SAV are ↘ because of pollution, and in many lakes we do not have information on SAV.
Lakes where SAV was measured for a long time.
restoration
invasive species
In the end, my thesis will inform SAV conservation and restoration.
And these changes vary by region.
Recently, however, many SAV meadows in lakes are ↗ because of their restoration.

Table des matières

Liste des tableaux

Liste des figures

Introduction

Chapitre 1

Chapitre 2

Chapitre 3

Liste des sigles et abréviations

AICc : sample-corrected Akaike information criterion

C : conductivity

D : distance

f : fraction

LDA : linear discriminant analysis

LSP : Lac Saint-Pierre

LSL : Lac Saint-Louis

LSF : Lac Saint-François

MAPE : mean absolute percentage error

ML : maximum likelihood

N : azote, nitrogen

NO_3^- : nitrate

NH_4^+ : ammonium

PCA : principal component analysis

PLSR : partial least square regression

R : proportional retention

R : rake

REML : restricted maximum likelihood estimation

RMSECV : root mean square error of cross-validation

SAV : submerged aquatic vegetation

Q : discharge

Q: quadrat

Q-R : quadrat-rake

R-E : rake-echosounding

SI: supporting information

SLR : Saint Lawrence River

SR : selectivity ratio

TP : total phosphorus

U : uptake rate

U_a : uptake rate of autotrophic assimilation

$U_{a\text{-}GPP}$: autotrophic assimilation rate from gross primary productivity

U_d : uptake rate of denitrification

U_h : heterotrophic assimilation uptake rate

U_t : total uptake rate

V_f : uptake velocity

$V_{f\text{-}t}$: total uptake velocity

$V_{f\text{-}a}$: uptake velocity of autotrophic assimilation

$V_{f\text{-}d}$: uptake velocity of denitrification

VAS : végétation aquatique submergée

À mon père Marc

qui m'a quitté pendant la réalisation de cette thèse

pour m'avoir insufflé la curiosité et la créativité

et à ma mère Lisa

sur qui je peux toujours compter

pour m'avoir transmis l'ambition et la persévérance

Remerciements

Une thèse c'est un peu comme pour un enfant, il faut un village pour l'élever, ou enfin, pour qu'elle arrive à maturité. J'aimerais remercier tous ceux qui m'ont aidé dans l'accomplissement de ce travail.

Merci à tous les collègues du laboratoire Maranger qui sont passés à travers les années, vous avez tous contribué avec vos commentaires, vos idées et votre énergie à cette thèse. Un merci particulier à Richard pour ton point de vue rafraîchissant, à J-O mon collègue en parentalité et à Lisa pour ton énergie tranquille. Merci, Steph, pour tous les cafés et les pomos, j'ai bien hâte de fêter la fin de nos thèses au spa. Merci aussi à mes nouveaux collègues du book club qui allument mon cerveau de nouvelles idées de science et de philosophie. Merci aux collègues croisés lors de mon stage à Duke qui eux aussi ont remplis ma tête d'idée. Merci à Cathy et Jim de m'avoir sorti de mon impasse et m'avoir fait saisir comment traiter les données de sonde. Merci aussi à la FAS et au cours Horizon de m'avoir donné une opportunité unique de créer un cours et d'explorer de nouvelles formes d'apprentissage. Je remercie aussi tous ceux qui m'ont donné les moyens techniques pour compléter la thèse. Merci aux innombrables aides de terrain et de laboratoire, dont le fabuleux Dominic, sans vous il n'y aurait pas de thèse. Merci aux guides du lac Saint-Pierre et à l'incomparable Roger Gladu, la vraie mémoire du lac. Merci au GRIL pour le financement et pour toutes les activités de formation.

Je remercie ma directrice et mes deux co-directrices, trois superbes modèles de femmes en sciences. Merci, Pascale, pour ta clarté et ta recherche du mot juste qui m'ont mieux fait comprendre des concepts en hydrologie. Merci, Christiane, pour ton souci du détail, le partage de tes connaissances encyclopédiques sur le fleuve et les plantes et l'opportunité que tu m'as donnée de travailler à Environnement Canada. Merci à mon incomparable directrice, Roxane, de m'avoir laissé explorer et m'avoir poussé dans différentes directions. Merci aussi pour toutes les opportunités dont tu m'as fait bénéficier. Merci surtout pour tes deux plus grands cadeaux qui me donnent le goût de poursuivre en sciences : un appui sur lequel je peux bâtir la suite et la réalisation que c'est possible d'avoir du plaisir à faire de la science.

Les derniers et non les moindres, merci à ma famille de m'avoir entouré pendant les années de doctorat, qui sans doute vous ont semblés longues. Merci Eliez et Esther pour votre lumière qui est ma motivation. Merci, Tommy, pour ton support indéfectible. Je suis choyée de vous avoir dans ma vie.

Introduction

La végétation aquatique submergée (VAS), la frange entièrement submergée des milieux humides, est une composante primordiale des écosystèmes aquatiques. Par son rôle structurant, la VAS modifie le fonctionnement des lacs et des rivières et elle a ainsi été qualifiée d'ingénieur écologique ou d'habitat fondateur (Caraco et al., 2006; Jeppesen et al., 1998; Orth et al., 2017). Par le fait même, nous en tirons des bénéfices et la VAS fournit plusieurs services écosystémiques culturels, de support et d'approvisionnement (Janssen et al., 2021). Par exemple, les structures subaquatiques de la VAS créent une complexité de surfaces colonisables qui supportent une diversité de niches écologiques (Thomaz & Cunha, 2010). La VAS est donc un important habitat pour la faune, en plus de lui procurer une source de nourriture (Lodge, 1991), et contribue de façon disproportionnée par rapport à la zone pélagique à la biodiversité des écosystèmes aquatiques (Vander Zanden & Vadeboncoeur, 2020). Ses structures ralentissent également l'écoulement de l'eau, ce qui promeut la sédimentation, limite la resuspension, favorise le maintien d'une eau claire et régule le cycle des nutriments (Barko & James, 1998; Scheffer et al., 1993).

Cependant, la VAS est soumise aux activités humaines qui ont radicalement transformé les écosystèmes et leur fonctionnement. Cette influence est si profonde qu'une nouvelle ère géologique a été proposée pour la décrire : l'Anthropocène (Steffen et al., 2007). Par la transformation des terres et l'altération des cycles biogéochimiques, l'activité humaine a engendré les changements climatiques (Vitousek et al., 1997). Ces modifications, en plus de la chasse, la pêche ou la facilitation des invasions, ont entraîné une diminution de la biodiversité, qui a été suggérée comme étant la 6^{e} extinction majeure de l'histoire de la vie (Chapin et al., 2000). Ce sont les écosystèmes aquatiques qui sont les plus touchés par ces modifications biotiques et expérimentent mondialement les plus grandes pertes de biodiversité (Sala et al., 2000). Un des problèmes les plus communs dans les écosystèmes d'eau douce est l'eutrophisation liée à l'augmentation des nutriments provenant du bassin versant, via l'agriculture ou l'urbanisation, qui stimule la production primaire aquatique et diminue la qualité de l'eau (Carpenter et al., 1998). Cet apport de nutriments modifie la structure des communautés et favorise la production pélagique au détriment de la production benthique algale ou végétale (Scheffer et al., 1993; Vadeboncoeur et al., 2003). La théorie des états alternatifs stables explique ces modifications apportées par l'eutrophisation qui entraînent le déclin de la VAS et le passage d'une eau claire à une eau turbide dominée par le phytoplancton (Scheffer et al., 1993).

Plusieurs études montrent les vastes changements de la VAS liés aux activités humaines, ce qui menace les fonctions et services écosystémiques qu'elle soutient. Les changements affectent les quantités de VAS qui dans certains cas est en déclin alors que dans d'autres elle augmente (p. ex. Körner, 2002; Vermaire & Gregory-Eaves, 2008). Bien que des modifications de la diversité et de l'identité des espèces de VAS soient aussi observées avec les variations environnementales (p. ex. Søndergaard et al., 2010; Steffen et al., 2013), dans cette thèse je me pencherai sur les variations des quantités de la VAS. Je considère la VAS comme une communauté dont la taille est le déterminant premier de son effet sur le fonctionnement des écosystèmes, ou de la modification des stocks est des flux d'éléments et d'énergie (Brown et al., 2004; Schramski et al., 2015; Yvon-Durocher & Allen, 2012). Ma thèse vise donc à mieux comprendre comment les quantités de la VAS répond aux pressions environnementales et quels sont les effets de ces modifications sur les fonctions et services soutenus par la VAS (Figure 1). Avant d'aller plus loin, je présente plus en détail ce qu'est la VAS, les facteurs déterminant sa distribution et souligne les lacunes dans les connaissances qui ont mené à l'élaboration des études spécifiques des chapitres 1 à 3.

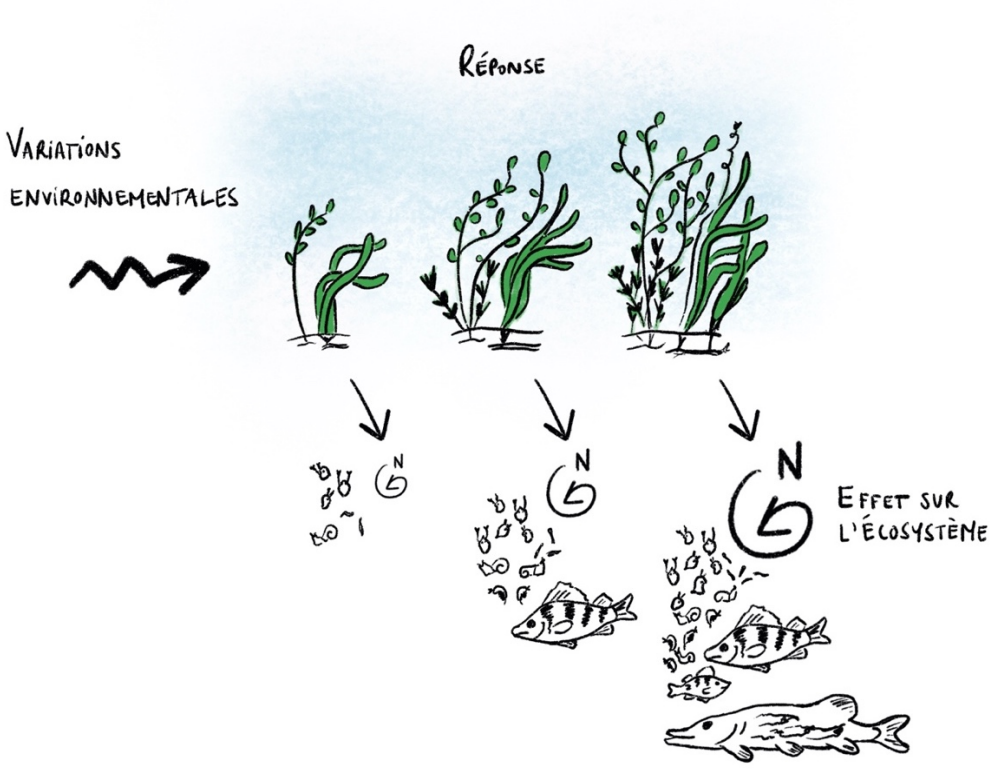

Figure 1. Cadre conceptuel de la thèse qui vise à comprendre la réponse de la VAS aux variations environnementales et quels sont les effets de ces modifications sur les fonctions et les services soutenus par la VAS. N: azote.

Qu'est-ce que la végétation aquatique submergée?

La végétation aquatique submergée, aussi appelée macrophytes submergés ou hydrophytes, comprend des organismes aquatiques photosynthétiques qui sont visibles à l'œil nu et qui croissent sous l'eau (Chambers et al., 2008). L'habitat de la VAS est l'herbier où elle est densément regroupée. Dans les eaux continentales, il est qualifié d'herbier d'aquatique alors que pour les océans il est l'herbier marin. La VAS continentale comprend plusieurs groupes taxonomiques dont des macroalgues (famille des Characeae — les genres *Chara* et *Nitella*), des mousses et hépatiques (bryophytes) et des plantes vasculaires dont des fougères (ptéridophytes) et des plantes à fleurs (angiospermes, Figure 2). La plupart vivent ancrées dans les sédiments : les Characées ont des cellules d'ancrages spécialisées, les rhizoïdes, et les plantes vasculaires ont un système racinaire, bien que certaines de ces dernières ne possèdent pas de racines et vivent suspendues dans la colonne d'eau (p. ex. cornifle nageant, *Ceratophyllym demersum*). Les plantes aquatiques vasculaires sont parfois appelées des espèces « secondaires aquatiques » puisqu'il s'agit de plantes terrestres qui se sont réadaptées à la vie sous l'eau (Rascio, 2002). Elles ont donc certaines caractéristiques des plantes terrestres, dont leur capacité à absorber les nutriments par leurs racines, mais ont des adaptations spécifiques au milieu aquatique. Par exemple, elles possèdent un aérenchyme, une série d'espaces intercellulaires connectés, qui leur permettent de faire circuler les gaz, d'oxygéner leurs racines et de supporter l'anoxie des sédiments.

La croissance clonale par dispersion végétative, notamment par rhizomes et fragmentation, est également très commune chez la VAS et probablement un prérequis à l'adaptation au milieu aquatique (Philbrick & Les, 1996). L'avantage de ce type de propagation est sans doute lié à la difficulté de la pollinisation sous l'eau et du transfert du pollen au stigmate ainsi qu'au médium aquatique qui génère des pousses fragiles qui se brisent facilement et qui se dispersent fréquemment dans le courant. Les rhizomes procurent l'avantage d'un meilleur ancrage dans des sédiments mous, ainsi qu'une résistance aux vagues et au courant ou à la sécheresse épisodique. De plus, la plupart des espèces de VAS sont des herbacées annuelles qui ont plusieurs stratégies pour assurer des propagules végétatives pour la saison suivante, dont le turion qui est une sorte de bourgeon hivernal spécifique aux plantes aquatiques. Cependant, certaines espèces de VAS sont pérennes et peuvent maintenir un métabolisme actif en hiver sous la glace (Boylen & Sheldon, 1976). Plusieurs espèces de VAS exotiques envahissantes exploitent les stratégies de reproduction asexuée pour se disperser rapidement. Hors de leur aire de répartition native, elles sont souvent perçues comme des

« mauvaises herbes » puisque leur croissance excessive peut limiter certains usages comme la production d'hydroélectricité, la navigation ou la baignade (Hussner et al., 2017). Les principales espèces de VAS envahissantes sont *Cabomba caroliniana*, *Elodea canadensis*, *Elodea nuttallii*, *Hydrilla verticillata*, *Lagarosiphon major* et *Myriophyllum spicatum*.

Par rapport à leurs équivalents terrestres, les espèces de VAS ont mondialement des aires de répartition beaucoup plus larges. Cette ubiquité est probablement encore due à la dispersion asexuée (Santamaría, 2002). À l'échelle globale, la distribution généraliste de la VAS s'explique par le transport des propagules par les oiseaux (Les et al., 2003) et plus récemment par les humains (Chambers et al., 1993) alors qu'à l'échelle locale la distribution est plutôt contrôlée par la connectivité entre les plans d'eau (Capers et al., 2010). Bien que plusieurs espèces aient de grandes aires de répartition, la VAS semble dominante dans les régions tempérées. En haute altitude et latitude, la faible température limite sa présence. Par exemple, le fond des lacs arctiques serait plutôt colonisé par des tapis microbiens (Rautio et al., 2011). En région tropicale, les plantes flottantes et le phytoplancton serait de meilleurs compétiteurs pour l'accès à la lumière (Feuchtmayr et al., 2009; Kosten et al., 2009; Netten et al., 2010). Une recension des patrons et de facteurs environnementaux affectant la distribution et la diversité des espèces de plantes aquatiques a récemment été publié et montré le manque d'information sur leur biogéographie (Alahuhta et al., 2021). De plus, on en sait très peu sur comment les quantités de VAS varie à travers le globe et à travers le temps.

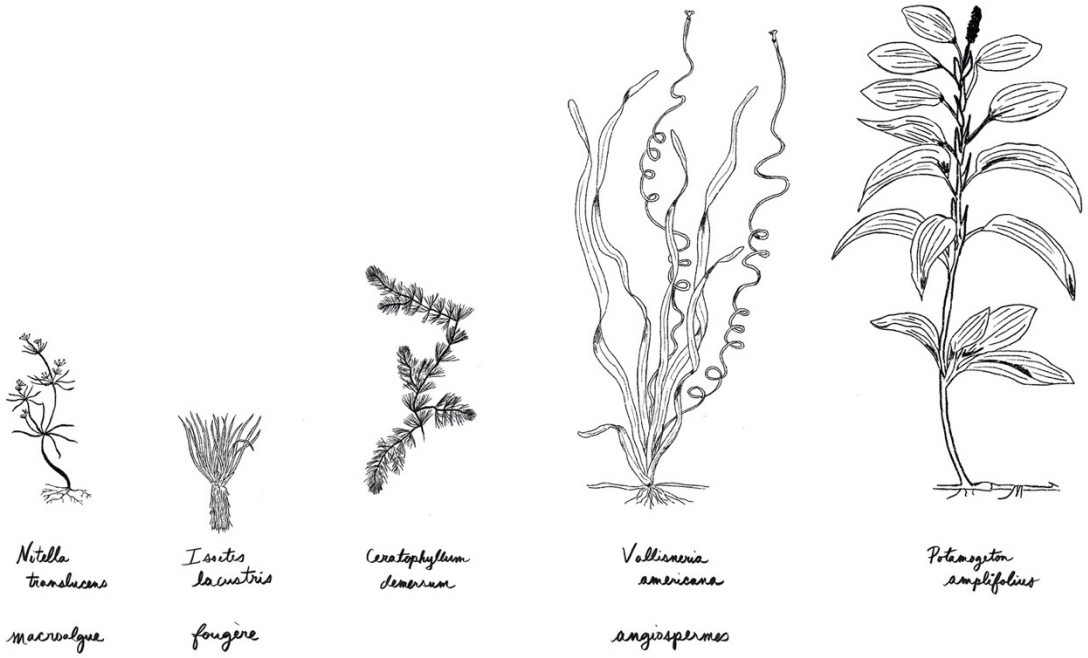

Figure 2. Quelques exemples d'espèces de végétation aquatique submergée.

Facteurs environnementaux contrôlant la VAS

La VAS se retrouve essentiellement dans les zones peu profondes des lacs et des rivières, dans les endroits abrités où la lumière pénètre jusqu'au fond, où la pente est faible et le substrat fin (Figure 3). En concevant l'écosystème aquatique comme une montagne inversée, on saisit immédiatement que le facteur premier qui limite la colonisation des plantes en profondeur est l'accès à la lumière, à l'image de la limite altitudinale (et latitudinale) des arbres qui s'explique par la température. En milieu aquatique, la disponibilité de la lumière est dépendante de la couleur de l'eau et de la concentration de particules en suspension et diminue de façon exponentielle avec la profondeur. Ainsi, plusieurs études établissent une relation entre la profondeur maximale de colonisation de la VAS et la transparence de l'eau (profondeur secchi ou coefficient d'extinction lumineuse, p. ex. Chambers & Kalff, 1985; Hudon et al., 2000; Middelboe & Markager, 1997). Cette profondeur se trouve en général à moins de 30 % de l'irradiance à la surface du plan d'eau, avec une zonation verticale de plantes et la présence des plus tolérantes à de faibles luminosités en profondeur, comme les Characées (Chambers & Kalff, 1985; Duarte & Kalff, 1987).

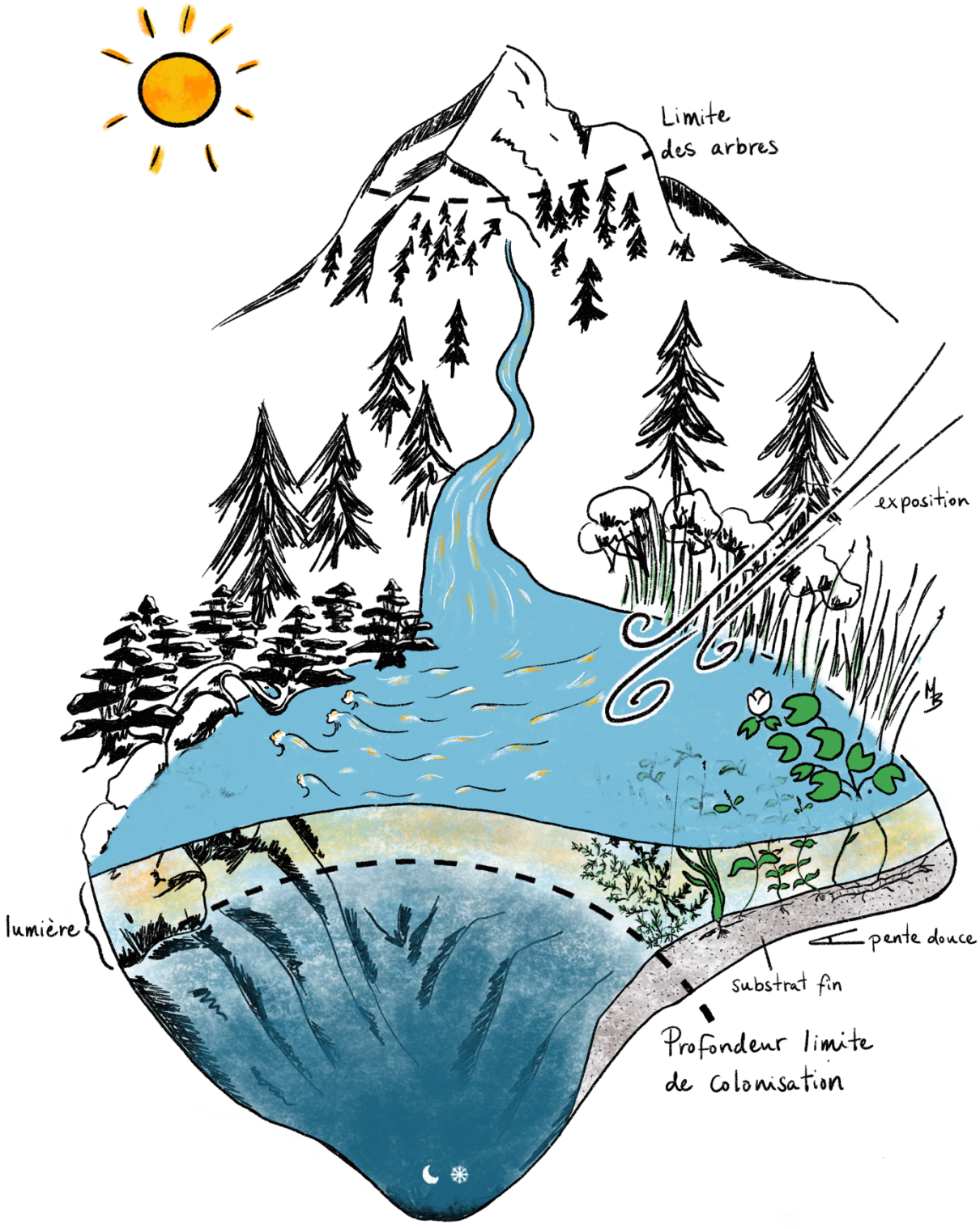

Figure 3. La montagne inversée : facteurs physiques contrôlant la distribution de la végétation aquatique submergée dans les lacs et les rivières.

Dans les lacs peu profonds où la lumière atteint les sédiments sur une grande proportion du fond, la VAS a donc tendance à être dominante. L'accès à la lumière a un rôle déterminant sur cette dominance et la VAS maintient plusieurs rétroactions favorisant une eau claire (Scheffer et al., 1993). Par exemple, elle limite la resuspension des sédiments, crée des habitats pour des organismes filtreurs ou sécrète des substances allélopathiques inhibant le phytoplancton. Ces rétroactions sont supplantées avec l'augmentation des nutriments et l'eutrophisation qui stimule la production pélagique ou des épiphytes et limite l'accès à la lumière par la VAS, entraînant leur déclin et le passage à un état turbide (Phillips et al. 2016). L'arrivée d'espèces qui modifient la clarté de l'eau peut aussi précipiter le passage à un état turbide via la resuspension (p. ex. arrivées de poissons benthivores) ou un allègement de la prédation sur le phytoplancton par cascade trophique (p. ex. déclin des piscivores, augmentation des planctivores, diminution du zooplancton). À l'inverse, certaines espèces peuvent favoriser le retour de la VAS, comme l'arrivée de moules qui filtrent l'eau (Reynolds & Aldridge, 2021). D'autres espèces peuvent également directement affecter la VAS par des interactions trophiques. L'herbivorie entre autres serait plus importante que pour les plantes terrestres à cause d'une plus grande palatabilité de la VAS (Bakker et al., 2016; Lodge, 1991). En général 40 à 48 % de la biomasse de la VAS serait consommée par les herbivores et des changements de régimes vers une eau turbide déclenchés par ceux-ci ont été rapportés (par des oiseaux ou des poissons).

En plus de la lumière, l'interaction avec la température est considérée comme un facteur déterminant la profondeur maximale de colonisation de la VAS et de leur distribution selon la latitude et l'altitude (Barko et al., 1982; Duarte & Kalff, 1987; Rooney & Kalff, 2000). La température contrôle la germination, le taux de croissance et l'amorce de la dormance de la VAS. La température de germination des propagules varie entre les espèces, mais est assez étendue et oscille entre 3 et 20 °C alors que la dormance est induite en deçà de 3 °C et au-dessus de 45 °C (Lacoul & Freedman, 2006). L'émergence des plantes est bien prédite par les degrés-jours accumulés selon la température des sédiments. Les espèces nordiques (p. ex. *Potamogeton nodosus, Stuckenia pectinata (Potamogeton pectinatus), Vallisneria americana*) nécessiteraient moins de degrés-jours pour émerger et seraient plus hâtives par rapport à des espèces méridionales (p. ex. *Hydrilla verticillata*, Spencer et al., 2000).

Outre la lumière et la température, d'autres contraintes physiques à la distribution de la VAS sont le mouvement de l'eau et type de substrat. Le mouvement de l'eau par les courants ou les vagues

peut étirer, briser ou déraciner la VAS. Certaines espèces, particulièrement celles qui sont longilignes, de plus petite taille et avec une grande biomasse racinaire peuvent résister à la traction imposée par le mouvement de l'eau (Bornette & Puijalon, 2011; Madsen et al., 2001). Malgré tout, le courant et les vagues limitent la distribution des plantes : elles colonisent généralement les régions avec des vitesses en deçà de 1 m/s et la profondeur minimale de colonisation est positivement reliée à la profondeur de mélange des vagues de surface (Chambers, 1987; Chambers et al., 1991). Le mouvement de l'eau a également des effets positifs à cause de la diminution de la couche de diffusion, un courant de faible vitesse (≤ 0,01 m/s) est corrélé à la photosynthèse et l'acquisition de nutriments (Madsen et al., 2001). Les zones de faible courant correspondent aussi à des zones de dépôt idéales pour la VAS dont le substrat préférentiel est fin, d'une densité intermédiaire, d'une texture entre l'argile et le sable et avec une proportion de moins de 20 % de matière organique (Barko et al., 1991). Ce substrat permet l'ancrage des racines et limite l'effet toxique de composés libérés lors de la décomposition en anaérobie de la matière organique comme l'éthylène ou le sulfure d'hydrogène. La pente du substrat limite aussi la VAS, elle se retrouve donc dans des zones de dépôt en deçà d'une pente critique de 15 % (Duarte & Kalff, 1990).

Enfin, la VAS peut être limitée par des éléments nécessaires à sa croissance, soit principalement le carbone, l'azote et le phosphore. La limitation par le carbone est causée par la diffusion lente des gaz dans l'eau (10 000 fois plus lent que dans l'air, Wetzel & Søndergaard, 1998). De plus, l'échange gazeux peut être entravé par la présence d'épiphytes qui isolent les plantes de l'eau et augmentent la couche limite de diffusion. La disponibilité du CO_2 pour la photosynthèse est dépendante du mouvement de l'eau qui permet la solubilisation et du pH qui contrôle les formes de carbone inorganique (le CO2 est très limitant à pH > 5,4, Bornette & Puijalon, 2011; Lacoul & Freedman, 2006). Certaines plantes peuvent également assimiler le CO_2 par les pousses ou les racines, mais également le bicarbonate (HCO_3^-) en milieu alcalin (Bornette & Puijalon, 2011). L'azote (N) plutôt que le phosphore tendrait à être le nutriment limitant de la VAS, contrairement au phytoplancton. Cette limitation par l'azote est suggérée par des expériences de fertilisation (Anderson & Kalff, 1986; Barko et al., 1988; Rogers et al., 1995). Les grandes réserves de phosphore accessible dans les sédiments via le système racinaire suggèrent aussi une limitation par l'azote (Barko et al., 1991; Barko & James, 1998; Carignan & Kalff, 1980). En effet, à cause des conditions réductrices des sédiments, les concentrations de phosphore dissous dans l'eau interstitielle des sédiments sont typiquement plus élevées que dans la colonne d'eau (p. ex. Barko et al. 1991 rapportent 1150 µg/L vs 10 µg/L). Dans la plupart des cas, les sédiments fourniraient au moins 50 %

du phosphore des plantes par rapport à la colonne d'eau dont le stock de nutriment est aussi accessible via l'assimilation par les parties vertes de la VAS (Barko et al., 1991; Carignan, 1980; Carignan, 1982,). De plus, certaines espèces de VAS développent des associations avec des mycorhizes pour accéder au phosphate (p. ex. *Vallisneria Americana*, Beck-Nielsen & Madsen, 2001; Wigand & Stevenson, 1997; Wigand et al., 1997).

Mesurer la VAS

Par sa nature subaquatique, mesurer la VAS est un défi. Je définis la quantité comme la taille et, à l'échelle d'un écosystème, les deux composantes de la taille sont l'aire couverte par l'herbier et sa densité. Mesurer l'aire se fait typiquement par des transects ou des techniques par la sélection de points sur un quadrillage permettant de délimiter l'herbier dans l'espace (Madsen & Wersal, 2017). La détermination de l'aire nécessite l'identification de la présence ou l'absence de la VAS. La densité est la quantité de plantes par unité de surface, ou la biomasse. C'est donc une mesure qui est tridimensionnelle et qui nécessite une estimation du volume ou de la masse de plantes présente. Cette mesure est plus complexe et il existe plusieurs façons de l'estimer, chacune ayant ses avantages et ses faiblesses. Le développement d'une méthode plus efficace pour mesurer la biomasse est donc abordé dans le **Chapitre 1**.

Milieu humide, rétention de l'azote et rivière

Bien qu'elle ne soit souvent pas considérée comme telle, les herbiers aquatiques sont un type de milieu humide. En effet, les classifications de milieux humides considèrent couramment les lacs et les rivières comme un seul grand type sans distinction pour la zone d'eau profonde des zones avec des herbiers (FGDC, 2013; Rattan et al., 2021). Cependant, les herbiers regroupent les trois caractéristiques principales qui définissent les milieux humides : l'eau, un substrat anoxique et la présence de plantes (Keddy, 2010). En effet, les milieux humides sont des écosystèmes où l'inondation produit des sols dominés par des processus anaérobiques qui forcent les végétaux à s'adapter à l'inondation. Les herbiers aquatiques constituent donc les milieux humides qui sont à la limite extrême entre la terre et l'eau, ou la portion sous l'eau des milieux humides. Il s'agit d'une perspective qui est adoptée dans le **Chapitre 3** où l'évolution de ce type de milieu humide en relation avec les activités humaines est mise de l'avant.

À cause de l'anoxie des sédiments et des conditions réductrices qui en résultent, une fonction typique des milieux humides est la régulation du cycle des nutriments, en particulier de la

rétention de l'azote. Dans les herbiers, cette capacité de rétention de l'azote est causée par différents mécanismes qui y sont entretenus (Figure 4). La présence de plantes peut notamment amplifier le couplage de la nitrification et de la dénitrification autour des racines (Reddy et al., 1989; Risgaard-Petersen & Jensen, 1997). L'oxygénation permet d'abord la nitrification qui transforme en milieu oxygéné l'ammonium (NH_4^+) en nitrate (NO_3^-). Le NH_4^+ est fourni par l'ammonification de l'azote organique provenant de la litière de plantes. Le NO_3^- qui diffuse dans les zones anoxiques peut ensuite fournir le substrat à la dénitrification qui le transforme en N_2, une forme d'azote non réactive, et occasionne une perte définitive d'azote du système. En rivière, le nitrate n'est souvent pas majoritairement produit localement et il vient d'un transport, ou de l'advection, et il peut être dénitrifié après diffusion dans les sédiments. Cette source extérieure est la plus importante lorsque les concentrations dans la colonne d'eau sont au-delà de ~ 10 µmol/L ou ~ 140 µg/L (Seitzinger et al., 2006). Dans les sédiments des herbiers, la dénitrification est également favorisée par l'apport de carbone de la litière végétale, mais aussi par l'exsudation du carbone organique dissous des racines (Cornwell et al., 1999; Karjalainen et al., 2001). Le NO_3^- peut aussi être directement assimilé par les plantes et ses épiphytes. De plus, la dénitrification peut se produire dans les épiphytes qui tapissent la VAS et où se trouvent de microzones anoxiques (Eriksson & Weisner, 1996).

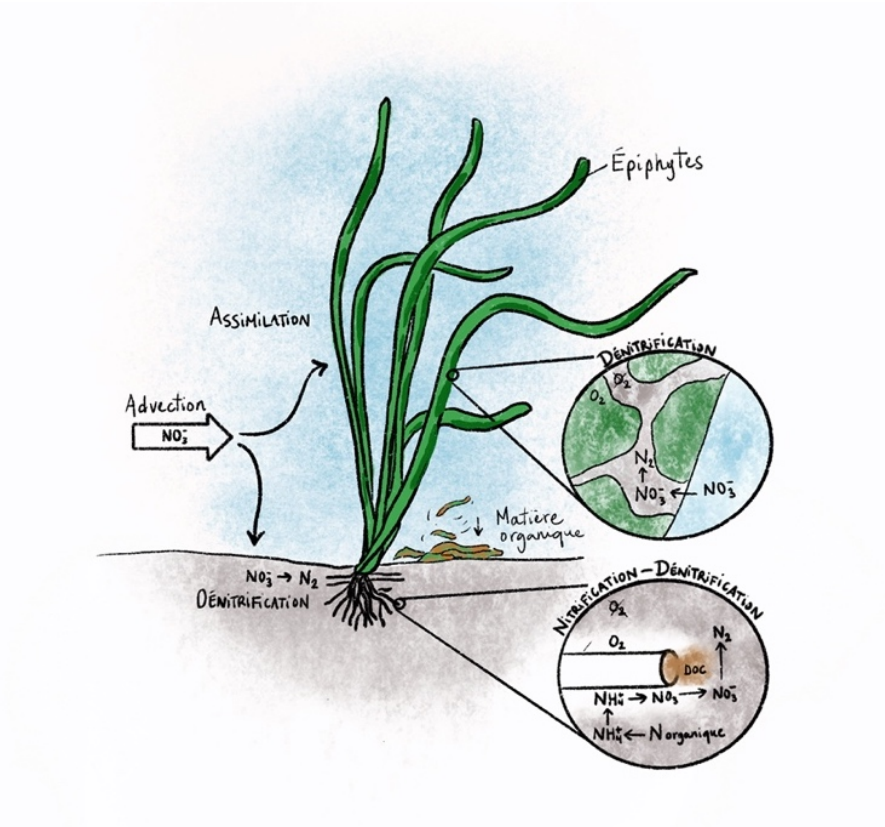

Figure 4. Mécanismes de rétention de l'azote dans les herbiers aquatiques.

La rétention de l'azote, qui est un important service écosystémique fourni par la VAS, est abordé dans le Chapitre 2 où elle est mesurée dans un lac fluvial au sein dans une grande rivière. Ce choix n'est pas anodin, car il existe peu de connaissance sur la VAS dans les milieux lotiques ainsi que sur les cycles biogéochimiques dans les grandes rivières. En effet, les connaissances sur la VAS viennent principalement des lacs peu profonds où elles sont typiquement dominantes. Ce n'est que récemment que les rétroactions entretenues par la VAS ont été montrées en rivières (Diamond et al., 2021; Hilt, 2015) et qu'un modèle conceptuel sur l'eutrophisation en rivière impliquant la VAS a été développé (O'Hare et al., 2018). Par ailleurs, la rétention de l'azote, surtout la dénitrification en rivière est très hétérogène (Piña-Ochoa & Álvarez-Cobelas, 2006). Des études indiquent que la VAS y serait un point de contrôle, contribuant disproportionnellement à la rétention de l'azote par rapport au reste de la rivière (sensu Bernhardt et al., 2017; e.g. Hudon & Carignan, 2008; Preiner et al., 2020). La rétention de l'azote suit également une réaction de premier ordre, c.-à-d. sa vitesse est proportionnelle à la concentration de son substrat, le nitrate. La rétention maximale a donc lieu là

où il y a une abondance de nitrate, une condition souvent rencontrée dans les rivières de grandes tailles qui concentrent l'écoulement et la pollution de multiples bassins versants. Les grandes rivières et les zones d'écoulement plus lent qui permettent l'établissement de la VAS sont donc potentiellement d'importants sites de rétention de l'azote. Cependant, la dynamique de l'azote en milieu lotique est mieux connue dans les ruisseaux et les difficultés méthodologiques font en sorte qu'il existe très peu de mesures directes de rétention de l'azote en grandes rivières (Ensign & Doyle, 2006; Tank et al., 2008). C'est pourquoi le **Chapitre 2** porte spécifiquement sur la VAS et l'azote dans une grande rivière.

Objectifs

La thèse s'organise en trois chapitres allant de l'échelle de l'écosystème à celle du globe et qui posent des questions sur les variations de quantités de VAS : comment les mesurer, quelles sont leurs réponses aux facteurs environnementaux et quels sont leurs effets sur l'écosystème (Figure 5).

Dans le **Chapitre 1**, puisque connaître la densité du stock de VAS est nécessaire pour déterminer leur rôle fonctionnel, l'objectif est d'établir une méthode pour mesurer plus facilement la biomasse des plantes et donc favoriser leur mesure à plus grande échelle spatiale et temporelle. L'idée est de combiner des techniques existantes afin de rendre leur utilisation plus efficace en bénéficiant de leurs avantages, tout en évitant leurs inconvénients. Pour ce faire, j'ai d'abord modélisé la biomasse récoltée par quadrat avec plongeur qui est exacte, mais dangereuse et onéreuse, par des mesures avec un simple râteau de la surface. Cette calibration avec les quadrats corrige le biais du râteau et permet son utilisation plus facile et rapide. Par la suite, j'ai comparé les mesures par râteau avec l'échosondage, une méthode de télédétection acoustique qui permet de mesurer un indice de biomasse à plus grande échelle, mais qui nécessite une calibration. La méthode est finalement validée en comparant des biomasses par quadrat à des mesures d'échosondage converties en biomasse par quadrat à l'aide de la double calibration.

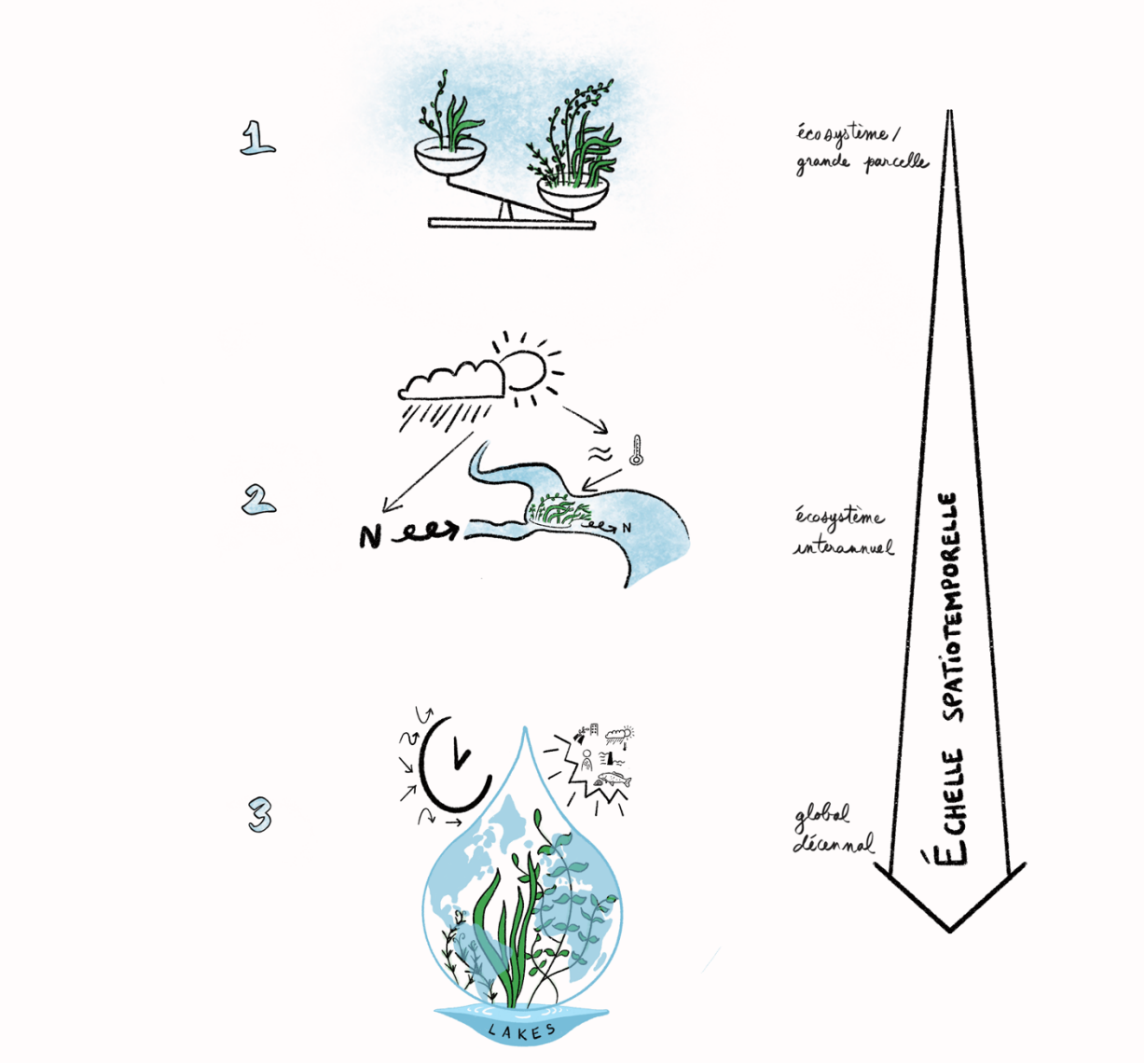

Figure 5. Présentation des trois études sur la réponse et l'effet de la VAS aux changements environnementaux et leur imbrication à travers le temps et l'espace.

Dans le **Chapitre 2**, j'évalue dans une grande rivière comment les variations environnementales de la VAS modifient un service écosystémique. Plus spécifiquement, l'objectif est de déterminer comment les variations climatiques affectent la rétention de l'azote soutenue par un herbier aquatique riverain. Pour ce chapitre, nous avons posé l'hypothèse que la rétention de l'azote devrait être fonction des apports en azote et de la biomasse de plante, tous deux soumis aux variations climatiques. À cet effet, les travaux ont été réalisés au cours de six étés au Lac Saint-Pierre, un lac

fluvial du fleuve Saint-Laurent, à la confluence avec deux tributaires agricoles, les rivières Saint-François et Yamaska. J'ai utilisé un indicateur de la biomasse de plante, calibré avec des mesures de terrain, qui a permis d'obtenir une mesure journalière et un portrait détaillé de l'évolution de la biomasse tout au long de la saison de croissance. Ces mesures ont été confrontées à un budget journalier d'azote établi par la différence entre les concentrations de nitrate en aval de l'herbier, mesurées par une sonde à haute fréquence, et les concentrations en amont. De plus, les variations diurnes du nitrate estimées par la sonde ont permis de séparer la rétention en deux voies métaboliques principales : l'assimilation autotrophe et la dénitrification. Ce chapitre constitue donc un défi méthodologique et conceptuel puisqu'il caractérise pour une rare fois sur une longue étendue et une fine résolution temporelle la dynamique de l'azote dans une grande rivière.

Dans le **Chapitre 3**, je dresse un portrait global des connaissances sur les tendances et les impacts des activités humaines sur les quantités de la VAS. L'objectif est de synthétiser les informations provenant des séries temporelles de quantité de VAS disponibles dans la littérature scientifique, incluant les régions d'étude, les tendances temporelles, les méthodes et métriques de mesures ainsi que les facteur contrôlant les changements de quantité. Dans ce but, j'ai effectué une revue de littérature à partir d'une recherche par mots clés dans une base de données bibliographiques. Les références pertinentes ainsi obtenues ont permis de compiler l'information de chaque article, rapport ou base de données. Ce portrait global informe sur l'état de la VAS à travers le monde, pointe les lacunes de recherche et les développements méthodologiques nécessaires tout en fournissant des pistes de solution pour une meilleure gestion de la VAS.

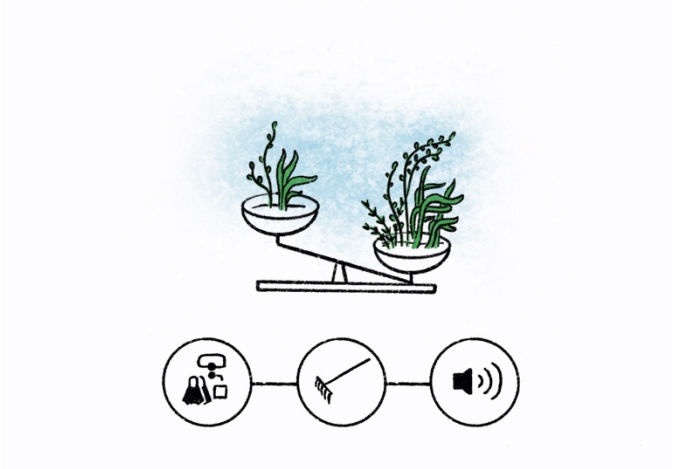

Chapitre 1 – Combiner quadrat, râteau et échosondage pour estimer la biomasse de la végétation aquatique submergée à l'échelle de l'écosystème

Combining quadrat, rake and echosounding to estimate submerged aquatic vegetation biomass at the ecosystem scale

Morgan Botrel[1,2], Christiane Hudon[2,3], Pascale M. Biron[2,4], Roxane Maranger[1,2]

[1] Université de Montréal, Département de sciences biologiques, Complexe des sciences, 1375 Avenue Thérèse-Lavoie-Roux, Montreal, QC Canada, H2V 0B3

[2] Groupe de recherche interuniversitaire en limnologie (GRIL)

[3]Environment and Climate Change Canada, Water Science and Technology, St. Lawrence Center, 105 McGill, Montreal, QC Canada, H2E 2Y7

[4]Concordia University, Department of Geography, Planning & Environment, 1455 De Maisonneuve Blvd. W., Montreal, QC Canada, H3G 1M8

Preprint accessible through bioRxiv, https://doi.org/10.1101/2022.03.15.484486

Data openly available on Zenodo, https://doi.org/10.5281/zenodo.5548402

Abstract

Measuring freshwater submerged aquatic (SAV) biomass at large spatial scales is challenging and no single technique can cost effectively accomplish this while maintaining accuracy. We propose to combine and intercalibrate accurate quadrat-scuba diver technique, fast rake sampling and large-scale echosounding. We found that the overall relationship between quadrat and rake biomass is moderately strong (pseudo R^2 = 0.61) and varies with substrate type and SAV growth form. Rake biomass was also successfully estimated from biovolume (pseudo R^2 = 0.57), a biomass proxy derived from echosounding, at a resolution of 20 m. In addition, the relationship was affected in decreasing importance by SAV growth form, flow velocity, acoustic data quality, depth and wind conditions. Sequential application of calibrations yielded predictions in agreement with quadrat observations, but echosounding predictions underestimated biomass in shallow areas (< 1.5 m) while outperforming point estimation in deep areas (> 3 m). Whole-system biomass estimations by calibrated echosounding data were either lower or higher by a factor of two than estimates from rake point surveys, suggesting echosounding has higher accuracy at large scale owing to the large sample size and better representation of spatial heterogeneity. We developed a step-by-step guideline to decide when an individual or a combination of techniques is profitable. Given the safety risk of quadrat-scuba diver technique, we recommend developing as a one-time event a series of quadrat and rake calibration. The use of rake and echosounding should be considered when sampling at larger spatial and temporal scale. In this case, rake sampling becoming an interesting ground truth for echosounding by providing species information or estimates in shallow waters where echosounding is inappropriate.

Introduction

Submerged aquatic vegetation (SAV) provides many aquatic ecosystem functions and services, from stabilizing sediments to maintaining critical habitat for fauna (Caraco et al. 2006; Carpenter and Lodge 1986; Hilt et al. 2017). Ecosystem service provisioning by SAV meadows is dependent both on plant patch density and size where high elemental fluxes and faunal populations are associated with high SAV standing stock (e.g. Brown et al. 2004; Cyr and Downing 1988; Rooney et al. 2003). However, SAV standing stock is sensitive to human pressures. For example, declining SAV abundance in shallow lakes mainly reflects loss of water transparency as a function of increasing eutrophication (Scheffer et al. 2001; Scheffer et al. 1993). Management efforts around SAV often attempt to restore abundant meadows, while invasive alien aquatic 'weeds' that impede multiple water usages are typically actively removed (Hussner et al. 2017; Madsen and Wersal 2017). Regardless of the management needs, accurate estimates of SAV standing stock are essential to assess their overall functional role in ecosystems and whether management strategies are working.

SAV standing stock or standing biomass is the density measure of aboveground living plant material in mass per unit area. Biomass can be either measured using destructive removal techniques or estimated using remote sensing (Figure 1a). Destructive techniques consist of harvesting plant material, either from below or above the water surface. These are measures of direct biomass, as opposed to a proxy, and represent SAV biomass spatially as a point phenomenon. Direct underwater harvest of SAV by scuba divers is the biomass measure with the least bias, reaching values closest to the truth (Downing and Anderson 1985; Madsen 1993). It is thus the most accurate biomass measure and also has the advantage of being applicable at all depths. However, this technique requires specialized scuba training. Additionally, because of long collection time, small quadrat size (< 1 m^2), and the associated safety risks and expenses, sampling of large areas or in turbid waters is not possible. To alleviate these shortcomings, destructive techniques using tools to grab samples from the surface have been developed. Multiple tools exist, but the double-headed rake with a variety of assembly features (on a telescopic pole, tongs or rope) and collection methods (dragged, griped or spun) is rather well adapted for use in large surveys (Johnson and Newman 2011; Madsen and Wersal 2017; Rodusky et al. 2005; Yin and Kreiling 2011). Indeed, the rake is convenient for large-scale recurrent SAV sampling due to its low purchase cost, ease of use, fast collection, robustness and simple maintenance. However, rake collection is restricted to shallow depths (< 3 - 4 m) and is biased since plant material is often not entirely collected or collected in excess (Johnson

and Newman 2011; Kenow et al. 2007; Rodusky et al. 2005). Furthermore, all destructive methods are point measurements and require the collection and processing of multiple replicates to reach a reasonably precise biomass at a given site due to the typical patchy distribution of SAV meadows at small scale (Downing and Anderson 1985). Accurate measurements of SAV biomass capturing SAV heterogeneity at larger spatial scales thus remain a challenge, since surveys using quadrats are accurate but only applicable at small scale whereas rake samples are biased but provide a broader estimate of biomass distribution.

At large spatial scales, SAV biomass estimates can be improved with remote sensing that represent SAV in space as a continuous surface phenomenon. These techniques provide a proxy of biomass where SAV is detected by a receiver that captures a signal (e.g. sound or light) reflected or emitted by SAV (Rowan and Kalacska 2021). Capturing the sound reflection made by gas vacuoles in plant tissue (the echo) using an active single beam echosounder, is the simplest and best remote sensing technique to estimate SAV biomass in turbid freshwaters (Duarte 1987; Rowan and Kalacska 2021; Sabol et al. 2002; Vis et al. 2003). Indeed, echosounders are transportable and increasingly affordable devices that, just like a sonar used for fishing, can be hooked on the side of a boat for a rapid, non-destructive and repeatable survey (e.g. Howell and Richardson 2019). The reflection of sound on bottom surfaces and canopies allows for the simultaneous measurement of SAV height and water depth, which is extremely useful as water depth strongly influences SAV biomass (Duarte and Kalff 1990). Because SAV height correlates to biomass, echosounding has successfully been used to model whole community biomass (Duarte 1987; Maceina et al. 1984; Sabol et al. 2002). However, the allometric relationship between height and biomass varies with species growth form and thus the calibration of SAV echo is species- or stand-specific and as such the measurement needs to be repeated frequently (Duarte 1987). Other drawbacks of echosounding include its lack of species differentiation, inability to take measurements in very shallow waters (< 0.4 – 0.7 m) or when plants reach water surface, and obligate sampling during calm weather conditions, since wind-induced gas bubbles strongly scatter sound (Sabol et al. 2002). Furthermore, the use of echosounding requires technical expertise, from maneuvering the instrument, electronic maintenance to processing data output.

Each of the aforementioned techniques has several advantages and disadvantages for estimating SAV biomass depending on the scale of study (Figure 1a). One promising approach would be to design a process enabling the benefits of all three techniques which could provide accurate

biomass estimates that take into account SAV heterogeneity at broad spatial scales. Therefore, our objective is to develop a process that assesses the interchangeability of quadrat, rake and echosounding techniques to render their use synergistic and cost-effective. To do so, we conducted two intercalibrations: one between biomass from quadrat and rake and the other between rake and a biomass proxy derived from echosounding (Figure 1b). Furthermore, we investigated how the predictions of both intercalibrations models are affected by environmental factors. The resulting two models were then sequentially applied to echosounding data to validate our approach. Finally, we assessed how increasing the sample size using echosounding modifies whole-system biomass estimation.

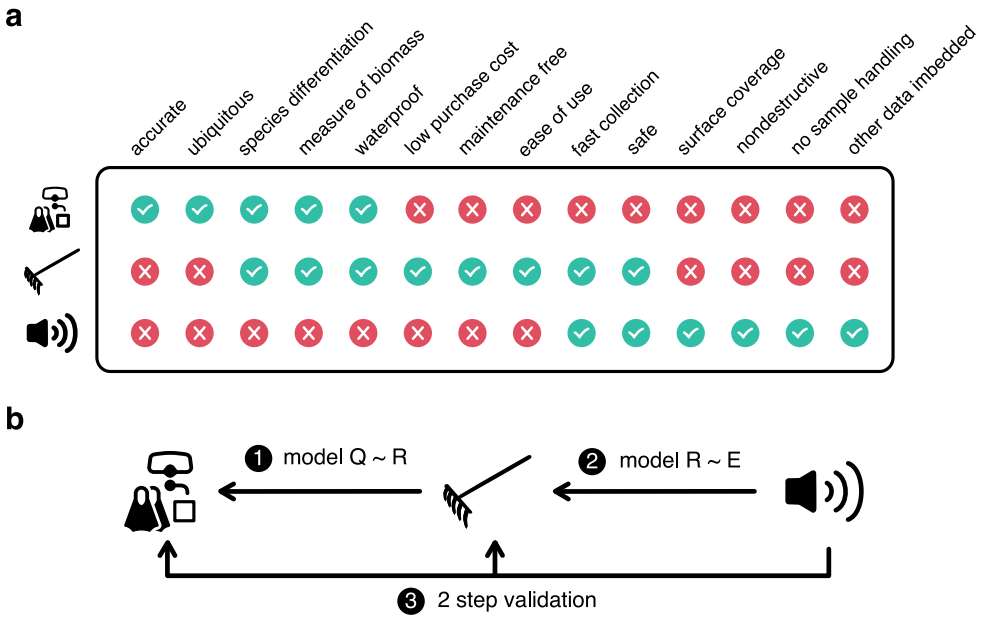

Figure 1. Comparison and combination of the quadrat, rake and echosounding techniques to estimate submerged aquatic vegetation biomass. a Strengths and weaknesses of the different techniques. b Approach and steps to combine techniques. Q: quadrat, R: rake.

Materials and Procedures

To compare, and integrate the different biomass assessment methods, three datasets were used: the quadrat-rake, the rake-echosounding and the validation datasets (Table 1). All datasets were collected in Lake Saint-Pierre (LSP), a ~300 km² widening of the Saint-Lawrence River in Quebec, Canada (Figure 2a, b). Part of the quadrat and rake dataset was also collected in the nearby upstream fluvial lakes, Saint-Louis and Saint-François.

Quadrat-rake (Q-R) dataset

The first dataset was used to assess the correspondence between biomass estimates derived from quadrat and rake samples (hereafter named the Q-R dataset). We had to compare destructive techniques that were measured on distinct sampled area but still represented the same site. Since at the time of the sampling such a comparison hadn't been done, we tested three different collection strategies: systematic pairs, haphazard pairs or blocks (Figure 2c). For the first two strategies, paired rake and quadrat samples were collected around the anchored boat, using either a systematic or a haphazard strategy. In the "systematic pair" strategy, a single quadrat (0.25 m x 0.25 m) was systematically collected to the upper right side of each rake sample (1 m x 0.35 m). In the "haphazard pair" strategy, bigger quadrats (0.40 m x 0.60 m) were located in the vicinity of the rake sample site. In the block sampling strategy, a block, which consisted of two rake samples positioned on both sides of a row of 4 individual quadrats (0.25 m x 0.35 m each) aligned to mimic the raked area, was collected on each side of the boat.

Quadrat plant samples were harvested by divers from within a PVC frame placed on the lake bottom by divers. All aboveground plant material was cut using grass-clippers or broken at the sediment surface. Rake samples were collected from the anchored boat, using a double-headed rake (0.35-m head width with fourteen, 8-cm long teeth on both sides) mounted on a telescopic pole (maximum length 5 m) following the method described in Yin and Kreiling (2011). The rake was lowered in the water and dragged toward the boat over the bottom on a length of approximately 1 m. As it was lifted from the water, the rake was flipped 180° to minimize plant loss.

Biomass samples were collected during the period of maximum SAV development during the summers of 2006 to 2009. Sites were chosen to cover a wide range of water depths, sediment types and SAV biomass. Water depth at each site was measured with a survey ruler and sediment type was classified as pebble, sand, silt, clay or a mixture thereof. SAV species composition of each

sample was visually assessed in decreasing abundance rank (1 = most abundant species). Plant material was washed on site to remove sediment and debris prior to further processing (on site, in the laboratory on fresh or thawed samples). Macrophytes (vascular plants and macroalgae such as *Nitella* and *Chara* spp) were separated from filamentous algal mats (Chlorophytes or the cyanobacterium *Microseira* (*Lyngbya) wollei*; each group was wrung out manually and either weighted with a hook-scale on site (precision 0.02 kg) or an electronic scale in the laboratory (precision 0.1 g). A subsample of filamentous algae was preserved in lugol for subsequent microscopic identification (250 X). Wet mass was converted to dry mass using previously established conversion factors for SAV (Hudon et al. 2012) and filamentous species (Cattaneo et al. 2013). All of the manipulations from sample collection to final biomass conversion are referred to 'biomass treatments'.

Both biomass and species information were aggregated per site. Biomass measurements were reported as a mean of 3-5 rake and quadrat replicates for the systematic and haphazard pair collection strategies or on 2 rakes and 4 quadrats for the block collection strategy. Species information per replicate sample was converted to dominant growth form type as either species forming dense canopy, short understory species or species with leaves growing from a basal rosette, using the dominant species only (rank 1). Canopy-forming plants (< 3 m) included mainly *Potamogeton richardsonii* but also *Heteranthera dubia*, *Stuckenia pectinata*, *Elodea* spp and *Myriophyllum* spp. *Chara* spp formed a low-lying (< 20 cm) layer on the bottom, while *Vallisneria americana* formed rosette of linear leaves extending towards the surface (< 1.5 m). When more than half of the replicates at a given site had the same dominant growth form, that growth form was allocated to the site.

Table 1. Summary of the three datasets used in this study. LSP Lake Saint-Pierre, LSL Lake Saint-Louis, LSF Lake Saint-François, sd standard deviation.

	Quadrat - rake	Rake - echo	Validation
Location	LSP 46°09'N 72°52'W LSL 45°24'N 73°54'W LSF 45°08'N 74°21'W	LSP 46°09'N 72°52'W	LSP 46°09'N 72°52'W LSP 46°13'N 72°53'W
Year	2006-2009	2012-2017	2013, 2016
Time of biomass collection	Jul, Aug, Sep	Jun 26-28 (2012 only) Jul 27 to Aug 17	Aug 13-16 2013 Aug 16-25 2016
Time of echosounding		June 18-20 (2012 only) July 27 to Aug 15	Aug 12-13 2013 Aug 3-4 and Sep 01-02 2016
Biomass treatment	fresh and frozen/thawed	frozen/thawed	frozen/thawed and fresh
Species identification	visual abundance rank	biomass per species	biomass per species
Type of comparison	3 dispositions systematic pair, haphazard pair, block	constant distance to rake station	constant distance to quadrat station
Number of biomass site	77	217	105
Size of the quadrat sampling unit (m)	0.25 x 0.25 0.40 x 0.60 0.25 x 0.35		0.25 x 0.25 0.30 x 0.30 (at low SAV density 1 to 100 m^2)
Size of the rake sampling unit (m)	0.35 x 1	0.35 x 1	
Biomass replicates per site	3-5 or 2-4	3-5	3
Variables used in analysis	quadrat biomass rake biomass collection strategy biomass treatment lake substrate type depth growth form	rake biomass biovolume biovolume sd depth growth form Chlorophyte biomass *Microseira (Lyngbya) wollei* biomass number of ping report mean distance to rake site flow velocity wind speed wind direction	quadrat biomass biovolume biovolume sd depth

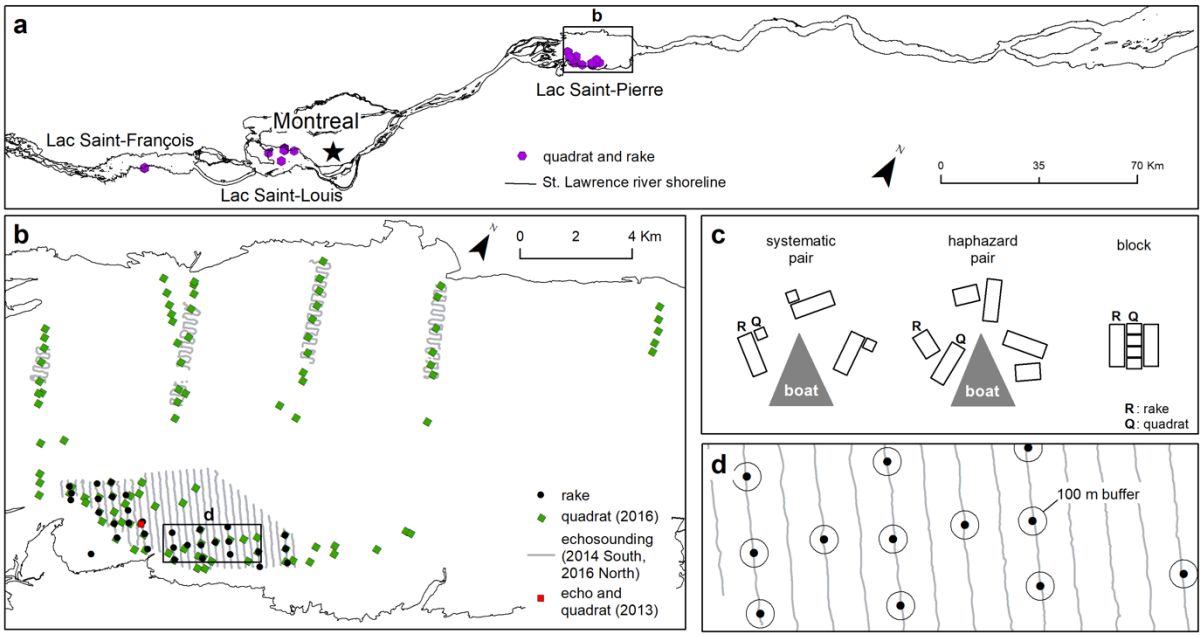

Figure 2. a Sampling locations in the St. Lawrence River for the quadrat-rake (Q-R) dataset; b rake-echosounding (R-E) and validation (echosounding - quadrat) datasets in Lac Saint-Pierre. c collection strategy to compare quadrat to rake; d collection strategy to compare rake to echosounding. For the R-E dataset in b, 2014 rake sampling sites and echosounding tracks are shown as an example (South-West sector in b). To clearly visualize the validation dataset, all the 2016 quadrats (green diamonds in b) are depicted but only part of the 2016 echosounding tracks (North section in b, South-West tracks are similar to R-E dataset) and the general location of the 2013 small scale sampling (red square, South-West sector in b) are shown.

Rake and echosounding (R-E) dataset

The second dataset was used to predict rake biomass from echosounding (hereafter named R-E dataset). Both acoustic and rake surveys were carried out in the southwest portion of LSP once a year from 2012 to 2017 during the moment of maximum biomass, but also once early in the growing season in June 2012 (Figure 2b, d). Acoustic surveys were conducted on 250 m-spaced transects perpendicular to the lake shore at low and constant speed (~1.1 m/sec). Acoustic data were collected using a downward-looking BioSonics single beam transducer mounted on an Ocean Science riverboat fixed to the side of the vessel by a steel rod. This set-up allowed the transducer to be constantly immersed below 5 cm of the water surface. Floating and drifting vegetation frequently became entangled with the transducer, which consequently was regularly cleaned. The transducer had a beam angle of 6.6° and a working frequency of 430 kH, which depending on water depth, represents a circle of 0.10 to 0.20 m cone diameter of sound reaching the sediment surface. Echosounding was controlled by a BioSonics DTX system running Visual Acquisition 6.06 with a pulse length of 0.1 msec and a ping rate of 5 ping/sec. Geolocation data were simultaneously recorded with a GNSS NovAtel Smart V1 receiver placed on top of the transducer. Real-time differential correction was obtained using the Omnistar VBS network in 2012 and 2013 (0.90 m precision) and the WAAS network in 2014 to 2017 (0.65 m precision). Acoustic data (echograms and geographic coordinates) were saved in dt4 files on a laptop PC for post-processing.

Acoustic data were processed using Visual Habitat 1. Lake bottom was first determined using a rising edge threshold of -47 dB and a rising edge length criterion of 10 cm. The resulting delineations on the echograms were manually corrected to have a bottom line following highest amplitudes. SAV was subsequently analyzed using plant detection threshold above ambient noise of -68 dB and a minimum height of plant detection of 10 cm. SAV delineations were again manually corrected when the plant line was going beneath the bottom line, mainly due to false detection of plants reaching the water surface. Invalid ping reports were removed, and remaining reports were exported for cycles of 5 pings to have a sample resolution similar to the raked length and a data point every ~1.1 m. For each cycle, mean plant height (m), plant cover (%), mean geographic position (decimal degree) and mean depth (m) were exported. SAV biovolume, a potential proxy of SAV biomass, was computed as mean plant height × mean plant cover.

Within one to two week of the acoustic surveys, rake samples were collected at 35 sites along the echosounding transects. Sites were positioned using a Trimble GeoXT (precision 0.50 m) in 2012-

2013, a SXBlue II GPS (precision 0.65 m) in 2014-2015 and a Garmin 64S (precision 3 m) in 2016 and 2017. Water depth (z) was measured with a survey ruler and, to be comparable with depth during echosounding, was corrected using the equation $z = z_{rake} - lvl_{date\ rake} + lvl_{date\ echo}$ and water level (lvl) at station 15975 (Fisheries and Ocean Canada, www.isdm-gdsi.ca, accessed 2017/11/27). Depth average flow velocity was also measured at the same time or one week prior to biomass sampling. Velocity was measured at 60 % of site depth using a rotating (Swoffer 3000) or electromagnetic (Marsh McBirney Flo-mate 2000 or Valeport model 801) flowmeter. At each site, 3-5 rake replicates were collected around the anchored, 7-m long boat, using the same apparatus and dragged length as the Q-R dataset. To ensure that a location was not raked twice, rakes were systematically collected in front and on each sides of the boat and as distant as possible when replicate number exceeded three. Plant material was similarly processed as described for the Q-E dataset, but plants were sorted by species in the lab and macrophyte biomass was measured on dried material. Total SAV biomass was computed from the species biomass and pooled by growth form. The same species as the Q-R dataset were found. All SAV biomass herein are reported as mean dry biomass in g m^{-2}.

Since rake collection and echosounding were conducted separately, we determined the spatial resolution at which they could be compared by inspecting the relationship between rake biomass and mean biovolume at increasing radial distance from rake site (see supporting information, SI, Text S1 and Figure S1). We conducted this comparison at radial distance ranging from 1 to 100 m (Figure 2d). Based on observed higher correlation and field observations, we chose a resolution of 20 m (or 10-m radius around rake site). Using the 20 m resolution, we calculated the biovolume standard deviation (sd) as an indicator of the acoustic error, the mean ping report distance to rake site as the acoustic proximity, and the number of ping reports per site as the acoustic frequency.

Echosounding and quadrat validation dataset

The third dataset was used to validate biomass estimation from echosounding and compare it to quadrat biomass (hereafter named the validation dataset). Acoustic and quadrat surveys were carried at the time of maximum biomass accumulation in 2013 and in 2016. In 2013, the survey was concentrated in a small (100 m x 100 m) area of high biomass in southwest LSP characterized by a narrow depth range (1.4 - 1.5m, Figure 2b). In 2016, the survey was conducted in both the southwest and the northern sector of LSP. The northern sector was characterized by greater depth range (0.5 - 7.0 m) due to the crossing of the St. Lawrence navigation channel. Quadrat sampling in this sector

was carried in 5 transects and the 250 m-spaced echosounding transects were perpendicular to the quadrat transects. The southwest sector had shallower depths (< 2.7 m) and echosounding transects were located following the same methodology as described for the R-E datasets. Processing of acoustic data and biomass samples were also conducted similarly to the R-E dataset, but aboveground biomass was collected in triplicates by scuba divers using a 0.30 m x 0.30 m quadrat in 2013, a 0.25 m x 0.25 m quadrat in 2016 and balance precision was 0.0004 kg. When SAV density was very low, divers evaluated the surface they patrolled without plants as a straight line or a circle around the anchor (up to 100 m^2) and collected the few plants they found. Quadrat and echosounding were spatially matched using the same resolution of 20 m determined from the R-E dataset.

Statistical analysis

To predict quadrat biomass from rake biomass, we conducted two distinct analysis with different purposes. First, to derive mean parameter estimates while allowing for a hierarchical structure, we used linear mixed model (LMM) with gaussian error. Only rake biomass was included as the fixed effect, and the random terms were date and sampling site. The random effect models were fitted with restricted maximum likelihood estimation (REML) and selected to minimize the sample-corrected Akaike information criterion (AICc) following the approach of Zuur et al. (2009). To assure the selected model captured spatial autocorrelation, absence of correlation was assessed by looking at correlograms of model residuals. Second, we investigated how environmental variables affected the rake and quadrat biomass relationship. The intention was to indicate which variable should be controlled for or included in the intercalibration to reach a higher accuracy. Since available variables were mostly categorical (collection strategy, biomass treatment, lake, substrate type and growth form, Table 1), we tested this using ANCOVA. When the relationship between quadrat and rake biomass exhibited different slopes and intercepts for a given condition, separate regression equations were computed for each category using ordinary least square regression. We also evaluated the effect of depth on the quadrat-rake biomass relationship using partial regression.

We applied a similar two-analysis approach to predict rake biomass from echosounding biovolume. LMM was used to derive mean parameter estimate, but to describe how environmental variables affected the rake biomass and biovolume relationship, we used partial least square regression (PLSR). This method was chosen based on the structure of the dataset that included many continuous and potentially correlated variables. Variables included in the analysis described

SAV growth form, macroalgae abundance, water depth, flow velocity, wind (hourly wind speed and direction acquired from Meteorological Service of Canada, climate.weather.gc.ca, accessed 2017/11/27) and acoustic data quality during surveys (Table 1). This method allowed us to visualize in reduced space the multiple covariates and is also robust when there is high collinearity among many predictors and when numbers of observations are low (Mevik and Wehrens 2007). For this, we selected components using the leave-one-out cross-validation and the one-sigma heuristic approach. We then selected variables using the filter method of selectivity ratio (SR), which is the ratio of the explained to the residual variance of the X variables on the y target projection. We chose SR over the commonly used variable importance of the projection (VIP) because the former selects important variables using a F-test and performs well for prediction (Farrés et al. 2015).

To validate our intercalibration approach, we applied our models in two steps. First, from echosounding biovolume, we predicted rake biomass and from that estimation we predicted quadrat biomass. We propagated model error with Monte Carlo simulations and used the root mean square error (RMSE) of the LMM residuals as the model error term. Second, we visually compared in space the quadrat-equivalent biomass predicted from echosounding to measured quadrat biomass. For this, we created spatially interpolated biomass maps from both quadrat and echosounding using kriging.

To compare the effect of sample size and spatial coverage on whole-system biomass, we compared biomass estimate from point sampling to remote sensing using the R-E dataset over five summer campaigns. We first calculated mean biovolume along echosounding transects in 20 m distance bins. We then created for each campaign a spatial polygon where both rake and echosounding had a good spatial coverage. To do so, we intersected for each campaign two 100 m buffers around concave hulls created from the rake sites and echosounding sites. Within the intersected spatial polygon, mean biomass for rake and echosounding sites were then calculated with bootstrapping confidence intervals. This resampling technique has been shown to be more appropriate for estimating seaweed confidence interval and is particularly suitable when the true distribution of the data is unknown or skewed (Johnson 2020). For echosounding, we also estimated a spatially interpolated average.

Due to high SAV heterogeneity ranging from bare patches to dense plant abundance, absence data (where quadrat or rake biomass = 0 and biovolume = 0) were excluded from modelling analysis. The three techniques had different sample unit size and sampling effort (Table 1). Therefore, techniques

with higher sample unit size, e.g. rake, or having a higher number of observations, e.g. echosounding, had a higher probability of finding SAV in low biomass regions compared to their correspondent explained variable (e.g. quadrat and rake respectively). The resulting models to predict rake and quadrat biomass were applied only to presence data (biovolume > 0 or rake biomass > 0) and absence recorded by both techniques were deemed true. When necessary, data used in statistical analysis were transformed to respect assumptions of normality. Data handling and statistical analyses were performed in R 3.6.3 (R core team 2020). Linear mixed models were computed with the lme4 package (Bates et al. 2015), with AICc compared using the MuMIn package (Bartón 2020). PLSR with variable selection was carried out using pls and plsVarSel (Mevik et al. 2020, Mehmood et al. 2012). Geospatial data was handled using the sp, sf, raster and concaveman packages (Pebesma and Bivand 2005, Pebesma 2018, Hijmans 2020, Gombin et al. 2020), while geostatistical modelling and kriging was performed using gstat (Pebesma 2004). Bootstrapping confidence intervals were computed using the boot package (Canty and Ripley 2021).

Assessment

Prediction of quadrat biomass using rake samples

The overall relationship between quadrat biomass and rake biomass was moderately strong with a pseudo R^2 of 0.61 (Figure 3a, Table 2, SI Table S1). The selected random effect of sampling site accounted for an additional 9% of variation (SI, Table S2 and S3). The quadrat and rake distributions were skewed, leading to non-normal regression residuals, therefore the modelled relationship was on $\log_{10}$ data. The quadrat biomass was generally significantly higher by a factor of 4 than biomass estimated using a rake (median_Q = 55 g m^{-2}, median_R = 14 g m^{-2}, paired *t*-test $p < 0.0001$). Quadrat estimates had 20 times higher variance (median s^2_R = 537 g m^{-2}, median s^2_Q = 30 g m^{-2}, $p < 0.001$) than rake equivalents, resulting in a higher standard error (SE, median SE_Q = 10 g m^{-2}, median SE_R = 4 g m^{-2}). There was a correlation between mean biomass and its associated error for both quadrat and rake (r_Q = 0.82, r_R = 0.77), indicating that the difference in error between methods could be caused by the higher biomass measured in quadrat sampling. Furthermore, this inflation of error with biomass was not constant: the ratio of variance to mean biomass ($s^2/\bar{x}$) increased with mean biomass and was generally higher for quadrat than rake ($\bar{x}_Q$ = 41, $\bar{x}_R$ = 17). As a result, both rake and quadrat measurements showed a spatial aggregation of biomass ($s^2 > \bar{x}$), although more markedly so for quadrats (99% of observations) than for rakes (67% of observations).

The discrepancy between rake and quadrat biomass comparison was not constant over the biomass gradient (Figure 3a, Table 2). The slope was less than one (0.64) and rake underestimation of quadrat biomass was highest at low biomass, while measurements from both methods converged at higher biomass (> ~ 100 g m^{-2}). The intercept was greater than 0 ($\log_{10}$(quadrat biomass) = 0.96 or quadrat biomass = 8 g m^{-2}), therefore application of the equation would result in systematically biased biomass estimation in the absence of SAV and has to be limited to presence data (Table 2).

Predictions of quadrat biomass from rake measurements were affected by substrate type and SAV growth form (Figure 3b and 3c), while no effect of collection strategy, biomass treatment, lake or depth was detected. The slopes and intercepts of the relationship differed significantly among substrate type ($F_{2, 61}$ = 4.44, p = 0.02), with silt displaying a higher intercept, lower slope and higher variability than sandy sediments (Table 1). This was indicative of the greater efficiency of rake to collect SAV, especially at low biomass, in sand bed areas compared to finer (silt) and more organic sediments (silt). For sandy sediments, the slope was not only closer to one, but the relationship also

had a better fit. In hard packed sediments (clay - pebble), rake sampling seemed to be unsuited and completely failed to collect any plant despite their known presence. However, this substrate type occurred only at a reduced number of sites (n = 6) and the biomass at these sites was very low (< 0.5 g m^{-2}).

In the case of the effect of the dominant growth form, the relationship slopes were similar for rosette and canopy-forming SAV ($F_{1,42}$ = 0.02, p = 0.88), but their intercepts were significantly different ($F_{1,43}$ = 6.93, p = 0.01). Understory were dominant at only 2 sites and were excluded from analysis. For the same rake biomass, the rosette had a quadrat biomass systematically higher than canopy by 1.95 g m^{-2}. Thus, rake was more efficient at sampling canopy-forming plants and tended to underestimate the biomass of rosette-forming *Vallisneria americana*. Inclusion of the dominant SAV growth form in the model resulted in an overall better fit and lower prediction error.

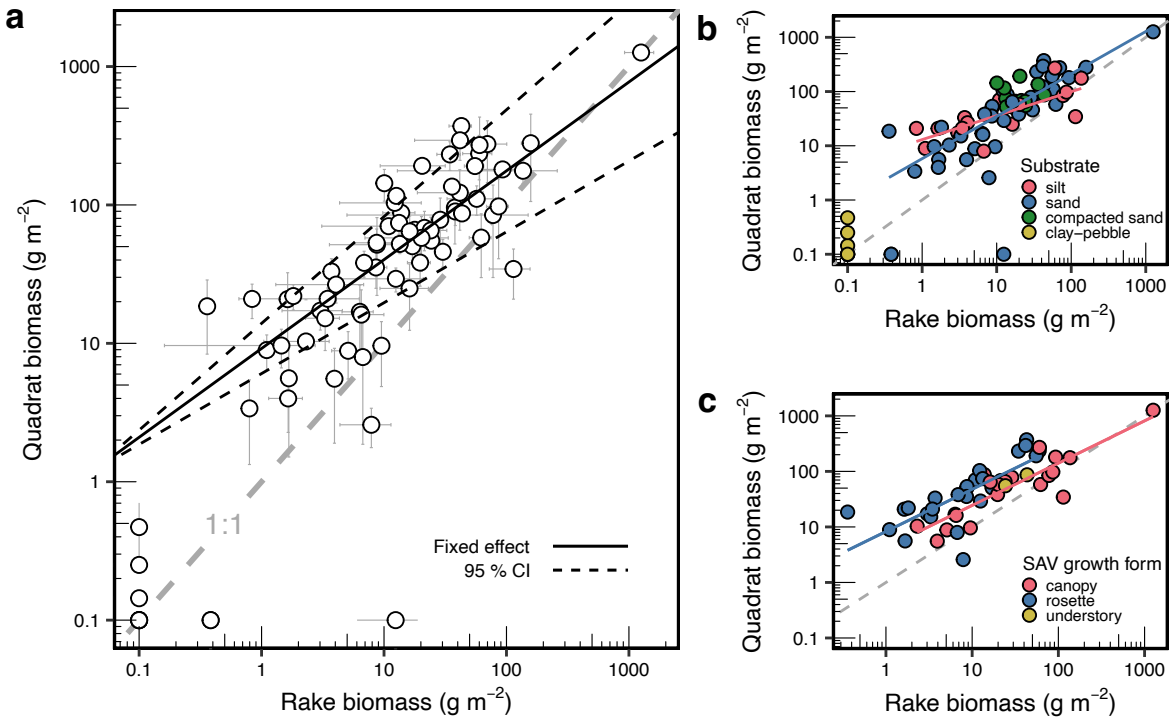

Figure 3. Relationships to predict quadrat biomass from rake biomass. Overall relationship is shown in a and effect of substrate and growth form are shown in b and c respectively. Regression line is represented by the dark solid line with 95% confidence intervals dashed lines and error bars are standard errors. Quadrat and rake absence (value displayed at 0.1) are depicted in a and b but are not included in regressions calculation.

Table 2. Equations and summary statistics of models allowing to predict quadrat biomass (log_{10} g m^{-2}) from rake biomass (log_{10} g m^{-2}). Models are shown for all available data and for different subsets with distinct environmental conditions having a significant effect on the quadrat and rake relationship. Equ. equation number, LMM linear mixed model, OLS ordinary least square, 1|site varying intercept per sampling site. For LMM, R2 indicate the marginal R^2 (for the fixed effect).

Equ.	Environmental condition	Coefficients		R^2	*n*	Rake biomass range (g m^{-2})	Model type	Random effect
		Intercept	Slope					
1	All data	0.96	0.64	0.61	67	0.36 - 1257.68	LMM	1|site
2	Silt	1.11	0.44	0.46	16	0.84 - 136.45	OLS	
3	Sand	0.76	0.78	0.69	40	0.36 - 1257.68	OLS	
4	Rosette	0.92	0.76	0.61	26	0.36 - 59.91	OLS	
5	Canopy	0.63			20	2.30 - 1257.68	OLS	

Prediction of rake biomass from acoustic data

When comparing rake biomass to biovolume, the distinct scale of the two methods was more apparent than for the quadrat-rake comparison. SAV were more spatially aggregated when looking at biovolume with 98% of observations having a variance higher than its mean ($s^2 > \bar{x}$) compared to 50% for rake. Nevertheless, the relationship between rake biomass and biovolume was moderately strong with a pseudo R^2 of 0.57 (Figure 4, SI Table S4). The following equation described the generalized relationship.

[6] $\log_{10}$ SAV rake biomass $= 0.37 \times \sqrt{\text{biovolume}_{10}} - 1.37$

An additional 27 % of variation was explained by the selected random effect of varying intercept per sampling campaign and site. This suggested that environmental condition affected the rake biomass biovolume relationship. To test for this influence, we performed a PLSR (Figure 4b, c). We first selected the number of components (or latent variables) using the root mean square error of cross-validation (RMSECV) which had a minimal value of 0.60 (log_{10}) at 8 components. To avoid overfitting, we chose the model with three components (RMSECV = 0.63), which was the model with the fewest components that was less than one standard deviation from the best model (one-sigma heuristic approach). As expected, biovolume was the most the most important variables explaining these components (Figure 4c). Biovolume sd was also a strong predictor and like

biovolume, it was correlated to rake biomass ($r_{biovolume}$ = 0.79, $r_{biovolume\ sd}$ = 0.61, SI Figure S2a, b). The two echosounding variables were also correlated to one another (r = 0.59, SI Figure S2c, Figure S3a), although above a biovolume of 15, there was increased scatter between the two variables and a reduced correlation ($r_{biovolume\ >\ 4}$ = 0.10). As a result, biovolume and biovolume sd were nearly orthogonal when looking at site configuration in relation to predictors (Figure 4b). Biovolume was more highly correlated to rake SAV biomass and canopy growth form, while biovolume sd was pulled by two extreme data points. This suggest that biovolume sd does not add much predictive power compared to solely modelling rake biomass from biovolume.

Other potential predictors of rake biomass included, in decreasing order, SAV growth form, flow velocity, mean distance to rake site, depth and wind direction (Figure 4c, Figure S3b-f). Mean distance did not display any coherent patterns on the relationships between biovolume and rake biomass in contrast to other variables. The presence of canopy growth form modified the relationships, where canopy had a higher rake biomass per biovolume than rosette-forming plants. Flow velocity was rather correlated with biomass, where site with low flow had higher biomass. Depth seem to induce a bias where shallow sites (< 1 m) tended to display a low biovolume for a given rake biomass. With regards to wind direction, sites sampled when winds were coming from North to North-West had high biovolume for their measured rake biomass (Figure S3f).

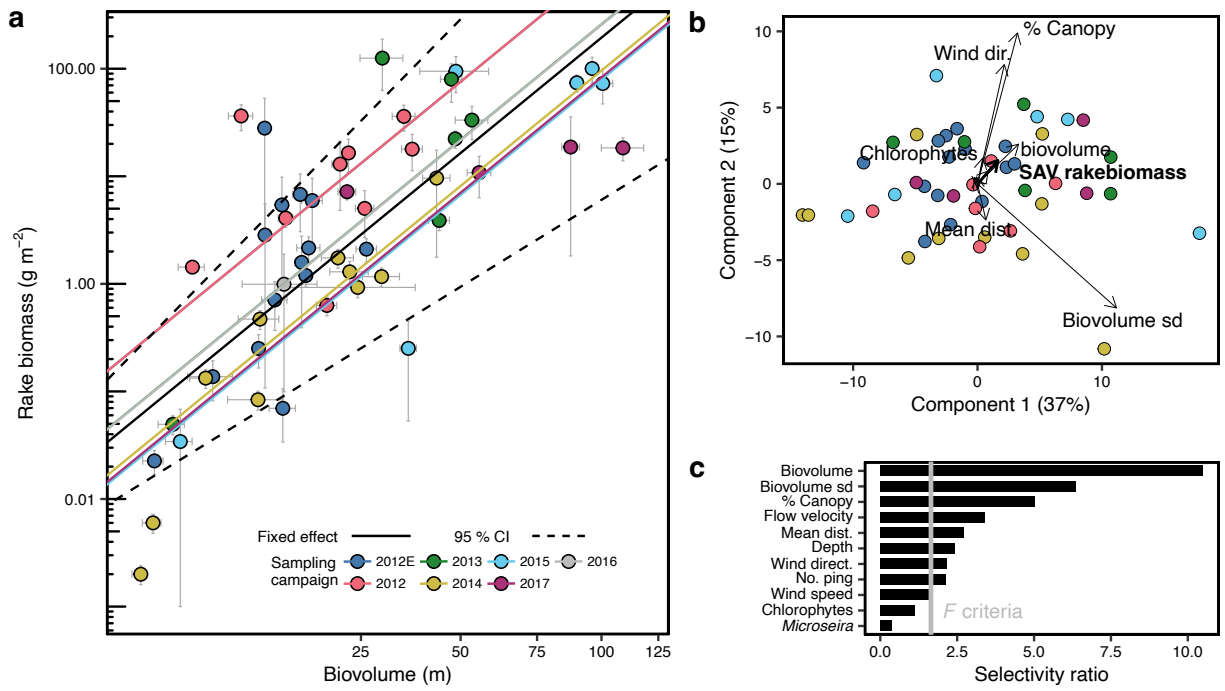

Figure 4. Relationship to predict rake biomass from echosounding biovolume, and effect of environmental variability on the relationship. Overall fixed relationship is shown as a black line in a with the colored line showing the random effect of different intercept per sampling campaign. Grey lines radiating from points are standard errors. The effect of the environmental variables is shown in b as score plot of the PLSR model describing data configuration in relation to predictors, with the explained variable in bold. c Depicts the importance of environmental variables as predictors of rake biomass, with each variable's bar crossing the green line having a significant discriminant power at $p < 0.05$. sd standard deviation, no. number, dist. distance, dir. direction, CI confidence interval.

Two-step model validation

To validate the two-step intercalibration approach, we predicted quadrat biomass by sequentially applying the general rake-biovolume equation 6 followed by the rake-quadrat equation 1. Predicted biomass was then compared to measured quadrat biomass. Three surveys carried out over different depth ranges were available for the comparison: a small-scale survey at constant depth (2013, 1.4 - 1.5 m), a survey in the deeper water in the North of LSP (0.5 - 7.0 m) and a survey in the shallow waters in the South of LSP (< 2.7 m). We first compared paired acoustic predictions at 10 m distance of quadrat measurements (Figure 5). The two step predictions were comparable to the

quadrat measurement and did not introduce any evident bias. The standard deviation of the Monte Carlo simulation was 4 g m^{-2} (log_{10} 0.59) which was an intermediate value between the RMSE of the two models (Q-R 1.9 g m^{-2} and R-E 2.4 g m^{-2}). However, the RMSE of the predictions 123 g m^{-2} was higher than the quadrat measured standard error (38 g m^{-2}). The mean absolute percentage error (MAPE) of the predictions was also higher than the relative error of the quadrat measurements (1718% vs 50% respectively), but it was driven by a single outlying data point in the North of LSP that, once removed yielded a MAPE of 87%. Indeed, when looking at each individual survey, the acoustic predictions in 2016 tended to have a higher error than the 2013 predictions ($RMSE_{2016}$ = 170 g m^{-2}, $MAPE_{2016}$ = 6433 %, $RMSE_{2013}$ = 86 g m^{-2}, $MAPE_{2013}$ = 68 %). The 2016 predictions were either well above or below the 1:1 line, while the 2013 predictions from sites at a constant depth had a majority of their confidence intervals overlapping the 1:1 line. In 2016, sites from the deeper North sector tended to have higher predictions compared to nearly absent quadrat biomass (< 1 g m^{-2}). Echosounding integrates a larger number of measured units and thus better describes the same areal extent than quadrat (up to 400 m^2 vs < 1 m^2) which, in this case, probably underestimates true biomass. Conversely, sites from the shallow South sector tended to have much lower acoustic predictions than that measured by quadrat, probably due to a bias from echosounding due to biomass accumulation at the surface from floating leaves. Overall, the predictions were not significantly different from quadrat measurements (paired t-test p = 0.17, Figure 5b), although acoustic predictions had somewhat lower mean and median ($\bar{x}_{pred}$ = 88 g m^{-2}, $\bar{x}_{obs}$ = 121 g m^{-2}, $median_{pred}$ = 98 g m^{-2}, $median_{obs}$ = 107 g m^{-2}).

Second, given that most quadrat measurements in our dataset were located beyond 10 m from the echosounding track, we compared spatially interpolated measured quadrat biomass to interpolated predictions derived from echosounding (Figure 6). In the 2013 constant depth range survey, the quadrat and echosounding estimation were very similar and small local differences were potentially caused by the higher sampling effort and surveyed area of echosounding (Figure 6a, b). In the deeper North sector of LSP, interpolated biomasses were similar for quadrat and echosounding above the SAV maximum colonization depth (3 m, Figure 6c, d). Echosounding clearly enabled the delimitation of SAV spatially because of a better accountability of limits imposed by depths. Quadrat interpolation tended to overestimate biomass in deeper waters where no sampling occurred. Conversely, in the shallow South (< 1.5 m, Figure 6e, f), echosounding underestimated biomass, again probably because of bent SAV that accumulated at the water surface and prevented efficient estimation of underwater biomass using acoustic signal.

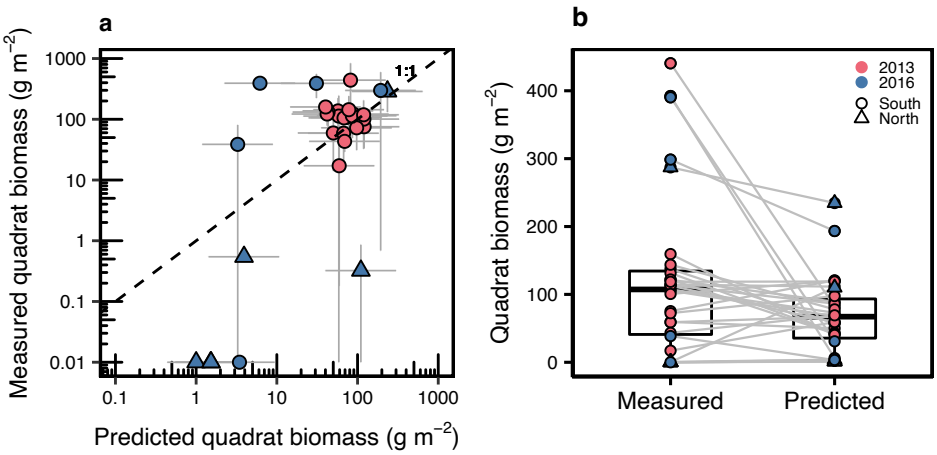

Figure 5. Validation of the two-step quadrat biomass prediction from echosounding (using equation 1, table 2 and equation 6 in text). a Scatterplot of measured vs predicted quadrat biomasses, error bars are the 95% confidence intervals and absence of measured biomass are depicted at 0.01 g m^{-2}. b Paired boxplot of measured vs predicted quadrat biomasses, solid horizontal line within boxes represents the median, boxes extent the 25th and 75th percentiles and whiskers the 10th and 90th percentiles.

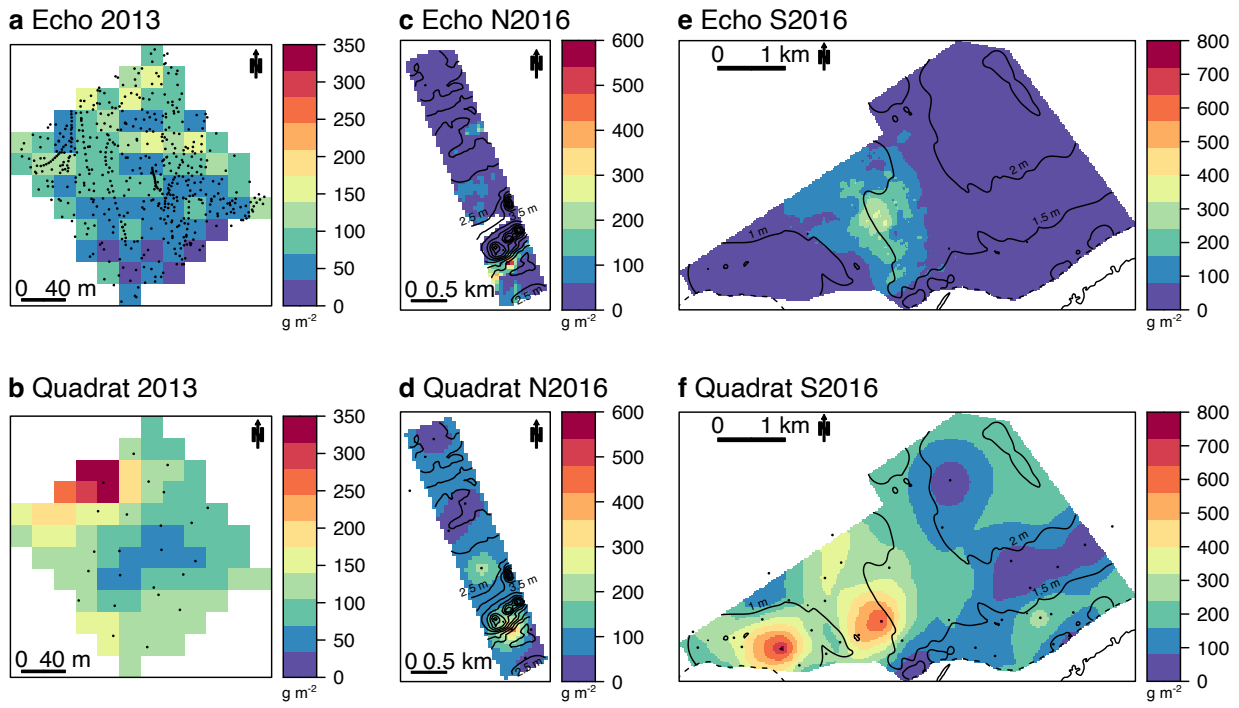

Figure 6. Comparison of spatially interpolated quadrat-equivalent biomass estimated from echosounding (top panels) and point measurements (bottom panels). A and b 2013 small-scale plot of constant depth, c and d North section of LSP with depths ranging from 0.5 to 7 m sampled in 2016, e and f South section of LSP with shallow depths (< 2.5 m). Lines are isobaths at 0.5 m increments and dots sampled sites (not displayed for clarity in c and e).

Effect of sample size on whole system estimation

Finally, we assessed how the increased sample size afforded by echosounding and the use of spatial interpolation method modify whole-system biomass estimation. Using the two models we developed, we predicted quadrat biomass from both rake biomass and biovolume for five independent SAV surveys where both rake sampling and echosounding had similar spatial extent. We then compared the mean from these estimated biomasses, either on the raw data or on spatially interpolated biomass (Figure 7). In all surveyed years, the study area displayed heterogenous biomasses, with clear high and low biomass zones (SI Figure S4). This combined with the different sampling effort of rake (n = 21 to 30) and echosounding (n = 1224 to 1934) created widely different mean biomass per survey. Biomass predicted from rake was, depending on the survey, either lower or higher than that from echosounding generally by a factor of 2. The mean estimate of each technique was distinct and there was almost no overlap with their confidence intervals. As a result,

the range across years of mean biomass from rake (15 to 59 g m^{-2}) was more limited compared to that from echosounding (9 to 84 g m^{-2}). The higher number of observations using echosounding generated more precise estimates with smaller confidence intervals compared to the very large uncertainty associated with the rake estimation. In contrast to the difference between techniques, spatial interpolation of biomass derived from echosounding did not affect whole-system mean biomass that was very similar to direct estimation from the original echosounding track. Largest differences between estimates were observed for surveys with interrupted echosounding tracks (2013, 2017) that consequently were not covering uniformly the study area (SI Figure S5).

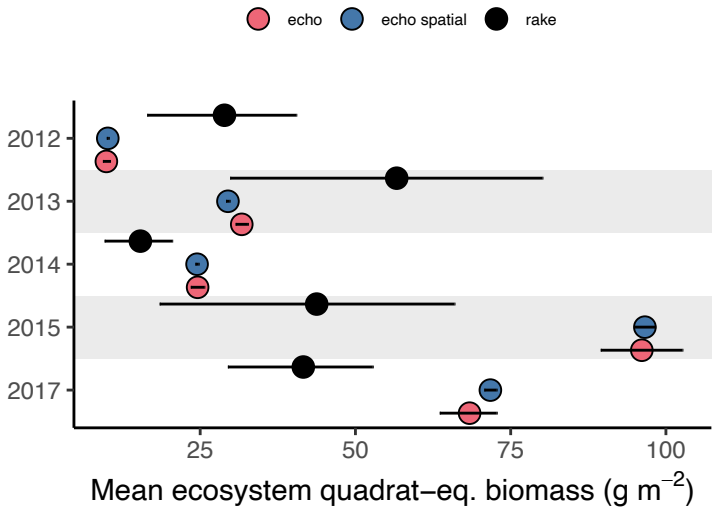

Figure 7. Comparison of whole-system average quadrat biomass using non-spatial predictions from rake and echosounding and spatially interpolated echosounding predicted biomass for five summertime yearly surveys. Horizontal bars represent 95% bootstrapped confidence intervals.

Discussion

We successfully developed two intercalibrations that allows for the interchangeable use of quadrat, rake and echosounding techniques to estimate SAV biomass. We first predicted quadrat biomass from rake biomass and showed the effect of substrate and species growth form on the predictions. Using a resolution of 20 m, we predicted rake biomass from biovolume, a proxy of biomass derived from echosounding. We also showed that this prediction is affected by multiple environmental variables, including SAV growth form, flow velocity, depth, wind conditions and acoustic data quality. By sequentially applying both models to echosounding tracks, we were able to accurately predict quadrat biomass. Since the bias of rake collection can be corrected, this faster and safer technique could thus be used instead of quadrats as the ground truth for echosounding. In rugged and deeper bottoms, echosounding outperformed point sampling techniques in estimating biomass, but underestimated biomass in very shallow waters. Use of echosounding combined with the intercalibrations are particularly useful at large spatial scales as the higher sampling effort from the greater number of observations provided by this technology increase accuracy by capturing SAV heterogeneity.

Intercalibration between quadrat and rake

Our intercalibration between quadrat and rake biomass confirmed that the two techniques are comparable, and that bias introduced by rake sampling can be corrected (Johnson and Newman 2011; Kenow et al. 2007; Rodusky et al. 2005). This correction is important and meaningful, since failure to correct biomass estimation from the rake can lead to a 4-fold underestimation of biomass, with even greater bias at low biomass. In real-world application, the correction can modify sample distribution which can reveal significant difference or patterns in space and time that would not be detected otherwise. Given that the correction is stronger below a rake biomass of 100 g m^{-2}, these effects will depend on the measured rake biomass ranges. The model error was also lower than the standard error of the measured quadrat biomass and was equivalent to the error associated with rake biomass collection. The smaller error and variance of rake were probably caused by the larger rake sample unit size that dampened small-scale heterogeneity captured by quadrat, which had consistently higher ratio of variance to mean biomass. Thus, gain in accuracy, did not come at the expense of precision.

Our finding that rake collection underestimated biomass confirms previous observations on rake and quadrat comparisons (Johnson and Newman 2011; Kenow et al. 2007; Rodusky et al. 2005).

This bias is probably introduced by saturation of plant material on the rake or to the loss of this material as it is lifted from the water. Work by Masto et al. (2020), who combined quadrat-rake apparatus and picked up remaining plant material after rake collection, also suggests that the rake does not completely break plant material at the sediment surface. This harvesting efficiency from rake was affected by the same factors explaining SAV anchorage strength from the natural pulling forces of waves, current or bird foraging: the size of SAV root system and sediment cohesive strength (Schutten et al. 2005). Indeed, we found that canopy-forming SAV tended to be more efficiently collected by rake in contrast to the rosette-forming *Vallisneria americana*. The latter has one of the higher root to shoot ratio among freshwater SAV (Stevenson 1988), thus being harder to break from the sediment and being systematically underestimated by the rake. We also observed that the rosette-forming linear leaves tended slip in between rake teeth compared to the canopy-forming that were entangled in them. Additionally, canopy-forming not only tend to have a reduced root system, but their intertwined stem could drag plant material from outside the rake sampled area. Dense stands of the canopy-forming species *Ceratophyllum demersum*, *Potamogeton zosteriformi*, *Hydrilla verticillata* have previously been overestimated by rake techniques (Johnson and Newman 2011; Rodusky et al. 2005).

Our results further indicate that rake harvesting efficiency is dependent on the substrate type. We did find that in hard packed sediments (pebble-clay), which provide higher anchorage strength, the rake technique failed to collect any SAV. Counterintuitively, plants were more easily and consistently pulled out from moderately compacted (sand) than from organic and soft sediments (silt). This finding could be an artifact of the more restricted biomass range measured from siltier sites as compared to sandier ones in our survey. However, Rodusky et al. (2005) similarly found a weaker relationship with quadrat biomass and a lower slope when rake collection was on peat-like organic sediments compared to sand. In very loose and organic sediments, the rake could have less grip and SAV be more elusive, being both dragged and buried in mud by the rake motion. SAV is also likely more dispersed in this type of substrate since it is not optimal for their growth (Barko et al. 1991). All of these effects would result in less consistent rake harvest in organic substrates. Therefore, calibration of rake biomass measurements could include of both species and substrate information to increase accuracy. Nevertheless, we derived a generalized relationship that can be used to derive community level estimate. We have also shown that the calibration is not impacted by the sampling strategy and the depth of the quadrat and rake comparison. Investigators

can thus use the simplest sampling strategy, such as the haphazard pair, and reduce sampling effort in deeper more hazardous areas for scuba diving.

Intercalibration between rake and echosounding

We also successfully developed an intercalibration between rake biomass and biovolume. Quadrat biomass has previously been related to biovolume or height measured by echosounder (e.g. Duarte 1987; Maceina et al. 1984; Thomas et al. 1990), but to our knowledge, only Howell and Richardson (2019) related rake biomass to biovolume. However, their biovolume was derived from a cloud-based data-processing platform and was not an absolute volumetric estimate; rather it referred to the percent volume inhabited by SAV in the water column (PVI, % cover/depth * height, (Thomas et al. 1990; Winfield et al. 2007). This metric is not appropriate to estimate biomass because it is a depth-standardized measurement that does not reflect variation in plant height. For example, given a surface cover of 100%, the same PVI of 80% is measured for a plant height of 2.4 m at a depth of 3 m (2.4/3 * 100) or a height of 0.8 m at a depth of 1 m (0.8/1 * 100). Comparison of these specimens' biomass would likely be very different given their 3-fold size difference. Thus, care must be taken when blindly applying measure from the manufacturer; the use of the simple biovolume as % cover multiplied by height is recommended to compare with biomass estimates.

We computed a generalized relationship between rake biomass and biovolume that allowed to validate the sequential application of rake-echosounding and quadrat-rake models. However, the echosounding and rake relationship was affected by multiples environmental variables, notably SAV growth form. Indeed, Duarte (1987) has previously shown that given their different biomass allocation with height, deriving calibration by SAV growth form increase accuracy in quadrat biomass estimation. Although not detected in our model, filamentous algae could further introduce bias in the biovolume-rake biomass relationship since they can be detected by echosounder (Bučas et al. 2016; Depew et al. 2009). Predictions were also affected by environmental conditions during sampling, with clear effect of flow velocity, depth and wind direction. The depth and flow effects could be due to differences in species composition that tend to vary by depth or decrease in biomass in deeper area more exposed to fast flow at our study site (Hudon 1997). Alternatively, underestimation in shallow areas could be due to detection problems either because of an overestimation of bottom depth, which is used to calculate plant height, or of floating plant material at the water surface that was not detected by the echosounder. Observations when wind was coming from North to North-West also had overestimated biovolume. In LSP, wind coming from this

direction are against water current and are in the general orientation of the lake, which increases the travelling distance on open water. Both of these factors can increase wave height and create bubbles that cause false echosounding plant detection. To account for these environmental variations, greater accuracy could thus be provided by conducting a calibration per sampling campaign (e.g. Figure 4b), for similar environmental conditions or during favorable wind conditions.

Versatility of using two intercalibrations

Compared to the application of a single technique, our two intercalibration approach allows for more versatility and the measurement of biomass at wider temporal and spatial scales. We provide in Figure 8 a step-by-step guideline composed of key questions that help decide when only quadrat collection, the rake-quadrat intercalibration or the full two-step intercalibration is profitable. First, the choice of the method should be guided by the desired spatial and temporal scale of the inquiry. When sampling effort is low, quadrats are likely to be the first technique of choice given its accuracy. Although accurate, collecting biomass from quadrats is rarely conceivable. Indeed, given that scuba-diving can be a life-threatening activity, it is increasingly regulated by institutions who establish strict safety protocols and limit its use. Rake becomes an interesting alternative as it can limit scuba-diving as a one-time event for the determination of the quadrat-rake intercalibration. Additionally, the use of rake saves time since that, depending on the diver's experience, a single quadrat collection can take up to half an hour (Downing and Anderson 1985) compared to a few minutes for rake. Time and resources gained by using the rake in combination with the improved underwater accessibility can be dedicated to additional sample collection, thus improving sample size, understanding of SAV diversity, and spatial coverage.

If a larger spatial and temporal resolution is required, echosounding likely becomes the technique of choice. The major impediment to apply echosounding would be its high purchase cost and the necessity to post-process results. These can be reduced by considering using consumer-grade echosounder coupled to cloud-based automated data-processing tools (Helminen et al. 2019; Howell and Richardson 2019; Munday et al. 2013). Once echosounding is chosen, it also requires a ground truthing as it only provides a proxy of biomass. Quadrats could be used for this purpose (Duarte 1987), and given the safety issues and cumbersomeness of the techniques it should be considered only if very few samples are needed. Rake and our two-step intercalibration approach would likely be more appropriate as rake is more simple, safe and rapid to sample. Using rake as a

ground truth provides the opportunity to use echosounding to cover SAV meadows in large extents in a uniform manner, thus capturing more of the spatial heterogeneity and increasing accuracy at the ecosystem scale. In our whole-system estimation, the different sampling effort yielded incomparable biomass between techniques. Although the precision of biomass predictions from echosounding at an individual site is lower than that of rake, that loss is counteracted by the sheer number of echosounding measurements. Reaching similar sampling effort would be impossible with the rake technique. We estimated that it would take 60 days using a rake to simply collect a similar ecosystem-scale sample size as observed in Figure 7, without taking into account processing time. We also saw that there is no real gain in using spatial interpolation techniques to estimate biomass if there is a thorough coverage of the study area with echosounding. This is more effective as it requires less post-processing and computing power. Furthermore, using the rake in combination with echosounding provides information on SAV species that is not available using echosounding. Using the two techniques also allows to increase the available depth range as rake are suitable in very shallow areas and echosounding in deeper ones.

Our approach also allows for retrospective decisions with a change in priorities. For example, many existing monitoring programs rely on rake measurements (e.g. Yin and Kreiling 2011, Rodusky et al. 2005). If more rapid sampling or higher coverage is needed, our approach could facilitate the substitution of rake technique to echosounding. To do so we provide an intercalibration that allows for this comparison, but we also point out that the ecosystem-scale biomass estimation depends on the sampling effort, which is inherently higher with echosounding. Thus, to have reliable SAV biomass trends through time, only the sites that were continuously sampled should be compared. This mean that a subset of the echosounding data, that would likely cover a greater area than rake sites, should be used for this temporal analysis.

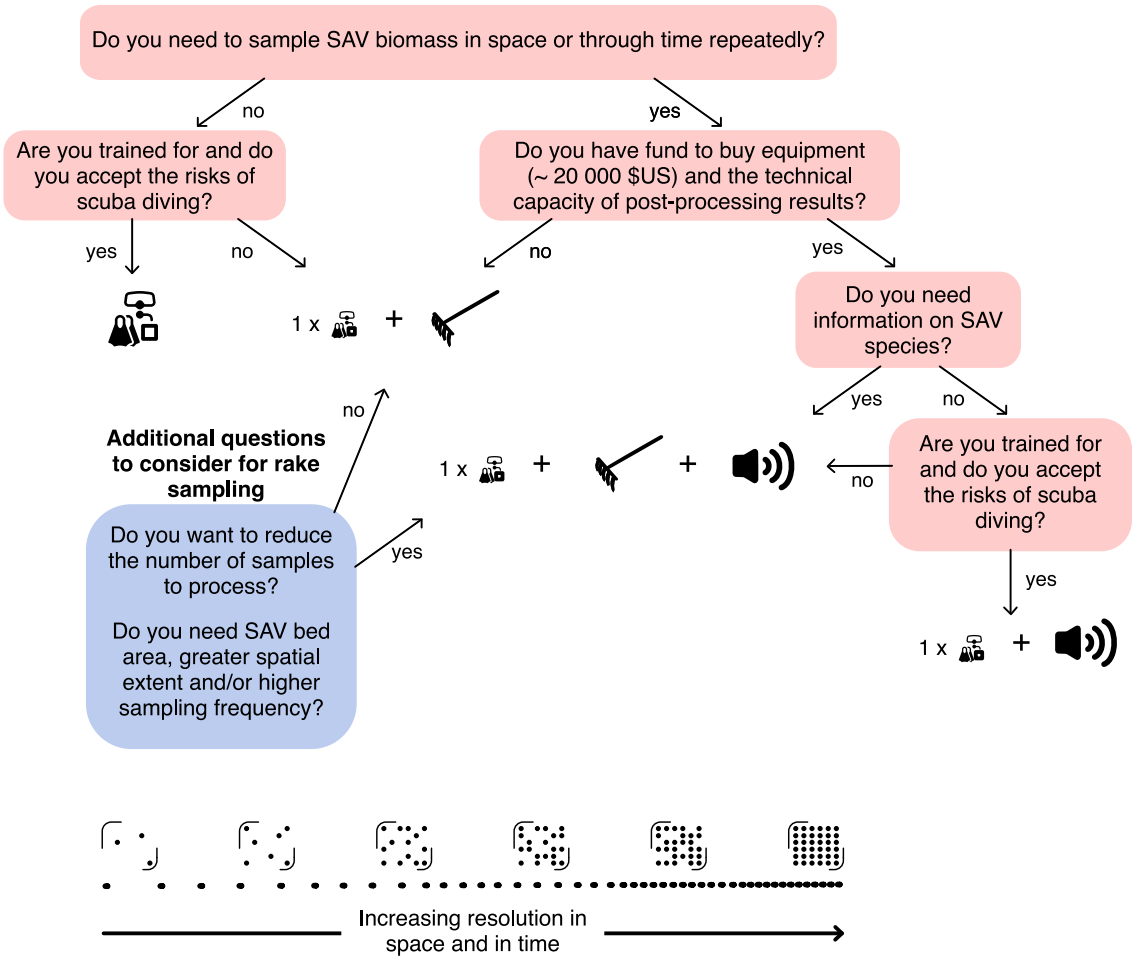

Figure 8. Step-by-step guideline to decide what biomass method to use and when combining them is desirable.

Comments and recommendations

The choice to use one or both intercalibrations will depend on the study goals, resources available and time granted. If one only intends to use rake, the quadrat and rake calibration can be conducted using the simplest sampling strategy, where only a one-time calibration is needed, with sites chosen to maximize a biomass gradient and ensure divers security. Increased accuracy can be achieved by deriving species- and substrate-specific equations. For the rake and echosounding combination, an even more efficient intercalibration can be achieved than the one presented here. For example, despite having a rake dataset of 217 sites, we only had 52 sites that spatially matched the echosounding tracks at 10 m radius resolution. Since the two sampling techniques were not used simultaneously, sampling with both techniques had to be conducted as close as possible to an

assigned geographic position. Over the 6-year sampling period, variations in staff and GPS accuracy resulted in reduced precision, yielding a lower number of matched pairs in later years, which affected predictions (Figure 5c). These shortcomings can be overcome by conducting the rake sampling and echosounding simultaneously. For example, buoys could be deployed as the echosounder is passing over the selected calibration sites for subsequent rake collection. Furthermore, when dense plant material is floating at the water surface, echosounding is inappropriate: the transducer is blinded which leads to drastically underestimated biomass. In contrast, the rake is not appropriate in deep waters (> 3 m) where other apparatus and collection strategies should be tested and compared to either quadrats or echosounding. Therefore, to maximize matched rake-echosounding sites and avoid sampling in inappropriate conditions, careful planning of sampling and training of field technicians are necessary.

Information needed regarding species composition, substrate type and time dedicated for biomass samples or echosounding post-processing should also be planned in advance. The rake has the advantage of providing species information, but each sample entails considerable sample processing time. Using a faster semi-quantitative approach such as applying a visual abundance scale based on the degree of each species filling the rake teeth can help increase sample size and provide community information at the ecosystem scale (Yin and Kreiling 2011), which can be used to more accurately predict biomass. When different SAV communities display distinctive heights, for example understory charophytes and taller angiosperms, applying height threshold to echosounding data can provide functional group information at large spatial scales (Bučas et al. 2016). Recent echosounders also provide information on substrate type that can increase accuracy when applying our two-step calibration approach (Helminen et al. 2019; Munday et al. 2013). New technological development in hydroacoustic autonomous boats (e.g. Goulon et al. 2021) are further promising to reduce sampling time and increase sampling frequency. Given the technological progress that were accomplished over the past decade, it is likely that future developments in GPS, echosounding and computing power will further facilitate and decrease costs related to large-scale estimations of SAV biomass over a wide range of environmental conditions.

Acknowledgements

We thank Stéphanie Massé, Caroline Chartier, Elena Neszvecsko, Geneviève Trottier, Magalie Noiseux-Laurin and François Messier from GRIL, Patricia Bolduc from UQTR and all other students that conducted field work and processed samples. The technical support of Jean-Pierre Amyot, Conrad Beauvais, Rollando Benjamin, Maude Lachapelle, Yasmina Remmal and Maxime Wauthy from Environment Canada is acknowledged with thanks. Bruce Gray and the Technical Operations diving team (Environment Canada, Canada Centre for Inland Waters, Burlington, ON) provided excellent field support for underwater sample collection. We also thank Richard Carignan and Andrea Bertolo for planning and troubleshooting during echosounding surveys. We thank Lars Iversen, Sabine Hilt, and two anonymous reviewers for insightful comments that improved the manuscript. Sampling was made possible thanks to the guides from pourvoirie Roger Gladu. This project was funded by the GRIL, a FRQNT Initiatives stratégiques pour l'innovation grant, FRQNT and NSERC scholarships to MB. This work was supported by Environment and Climate Change Canada (ECCC) as part of the Canada-Québec St. Lawrence Action Plan (SLAP) (CH).

Supporting information

Text S1

To assess the correspondence between rake biomass and the biomass proxy from echosounding, we first needed to spatially match rake site to the echosounding track and, second, determine the spatial resolution of the aggregated rake replicates to which we could compare the echosounding data. Our approach was to calculate the mean biovolume of the acoustic data falling in a circle at increasing radial distance from the rake site, ranging from 1 to 100 m (Figure 2d). Higher correlations between the biovolume_D calculated at a given distance (D) and rake biomass were interpreted as closer to the resolution of rake collection. To do so, we first imported ping reports and biomass site positions transformed in UTM 18N in QGIS (QGIS Development Team). We computed a 100 m-radius buffer around each biomass site and echosounding track data were intersected with the buffers. Using the intersected layer, all geographic distances between the individual ping reports and the nearest biomass sites (i.e. the target layer) were calculated using the distance matrix tool. In R and using the intersected table, we then calculated mean biovolume_D per radial distance, at 1m increments between 1 and 40 m and at 5 m increments between 40 and 100 m. This set-up also allowed us to evaluate the effect of acoustic data quality (error, proximity, and frequency) on biomass prediction. We calculated the biovolume standard deviation (sd) as an indicator of the acoustic error, the mean ping report distance to rake site as the acoustic proximity, and the number of ping reports per site as the acoustic frequency.

To determine the spatial resolution of rake biomass at which we could compare acoustic data, we inspected the relationships between rake biomass and mean biovolume at increasing radial distance from rake sites (Figure 4a). As expected, the correlation coefficients between biovolume and rake biomass were highest close to the rake site and decreased with distance. However, the difference in correlation with distance were subtle and the observed range narrow (r_{min} = 0.66, r_{max} = 0.74). Deviation from the general decreasing trend and slight increases in the strength of the correlation were observed starting at 7 m, with a maximum increase reached around 10 m. The correlation increased again around 25 m radius and decrease thereafter to reach a minimum correlation value. The overall decreasing correlations were computed using an increasing number of paired observations with distance, which also increased their significance level (Figure 4b). These results justified our selection of a 10-m radius for the spatial resolution of biovolume, corresponding to an intermediate correlation value (r_{10m} = 0.73) derived from a reasonably high number of paired

observations (n = 52). Furthermore, a resolution area coinciding with a 10-m radius is consistent with field observations and rake site area, taking into consideration boat size (7 m long), its movements around the anchor, rake collection at 2 m from boat sides and positioning error (up to ~ 3 m).

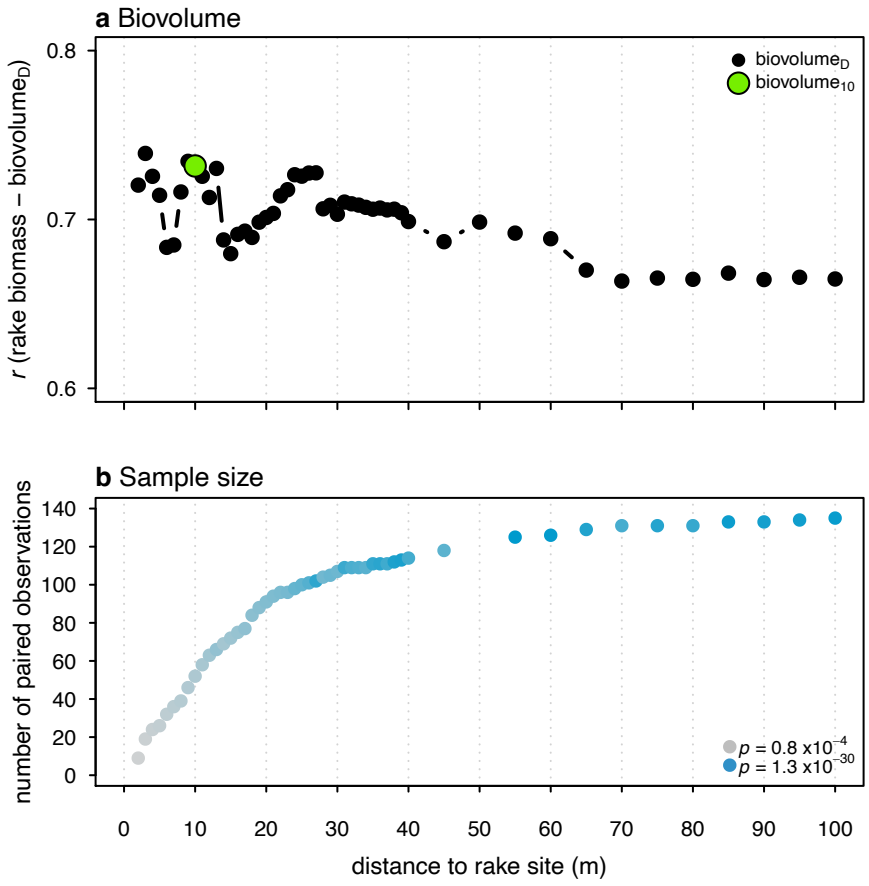

Figure S1. Effect of spatial resolution on the relationship strength between rake biomass and echosounding biomass proxy (biovolume). A) Pearson correlation (r) between rake biomass and mean biovolume aggregated at increasing radius distance from rake site (biovolume$_D$). The green dot indicates the correlation at the selected resolution of 10-m radius. B) Number of paired observations and significance level for the correlations.

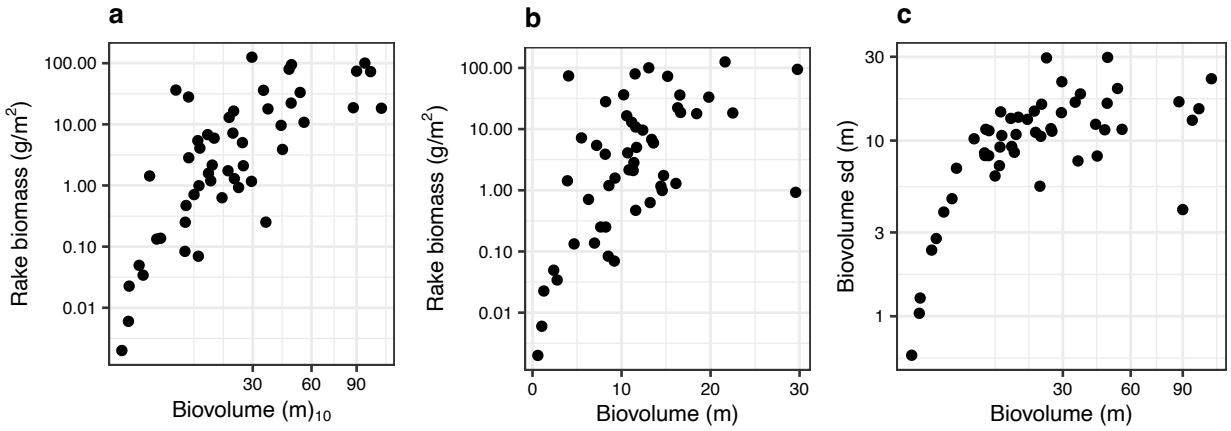

Figure S2. Scatterplot of the echosounding variables with high discriminant power in the PLSR model. a) Rake biomass as a function of biovolume. b) Rake biomass as a function of biovolume sd. c) Relationship between biovolume and biovolume sd.

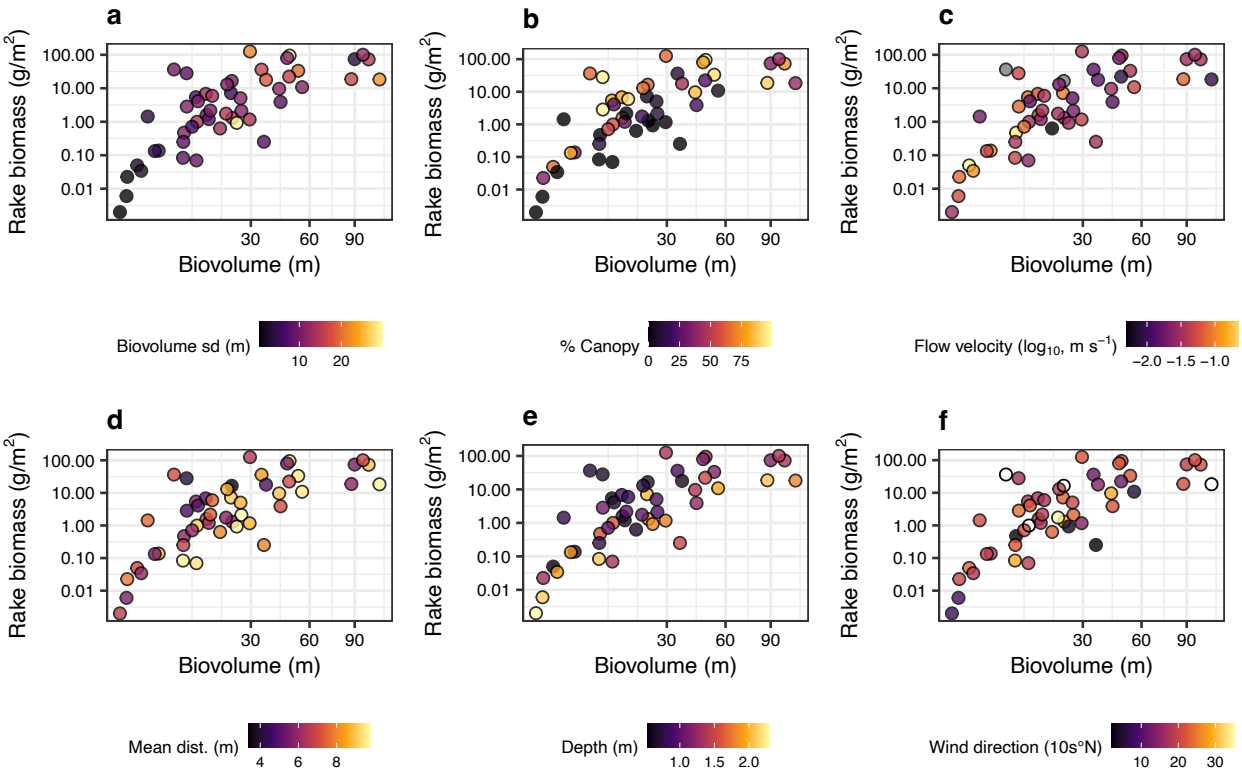

Figure S3. Scatterplot of the variables with higher discriminant power in the PLSR model. Biovolume (a) and biovolume sd (b) are predictors of rake biomass and are correlated to one another (c). Other variables (d - % canopy, e- depth, f- wind direction) modify the biovolume-rake biomass relationships. In f, Est is 9, South is 18, West is 27, North is 36 and 0, which indicate calm wind conditions, is not colored (n = 1).

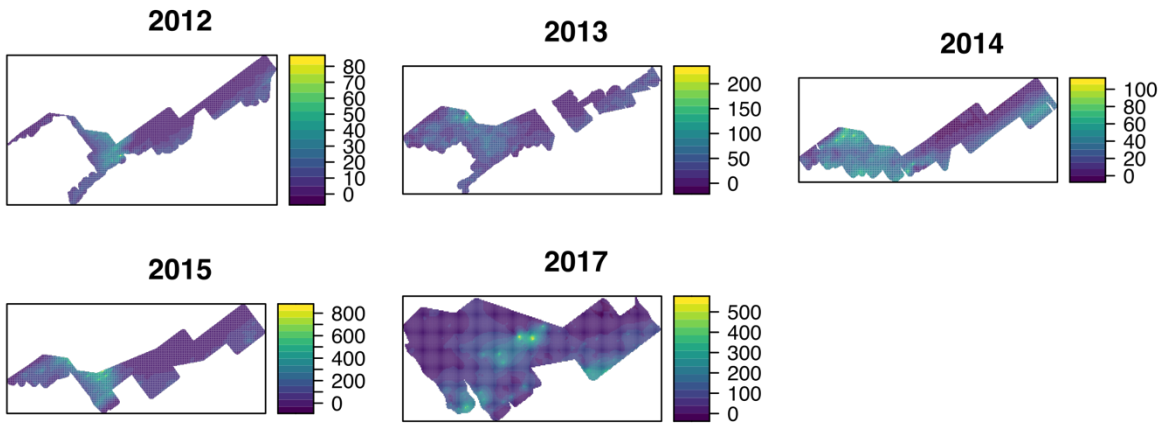

Figure S4. Kriging maps of biomass (g m^{-2}) for whole-system estimation. Kriging surfaces are derived from two-step predictions of echosounding biovolume.

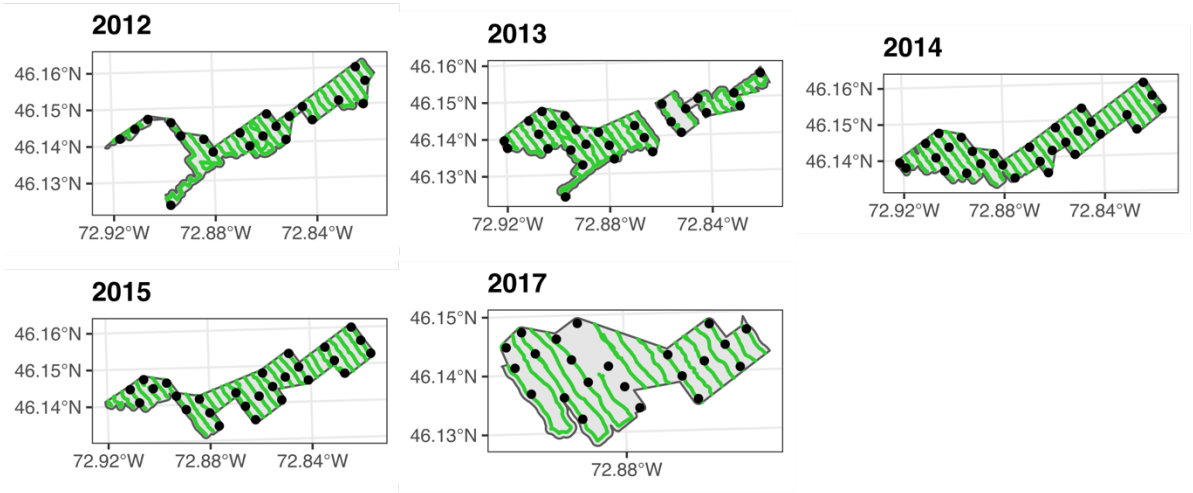

Figure S5. Location of rake samples (black dots) and of echosounding tracks (green lines) used for the whole-system SAV biomass estimations (2012-2017).

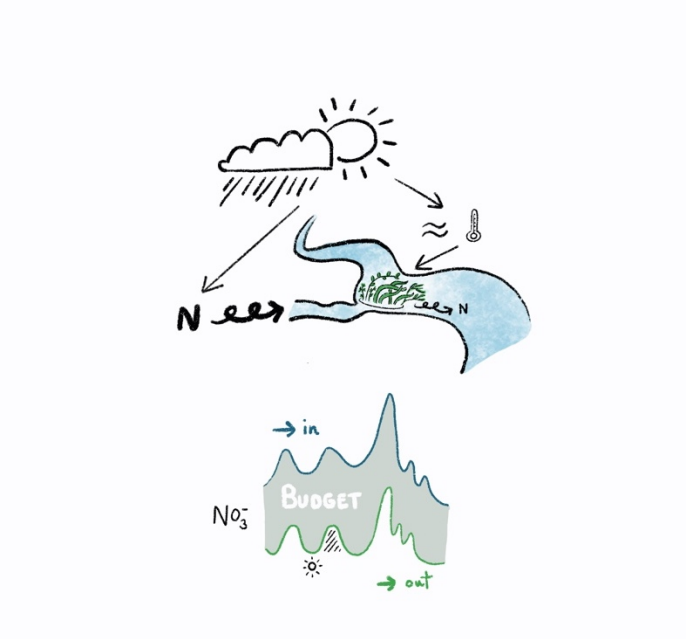

Chapitre 2 – Effet des variations climatiques sur la rétention de l'azote dans un herbier aquatique riverain

Climate-driven variations in nitrogen retention from a riverine submerged aquatic vegetation meadow

Morgan Botrel[1,2], Christiane Hudon[2,3], James B. Heffernan[4], Pascale M. Biron[2,5], Roxane Maranger[1,2]

[1] Université de Montréal, Département de sciences biologiques, Complexe des sciences, 1375 Avenue Thérèse-Lavoie-Roux, Montreal, QC Canada, H2V 0B3

[2]Groupe de recherche interuniversitaire en limnologie (GRIL)

[3]Environment and Climate Change Canada, Water Science and Technology, St. Lawrence Center, 105 McGill, Montreal, QC Canada, H2E 2Y7

[4]Nicholas School of the Environment, Duke University, Durham, NC, USA

[5]Concordia University, Department of Geography, Planning & Environment, 1455 De Maisonneuve Blvd. W., Montreal, QC Canada, H3G 1M8

Published in *Water Resources Research, volume 58,* https://doi.org/10.1029/2022WR032678

Preprint accessible through ESSOAr, https://doi.org/10.1002/essoar.10511089.1

Data openly available on Zenodo, https://doi.org/10.5281/zenodo.7052193

Minor edits to the published text and to the supporting information have been made here, following suggestions by the thesis committee.

Key Points:

- Nitrogen retention and biomass were measured at high resolution over six summers in a submerged aquatic vegetation meadow of a large river
- Among the highest riverine nitrate uptake rates were recorded and 47-87% of loads were retained with plants favoring denitrification
- Interannual climate variation influenced nitrate retention by altering water levels, temperature, plant biomass and tributary nitrate load

Abstract

Large rivers can retain a substantial amount of nitrogen (N), particularly in submerged aquatic vegetation (SAV) meadows that may act as disproportionate control points for N retention. However, the temporal variation of N retention in large rivers remains unknown since past measurements were snapshots in time. Using high frequency plant and NO_3^- measurements over the summers 2012-2017, we investigated how climate variation influenced N retention in a SAV meadow (~10 km^2) at the confluence zone of two agricultural tributaries entering the St. Lawrence River. Distinctive combinations of water temperature and level were recorded between years, ranging from extreme hot-low (2012) and cold-high (2017) summers (2 °C and 1.4 m interannual range). Using an indicator of SAV biomass, we found that these extreme hot-low and cold-high years had reduced biomass compared to hot summers with intermediate levels. In addition, change in main stem water levels were asynchronous with the tributary discharges that controlled NO_3^- inputs at the confluence. We estimated daily N uptake rates from a moored NO_3^- sensor, and partitioned these into assimilatory and dissimilatory pathways. Measured rates were variable but among the highest reported in rivers (median 576 mg N m^{-2} d^{-1}, range 60 – 3893 mg N m^{-2} d^{-1}) and SAV biomass promoted greater proportional retention and permanent N loss through denitrification. We estimated that the SAV meadow could retain up to 0.8 kt N per year and 87% of N inputs, but this valuable ecosystem service is contingent on how climate variations modulate both N loads and SAV biomass.

Plain Language Summary

Large rivers remove significant amounts of nitrogen pollution generated by humans in waste waters and from fertilizers applied to agricultural lands. Underwater meadows of aquatic plants remove nitrogen particularly well. To keep the river clean, plants use the nitrogen themselves, and promote conditions where bacteria can convert this pollution to a gas typically found in air. Measuring nitrogen removal in rivers is really difficult, and we don't know how climate conditions influences this removal or plant abundance. We successfully measured nitrogen pollution removal from an underwater plant meadow in a large river over six summers. We found that plant abundance and river nitrogen inputs were critical to determine how much pollution was removed, and that these were controlled by climatic conditions. Plant abundance was controlled by both water temperatures and levels. When water was warm and levels were neither too high nor too low, conditions were perfect for lots of plants to grow who mainly stimulated bacteria that permanently eliminated nitrogen. We showed that the amount of nitrogen pollution removed over the summer by the meadow changes with climatic conditions but in general represents the amount produced by a city of half a million people.

Introduction

Human activities on land has led to increased delivery of nitrogen (N) to aquatic ecosystems, resulting in the degradation of receiving waters (Carpenter et al., 1998; Galloway et al., 2003). During the transfer from land to sea, these impacts are modulated by river networks that retain a considerable amount of N, either through temporary biotic uptake from the water column or permanent removal by denitrification in anoxic sediments (Hall et al., 2009; Seitzinger et al., 2006). Within hydrographic networks, modelling efforts suggest that large rivers have a substantial influence on basin-wide N retention (Seitzinger et al., 2002; Wollheim et al., 2006; Ye et al., 2017). This influence is explained by their broader reaches that increase water residence time and contact rate with reactive surfaces, combined with higher N loads due to their downstream position. However, N retention in rivers is highly heterogeneous (Piña-Ochoa & Álvarez-Cobelas, 2006) and specific locations, like submerged aquatic vegetation (SAV) meadows, can display a disproportionate retention, thus acting as control points (sensu Bernhardt et al., 2017; e.g. Pinardi et al., 2009; Preiner et al., 2020).

This disproportionate role of SAV meadows can be explained by a suite of positive feedbacks enhancing plant growth and N uptake. For example, SAV reduce flow velocities and increase water transparency through sediment deposition (Hilt, 2015; Scheffer et al., 1993). The role of SAV in N dynamics might be amplified by their location within rivers. For example, high N retention has been observed in a meadow located in a confluence zone of one river (Hudon & Carignan, 2008), but near undetectable denitrification rates were reported at one located in the main channel of another river (Tall et al., 2011). This might be due to the specific geomorphologies, like deltas, at confluence zones that increase water residence time and favors N retention in comparison to the higher velocities in main channels. Greater N retention at confluence zones can also be explained by their typically high productivity caused by the increased nutrient supply from incoming tributaries (Benda et al., 2004; Rice et al., 2008). Nevertheless, information on the effect of SAV on N dynamics in rivers remain scarce, with only a handful of studies addressing the topic in rivers with discharges greater than 100 $m^3 s^{-1}$ (Diamond et al., 2021; Hudon & Carignan, 2008; Hudon et al., 2017; Tall et al., 2011) and a few in rivers with discharge of less than 20 $m^3 s^{-1}$ (Audet et al., 2021; Desmet et al., 2011; Heffernan & Cohen, 2010; Pinardi et al., 2009; Preiner et al., 2020). As a result, we have some understanding, albeit fragmented, of N dynamics in SAV meadows across rivers. Yet, past evidences are snapshots

over a day, a season, or a year at most, and do not capture the temporal variability in N retention imposed by climate.

Indeed, N retention fluctuates among years as a function of climate variations as shown by previous studies relating net human watershed N input to riverine exports (Ballard et al., 2019; Goyette et al., 2019; Howarth et al., 2012). In temperate regions, water flow (levels or discharge) and temperature tend to be negatively correlated because of higher evapotranspiration of land plants with increased temperatures (e.g. Hudon et al., 2010). As a result, colder than average growing seasons should exhibit higher runoff watershed losses, faster within-river flow, and consequently increased N export. In contrast, warmer growing seasons should result in lower discharge and higher N retention through enhanced plant and microbial activity, potentially compounded by lower precipitation and higher water residence times. However, the effect of climate and temperature variation on riverine SAV dynamics and overall N retention remains unknown. Rising temperatures can affect SAV quantities either by directly increasing growth rate (Brown et al., 2004; Farquhar et al., 1980) or by improving light availability through water level decline. During extreme drought, water levels can go below a deleterious threshold after which air exposure can lead to the dry-out of above ground plant material (Ersoy et al., 2020; Hudon et al., 2010). Growth rates could also increase to a temperature optimum where SAV thereafter could be outcompeted by periphyton or phytoplankton (Short et al., 2016), which may result in a decrease in N retention through reduced reactive surfaces and higher flow velocities. As SAV meadows in rivers represent a potential control point for N loss, characterizing how climate variations influence this critical ecosystem service is of high importance.

Accurate estimates of N loss in large rivers are particularly challenging because methods for measuring SAV quantities and N retention throughout or over multiple growing seasons are restricted and time consuming. Capturing changes in SAV density, or biomass, over a growing season requires the processing of many plant samples, or in typically turbid waters, conducting numerous remote sensing surveys using a sonar (Botrel et al., 2022). One potential solution to track temporal SAV biomass is to use the difference in slope in surface water level between gauging stations around large riverine meadows. Variations in water level slope tend to follow plant development because as SAV accrues biomass, flow is obstructed by the biomass in large meadows resulting in an increase surface water elevation upstream (Boudreau et al., 1994). This approach has been used successfully to estimate biomass in a large river (Giacomazzo et al., 2020; Vis et al., 2007).

As for N uptake measurements, few reliable methods exist in large rivers. The typical isotopic or nutrient release experiments used to measure N uptake rates in streams are impractical in large rivers because of the enormous quantities of injected N needed to detect and track a downstream signal in a large water mass (e.g. Mulholland et al., 2002; Newbold et al., 1981; Peterson et al., 2001). Consequently, past N uptake estimates in large rivers are very coarse as they were either derived from large scale mass balance (Alexander et al., 2000; Howarth et al., 1996) or from models that upscaled measurements taken in small streams (Hall et al., 2013; Wollheim et al., 2006; Ye et al., 2017). However, the development of in situ high frequency NO_3^- sensors provides a unique opportunity to directly measure variation in N uptake rates, particularly in rivers subjected to human derived N inputs where NO_3^- is typically the dominant N form (Caraco & Cole, 1999). Using these sensors, N uptake can be estimated daily by a passive mass balance between two stations along a river reach. Furthermore, when autochthonous primary production is high, NO_3^- concentrations tend to display a diel variation driven by daily change in sunlight and gross primary productivity (GPP) that can be used to estimate autotrophic NO_3^- uptake (Hall et al., 2009; Heffernan & Cohen, 2010). As a result, high frequency NO_3^- signals allow for the partitioning of total N uptake rates into assimilatory and dissimilatory pathways, providing additional information on N fate.

Given the lack of knowledge on temporal N retention dynamics in riverine SAV bed, our objective is to characterize how interannual climate variation affects N retention in a large riverine SAV meadow located at a confluence zone. We hypothesized that retention would be a function of NO_3^- loads and of vegetation biomass, both of which are related to climate-driven variations. To do so, we estimated SAV biomass and environmental conditions over six summers in a natural widening of the St. Lawrence River (SLR), a large temperate river with seasonal ice cover. Using a passive mass balance approach with an in situ sensor, we contrasted interannual variations of N retention within the flow path of the SAV meadow and partitioned retention into autotrophic assimilation and denitrification. N retention was then upscaled to the entire SAV bed using a simple regression model.

Materials and Methods

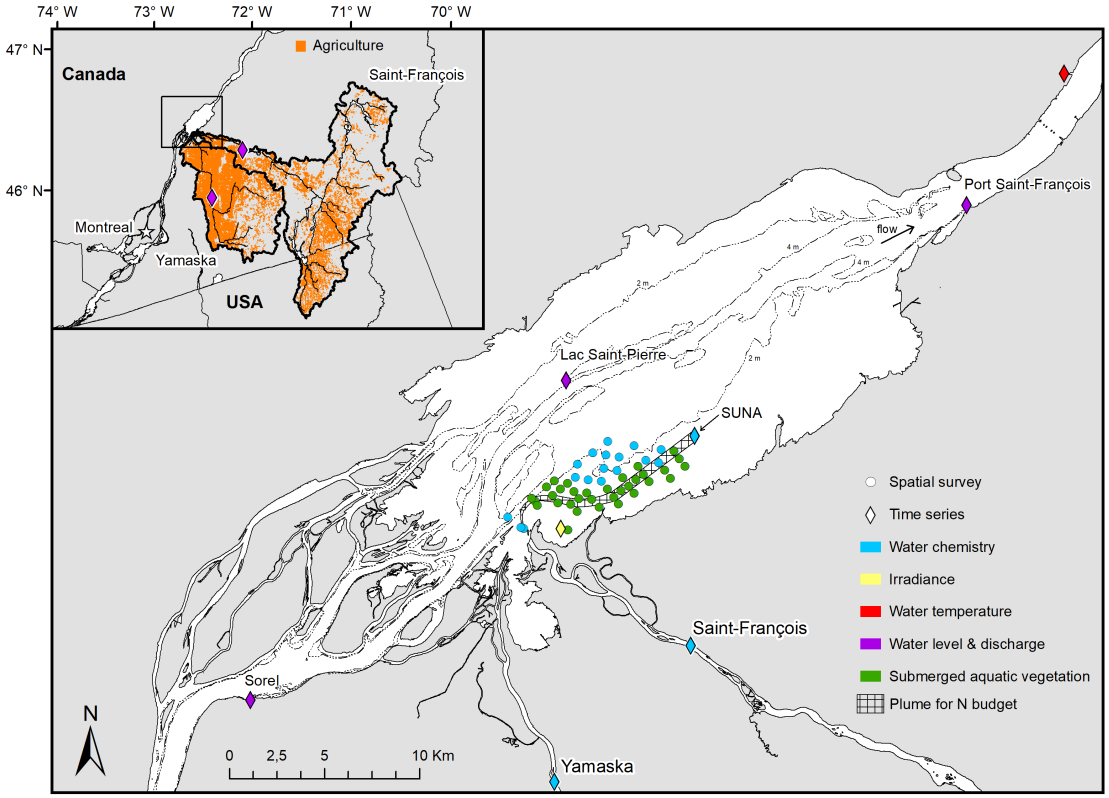

Figure 1. Map of the study area and site locations in Lake Saint-Pierre. The limits of Yamaska and Saint-François river watersheds (thick outline) and farmlands (orange) are delineated and the frame indicates the location of the enlarged area (inset). The dotted lines in the lake are the 2 m and 4 m isobaths. Notice that tributaries gauging stations are only shown in inset.

Study site

We studied N retention in a large (~10 km²) SAV meadow receiving waters at the confluence of two agriculturally impacted rivers (Goyette et al., 2016), the Saint-François (10.18 x 10^3 km², 2012-2017 median summer discharge = 74 m^3s^{-1}) and the Yamaska (4.45 x 10^3 km², 20 m^3s^{-1}). At the same location, these two tributaries join the fluvial Lake Saint-Pierre (LSP), a ~ 400 km² shallow widening (mean depth of 3 m) of the St. Lawrence River (SLR, 8th order, 9640 m^3/s), Québec (Canada, Figure 1). Annual loads of total N from the Yamaska (7.03 x 10^3 tons yr^{-1}) far exceeded those of the Saint-François River (4.45 x 10^3 tons yr^{-1}), in spite of its much smaller watershed (Hudon et al., 2017). The impact of intensive farming on the Yamaska drainage basin was also shown by its high conductivity

and high flashiness after local rain events. Conductivity in the tributaries and main stem is distinct (median, $med_{Yamaska}$ = 370 µS cm^{-1}, $med_{Saint\text{-}François}$ = 206 µS cm^{-1}, med_{SLR} = 270 µS cm^{-1}), allowing for its use as a conservative tracer of water mass.

Located at the mouth of their confluence with the SLR, the SAV meadow under study was well positioned to intercept and filter the nutrient-rich waters from both tributaries, as was previously suggested by a nutrient mass balance study in LSP (Hudon & Carignan, 2008). Lake Saint-Pierre supports about half of the remaining SLR wetlands (Hudon et al., 2018; Jean et al., 2002), and has been designated as both a Ramsar site and a UNESCO biosphere reserve. Although its natural capital has been recognized, LSP hydrodynamics have been highly modified by human activities. Discharge from the Great Lakes to the SLR is regulated at the Moses-Saunders dam (Cornwall, ON, Massena, NY), which has resulted in an overall reduction in water level extremes in LSP of 0.7 m on average between 1912 and 1994 (Hudon, 1997; Hudon et al., 2006). The effects of flow regulation have been compounded by the dredging of a 11.3 m-deep navigation channel that focuses water flow from the Great Lakes to the central part of the lake (0.5-1 m s^{-1}, representing 55-88 % of total discharge (Hudon & Carignan, 2008; Morin & Côté, 2003; Figure 1). As a result, flow is markedly slower (< 0.5 m s^{-1}) in the lateral shallow zones particularly during summer, when mixing of incoming tributaries with this central water mass is limited (Vis et al., 2007). Reduction in flow velocity in the lateral zones is also explained by the presence of extensive SAV present up to a maximum depth of 3 m (Hudon, 1997).

While the bulk of SLR flow is controlled anthropogenically, water levels nevertheless follow interannual fluctuations as a function of climate variation. Flow regulation has a stabilizing effect on waters originating from the Great Lakes (772 x 10^3 km^2), which account for approximately 70 % of the SLR waters entering LSP (Hudon et al., 2017). The climate effect is thus primarily the result of tributary inputs, the largest of which is the Ottawa River (146.3 x 10^3 km^2), a North shore tributary accounting for ~20% of water inputs in LSP. The much larger sizes and areas covered by the SLR watershed compared to its individual tributaries further induce a potentially complex influence of climate at confluence zones. The SLR main stem climate variation is an aggregate of the basin-wide Great Lakes and overall tributaries water inputs, while individual tributaries discharges and NO_3^- concentrations are independent of these large-scale variations and represent localized precipitation patterns.

Spatial survey of SAV biomass and water chemistry

Field surveys were carried out during maximum SAV biomass accumulation, around early August from 2012 to 2017, and once during the early growing season in June 2012. We measured SAV biomass at approximately 35 sites. Water temperature and conductivity were measured using a YSI 556 MPS or a YSI 600XL at each site as well as at ~17 additional sites within and around the meadow (Figure **1**). SAV was collected every summer using the rake technique, with additional diver-collected quadrats in 2016. For the rake technique, a 0.35 m-wide double-headed rake was lowered in the water and dragged toward the boat over a length of approximately 1 m. In 2016, divers harvested all plant material within a 0.30 m by 0.30 m PVC frame placed on the lake bottom. At each site, 3 to 5 replicates were collected, and plant material was rinsed on-boat, stored in plastic bags, and frozen once on shore. Upon return to the laboratory, plant samples were thawed, wrung out manually, sorted by species, separated from filamentous algae, dried to a constant mass at 60°C, and weighed (0.001g). The sum of species dry biomass in g m^{-2} was calculated per sample and averaged at each site (3-5 replicated) SAV species composition was dominated by *Vallisneria americana* and *Potamogeton richardsonii*, but also included *Heteranthera dubia*, *Stuckenia pectinata*, *Elodea* spp, *Myriophyllum* spp. and *Chara* spp. Because rake biomass collections are underestimated due to loss of plant material during sampling, rake estimates were converted to quadrat equivalency using a previously determined general relationship (Chapitre 1).

Time series data

Temporal SAV biomass estimates

Daily SAV biomass was estimated between June and November using the slope in surface water level between gauging stations (Figure 1). Slopes were calculated as water surface elevation upstream minus downstream divided by distance between successive stations (23 km, Supporting information, SI, Text S1). As variations in water level slope are also affected by signals other than SAV growth, such as tides and winds (Vis, 2004), we extracted the SAV signal with the Hilbert-Huang transform method using the hht and EMD packages in R (Bowman & Lees, 2013; Huang et al., 1998; Kim & Oh, 2018; Wu & Huang, 2009). We chose this signal extraction method because it is adaptative and intrinsic, and is entirely based on data without imposing an a priori hypothesis on the shape of the SAV growth curve (Wu et al., 2007). We analyzed water level slopes only during the growing season (June 21 to September 22), therefore SAV signal corresponded to the EMD

residuals or the seasonal trend (SI Figure S1). To reduced signals mixing at different time scales (i.e. mode mixing), we used a noise-assisted version of EMD, ensemble empirical mode decomposition (EEMD; Bekka & Berrouche, 2013). Confidence levels were estimated to assess between year differences using the bootstrapping approach of Ezer & Corlett (2012; SI Text S1).

To reconstruct SAV growth using changes the seasonal trend in water level slopes as an indicator of daily biomass, we assessed the optimal gauging station representative of SAV biomass. For this validation, we used the Pearson correlation between the slope signal to the overall biomass measured during spatial surveys (SI Text S1 and Figure S2). The slope calculated between the downstream gauging stations (Port St-François) to the middle LSP station yielded a higher correlation (r = 0.98) than the slope between upstream Sorel station and the same middle station (r = 0.33). Using this former slope value and to provide estimates using a common metric, we calculated maximum summer SAV biomass using a simple linear regression between rake estimated biomass and slopes (r^2 = 0.97, p < 0.0001). For visualization of SAV growth patterns and statistical analysis, we directly used the slope EEMD residuals between the Port St-François and LSP station as an indicator of temporal SAV biomass changes.

Nutrient inputs

To estimate daily NO_3^-, total phosphorus (TP) and turbidity in the tributaries, we used the composite approach from the R package loadflex that includes regression modelling using discharge as a predictor of discrete water chemistry and a residual correction using additional water chemistry measurements (Appling et al., 2015). The best regression models were selected using Akaike information criterion (AIC) from among 9 models fitted for data between 2009 and 2018 in the rloadest package (Johnson & Omland, 2004; Runkel & De Cicco, 2017). Weekly water chemistry data from both provincial and national agencies collected in the Saint-François and Yamaska rivers (Table S1) were used to derive models. To avoid autocorrelation when fitting models, a subset of data at time intervals greater than 7 days was used; the complete dataset was used for the residual correction. Daily discharge data was acquired at upstream stations in Drummondville for Saint-François and Saint-Hyacinthe for Yamaska (Table S1). Missing data (3 days) from Saint-François were filled using data available from a station 1 km upstream, Hemming Falls (r = 0.93), while missing data from the Yamaska dataset (22 days) were filled using the linear regression between daily discharge at Saint-Hyacinthe and the sum of discharges at the two main upstream sub-watershed stations (Farnham and Noire, R^2 = 0.96).

Water chemistry monitoring stations were located near the mouth of the tributaries, but discharge stations were located 47 km and 63.5 km upstream for Saint-François and Yamaska respectively. Discharge was corrected for additional water inflow using the pro-rate technique and was multiplied by the proportional increase in drainage area at the respective water chemistry stations (1.05 and 1.34 for Saint-François and Yamaska; Morse, 1990). We also corrected daily discharge according to transit time estimated with Saint-Venant equations which included information on channel geometry and friction coefficients (P. Fortin ECCC pers. comm.). During summer (from June 21 to September 22), transit time was longer than 24h for 4% and 65% of dates for Saint-François and Yamaska respectively. Longer transit times in Yamaska were probably due to its smaller watershed size and the higher distance between the gauging station to the river mouth. To describe total tributary inputs during the SAV growing season, discharges are reported as the sum of both tributaries. Summertime concentrations received by the SAV bed were weighted by the proportion of individual tributary (*i*) discharge to the total discharge ($[NO_3^-]$ (mg L^{-1}) = $\sum_i^2([NO_3^-]_i \times {Q_i}/{Q_{total}})$).

Downstream NO_3^-, temperature and light estimates

To estimate NO_3^- concentrations downstream of the SAV meadow, a SUNA V1 sensor (Satlantic) using in situ ultraviolet absorption spectroscopy (200-400 nm spectra) was moored from the end of June to end of September in 2012 to 2016 (Figure 1). The sensor, equipped with a battery pack, flow cell, and a Sea-Bird electronic pump, was mounted on an aluminum stepladder which kept the sensor at 75 cm above the sediment. Before and after moorings, calibration was verified using distilled water and known NO_3^- concentrations. To limit the interference of large particles on the ultraviolet lamp, a pre-filter with a mesh size of 5 mm was installed at the water intake. Each hour, water was pumped, and four measures were recorded. Only measurements within manufacturer-specified accuracy (+- 0.028 mg N L^{-1}) were deemed acceptable and median values were kept for further analysis. A sensor to measure hourly dissolved oxygen concentrations (D-Opto) was also deployed in 2016, with intermittent measurements over other years.

Continuous local water temperature was taken from the SUNA sensor, and validated with D-Opto measurements in 2016 (r = 0.99). Additional water temperature time series were acquired at Trois-Rivières station (Table S1) and correlated with daily water temperature measured by the SUNA and mean water temperatures measured during spatial surveys (r = 0.72 and r = 0.75,

respectively). Hourly short-wave radiation was acquired from NASA datarod at a location close to the SAV bed (46.1247 N, 72.9018 W; Teng et al., 2016), apps.hydroshare.org/apps/data-rods-explorer). Short-wave radiation flux (300-2000 nm in Wm^{-2}) was converted to photosynthetically active radiation (PAR, 400-700 nm) in photon flux density units (mol m^{-2} h^{-1}) using a conversion ratio of 2.114 (Britton & Dodd, 1976). To describe SAV growing season, we calculated the accumulated degree days using a reference temperature of 7°C, which corresponds to the known sprouting temperature of *Vallisneria americana* (Paresh Lacoul & Bill Freedman, 2006), a common species at our study site. Similarly, cumulative PAR was calculated as the sum of daytime hourly irradiance.

NO_3^- budget and fate

We calculated a nitrate (NO_3^-) budget for a plume spanning from the mouths of the tributaries (input) to the downstream edge of the SAV meadow where the SUNA was located (output, Figure 1). NO_3^- was the dominant N form in these tributaries (60 % on average) and is a significant agricultural pollutant. A complete summary of equations used to derive budgets is presented in Table 1. The shape of the plume was drawn from trajectories of drifters deployed in 2005, 2006 and 2012 (SI Figure S3). A plume width of 500 m was used for calculations, corresponding to the distance between stations of the spatial survey and was chosen based on conductivity measurements as a conservative tracer of water masses. When choosing the location for the outflow station in 2012, the objective was to measure NO_3^- from the Saint-François water mass flowing through the SAV bed. Since 2012 was an extremely low water level year, the sensor was placed at the offshore limit of this water mass to ensure water was deep enough to allow measurements throughout the summer. However, the study area is a complex zone at a confluence of the Saint-François and Yamaska rivers. Based on delineation using optical properties from satellite observations (pers. comm. P. Massicotte) and conductivity, we observed that in subsequent higher water level years, the same outflow location was most likely exposed to a mixture of waters from both rivers. Daily upstream NO_3^- concentrations were thus estimated from the NO_3^- loadflex predictions multiplied by the contribution of Saint-François and Yamaska to the water flowing at the downstream site (Table 1, equation 1). To estimate contributions, we used a two-end member mixing model with conductivity as the conservative tracer and applied an analytical solution (Table 1, equation 2). Contributions were estimated once per summer using matching monthly

conductivity at the nearest sampling station to the SUNA and conductivity measurements in the tributaries from this study and the provincial monitoring station (Table S1).

Daily discharge at the outflow site was computed as the area of the plume cross-sectional transect multiplied by flow velocity (Table 1, equation 3). The cross-sectional area was estimated from the sum of cell depths measured for the outflow transect on a bathymetric raster map (Hudon & Carignan, 2008), corrected for daily water level height, and multiplied by the bathymetric cell width. Daily velocity was estimated from Delft3D simulations, a tridimensional hydrodynamic model established for our study area (Bulat et al., 2019). Model simulations were run for each year using median, minimum, and maximum input discharges at Saint-François over the SUNA mooring period, and yearly spatial polygons of SAV height established from SAV echosounding surveys (this thesis, chapitre 1). Mean depth-average velocity was computed on the resulting spatial polygon grid of 70 m resolution at the outflow transect (7 polygons). Mean residence time was also estimated from depth-averaged velocity assuming a travelling distance of 11.61 km, but the mean was computed over the complete plume surface area. To estimate both daily velocity and daily residence time, interpolations were computed using yearly linear regressions between daily Saint-François discharge and the mean depth average velocities or the mean residence time (i.e. Delft3D inputs and outputs).

Daily total areal uptake (U_t) was considered to be the sum of daily autotrophic assimilation (U_a), denitrification (U_d), and heterotrophic assimilation (U_h, Table 1, equation 4). U_t was calculated as the difference in daily median outflow NO_3^- concentration between upstream input and output (downstream) while taking residence time into account, multiplied by the ratio of outflow discharge divided by the plume area (Table 1, equation 5). Daily proportional uptake (R) was calculated as the median NO_3^- concentration at the outflow minus upstream inputs, divided by those inputs (Table 1, equation 6). U_a was calculated from diel NO_3^- variation using equation 7, Table 1, and U_d as the difference between U_t and U_a. Since hourly NO_3^- data at the downstream station was a composite of multiple frequency signals, we extracted diel variations using Hilbert-Huang transform, similar to the SAV time series (SI, Text S1) and to the protocol of Chamberlin et al. (2021). This method is best suited for nonstationary data, a common feature of hydrological time series (Lloyd et al., 2014). Days for which more than five consecutive hourly measurements were missing were excluded from the time series (5 days in 2012 and 2013, 1 day in 2014), otherwise missing values were linearly interpolated. The diel signal was consistently detected and corresponded for the five NO_3- time

series (2012-2016) to the intrinsic mode function (IMF) 4 with mean instantaneous periods between 21 and 23 hours. This signal was distinct from the tide effect of IMF 3 with a shorter period. NO_3^- spike sometimes introduced oscillations on the diel IMFs and biased the dial signal (Stallone et al., 2020), those sections were thus removed from the analysis.

The approach we used to partition uptake rates assumes that autotrophic assimilation is temporally coupled to primary production and is the only diurnally varying NO_3^- removal pathway. The diurnal variation is also solely ascribed to the SAV meadow without interference from the NO_3^- input signal (the tributaries). These assumptions may not always be met as assimilation can occur at different times of day (Appling & Heffernan, 2014), other processes can vary and explain diurnal variation, such as nitrate consumption from denitrification (Laursen & Seitzinger, 2004), and input signals could vary diurnally. To validate the assumptions, we compared U_a estimated from NO_3^- time series to autotrophic assimilation estimates based on gross primary production (GPP) calculated from the 2016 oxygen time series assuming a photosynthetic coefficient of 1, an autotrophic respiratory coefficient of 0.5, and using a mean C : N ratio measured for both SAV and macroalgae in LSP (molar ratio of 13 : 1, equation 8, SI Text S1). Validation of the estimates showed that U_a and $U_{a\text{-}GPP}$ were comparable. The timing of NO_3^- maxima and minima was more variable than for O_2 and resulted in dispersion around the $U_{a\text{-}GPP}$ to U_a 1:1 line, with most values being similar (SI Figure S4). This suggest that either NO_3^- was more subject to hydraulic dispersion than O_2 (Hensley & Cohen, 2016), or that assimilation occurred continuously. Nonetheless, overall mean U_a and $U_{a\text{-}GPP}$ were similar, suggesting that autotrophic assimilation was the dominant process controlling NO_3^- diurnal variation (SI Figure S4). To limit the effect of hydraulic dispersion, we filtered the resulting U_a to obtain time intervals between daily maximums of 20 to 28 hours.

Similarly to GPP, we estimated ecosystem respiration (ER) from the oxygen time series (SI Text S1), allowing for the calculation of U_h in 2016, assuming a heterotrophic growth efficiency of 0.2 and molar C : N ratio of 20 : 1 (Table 1, equation 9, Hall & Tank, 2003; Heffernan & Cohen, 2010). As U_h represented less than 0.05% of U_t, this term was negligible and was not considered in denitrification estimates. Finally, to isolate the effect of biotic activity on retention (Wollheim et al., 2006; Stream Solute Workshop, 1990), we calculated the uptake velocity (V_f), or the mass transfer coefficient from water to the benthos (Table 1, equation 10). We calculated both total ($V_{f\text{-}t}$) and process-specific velocity (for autotrophic assimilation $V_{f\text{-}a}$ and denitrification $V_{f\text{-}d}$).

Statistical analysis

We used linear discriminant analysis (LDA) to assess the occurrence of among-year differences in environmental variables and N budget during summertime, and to identify which variables generated those differences. Given the smaller number of observations for process-specific rates (*n* total uptake = 292, *n* process-specific = 99), interannual differences were assessed using nonparametric Kruskall-Wallis tests. A principal component analysis (PCA) was used to describe correlations between NO_3^- budget terms and environmental variables. We then determined predictors of U_t using a regression approach. As our data were nested per year and displayed temporal autocorrelation, we conducted regressions as linear mixed models with a gaussian error structure. To find optimal model structures, we applied the protocol of Zuur et al. (2009). We first removed collinear variables and kept the variables that were most correlated to our response variable, U_t. We then selected random effects using a fixed structure of all possible covariates with restricted maximum likelihood estimation (REML). The best model was selected to minimize the sample-corrected Akaike Information Criterion (AICc). Using this optimal random structure, fixed effects were similarly selected using AICc but with maximum likelihood estimation (ML). The final model was fitted using REML and validated for normality and homogeneity by visual inspections of standardized residuals against fitted values and explanatory variables. Using the fixed component of the mixed model, daily retention was predicted from the weighted discharge estimates of NO_3^- concentrations inputs as the explanatory variable. Total summertime retention was estimated by multiplying these predictions with the SAV meadow area (10 km^2) and summing these daily values. Similarly, we estimated total NO_3^- inputs by summing daily loads from the two tributaries. All statistical analyses were conducted in R (R Core Team, 2020) using the MASS package for LDA, vegan for PCA and nlme for linear models (Oksanen et al., 2020; Pinheiro et al., 2020; Venables & Ripley, 2002). Prior to analysis, data were transformed when necessary to satisfy normality and homoscedasticity assumptions.

Table 1. List of equations used for nitrate budget calculations. No. equation number. In the 'Abbreviated description' column, abbreviations that are used in subsequent equations are only described once in sequential order.

No	Equations	Abbreviated description
1	$[\mathbf{NO_3^-}]_{\mathbf{in}}\ (\mathrm{mg\ L^{-1}}) = [NO_3^-]_{StF} \times f_{StF} + [NO_3^-]_{Yam} \times f_{Yam}$	**Nitrate input ($[NO3\text{-}]_{in}$)**: StF Saint-François River, Yam, Yamaska River, f fraction where $f_{Stf} + f_{Yam} = 1$
2[a]	$\mathbf{f_{StF}} = {(C_{out} - C_{Yam})}/{(C_{StF} - C_{Yam})}$	**Fraction of Saint-François River water mass (f_{Stf})**: out outflow, C conductivity
3	$\mathbf{Q_{out}}\ (\mathrm{m^3 s^{-1}}) = (\sum_{i=1}^{n} h_{out,i} \times w_i) \times u_{out}$	**Discharge at outflow (Q_{out})**: h depth, i ith bathymetric raster cell, w width, u depth average velocity
4	$\mathbf{U_t}\ (\mathrm{mgN\ m^{-2} d^{-1}}) = U_a + U_d + U_h$	**Total nitrate uptake rate (U_t)**: U_a autotrophic assimilation, U_d denitrification, U_h heterotrophic assimilation
5	$\mathbf{U_t}\ (\mathrm{mgN\ m^{-2} d^{-1}}) = \frac{Q_{out,d}}{A}([NO_3^-]_{in-\tau} - [NO_3^-]_{out,med})$	**Total nitrate uptake rate (U_t)**: A area of the plume, τ residence time in days, med median
6	$\mathbf{R}\ (\mathrm{unitless}) = 1 - \frac{[NO_3^-]_{out,med}}{[NO_3^-]_{in-\tau}}$	**Proportional retention (R)**
7[b]	$\mathbf{U_a}\ (\mathrm{mgN\ m^{-2} d^{-1}}) = \frac{Q_{out,d}}{A} \sum_{t=hmax0}^{hmax1} ([NO_3^-]_{max\ (hmax0)} - [NO_3^-]_h)$	**Autotrophic assimilation (Ua)**: t time of day, hmax0 hour of first daily NO_3^- maximum, hmax1 hour of last daily NO_3^- maximum, h hour
8[b,c]	$\mathbf{U_{a-GPP}}\ (\mathrm{mgN\ m^{-2} d^{-1}}) = {(GPP \times h \times p \times r_a)}/{C:N}$	**Autrotrophic assimilation from GPP ($U_{a\text{-}GPP}$)**: GPP gross primary productivity, p photosynthetic coefficient, r_a autotrophic respiratory coefficient, C : N carbon to nitrogen ratio
9[b,c]	$\mathbf{U_h}\ (\mathrm{mgN\ m^{-2} d^{-1}}) = {((ER - (r_a \times GPP)) \times HGE)}/{C:N}$	**Hetetrophic assimilation (U_h)**: ER ecosystem respiration, HGE heterotrophic growth efficiency
10[d]	$\mathbf{V_f}\ (\mathrm{m\ d^{-1}}) = {U}/{[NO_3^-]_{out,med}}$	**Uptake velocity (V_f)**: U uptake rate

Equations are derived from [a] Phillips & Gregg (2001), [b] Heffernan & Cohen (2010), [c] Hall & Tank (2003), and [d] Ensign and Doyle (2006).

Results

Interannual variation in environmental variables and temporal SAV biomass

There were strong and significant interannual variations in environmental conditions during the SAV growing seasons (MANOVA, $p < 0.0001$) caused by several variables that varied differently across summers. Variables that contributed to among-year differences were mainly water level, water temperature, tributary discharge, and NO_3^- input concentrations (LDA, SI Table S2). These conditions created a sharp gradient among summers, ranging from hot temperatures with low water levels to cold summers with high water levels. Mean summer water levels and temperatures spanned 1.4 m and 2°C, respectively coinciding with historical extremes in 2012 and 2017 (Figure 2). Exceptionally low water levels and high temperatures were observed in 2012, whereas 2017 coincided with major flooding from the Ottawa River during the spring freshet and sustained high discharge throughout the season. The other four years, either tended to be hot with low water levels (2016) or had intermediate water levels (0.69 to 0.77 m CD) but varying mean water temperatures (2013, 2014, 2015). In these latter years, 2014 was colder, both in mean temperature (21°C) and accumulated degree day (Figure 2b). For the remaining two years (2013, 2015), the mean temperatures were similar. However, the greater variability in daily temperatures with sporadic colder days in 2013 (min_{2013} = 17°C, min_{2015} = 18.8°C, SI Figure S5) resulted in a lower accumulated degree day that year compared to 2015.

Hotter years (2012, 2015, 2016), with both higher accumulated degree days and mean water temperature, tended to receive more PAR than colder years, but this was not always the case. For example, the second hottest summer (2016) had similar irradiance levels to the two coldest ones (2014, 2017). Whereas mean water temperature and water levels followed a pattern of negative correlation in the SLR, there was no correlation between SLR temperatures and tributary variables (Figure 2e-g). This suggests that tributary loadings were influenced asynchronously from flow patterns in the mainstem. Tributary discharge and weighted NO_3^- had similar patterns albeit NO_3^- concentrations were markedly lower in 2012 as compared to other years (med_{2012} = 0.26 mg N L^{-1}, med_{other} = 0.46-0.72 mg N L^{-1}). This was a function of more variable NO_3^- and considerably higher concentrations in the Yamaska as compared to the Saint-François since its proportion to total discharge stayed relatively stable throughout the different summers (med_{all} = 0.20, med_{year} 0.27 to 0.13, SI Figure S6). NO_3^- concentrations from Yamaska were particularly high during the intermediate temperature years (med_{2015} = 1.75 mg L^{-1}, med_{2013} = 1.77 mg L^{-1}, med_{other} = 0.08 to 0.82

mg L^{-1}), up to 5.5 mg L^{-1}. In contrast, TP and turbidity did not show any obvious differences among years, but TP was lower in 2015 (med_{2015} = 30.2 µg P L^{-1}, med_{other} = 33.6 to 44.0 µg P L^{-1}, Figure 2g) and turbidity higher in 2012 (med_{2012} = 17 NTU, med_{other} = 10 to 15 NTU, SI Figure S5) as compared to other years.

From our comparison with field biomass estimates, we deemed the downstream LSP water level slope a good indicator of SAV biomass. Looking at the estimated temporal SAV biomass changes throughout the six summers, two patterns of seasonal progression were revealed (Figure 3). The first pattern reflected a reduced SAV biomass reaching its peak earlier during the season (late July to late August). This pattern was observed over both the colder years with high water levels (2013, 2014, 2017) and the hottest year with very low water levels (2012), suggesting that extreme environmental conditions can restrict SAV growth. In addition, three of these four years (all but 2013) experienced lower NO_3^- inputs from tributaries. The second pattern occurred over years of highest SAV biomass, peaking later during the season (September). SAV growth was favored by warm summers (2015, 2016) with intermediate water levels and high NO_3^- inputs. Overall, these observations suggest that maximum SAV biomass could vary following a dome-shaped curve where the optimum coincided with summers of warm temperature, average water levels and abundant nitrate.

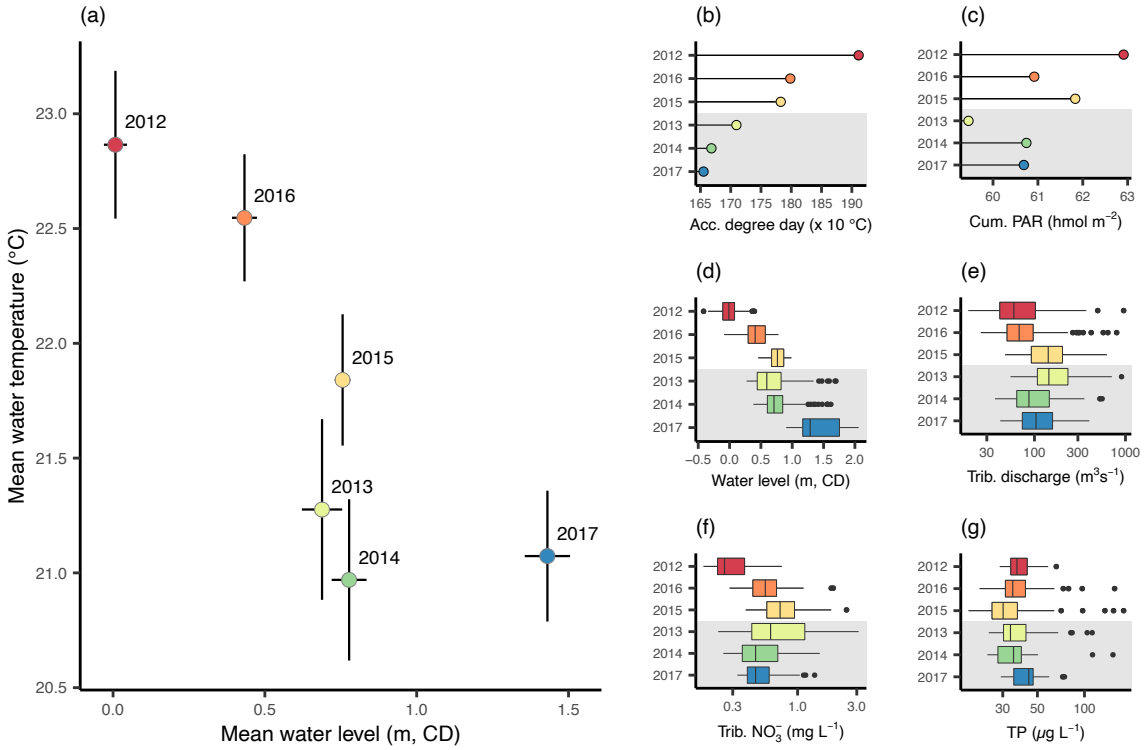

Figure 2. Interannual variation in environmental variables during summers from 2012 to 2017 (June 21 to September 22) for the main stem (a-d) and tributaries (e-g). Error bars are 95% confidence intervals around the mean. Dot and boxplots are ordered by decreasing water temperature as accumulated degree day using a warm to cold color gradient; cold summers are indicated by the light grey shaded background. Vertical bars within boxes indicate median value, box boundaries represent 25th and 75th percentile and whiskers range from 10th to 90th percentiles. Cum. cumulative, PAR photosynthetic active radiation, Acc. accumulated, CD Chart Datum, Trib. Tributaries, TP total phosphorus. Cumulative summer PAR and degree-days > 7°C were calculated from May 1st to September 22 . Water levels are from LSP station and SLR temperature from Trois-Rivières. Tributaries discharge correspond to the sum of Yamaska and Saint-François discharges. Nitrate and TP are flow-weighted concentration from the two tributaries.

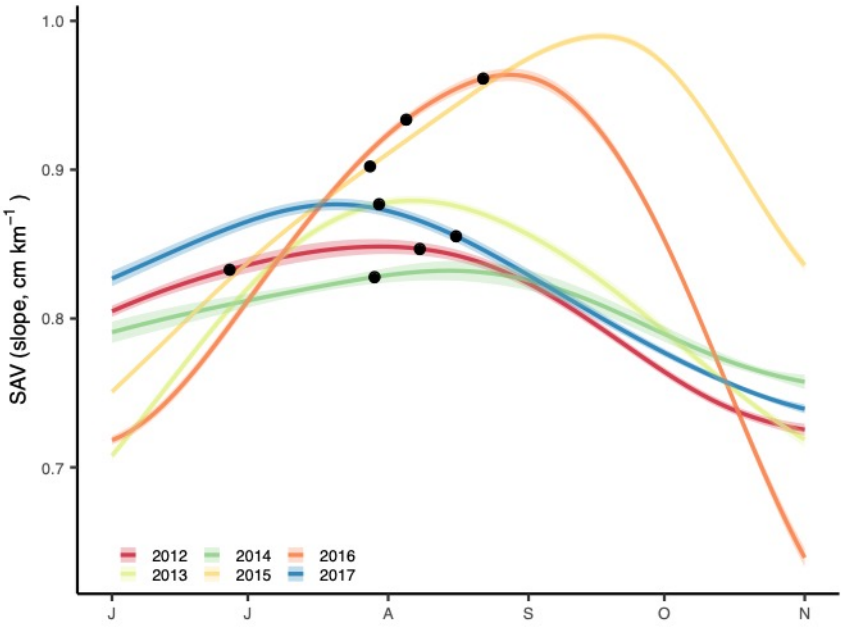

Figure 3. Interannual variation in temporal SAV biomass changes estimated daily from water level slope. Light-colored bands are 95% confidence intervals, but are not always visible given their small sizes. For each year, a date of formal biomass measurement allowed for estimated SAV biomass to be validated (black points). Slopes are the trend extracted using EEMD from raw surface water elevation, which corresponded to the SAV flow obstruction effect. SAV submerged aquatic vegetation, LSP Lac Saint-Pierre. Lines are color-coded by water temperature using a warm to cold color gradient.

NO_3^- budget

To estimate the NO_3^- budget for the plume flowing across the SAV meadow (Figure 1), we first compared the modelled NO_3^- input to the output of the in situ sensor measurements over five summers (Figure 4). The time series for the sensor were complete for 2012 and 2015 (88 and 93 days) and truncated by about 29 days for the other years due to instrument failure, with 2014 having the shortest time series (24 days). The comparison revealed that the NO_3^- output followed the same temporal pattern as the estimated inputs from the tributaries, but at markedly lower concentrations, regardless of the contribution of each tributary to NO_3^- inputs.

The contribution of each tributary to the incoming NO_3^- loads to the plume, estimated from conductivity, varied among years. Over the hot summers of 2012 and 2016, NO_3^- inputs to the plume originated solely from Saint-François River (Figure 4), whereas over the remaining years (2013-2015), both rivers contributed approximately equally. We also observed that the daily NO_3^- concentration range measured at the outflow, which reflected daily retention by autotrophic assimilation, was most often considerably below estimated inputs, suggesting substantial removal by denitrification. The sensor occasionally exhibited abrupt changes and elevated daily concentrations, sometimes above estimated inputs, particularly in years when the Yamaska was contributing to the inputs. These changes coincided with both high NO_3^- concentrations from the Yamaska River combined with short-term high discharge events that increased its proportion to the total water inputs (SI Figure S6). We thus evaluated that on those days, tributary contributions to the outflowing water mass were poorly estimated. As such, we excluded these dates from budgets ($n_{excluded}$ = 31, n_{budget} = 292) and assumed that the remaining NO_3^- inputs were accurately estimated.

The NO_3^- budget in the plume flowing across the SAV meadow also displayed high interannual variability (MANOVA $p < 0.001$, Figure 5) similar to the observed variation in temporal SAV biomass, and NO_3^- inputs and outputs for the complete SAV meadow (Figure 5). All variables contributed to among-year differences in budgets (LDA SI Table S3 and for process-specific rates and velocities $p < 0.03$). Using PCA, we observed that the uptake rates (particularly for U_t, U_a and U_d) were highly correlated to NO_3^- concentrations and tributary discharge ($r > 0.53$, Figure 5a). Variables describing proportional uptake (R and U_d/U_t) and V_f, both total and process-specific, where orthogonal to the uptake rates and were related to temperature and SAV abundance, both of which were markedly higher in August 2016 (up to day 228 of the year, last observation that year). In contrast, overall uptake rates tended to be differentiated by more generalized annual conditions where hotter and lower water levels years resulted in lower NO_3^- inputs and total retention than colder, higher water level years.

As such, this pattern of higher uptake measured in the plume was explained by the high NO_3^- loads in the colder years where both discharge and NO_3^- concentrations from tributaries (inputs) increased simultaneously (r = 0.82) and were strongly correlated to U_t (r_{NO_3} = 0.95, r_Q = 0.84). Interannual variations in NO_3^- loads entering the meadow induced sharp differences in measured areal total uptake rates among years with median differences of up to 1.6 g m^{-2} d^{-1} (range: med_{2012} = 0.1 g m^{-2} d^{-1}, med_{2014} = 1.7 g m^{-2} d^{-1}, Figure 5b). Similarly to total NO_3^- inputs to the overall

SAV meadow (Figure 2), high inflowing NO_3^- concentrations from the tributary to the plume reflected the greater contribution of the heavily enriched and flashy Yamaska River waters. Inflowing NO_3^- concentrations to the plume were generally similar to those for the complete SAV meadow (Figure 2), except for 2013 and 2014 (Figure 5c). These discrepancies were due to the shortened periods when sensor data were available those years, with midsummer 2013 and early June 2014 having lower and higher NO_3^- inputs, respectively, than the rest of the summer (Figure 4). Both U_a and U_d followed a somewhat similar pattern as NO_3^- inputs (SI Figure S7), but 2013 displayed a distinctive pattern of high U_a as compared to its low inputs in NO_3^-. This is in part explained by lower U_d values, likely resulting from higher discharge and lower plant biomass. Apart from that year, U_d tended to be higher and had a wider range than U_a, reaching its maximum at 2.6 g m^{-2} d^{-1} (in 2015) compared to the maximum U_a of 1.9 g m^{-2} d^{-1} (in 2014).

In contrast to uptake rates, R was highest during hotter summers with a median increase of 5 to 27% as compared to colder years (med_{hot} = 69 to 82 %, med_{cold} = 55 to 64 %, Figure 5d). The low R measured over the two hottest years (2012 and 2016) could be explained by the up to three-fold reduction in discharge in comparison with colder years ($med_{2012,2016}$ = 36-69 m^3 s^{-1}, $med_{2013,\ 2014}$ = 78-100 m^3 s^{-1}). The low tributary discharge in 2012 and 2016 also nearly doubled water residence time in the plume ($med_{2012,\ 2016}$ = 50-60 h) compared to other summers ($med_{2013\text{-}2015}$ = 35-38 h, Figure S7). However, in 2015 the residence time and discharge were similar to the colder summers (med_{2015} = 35h, $med_{2013,\ 2014}$ = 35-38 h). In this case, the high R could be attributed to the higher SAV biomass of that year compared to colder ones; this factor likely also contributed to the high R in 2016. The higher total V_f ($V_{f\text{-}t}$) in the high biomass years (2015, 2016) also suggested that the increased biotic activity resulted in higher overall retention and uptake rates (Figure 5e-g). Additionally, the summers of 2015 and 2016 tended to have proportion of denitrification from total uptake (U_d/U_t) 11 to 37 % higher than others, suggesting an interplay between climate and SAV biomass on N fate (SI Figure S7). To further investigate whether the changing SAV biomass affected the partitioning of N retention pathways, we compared yearly medians of process-specific ($V_{f\text{-}a}$, $V_{f\text{-}d}$) to total uptake velocity ($V_{f\text{-}t}$, Figure 6). The higher $V_{f\text{-}t}$ in the high biomass years could be attributed to either generally higher uptake velocity due to denitrification ($V_{f\text{-}d}$, in 2015) or higher daily values that increased variation around the estimate (2016). By comparison, when SAV biomass was reduced, $V_{f\text{-}d}$ was lower (2013) or similar (2012, 2014) to uptake velocity due to autotrophic assimilation ($V_{f\text{-}a}$).

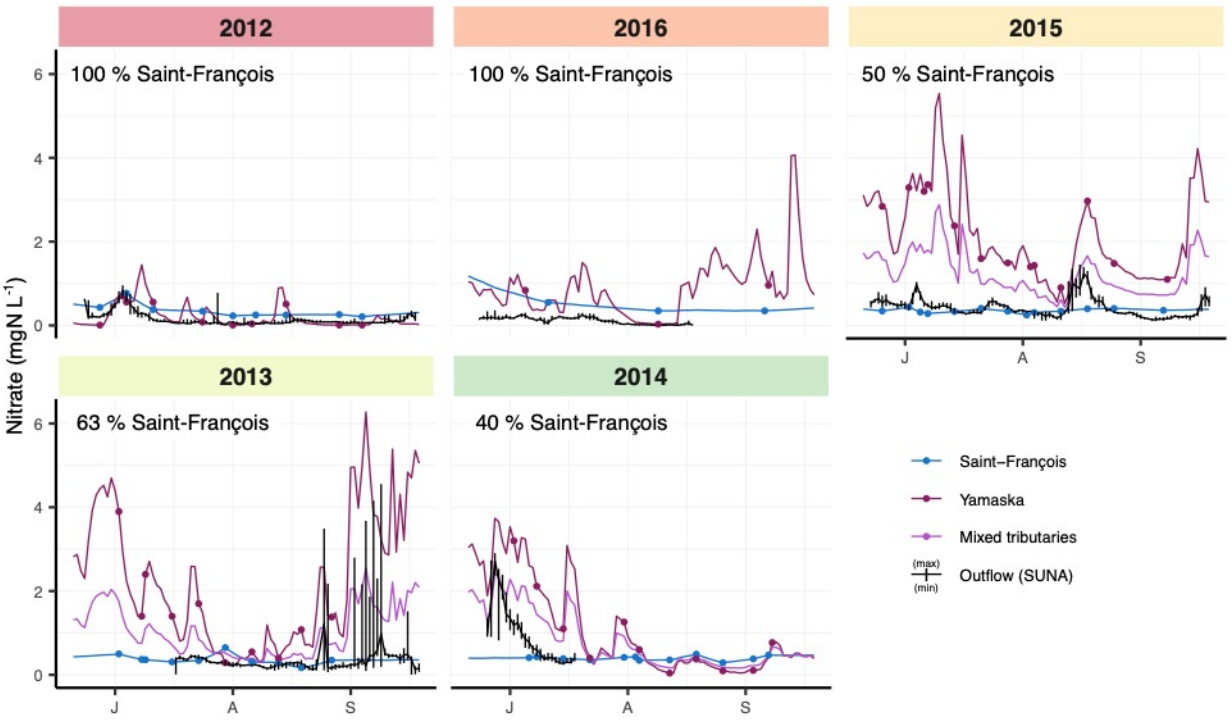

Figure 4. Daily NO_3^- inputs from individual tributaries as well as their estimated mixing concentrations in the plume compared to the median NO_3^- measured at the SAV bed outflow by the in situ sensor. Black vertical bars represent daily minimum and maximum NO_3^- concentration at the outflow. For tributaries, lines are fitted concentration values from the loadflex composite approach and points are measurements. Estimated input contributions from the Saint-François River are indicated on each panel with the remaining proportion coming from the Yamaska River. Mixed tributary lines for 2012 and 2016 are not presented since estimated inputs are solely from the Saint-François River. Panels are ordered by summer water temperature and water level (from hot-low level on top to cold-high on the bottom).

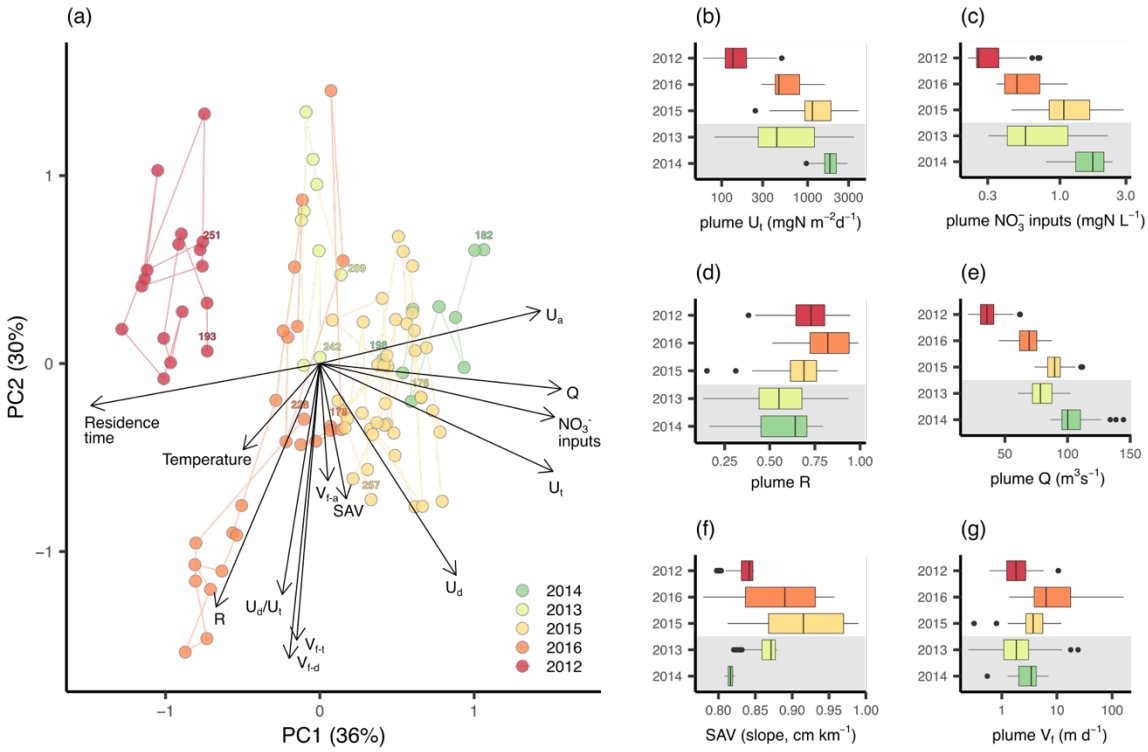

Figure 5. Correlative relationships and interannual variation in NO_3^- budget terms and their potential predictors in the plume flowing across the SAV meadow. A) principal component analysis (PCA) using scaling 2 where angles between arrows approximate correlation between variables. B) to G) show interannual distributions with vertical bars within boxes indicating median value, box boundaries representing 25th and 75th percentile and whiskers ranging from 10th to 90th percentiles. PC principal components with explained variance in parentheses, U uptake rate, R proportion of NO_3^- retained, Q discharge, SAV submerged aquatic vegetation, V_f uptake velocity, $_t$ total, $_a$ autotrophic assimilation, $_d$ denitrification. In a), colored numbers correspond to the first and last day of the year of estimation, and lines connect observations in temporal order. Years are ordered by decreasing water temperature using a warm to cold color gradient; cold summers are indicated by light grey shaded background.

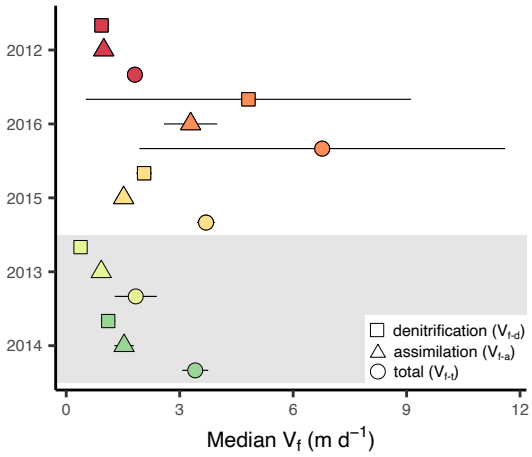

Figure 6. Comparison of median uptake velocity (V_f) from denitrification and autotrophic assimilation to total uptake velocity per summer. Error bars are standard error. Years are ordered by decreasing water temperature using a warm to cold color gradient; cold summers are indicated by the light grey shaded background.

Prediction of total NO_3^- retention by the SAV meadow

To estimate summertime NO_3^- retention in the complete SAV meadow, we built regression models using our NO_3^- budget in the plume and its relationship with environmental variables. The model to predict U_t with the highest AIC included both NO_3^- inputs and the temporal SAV biomass estimate (SI Table S4, Figure S8) but this model was not selected because the AIC improvement was minor (< 2) compared to the simplest model with only one predictor. Given the strong relationship between retention and inputs, U_t could be predicted solely from NO_3^- concentration of those inputs (marginal R^2 = 0.88, SI Table S5). The intercepts of the NO_3^- and U_t relationship differed among years (conditional R^2 = 0.92, Figure S8). Although the AIC difference was minor with the model without random structure, variable intercept per year was selected because it homogenized the residual variance among years (SI, Table S6). Most importantly, the model was substantially improved by adding an autocorrelation structure per date (autoregressive model, AR-1), which considers that consecutive observations were highly correlated with each other (r = 0.82). Using the fixed effect of the model with only NO_3^- as a predictor (SI Table S5) and weighted concentrations of tributaries derived from the plume, we predicted U_t for the complete SAV bed and summer period and derived R from yearly NO_3^- load (Table 2). Retention was highly variable among years, showing a fourfold difference between extremes. The interannual pattern in retention was similar to patterns in inputs, albeit the inputs exhibited a much higher interannual variation than the outputs, with

almost a sixfold difference between extreme N loads. As a result, R tended to be somewhat higher (63-87%) in the warmer years (2012, 2016, 2015) than in colder years (47-62%). A nearly complete retention (87%) was observed in 2016, concomitant with lower NO_3^- inputs. When calculating U_d from the overall SAV bed U_t using the median plume U_d/U_t, these differences in retention with climate were more important. Year with higher SAV biomass or lower NO_3^- inputs had 30 to 58% of inputs permanently removed through denitrification compared to 18-22% during colder years with reduced SAV biomass and higher NO_3^- loads.

Table 2. Whole-SAV meadow summertime NO_3^- inputs, total and denitrification uptake (U_t, U_d), and proportional retention (R) modelled for six summers (June 21 to September 22). Nitrate inputs were estimated from the sum of daily tributary loads. U_t was modelled from daily inputs, using NO_3^- concentrations as the predictive variable, while U_d was estimated by multiplying U_t by the plume yearly median proportion of U_d on U_t. Maximum SAV biomass was estimated from the linear regression between rake estimated biomass and water level slope. CI confidence intervals, denit. denitrification. Summers are ordered by decreasing water temperature.

Year	Total NO_3^- inputs (tonnes)	U_t (tonnes)	U_t 95% CI (tonnes)	U_d (tonnes)	R total (%)	R denit. (%)	Maximum SAV biomass (g m^{-2})
2012	304	192	[173, 214]	91	63	30	31
2016	533	466	[392, 555]	311	87	58	109
2015	1188	751	[610, 927]	441	63	37	127
2013	1811	846	[670, 1073]	250	47	14	52
2014	726	444	[373, 529]	158	61	22	20
2017	622	384	[329, 448]	113	62	18	50

Discussion

In this study, we provide high frequency measures of N retention and its partitioning into autotrophic and heterotrophic pathways across multiple years from a riverine SAV meadow, in one of the largest rivers studied to date. We hypothesized that retention, measured as either uptake rates (U) and proportion retained from inputs (R), would be a function of NO_3^- loads and of vegetation biomass, both of which expected to be subject to climate-driven variations. We found that N retention by the meadow in the main stem significantly attenuated the incoming loads from two enriched agriculturally impacted tributaries. Estimated rates were among the highest reported so far in rivers (U_t median 576 mg N m^{-2} d^{-1}, range 60 – 3893 mg N m^{-2} d^{-1}), showing both intra-annual and interannual variations of this ecosystem service as a function of climate conditions. This variation highlights the importance of measuring N retention rates multiple times within a year and across several years. NO_3^- uptake rates in the SAV meadow were a function of NO_3^- loads, which varied largely as a function of climate driven changes in discharge from the tributaries. However, the climate effect on loads were not in synchrony with the water level changes in the main stem. This was probably due to differential effect of precipitation patterns on basin-wide water inputs and aspects related to regulated flow upstream from the study site versus localized water inputs at the confluence. Proportional retention was higher in the hottest years and coincided with either higher water residence time or higher SAV biomass in the meadow or both. Maximum summer SAV biomass appeared to vary along a dome-shaped curve, and optimal conditions were observed in summers with warm water temperatures, average water levels, and loadings of abundant NO_3. Higher SAV biomass also influenced the partitioning of N retention pathways by promoting permanent removal through higher denitrification. Our work indicates that this riverine SAV meadow provides an important ecosystem service by reducing N export to downstream waters by 47 to 87% and permanently removing between 14 and 58% of N inputs. Thus, management actions should aim at preserving or restoring such critical riverine N removal control points.

Nitrogen retention in riverine SAV meadows

Vegetated sites in rivers are recognized for performing multiple aquatic ecosystem services including N removal (Caraco et al., 2006). However, measuring seasonal and interannual changes in SAV quantities and how it affects N processing in large meadows remains a challenge due to the restricted ability to assess biomass changes underwater and the difficulty to measure N retention in large river. We successfully followed SAV biomass daily using the indirect measure of water level

slope and N retention using a high frequency sensor. Using this information, we found that only part of our hypothesis was supported as there was no conclusive evidence of a strong relationship between uptake rates and SAV biomass. This was likely due to the overriding role of NO_3^- inputs in determining total uptake rates (U_t) of the meadow. The strong relationship between inputs and U_t is not suprising as N retention is typically modelled using first-order kinetics, where process rates are a linear (log-log) function of substrate concentrations (e.g. Seitzinger et al., 2006; Wollheim et al., 2006). For a maximal functioning, N removal sites thus have to be spatially connected to high N loading locations, as is the case for the confluence zone of this study (Cheng et al., 2020; Mitsch et al., 2001).

The strong positive effect of SAV quantities on N uptake rates has previously been reported when comparing river reaches with contrasting plant cover (85% vs 45%, SI Table S7, Preiner et al., 2020). We probably did not observe a clear pattern between our measure of plant quantities and uptake because SAV cover was always high across the N budget plume, thus always favoring high N uptake. Rather, the interannual differences in SAV was one of plant density, or biomass, which likely changed SAV surface area as these two measures of SAV are well correlated (Armstrong et al., 2003). Greater SAV surface area obstructs flow, which reduces velocity and increases water residence time (Madsen et al., 2001). This latter increase should also increase the proportion of N retained since a prolonged contact between water column NO_3^- with plants and sediments can lead to the exhaustion of this substrate pool. Indeed, and as typically observed (Seitzinger et al., 2006), there was a general inversed interannual pattern between proportion retained and discharge (Figure 5d-e). However, high biomass years (2015, 2016) had higher than expected retention (1st and 3rd highest) given their fast flow and high discharge (4nd and 2nd highest). Higher biomass years therefore probably had added plant surface area facilitating N exchange between plants, their epiphytes, sediments, and water column.

Additionally, our results suggest that changing SAV biomass affected N fate. When SAV was abundant, denitrification rates in the plume were high and accounted for 59 to 67% of total uptake in contrast to 30 to 48% during years when biomass was reduced. Similarly, when using V_f, a metric that is independent of concentrations and hydrologic characteristics (Ensign & Doyle, 2006; Wollheim et al., 2006), the biotic demand of denitrification ($V_{f\text{-}d}$) was higher than that of assimilation during high biomass years, and vice versa. At the scale of the SAV bed, these differences translated into an up to four times higher rate of permanent removal in high biomass years

compared to lower ones. These results are in agreement with studies that considered both assimilatory and dissimilatory pathways (Heffernan & Cohen, 2010; James, 2010; Pinardi et al., 2009; Preiner et al., 2020; summarized in SI Table S7), while reports focusing solely on N assimilation by SAV and their epiphytes generally found that overall uptake of water column NO_3^- concentrations were typically lower (Desmet et al., 2011; Diamond et al., 2021). The dominance of denitrification in a higher biomass year can be explained by the structural complexity of SAV and increased surface area that supports biofilms where denitrification can occur (Eriksson & Weisner, 1996). SAV also favors denitrification in sediments, by promoting organic matter particle settling, which increases sediment respiration rates and the anoxic conditions needed for denitrification (Cornwell et al. 1999). Furthermore, SAV provide labile dissolved organic matter directly to denitrifiers within the sediments through the release of exudates from their roots (Karjalainen et al., 2001). Overall, in advection-dominated systems such as rivers where NO_3^- is continuously supplied from the watershed (Seitzinger et al., 2006), the dominance of denitrification on total uptake in SAV beds is likely a function of how plants amplify reactive surface areas, enrich sediments, and increase contact rates through a reduction in flow creating optimal environmental conditions for denitrifying microbes.

Given the optimal conditions for N processing at our SAV control point, both total N uptake and denitrification rates measured in this study (U_t = 576 [60-3893 mg N m^{-2} d^{-1}] ,U_d = 338 mg N m^{-2} d^{-1} [1-2624 mg N m^{-2} d^{-1}] SI Table S7) are among the highest reported, but remain within the range of previous estimates derived from similar methods in SAV meadows [up to 840 mg N m^{-2} d^{-1}], Heffernan & Cohen, 2010; Preiner et al., 2020). Our estimates are also higher than those previously reported in a meta-analysis of denitrification in rivers worldwide (up to 1143 mg m^{-2} d^{-1}, Piña-Ochoa & Álvarez-Cobelas, 2006). This may be due to differences across methods, the temporal and spatial scales of inquiry or a dilution effect from SRL water. The meta-analysis involved short-term laboratory (cores) or in situ (chambers) incubations providing discrete denitrification rates in time. We report daily and interannual net uptake rates at the reach-scale that reflect the balance between processes that produce (nitrification) and consume NO_3^- (assimilation, denitrification), and its variability throughout multiple growing seasons. Our estimates may be higher because of a greater sensitivity of the two-station mass-balance approach to increase in NO_3^- concentration and reach length (von Schiller et al., 2011). Still, the uptake rates from this method are generally in agreement with multiple site mass-balance and incubation approaches (Piña-Ochoa & Álvarez-Cobelas, 2006; von Schiller et al., 2011). Another methodological bias that we did not account for is the potential

mixing of SLR water at the downstream site. This would also have resulted in an overestimation of uptake rate as concentrations in the main stem were typically lower than in the tributaries (SLR med_{NO_3} = 0.17 to 0.25 mg L^{-1} at Tracy station). However, care was taken to ensure water mass contributions in the plume came from the tributaries.

The high rates we report may also be explained by the presence, size and location of the SAV bed under study. This is highlighted by the similar denitrification rates measured in a dense floating bed of *Trapa natans* in a sheltered bay of the Hudson River (1.5 km^2, 518-994 mg N m^{-2} d^{-1}), in contrast to the undetectable rates in a small (0.6 km^2) *Vallisneria* meadow in a fast-flowing channel from the same river (Tall et al., 2011). The floating meadow acted in a similar way to this study large SAV meadow (~10 km^2) that both intercepted nutrient-rich waters and reduced velocities (Bulat et al., 2019), thus promoting high nitrate removal. Another line of evidence supporting the robustness of our estimates is that our measured uptake velocities (V_f, median 3.0 m d^{-1}) were similar to those reported for the Upper Snake River (WY, USA, 12 m^3 s^{-1}, 0.6 to 13.0 m d^{-1}, Tank et al., 2008). However, our estimates were much more variable both within and among seasons (range 0.2 – 160.8 m d^{-1}), highlighting the considerable heterogeneity of biotic activity, load and NO_3^- retention capacity in time at this dynamic confluence zone.

Complex effects of climate at a confluence zone

By measuring environmental conditions over 6 summers, we showed that different climatic variables drove complex variations in SAV biomass and N retention in a large riverine SAV meadow. The predominant influence of climate on SAV biomass was perceptible through the large range of water levels and temperatures among years: our observations spanned the lowest (2012) and highest (2017) mean summer water levels recorded at LSP gauging station for more than a century (data available since 1914, meds-sdmm.dfo-mpo.gc.ca). Our observations also included the warmest (2012) and the third coolest (2014) mean summer water temperature over the last 20 years (data available since 2000, ogsl.ca). These climatic variations translated into a ≈6-fold range in maximum SAV biomass within the study area during the 2012-2017 period (Table 2).

The range in climate variation captured on such a short time scale reflect the sensitivity of rivers to these changes and impacts that are likely already taking place (Gudmundsson et al., 2021; Nijssen et al., 2001). Among these impacts, we could expect that increased precipitation should favor N transport, as is generally seen in anthropogenically altered river networks (Goyette et al., 2019;

Howarth et al., 2012). Inflowing NO_3^- concentrations to the SAV meadow were correlated to the discharge of incoming tributaries, but concentration changes were mostly a function the relative contribution of each tributary to the total at the confluence site, particularly from the smaller, more NO_3^- rich, and flashier Yamaska River. This river displayed the typical seasonality of agricultural watershed where discharge and NO_3^- concentrations vary in synchrony (Van Meter et al., 2020). Indeed, in smaller catchments like the Yamaska, riverine nutrient loads are typically more variable than in larger catchments, like the Saint-François (2.1 times larger than Yamaska) and the SLR main stem, which integrate loads from many sub-watersheds that dampens individual basin signals (Burt & Pinay, 2005; Chezik et al., 2017). However, the variation in NO_3^- inputs was disconnected from temperature and water level variation in the main stem that was more reflective of water inputs at the scale of the entire SLR watershed. These asynchronies might become more common as more pronounced climate-driven changes and reduced summer discharge are expected over the next decade in southern SLR tributaries, in contrast to maintained or amplified discharge in northern SLR tributaries (Boyer et al., 2010; Ouranos, 2015). Regardless, the highest SAV biomass were recorded at the confluence zone over years of intermediate water level and temperature conditions.

Past observations suggest that optimal conditions for SAV biomass are met when water levels are high in LSP, and are limited when levels are low, favoring reed bed expansion (Hudon, 1997). We observed the latter in the extremely low-level year of 2012. SAV biomass was among the lowest recorded during this study and can be explained by the large areas of riverbed being exposed to air that year, potentially leading to SAV loss through the dry-out of above ground biomass. The elevated water temperatures might also have favored phytoplankton and metaphyton growth that year through slow water transit time, high water column illumination and increased nutrient release from the sediments. Indeed, low water levels in LSP are associated with increased filamentous green algae biomass (Cattaneo et al., 2013). Overall highest TP (~39 µg L^{-1}), chlorophyll *a* (~3.6 mg L^{-1}) and lowest secchi depths (~67 cm) were also measured within the bed in 2012 despite average TP inputs (Figure 2g). In contrast with Hudon (1997), however, our result suggests that SAV biomass is also constrained at extremely high water level years when temperatures are cold. The effect of high waters can be explained by SAV light limitations through the typical positive relationship between maximum SAV colonization depth and water transparency (e.g. Chambers & Kalff, 1985). Incoming turbidity did not display a coherent pattern as a function of water level changes (Figure S5), and increased water height in itself likely created deep areas where light did not reach the bottom, thus

restricting plant colonization. In the LSP fluvial lake, the deeper waters also correspond to an increased exposure to fast currents, further limiting SAV growth (Hudon et al., 2000).

When water depth and transparency allowed light penetration to the sediments and thus plants were not limited by light, increases in temperature probably directly favored SAV growth and biomass accumulation. This has previously been shown in nearby shallow lakes where sharp differences in SAV biomass for the same lakes were observed in a cold and a hot year (Rooney & Kalff, 2000). The direct effect of temperature is likely a function of increased photosynthetic rates that drive plant growth (Brown et al., 2004; Farquhar et al., 1980; Riis et al., 2012). Experimental studies support this potential direct effect in mesotrophic conditions, when light availability does not limit plant growth (Barko et al., 1982; Ersoy et al., 2020). These conditions were met in intermediate water level and hotter years (2015-2016) where TP within the meadow ranged from ~19-26 μg P L^{-1}. During those years, SLR temperature was near the previously determined growth optimum of ~25-28°C, below deleterious temperatures (28-30 °C; Barko et al., 1982; Riis et al., 2012). Indeed, during our field survey, water temperatures were always below 27.2 °C and generally around 24 °C during 2015 and 2016. The intermediate water level of those years likely also increased light availability to a more extensive area for SAV growth (Beklioglu & Altinayar, 2006). SAV growth during those years might also have been facilitated by the time lag that allowed for plant bed recovery following the 2012 drawdown that potentially damaged winter buds and reduced biomass the subsequent years. We argue that this is unlikely as SAV bed can regenerate from seed banks (Kimber et al., 1995), and the 2012 event still left large meadow areas covered with water. Additionaly, the highest biomass year (2016) was followed by a low biomass year, suggesting that autocorrelation between consecutive years was not a dominant driver of SAV biomass during our study period. Our results rather indicate that water levels combined with water temperature seems critical in determining biomass as for example in 2014 when water levels were similar to the high biomass year of 2015 and 2016, temperatures were coldest and SAV biomass was lowest. As such, when areal light to sediment is apparently equal, temperatures in hot years directly stimulated SAV growth in LSP.

Conclusions

In this study, we showed the complex influence of climate on N retention in a SAV meadow in the SLR and report some of the highest measured estimates in a large river from this control point. This influence includes modulating N loads to the meadow combined with SAV biomass and

water residence time within it, mitigating the total amount and the proportion of N retained, as well as N fate. Our results suggest that SAV biomass is restricted by extreme dry and wet years, which may increase in frequency with climate change, thus suggesting a diminishing role of SAV on N retention in the SLR. Indeed, SLR water levels have been decreasing since the 1970s (Hudon et al., 2018), and climate projections of increasing summer air temperatures will further reduce levels through higher evaporative loss. However, higher precipitations are projected with climate change, particularly in the North (Ouranos, 2015), which might also lead to more floods as observed in 2017 and sustained high water levels throughout summers. There was no direct correlation between SLR water levels and tributary NO_3^- loads at our confluence site, probably due to asynchronous precipitation patterns across sub-watersheds in the SLR basin. During years with overall higher tributary discharge, short-term, heavy precipitation patterns favored the flashiness of the Yamaska River, yielding high inflow of turbid, nutrient-rich waters. Our sensor time series displayed more frequent NO_3^- spikes following summer rain, potentially reflecting higher N export during these events due to reduced water residence time. As extreme precipitation events are expected to become more common with climate change, these moments might increasingly contribute to N exports (Goyette et al., 2019; Lu et al., 2020). However, we could not calculate N budgets during these events because of the changing tributary contribution to waters flowing through the SAV meadow. Future studies should investigate how such events contribute to overall N exports and assess whether SAV lose their capacity to dampen hydraulic flows and retain N under such circumstances.

Although wetlands in watersheds are considered to have a disproportionate role in N retention on the landscape (Cheng et al., 2020), we argue that shallow-water underwater plant meadows should also be considered in conservation assessments. Even when SAV biomass was low, the meadow provided an important ecosystem service by retaining large amounts of N, thus decreasing impacts of overall N delivery from agricultural rivers to the SLR estuary. The proportion retained and permanently removed was highest during hotter years with high SAV biomass, while the absolute amount retained was related to N loads which reflected localized precipitation patterns from the two tributary watersheds. Although the effect of SAV is seasonal, it coincides with the period when N export has the highest potential impact in the SLR estuary by contributing to the reported eutrophication, which partially explains growing hypoxia in its deep waters (Gilbert et al., 2005; Lehmann et al., 2009). We estimate that during the SAV growing season, between 2 to 9 t N per day could be retained, which is higher than previous estimates of 1.5 t N per day from this same location using a coarser mass-balance approach (Hudon et al., 2017). Assuming a 1.1 kg N per

summer based on an annual per capita excretion of 4.4 kg N yr^{-1} (Howarth et al., 1996), this would be the equivalent of retaining the N generated by a city of 0.17 to 0.77 million people over the SAV growing season. Although we illustrated the value of SAV meadows from a N perspective, other cultural and provisioning services are supplied by SAV in general (Hilt et al., 2017) and in particular at our site, commercial and recreational fisheries (Giacomazzo et al., 2020; He et al., 2016). Therefore, management action should aim at preserving or restoring such critical sites within the shallow-water areas of large rivers.

Acknowledgments

We thank the numerous people that provided assistance for sample and biomass collection and subsequent lab analyses throughout the years, Jean-Pierre Amyot and Conrad Beauvais for installation and maintenance of the SUNA, as well as Nicolas Fortin St-Gelais, Richard Labrie and Pierre Gagnon for advice on data analyses. We thank Robert Hensley and an anonymous reviewer for insightful comments that improved the manuscript. This project was funded by the Groupe de recherche interuniversitaire en limnologie (GRIL) through a Fonds de recherche de Québec - Nature et technologies (FRQNT) Initiatives stratégiques pour l'innovation grant, National Sciences and Engineering Research Council of Canada (NSERC) Discovery to RM, and FRQNT and NSERC scholarships to MB. This work was also supported by Environment and Climate Change Canada (ECCC) as part of the Canada-Québec St. Lawrence Action Plan (SPLAP, CH). We acknowledge that this work was carried out on the traditional lands stewarded by the N'dakina (Abenaki / Abénaquis).

Supporting information

Text S1. Supplementary methods

Estimating confidence intervals from slope SAV signal

In order to test the ability of water level slope to act as a surrogate to plant biomass and enable seasonal extrapolation of biomass related to growth dynamics, we needed to ensure that the information related to change in water levels and the subsequent slope was only a function of biomass changes and not related to other factors like wind. As such we used Hilbert-Huang transform, which is a type of spectral analysis where empirical mode decomposition (EMD) combined with the Hilbert spectrum, disentangles the original signal into a set of intrinsic mode functions (IMF) with distinct local frequencies. This can then be used to identify competing signals and isolate the one of interest. Therefore, to estimate the confidence interval of the SAV slope signal, we applied the bootstrapping approach of Ezer & Corlett (2012) where artificial resampled data are created many times from the anomaly between original data and the extracted ensemble EMD trend (noise-assisted version of EMD that reduce mode mixing). The artificial data is then decomposed as artificial trends, and the standard deviation of each daily observation is calculated from all the artificial trends. The resample technique requires a high computation time. As such, confidence levels were estimated using the basic EMD algorithm on 1000 trend extraction iterations.

SAV biomass from gauging station slope difference

To determine the optimal stations representative of SAV biomass, water level data at the Sorel gauging station (upstream, 3.775 m above sea level, referenced to the International Great Lakes Datum of 1985, IGLD85), was compared to a station within LSP (3.383 m IGLD85), and the latter station was compared with that of Port Saint-François (PSF, further downstream, 2.967 m IGLD85, see table S1 for station identifiers and data sources). Slopes were calculated as water surface elevation upstream minus downstream divided by distance between successive stations (23 km).

We found that the SAV signal from water level slope, determined from the upstream gauging stations between Sorel islands and LSP, was not a good predictor of mean SAV biomass (r = 0.33), largely due to the 2014 outlier where slope was highest and measured biomass was lowest (Figure S2). This is likely a function of physical and anthropogenic features modifying flow in that region. The upstream presence of an archipelago and numerous dykes in between islands, built to elevate

water levels in the navigation channel, probably changed the expected flow obstruction effect from SAV biomass alone. Indeed, Boudreau et al. (1994) reported that these upstream features amplified water levels at that site especially when water levels in the mainstem were higher, as was the case in 2014. By comparison, the downstream gauging stations slope between LSP and PSF was highly correlated with the measured SAV biomass (r = 0.98, excluding 2016 quadrat measurement). The 2016 quadrat biomass was much higher than would be expected from a perfect linear relationship between slope and biomass. This may be due to differences among methods and from sampling at slightly different sites. Regardless, this quadrat estimate indicated increasing biomass later during the 2016 growing season, in agreement with an observed increase in lower LSP water level slope.

Estimating gross primary production and ecosystem respiration in 2016

Daily gross primary production (GPP) and ecosystem respiration (ER) were calculated using the bookkeeping method in the R package LakeMetabolizer (Winslow et al., 2016). For gas exchange estimation, the depth of the surface mixed layer was assumed to be the depth at the outflow site, and oxygen saturation was calculated using in situ water temperature, and atmospheric pressure estimates at the Nicolet weather station (Table S1). The coefficient of gas exchange was computed using wind speed (Cole & Caraco, 1998) estimates from LSP weather station or, when data were missing, from Nicolet. Nighttime and daytime periods were estimated using the R package suncalc (Thieurmel & Elmarhraoui, 2019).

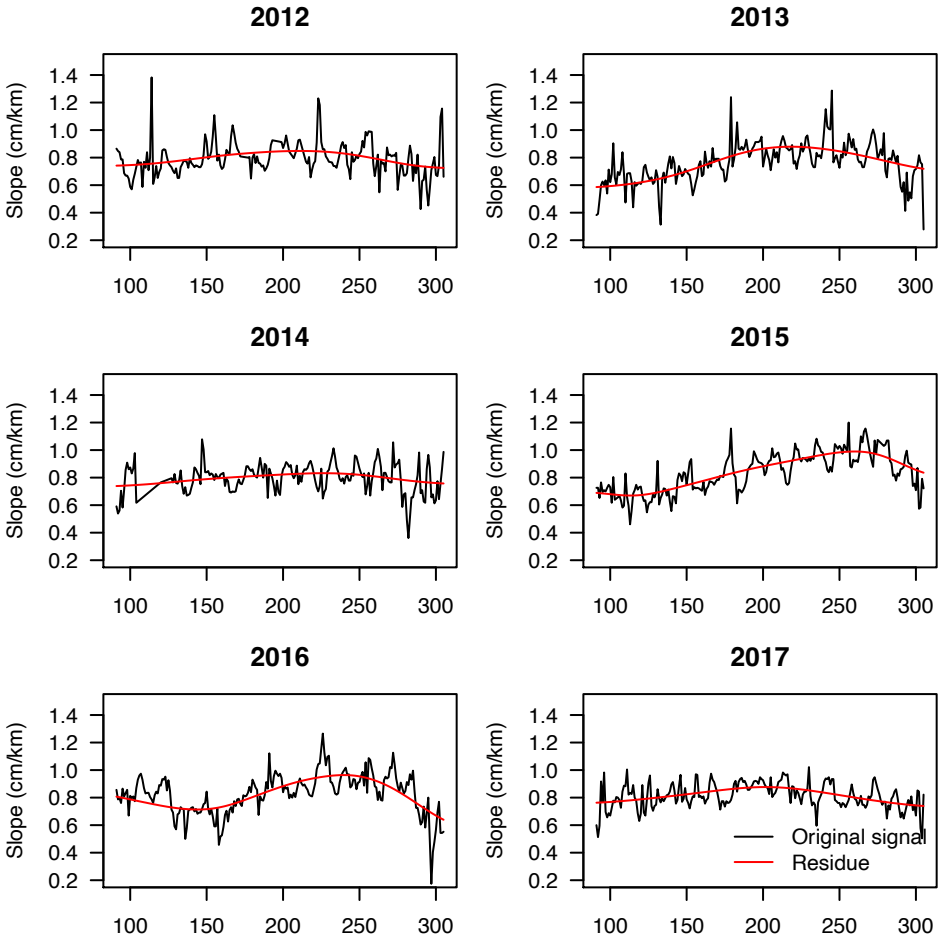

Figure S1. Comparison of original slope data between Lac Saint-Pierre and Port Saint-François (black) and the residual EEMD (red) interpreted as SAV signal along time in day of the year. Summer starts at day 172 (June 21th) where SAV signal begins to be apparent.

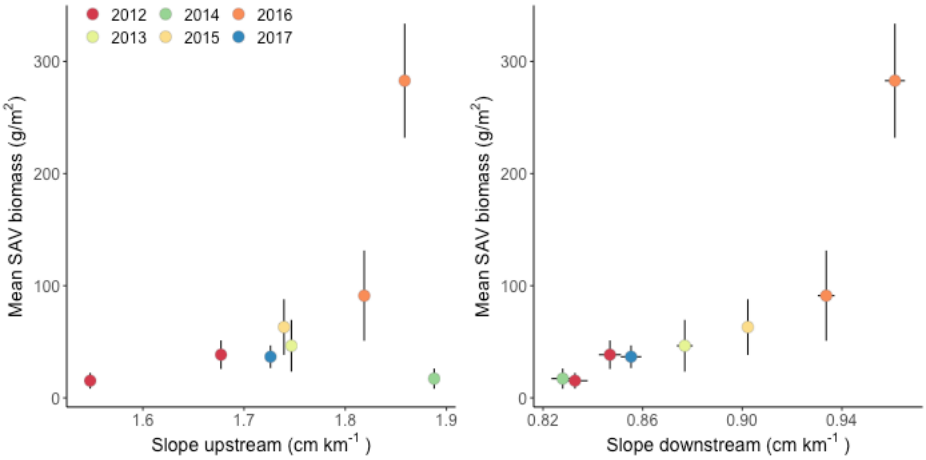

Figure S2. Relationships between SAV biomass and water level slopes calculated between LSP gauging station and with upstream (A) or downstream (B) station. All biomass measurements are derived from rake collections corrected to quadrat equivalent, except for late August 2016 that was directly estimated from quadrat sampling

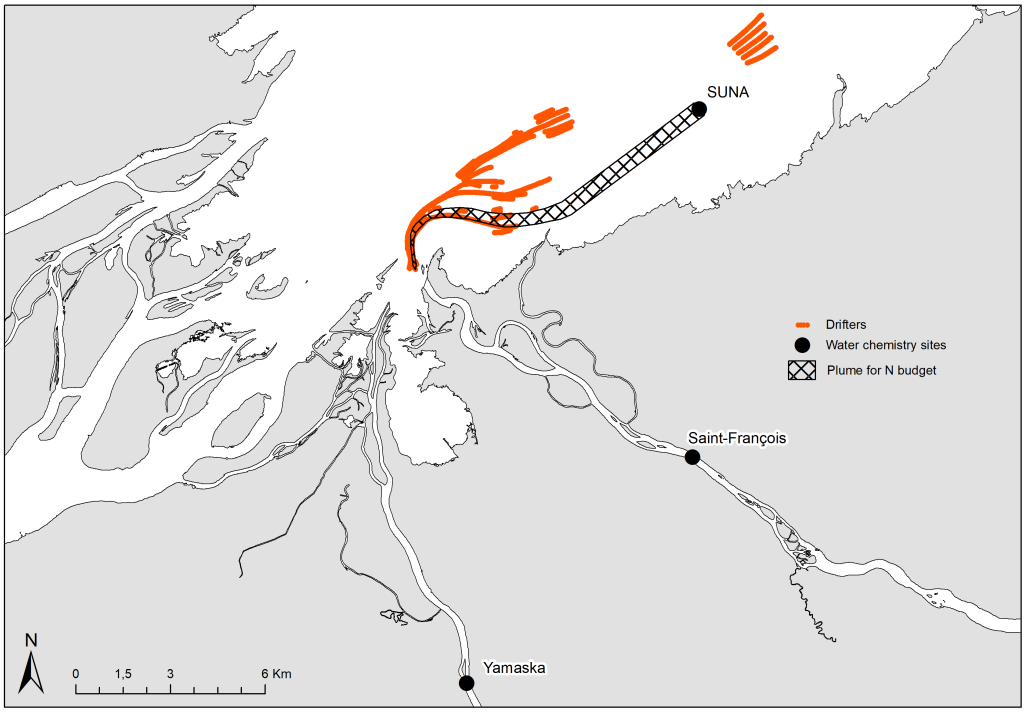

Figure S3. Map showing the estimated plume for N budget estimation between the tributary stations and the SUNA outflowing station.

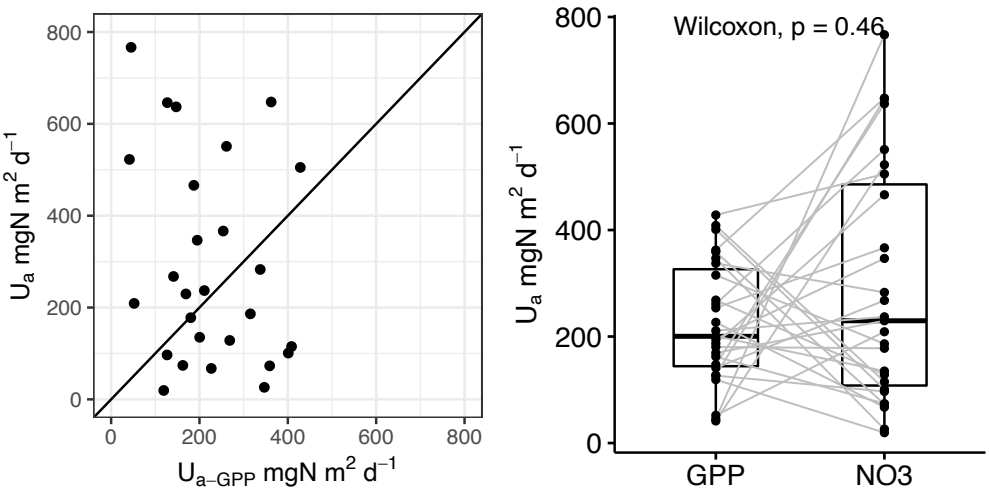

Figure S4. Comparison of nitrogen autotrophic assimilation in 2016 estimated from NO_3^- and from dissolved O2 time series and gross primary productivity (GPP). The black diagonal line is the 1:1 line.

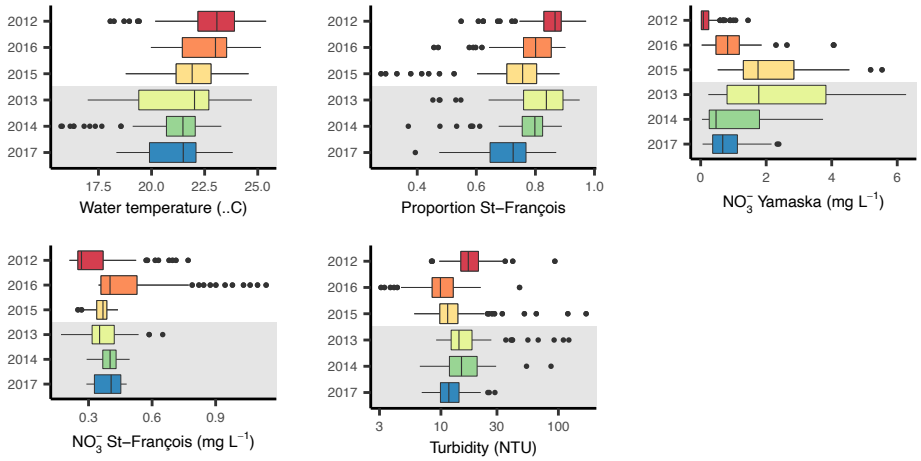

Figure S5. Boxplot of water temperature at Trois-Rivières, proportion of discharge from Saint-François River on total tributaries discharge, NO_3^- concentrations in each tributary and flow-weighted turbidity during summers from 2012 to 2017 (June 21 to September 22). Summers are ordered by SLR water temperature and level with hot-low level on top and cold-high level at the bottom and with grey background. Vertical bars within box indicate median value, box boundaries represent 25th and 75th percentile and whiskers range from 10th to 90th percentiles.

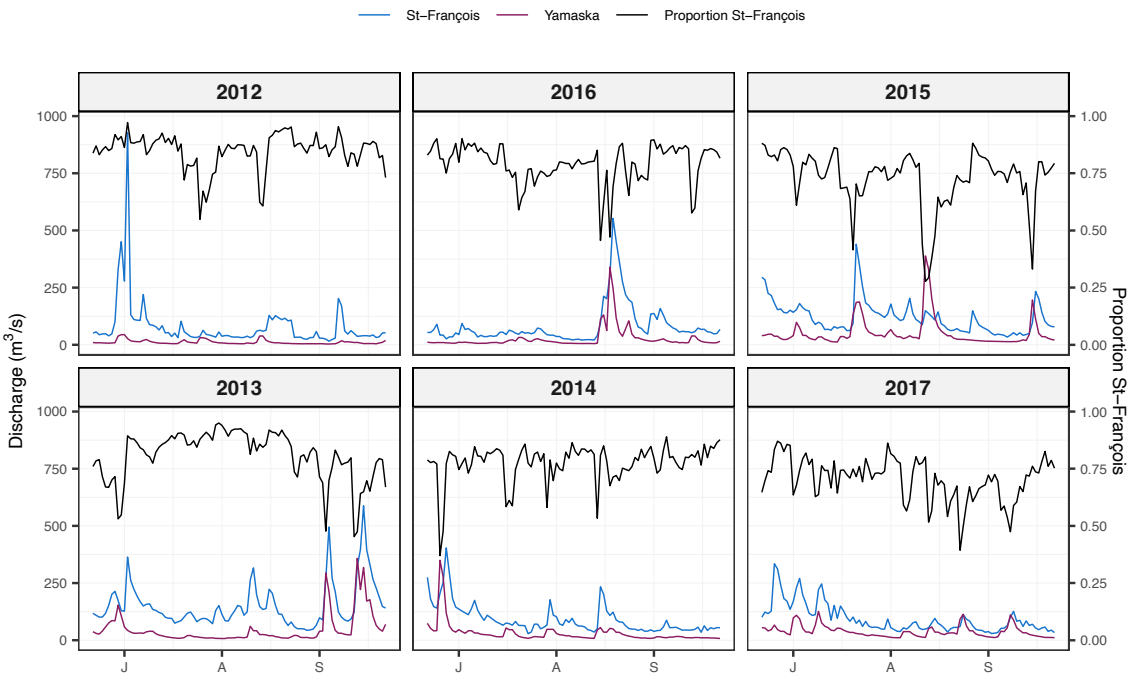

Figure S6. Daily variation in discharge and proportion of Saint-François discharge to total discharge of tributaries.

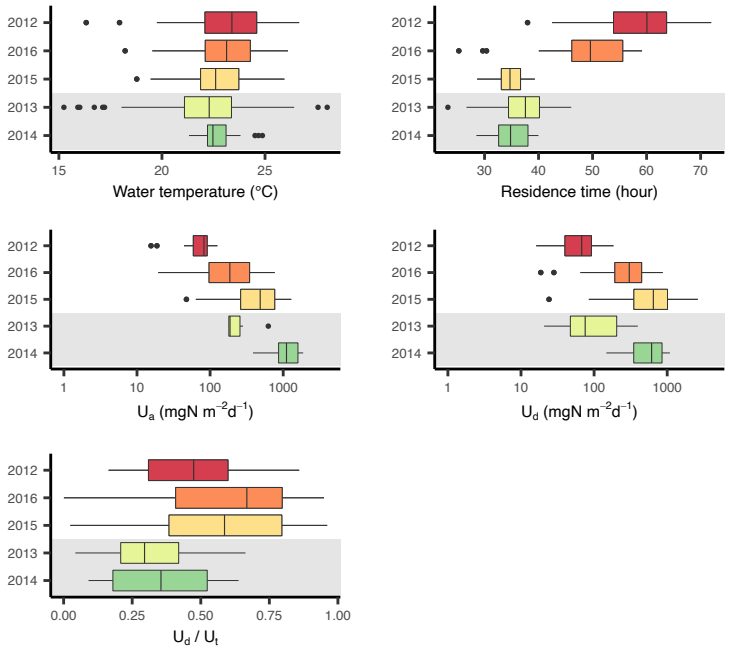

Figure S7. Boxplot of proportion of water temperature, residence time, autotrophic assimilation (U_a), denitrification (U_d), and proportion of denitrification on total uptake (U_d/U_t) over five summers. Summers are ordered by water temperature and level with hot-low level on top and cold-high level at the bottom and with grey background. Vertical bars within box indicate median value, box boundaries represent 25th and 75th percentile and whiskers range from 10th to 90th percentiles.

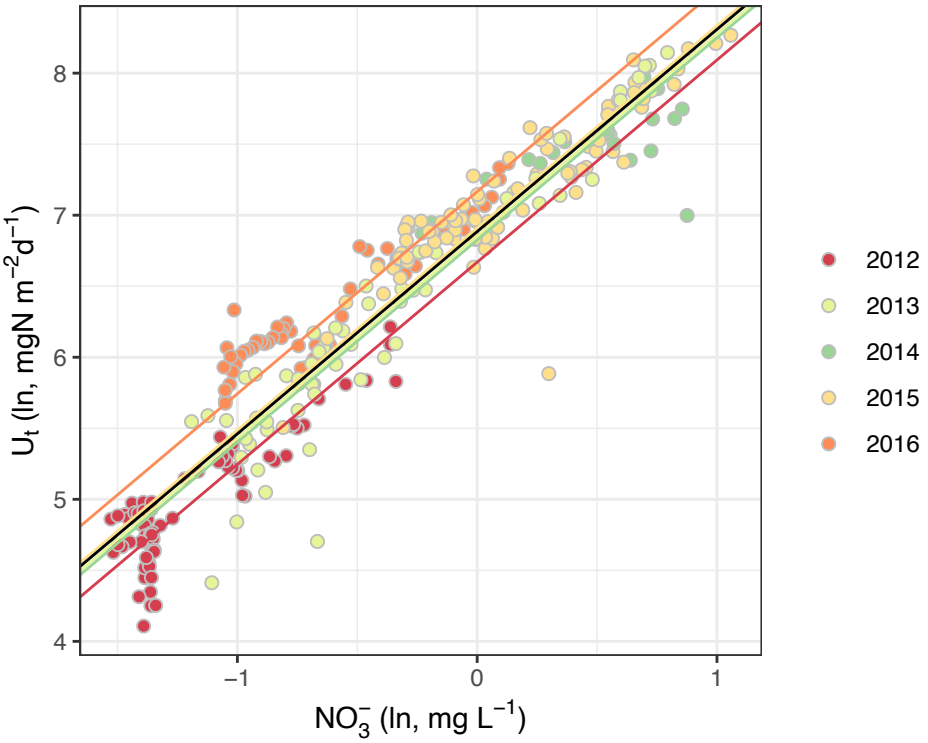

Figure S8. Relationship between total uptake rate (U_t) and NO_3^- inputs to the SAV plume showing the random structure selected (varying intercept per year). The black line is the fixed effect.

Table S1. Information on stations where data was acquired for time series analyses. DFO Department of Fisheries and Oceans Canada meds-sdmm.dfo-mpo.gc.ca; BQMA Banque de données sur la qualité du milieu aquatique www.donneesquebec.ca/recherche/fr/dataset/suivi-physicochimique-des-rivieres-et-du-fleuve; HYDAT National Water Data Archive wateroffice.ec.gc.ca/; CEHQ Centre d'Expertise Hydrique du Québec www.cehq.gouv.qc.ca/hydrometrie/historique_donnees/info_validite.htm; HQ Hydro Québec personal communication, CHS Canadian Hydrographic Service SINECO tide gauge network ogsl.ca, MSC Meteorological Service of Canada, climat.meteo.gc.ca. For discharge stations, watershed names are indicated in parenthesis.

Data type	Station name	Watershed area (km^2)	Station ID	Data source
Water levels	Sorel		15930	DFO
Water levels	Lac Saint-Pierre (Courbe No. 2)		15975	DFO
Water levels	Port Saint-François		03365	DFO
Water chemistry	Saint-François River	10176	3020031	BQMA
Water chemistry	Yamaska River	4464	3030023	BQMA
Water chemistry	Saint-François River	10176	QU02OF3004	ECCC
Water chemistry	Yamaska River	4464	QU02OG3007	ECCC
Discharge	Drummondville (Saint-François)	9630	02OF019	HYDAT
Discharge	Saint-Hyacinthe (Yamaska)	3334	030345	CEHQ
Discharge	Hemming Falls (Saint-François)	9610	02OF002	HQ
Discharge	Farnham (Yamaska)	1231	030302	CEHQ
Discharge	Noire (Yamaska)	1505	030304	CEHQ
Water temperature	Trois-Rivières		03360	CHS
Weather	Nicolet		7025442	MSC
Weather	Lac Saint-Pierre		701LP0N	MSC

Table S2. Standardized coefficients for the first two linear discriminant canonical functions (LD1, LD2) for summers of 2012-2017.

	LD1	LD2
Water level	2.21	0.07
Discharge of tributaries	-0.38	0.78
Water temperature	-0.29	0.38
PAR	-0.18	-0.20
NO_3^-	-0.40	0.87
TP	0.07	-1.23
Turbidity	-0.06	0.64

Table S3. Standardized coefficients for the first two linear discriminant canonical functions (LD1, LD2) for the N budget. U_t total uptake rate, R proportional retention, V_f uptake velocity.

	LD1	LD2
Submerged aquatic vegetation (slope)	-0.81	-0.75
Discharge of tributaries	-0.89	0.64
Residence time	0.44	1.5
Water temperature	0.02	0.01
NO3- inputs	0.43	-2.98
Ut	-1.81	3.06
R	0.69	-2.12
Vf	-0.20	2.08

Table S4. Table to select fixed effect to predict ln U_t (total uptake rate, mg N m^2 d^{-1}). The model included an autoregressive structure per date (AR-1, R = 0.84) and variable intercept per year (1|year). DF degree of freedom, logLik log likelihood, AICc sample corrected Akaike Information Criterion, delta difference in AICc from best model. Ln.NO_3 ln transformed NO_3^- (mg L^{-1}), temp temperature (°C), sav submerged aquatic vegetation index (cm km^{-1}). The second model was selected given the delta AIC difference was < 2.

Fixed structure	DF	LogLik	AICc	Delta
Ln.NO_3 + sav	6	96.8	-181.3	0.0
Ln. NO_3	5	94.9	-179.6	1.7
Ln. NO_3 + sav + temp	7	96.8	-179.22	2.1

Table S5. Model to predict ln U_t (total uptake, mg N m^2 d^{-1}) from ln NO_3^- (mg L^{-1}). Phi indicates correlation between consecutive temporal observations. Std.Error standard error, marg. marginal, cond. conditional. Model was fitted using an autoregressive structure per date (AR-1) and variable intercept per year (1 |year). This random structure was used because variable intercept and slope per year as a function of NO_3^- (1 + ln.NO_3|year) had singular convergence.

Year	Parameter	Value	Std.Error	Phi	marg. R^2	cond. R^2
all	intercept	6.88	0.11	0.82	0.88	0.92
	ln.NO_3	1.42	0.05			

Table S6. Selection of random effect for the prediction of ln U_t (total uptake, mg N m^2 d^{-1}). DF degree of freedom, logLik log likelihood, AICc sample corrected Akaike Information Criterion, delta difference in AICc from best model. Ln.NO_3 ln transformed NO_3^- (mg L^{-1}), temp temperature (°C), sav submerged aquatic vegetation index (cm km^{-1}). 1|year varying intercept per year, 1 + *x*|year varying intercept and slope per year as a function of variable *x*, AR-1 autoregressive structure per date, ARMA(*p*,*q*) autoregressive moving average model where *p* in the order of AR and *q* the order of MA. The random structure 1 + ln.NO_3|year with AR-1 is absent because it was not converging.

Response	Fixed structure	Random structure	Correlation structure	DF	LogLik	AICc	Delta
ln.U_t	ln. NO_3 + temp + sav	1|year	AR-1	7	90.5	-166.5	0.0
		-	AR-1	6	88.6	-164.9	1.6
		1 + temp|year	AR-1	9	90.0	-161.3	5.2
		1|year	ARMA(1,1)	10	70.6	-126.7	39.8
		1|year	ARMA(2,0)	10	71.0	-125.5	41.1
		1 + ln.NO_3|year	-	8	-2.0	20.6	187.1
		1 + temp|year	-	8	-8.0	32.6	199.2
		1|year	-	6	-12.5	37.3	203.9
		1 + sav|year	-	8	-12.5	41.6	208.1
		-	-	5	-55.0	120.2	286.8

Table S7. Summary table of uptake rate and uptake velocity measured in rivers and riverine vegetated meadows. Dominant vegetation that are not submerged are denoted by F (floating) or E (emergent). For uptake rates, one number in parenthesis indicate the standard deviations and two the range.

Ecosystem	Size of river or water inputs	Dominant vegetation	Vegetation size and location	Method	Process	Uptake rate (mg N m^2 d^{-1})	Uptake velocity (m d^{-1})	Time and sampling frequency	Reference
USA and Denmark rivers (metaanalysis)				N_2 flux and acetylene inhibition	Denitrification	80 (42-134)		rate averaged over a year	(Piña-Ochoa & Álvarez-Cobelas, 2006)
USA, Europe and Antartica rivers (metaanalysis)				N_2 flux, acetylene inhibition, 15N addition	Denitrification	249 (0-1143)		daily rate at maximum yearly water temperature	
Hudson River (USA)	490 m^3 s^{-1}	*Vallisneria americana*	dense beds over 0.6 km^2 in the main channel	in situ N_2 production	Denitrification	0		daily rate at annual maximum biomass	(Tall et al., 2011)
		Trapa Natans (F)	dense beds over 1.5 km^2 in a bay		Denitrification	(518-994)			
Mincio River (IT)	10-12 m^3 s^{-1}	*Vallisneria spiralis*		incubation, isotope pairing in sediment cores	Total retention	175 (53)		monthly measurements over a year	(Pinardi et al., 2009)
					Denitrification	106 (24)			
		Bare sediments			Total N retention	66 (33)			
Fisha River (AT)	2nd order, 1.2 m^3 s^{-1}, 250 km_2	*Berula erecta*	80-90% cover over 6.3 km^2 in the main channel	mass-balance with grab samples	Total N retention	840 (630)		monthly measurements over a year	(Preiner et al., 2020)
			45% cover over 6.9 km^2, main channel			510 (1330)			
		Bare sediments	12.9 km^2, main channel			170 (440)			

		Berula erecta	80-90% cover over 6.3 km², main channel	mass-balance with grab samples and O_2 sensor	Denitrification	690 (220)			
		Bare sediments	12.9 km², main channel			270 (140)			
Ichetucknee River (USA)	20 $m^3 s^{-1}$	*Sagittaria kurziana* and *Vallisneria americana*	dense beds over 0.154 km² in the main channel	mass-balance with one station NO_3^- sensor	Denitrification	568 (10)		daily rate during spring	(Heffernan & Cohen, 2010)
						288 (16)		daily rate during fall	
				NO_3^- sensor	Assimilation	131 (2)		daily rate during spring	
						58 (4)		daily rate during fall	
Mississippi backwater lake	2 $m^3 s^{-1}$	*Ceratophyllum demersum*, *Lemna* sp. (F), *Nymphea odorata* (F)	65-80 % of lake surface area	mass-balance with grab samples	Total N retention	137 (20-480)		biweekly sampling over the growing season	(James, 2010)
				Sediment flux assays	Denitrification	93.7			
Aa River (BE)	1-3 $m^3 s^{-1}$, 25 km²	*Potamogeton natans*, *Callitriche platycarpa* (F)	dense bed on a 1.5 km² strech	mass-balance with grab samples and assimilation experiment	Assimilation	(0.07 - 0.46)		seasonal sampling over 2 years	(Desmet et al., 2011)
Agricultural streams (DK)	3-4 order	*Sparganium erectum* (E)	100% cover	in situ isotope pairing in benthic chambers	Denitrification	35 (18-64)		3 monthly sampling	(Audet et al., 2021)
		Berula erecta (E)			Denitrification	35 (18-54)			
		Callitriche sp.			Denitrification	10 (2-18)			
		Ranunculus aquatilis			Denitrification	3 (0-23)			
		Bare sediments			Denitrification	1 (0-4)			
Upper Snake (USA, main river and streams)	7^{th} order, 12 $m^3 s^{-1}$	-	-	in situ pulse addition	Total N retention		(0.6-13.0)	once during summer	(Tank et al., 2008)

St. Lawrence River (CA)	9640 $m^3 s^{-1}$, 8^{th} order	*Vallisneria americana*, *Potamogeton richardsonii*	Dense beds over 10 km^2 at a confluence zone	mass-balance with one station NO_3^- sensor	Total N retention	576 (60-3893)	3 (0.2-160.8)	daily measure over 5 growing seasons (June-September)	This study
					Denitrification	338 (1-2624)	1.6 (2.8 - 104.5)		
				NO_3^- sensor	Assimilation	256 (15-1875)	1.4 (0.1-21.2)		

Chapitre 3 – Tendances et facteurs globaux déterminant les quantités de végétation aquatique submergée dans les lacs

Global historical trends and drivers of submerged aquatic vegetation quantities in lakes

Morgan Botrel[1,2] and Roxane Maranger[1,2]

[1] Université de Montréal, Département de sciences biologiques, Complexe des sciences, 1375 Avenue Thérèse-Lavoie-Roux, Montreal, QC Canada, H2V 0B3

[2]Groupe de recherche interuniversitaire en limnologie (GRIL)

In revision at *Global Change Biology*

Data openly available on Zenodo, https://doi.org/10.5281/zenodo.6502355

Abstract

Submerged aquatic vegetation (SAV) in lake littoral zones are an inland water wetland type that provides numerous essential ecosystem services, such as supplying food and habitat for fauna, regulating nutrient fluxes, and stabilizing sediments. However, little is known on how inland SAV quantities are changing globally in response to human activities, where loss threatens the provisioning of these ecosystem services. In this study, we generate a comprehensive global synthesis of trends in SAV quantities time series from lakes and identify their main drivers. We compiled trends across methods and metrics, integrating both observational and paleolimnological approaches as well as measure of SAV quantities, including extent, density or abundance classes. The compilation revealed that knowledge on SAV is mostly derived from developed countries, with major gaps in tropical, boreal and mountainous lake-rich regions. We found a tendency similar to other wetland types where in 41 % of times series SAV is largely decreasing mostly due to land use change and eutrophication. SAV is, however, increasing in 28% of cases, primarily since the 1980s. We show that SAV trends and drivers vary regionally, with increases in Europe explained largely by management of lakes, decreases in Asia as a function of eutrophication and land use change, and variable trends in North America due to invasive species arrival. By providing a quantitative portrait of SAV trends worldwide, we indicate knowledge gaps and future SAV research priorities. By considering the drivers of different trends, we also offer insight to future lake management related to climate, positive restoration actions, and change in community structure on SAV quantities.

Graphical abstract

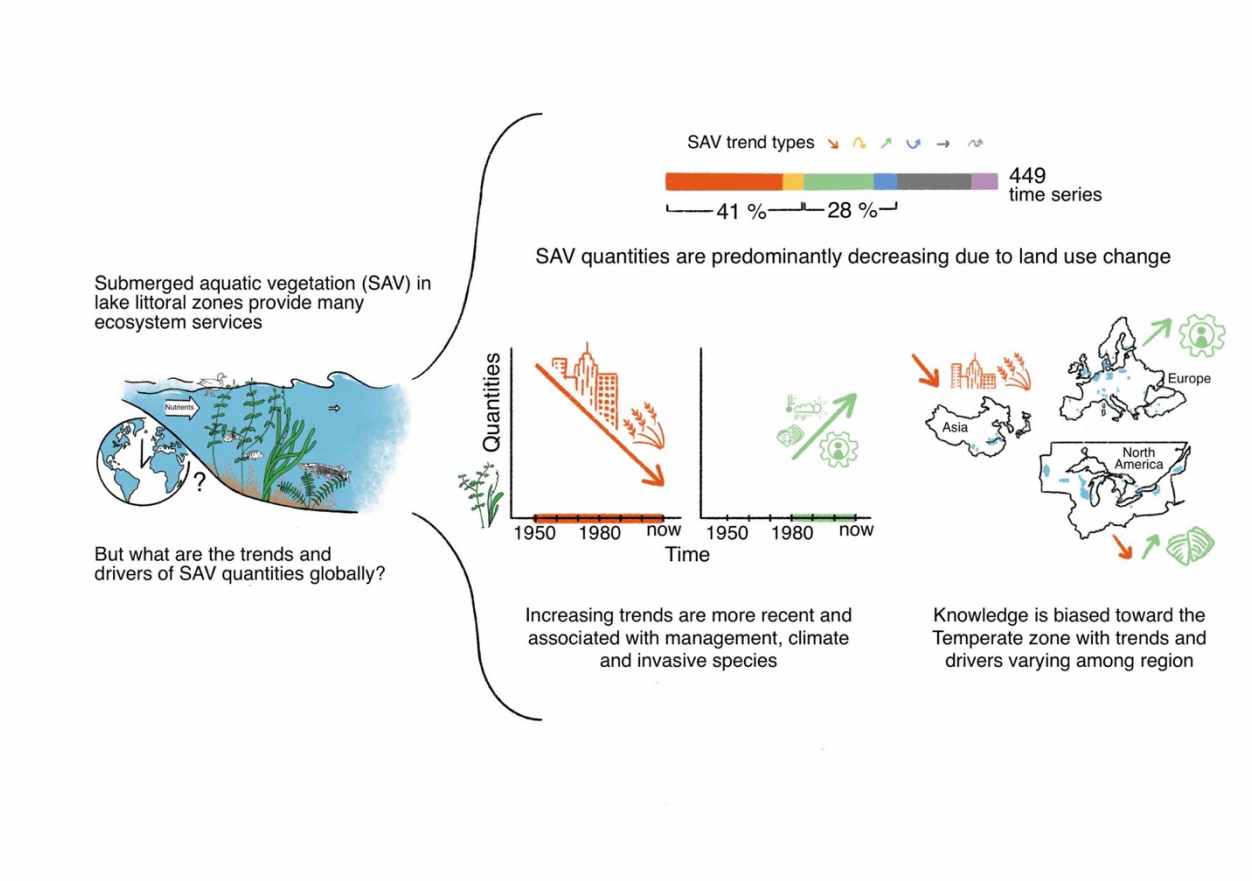

Introduction

Inland wetlands are ecosystems with among the highest rates of global decline, which given their social and ecological value, has led to a wide range of conservation and restoration initiatives worldwide (MEA, 2005; Rattan et al., 2021). These wetlands include peatlands, marshes, and swamps, but also the underwater vegetated zones surrounding lakes and rivers. Submerged aquatic vegetation (SAV) creates a typically unrecognized and understudied wetland type located within the littoral zones of many aquatic ecosystems, which is distinctive from open-water habitats (Gopal, 2016; Vander Zanden & Vadeboncoeur, 2020). Much like the representative plants of other wetland types, SAV is a foundational habitat that modifies the functioning of inland waters, delivering high-value ecosystem services such as providing food, promoting water clarity through particle settling, and stabilizing sediments, which strongly regulates nutrient and carbon cycling (Janssen et al., 2021; Jeppesen et al., 1998; Orth et al., 2017). However, global assessments of inland water SAV littoral extent and trends through time are lacking. The underwater nature of SAV has conceptually and practically hampered these assessments. Wetland classification schemes are limited to emergent vegetation, and typically lump SAV with open-water habitats more generally (e.g. FGDC, 2013; Gopal, 2016; Ramsar Convention, 2012). Furthermore, limnologists that study inland waters have traditionally focused research on the pelagic zone and have tended to neglect littoral areas (Vander Zanden & Vadeboncoeur, 2020). Mapping inland SAV is a challenge that has restricted global assessments as airborne or satellite remote sensing cannot detect plant canopies deeper than a few meters in turbid waters (Rowan & Kalacska, 2021). Additionally, the one reported global littoral assessment has lumped SAV with marsh-type, emergent and floating aquatic plants (Zhang et al. 2017). Given that broad scale assessments of inland waters do not distinguish littoral from open-water areas or SAV from other aquatic plants (Davidson, 2014; Hu et al., 2017; Lehner & Döll, 2004, Zhang et al. 2017), our understanding of how SAV in inland littoral zones of lakes are changing in response to human activities remains fragmented.

In contrast to inland SAV, thorough compilations of changing aerial extents exist for seagrass meadows, their underwater marine counterpart, and are linked to various anthropogenic drivers (Dunic et al., 2021; Waycott et al., 2009). In freshwaters, extents compiled for all aquatic plant types, including emergent and floating, were found to be declining (Zhang et al. 2017). This is in contrast to individual studies monitoring inland SAV quantities that suggest, similar to reports on seagrasses, that temporal changes are dynamic and vary according to location. Some show widespread regional

declines (Korner, 2002; Sand-Jensen et al., 2000) whereas others observe increases (Vermaire & Gregory-Eaves, 2008), which may include successful restoration actions of lost habitats (Hilt et al., 2018). The contrast could be due to the different plant groups considered, differences among methods and time periods assessed or a bias in aquatic plant records toward Temperate regions and China. To increase the number of SAV time series and widen the geographic range, one possibility is to consider the different metrics to measure SAV quantities, as and they can be reported as areal extent (e.g. Wang et al., 2019), percent volume inhabited (or 'infested' – PVI, e.g. Hanlon et al., 2000), ordered abundance class (e.g. Beklioglu & Altinayar, 2006), or density (e.g. Xiao & Liu, 2013). Additionally in lakes, SAV changes can be reconstructed from sediment archives using paleolimnological techniques (e.g. Ayres et al., 2008; Davidson et al. 2005). Although the latter provides a longer time frame than direct observational methods, the two can overlap at the decadal scale (Smol 1992; e.g. Kornijów et al. 2016; Madgwick et al. 2011). The challenge is then to find a way to compare the results among these different methods and metrics to determine worldwide spatiotemporal patterns in inland water SAV quantities.

Because global SAV trends are unresolved, we also know little about the drivers of SAV changes at broader scales. Indeed, various human activities impacting nutrient inputs, water levels and trophic community structure can have a negative effect on SAV. However, SAV ecology and the environmental variables controlling their quantities have been mostly described locally, particularly in shallow lakes (Wetzel, 1990). A central conceptual framework in SAV ecology is alternative stable state theory that highlights the key role of light and its interaction with nutrient inputs, water level and trophic interactions in regulating SAV quantities (Scheffer et al., 1993). In this framework, the temporal variability in long-term SAV quantities is a function of eutrophication history where an increase in nutrients favors high phytoplankton biomass or the proliferation of epiphytes that shade SAV, eventually leading to their collapse. The few regional assessments of changes in SAV quantities have been largely attributed to this eutrophication effect or to its reversal (e.g. Korner, 2002; Sand-Jensen et al. 2000; Vermaire & Gregory-Eaves, 2008; Vermaire et al. 2012; Hilt et al., 2018). However there is evidence of a unimodal relationship with eutrophication, where a moderate increase in nutrients in pristine ecosystems stimulate SAV growth before having a negative effect. Furthermore, the alternative stable state theory indicates that a reduction in water levels tends to promote SAV expansion through greater light exposure to bottom sediment, while a change in community structure could lead to a decline when the new species promotes higher turbidity, like benthivorous fish that resuspend sediments. In contrast, new species can facilitate SAV growth when they favor

clear water, like the addition of piscivorous fish that can indirectly regulate phytoplankton quantities through a trophic cascade. These top-down effects can also control SAV quantities through the modification of macroinvertebrate grazers and epiphytes (Phillips et al., 2016). Although the mechanisms of how these individual factors control SAV are known and we are learning about the effect of combined stressors (e.g. Vijayaraj et al., 2022), how human activities shape these environmental factors across space and time is yet to be determined.

Therefore, our objective is to characterize how SAV quantities in lakes have changed globally in response to human activities at longer term time scales. To do so, we synthesize trends, measurement methods and metrics of SAV time series, and report the global distribution of trends and mains drivers of change. As we were interested in human influences on SAV in inland waters, time series from 1850 onward, where anthropogenic activities have more significantly impacted the planet, were used (i.e. the Anthropocene, Steffen et al., 2015). As a preliminary survey showed that most SAV studies were conducted in lakes rather than lotic ecosystems, our study focuses on lakes. This finding is consistent with a recent review on macrophyte macroecology (Alahuhta et al. 2021) and earlier development of theories on eutrophication and alternative stable states where SAV plays a central role, compared to their more recent application in rivers (Hilt, 2015; O'Hare et al., 2018). By applying a novel trend typology approach, we synthesized information from observational and paleolimnological studies from 431 lakes, creating the most comprehensive spatial dataset on freshwater SAV time series trends and main drivers of change to date.

Methods

Using a literature search, we compiled a data set describing SAV quantities time series from lakes and reservoirs at the decadal time scale, synthesizing trends across observational and paleolimnological methods (Figure 1). Inspired by similar work on seagrasses (Waycott et al, 2009), references on SAV time series were identified using a keyword search on Scopus in November 2018 of the following terms describing SAV (macrophyte* or hydrophyte* or "submer*e* aquatic vegetation" or "submer*e* plant*" or "aquatic plant*"), lentic water bodies (lake* or pond or billabong or reservoir) and potential changes (cover or map or paleolimnology or "remote sensing" or "aerial photograph*" OR biomass or area or trend or long-term or historical or change or change or proliferation or increase or gain or decline or loss or recovery or stability or dynamic or impact). To restrict the search, we excluded terms in reference to marine, riparian or riverine habitats (not (seagrass* or tidal or marsh or riparian or river or marine)). This resulted in 2197 bibliographic records that were exported on EndNote X9 (Clarivate™) and first screened using title and abstract. To compare observational and paleolimnological approaches, we used titles and abstracts to remove either longer term millennial studies describing Holocene dynamics prior to 1850, or short term studies lasting less than a year, concentrating on those that covered decadal time frames. We also removed studies when results were from experimental assays, models or describing other types of aquatic plants (emergent and floating) or organisms.

The full texts of the remaining 510 documents were screened a second time to extract trend information. For this detailed data extraction, references were removed using similar criteria as for the first screening as well as when SAV changes were focused on diversity, when a single invasive SAV was described, or when SAV could not be distinguished from other growth forms. Reference bibliographies were also scanned. Two documents were examined in detail for additional SAV trends as they were peer-reviewed syntheses on SAV restoration (Hilt et al., 2018), and aquatic vegetation extent changes in lakes (Zhang et al., 2017), with references from the grey literature. These syntheses provided valuable information for lakes located in Germany, Denmark, England, the Netherlands, and China. When documents cited in the syntheses were not available due to either a language barrier or limited accessibility to grey literature, trends were extracted directly from the synthesis. A book chapter (Scheffer, 2004) reviewing SAV stories in lakes, was also instrumental in identifying SAV time series. We also accessed regional SAV monitoring datasets from the North Temperate Lakes LTER (Long Term Ecological Research network, Magnuson et al.,

2016a; Magnuson et al., 2016b; Nichols, 2021), the New Zealand NIWA (National Institute of Water and Atmospheric Research, de Winton, 2018) and the United Kingdom Broads Authority (Broads Authority, 2013; Tomlinson et al., 2019). Several references were identified that were promising, but data on SAV trends were not accessible (Supporting information, SI, Text S1).

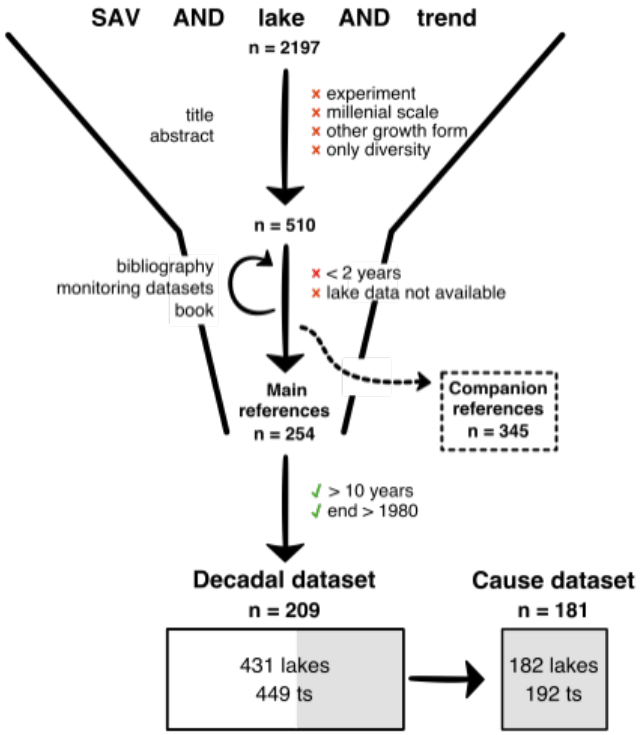

Figure 1. Filtering process for literature search and reference selection for the creation of the decadal scale and associated cause datasets compiling data describing SAV quantities time series. The grey areas illustrate that the cause dataset is a subset of the decadal dataset. Ts time series.

From the identified references, we compiled information on lake location and characteristics, SAV trends, methods, and measurement metrics as well as causes of observed trends. When a given lake had a SAV time series reported in multiple references, all were used in extracting pertinent information. For lake identification and to avoid duplication, lake coordinates were extracted from Google Maps from any geographic information available in the original references. Any information on lake shape, watershed, and contemporary trophic status were also noted from the texts. For a number of lakes, information on lake mean depth (n = 132), lake area (n = 73) and watershed area (n

= 189) were derived from the HydroLAKES dataset (Messager et al., 2016) using the select by location option in QGIS (QGIS.org, 2019).

We characterized SAV trends as how their quantities were changing through time using a visual classification of six possible trend types (Figure 2). These categories were determined during data extraction as we observed that the simple increasing, decreasing, and stable trends did not capture time series with inflection points and more complex trajectories, such as unimodal, recovery, and oscillating trends. As we were interested in relating changes in SAV to their drivers, we characterized and compared the shape of SAV trajectories, not just end points and rate of changes. To decide whether a time series had a directional change in SAV and was not stable, we looked for high magnitude differences between SAV quantities data points. For example, a trend was considered an oscillation not only when quantities were noticeably increasing and decreasing, but also when shifts were very abrupt i.e., going from almost no vegetation to sudden high quantities. These were usually indicated by the study authors. For paleolimnological data, changes were determined from inferred SAV quantities or the proxies interpreted by the study authors to reflect SAV quantities. These were typically identified in the text and were most often the abundance of fauna and flora associated to SAV (e.g. diatoms, Cladocera), SAV remains, or both. Trends were most often obvious and directly extracted from the original reference, either from the text or figures. In datasets that we needed to directly process in R (R Core Team, 2020), to visualize yearly maximum colonization depth for example (de Winton, 2018; Nichols, 2021), changing trends were assigned when interannual variations were at least of 1 m, which seemed reasonable given the typical colonization depth of 3 m. Trends were also characterized by noting the start, end, and number of years of observations.

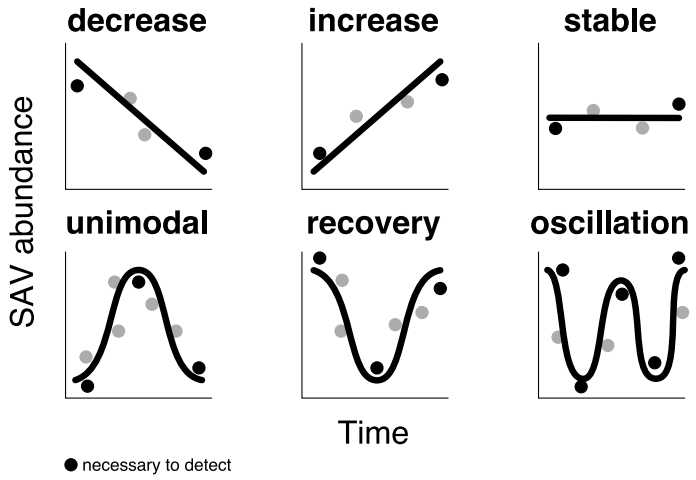

Figure 2. Typologies of SAV trends and minimal number of observations for their classification at the decadal scale.

SAV time series were largely reported from repeated field surveys, remote sensing or from variation in paleolimnological indicators. Surveys included the assessment of SAV from a planned sampling using either visual estimation of cover or from plant harvest. Remote sensing included any plant detection from a sensor at a distance, either optical or acoustic. Paleolimnology referred to the evaluation of SAV from fossils in the sediment archives. Sometimes, however, the information on SAV was from oral reports or old photographs and these were classified as 'historical knowledge'. For others, the method could not be determined and was classified as 'unknown'. This sometimes occurred when the reference was in another language than English, French or Spanish, i.e. languages known by the authors. Many paleolimnological studies combined direct methods (survey, remote sensing, historical knowledge) with sediment archives and were classified as 'paleo+'. Regardless of methods, we also noted the scale within the lake at which SAV quantities were reported and metric used. Scale was noted as either 'global' or 'local' or both as SAV was typically measured over the entire lake and/or only within the littoral zone. The metric types were classified as 'cover' when SAV extent was reported as area and proportion of lake bottom with SAV or as maximum colonization depth. 'Abundance' referred to SAV quantities reported using classes (e.g. low, medium, high), relative abundance, abundance scores or frequency of occurrence, while 'density' referred to biomass measurements, and 'fossil' represented sedimentary indicators of SAV (e.g. diatoms, benthic macroinvertebrates, SAV remains) used in paleolimnology.

Trend causes were determined from the abstract and main text. Various causes were identified and classified into broad categories to facilitate interpretation as a root cause rather than a precise environmental variable. For example, many studies reported changing nutrient levels (environmental variable) resulting in eutrophication. When eutrophication was related to increased agricultural or urban areas within watersheds, we categorized the driver as 'land use' (root cause). Land use was expanded to also include water use and further subdivided in more specific categories describing the process impacting SAV (e.g. 'browning', 'siltation', 'eutrophication') or direct lake use resulting in increased turbidity ('aquaculture', 'navigation'). Other categories of causes were 'management', 'biotic', 'climate' and 'geomorphology'. Management included any deliberate change to the lake with the goal of controlling SAV. Management aiming at reducing SAV always occurred within lakes (e.g. using herbicide or harvest), while efforts attempting to restore SAV involved management actions both in the lake and within its watershed, and these were classified in different subcategories (SAV reduction, restoration internal, and external). Changes in SAV driven by invasive alien species or a change in community structure were categorized as biotic. These were subdivided by feeding behavior ('filter feeder', 'piscivore', 'planktivore', 'benthivore', 'herbivore') or biological kingdom ('plant') or a characteristic unrelated to foraging ('guano'). Climate referred to causes related to changes in general weather conditions and were subdivided into environmental drivers ('water level', 'temperature') or specific climate events and processes (e.g. 'North Atlantic Oscillation', 'event', 'browning'). Finally, geomorphology encompassed any changes to lake and watershed shape and associated water flow. This was subdivided as 'drainage system' (mainly dams), 'embankment', 'land reclamation' and 'drawdown'. For individual time series, up to three drivers could be identified.

The search resulted in 599 references on 665 SAV time series in 627 lakes. Some references reported the same time series, while others provided additional information. To clarify what information was extracted from each reference, we separated the references into 'main reference' and 'companion information'. We identified 254 main references that included SAV time series and associated trend cause used for this study. Each lake typically had one time series that came from one reference where the complete information was available ($n_{\text{time series}} = 581$, $n_{\text{reference}} = 182$), but an individual reference could also contain information on many lakes. Additionally, time series were sometimes determined based on multiple documents that had continuous, non-overlapping and comparable data given the similar metrics for SAV quantities used. When lakes had multiple time series with metrics that could not be compared (e.g. biomass versus colonization depth), they were

recorded as distinct time series, and these typically had limited time overlap. Some large lakes (e.g. the Great Lakes) had multiple time series at different locations within their shoreline (e.g. in basins or bays). The companion information dataset included 345 documents that either had trend information that was similar but on a shorter time scale than the associated main references, or additional information on lakes and SAV related environmental variables. To limit duplicate entries and errors, all data were integrated in a relational database framework using PostgreSQL and are openly available (Botrel & Maranger, 2022). This overall global metadata of SAV time series includes trends beyond those used in this study as we provide all the information that was found with a minimum of two observations over two years. The intension is to share and grow it over time to serve future research.

Statistical analysis

For this study, we focus on decadal scale trends that include a time span of 10 years or greater, ending after 1985 (209 main references, 449 trends in 431 lakes, Figure 2). In a subset, causes were identified (181 main references, 192 trends across 182 lakes). Significant differences among categories were assessed using Kruskal-Wallis tests, and pairwise differences using Wilcoxon tests with Holms corrected p-values calculated from the R package ggpubr (Alboukadel, 2020). χ^2 goodness-of-fit tests was used to assess associations between two categorical variables. Prior to testing, categories with fewer than 10 observations were removed. For graphical representation of association, we only represent X^2 residuals under -1 or above 1.

Results

Global distribution of trends

By compiling time series of SAV trend typologies that spanned 10-years or longer, we found that SAV decreasing and unimodal trends, were the most common, accounting for 41% of time series overall (Figure 3). The remaining two thirds were equally divided between those that increased and recovered, and those with no clear directionality (stable, oscillation). Trend types covered different time frames. This was more a function of start year, as the median end year of 2006 was similar across all trend time series (p = 0.15). Decreasing and stable trends started around 1950, while increasing trends started later, around 1980 (p < 0.01). As a result, time series of decreasing and stable trends tended to be almost two times longer compared to increasing ones with a median time span of 46 and 28 years respectively. Recovery and oscillation trends, which included two types of monotonic changes (increasing and decreasing), lasted ~32 years and started in ~1977. As expected, trends also had a different number of observational years, where the simpler trends (decrease, increase, stable) typically had fewer observations compared to those with inflection points. Unimodal and recovery had 8-9 observations, oscillation up to 16 (p < 0.01, Figure S1). However, simple increasing trends had significantly more observations (median = 5) than decreasing and stable ones (median = 2).

Trends were derived from predominantly small and shallow lakes as the median area and mean depth were 0.6 km^2 and 2.6 m (SI Table S1), respectively. Our dataset, however, also covered large lakes up to 3753 km^2 (Poyang Lake, China). Two third of the lakes where we could identify contemporary trophic status (n = 299, n missing = 150) were classified as eutrophic or hypereutrophic, while 21% were mesotrophic and 9% oligotrophic. The majority of aquatic ecosystems used in this synthesis were natural freshwater lakes. Artificial lakes constituted 15% (68) of the total, and were mostly infilled excavation ponds from peat mining or polder lakes (in the Netherlands). Other ecosystem types included 15 reservoirs and five saline lakes, with the latter ones being enclosed coastal lakes with some seawater intrusion.

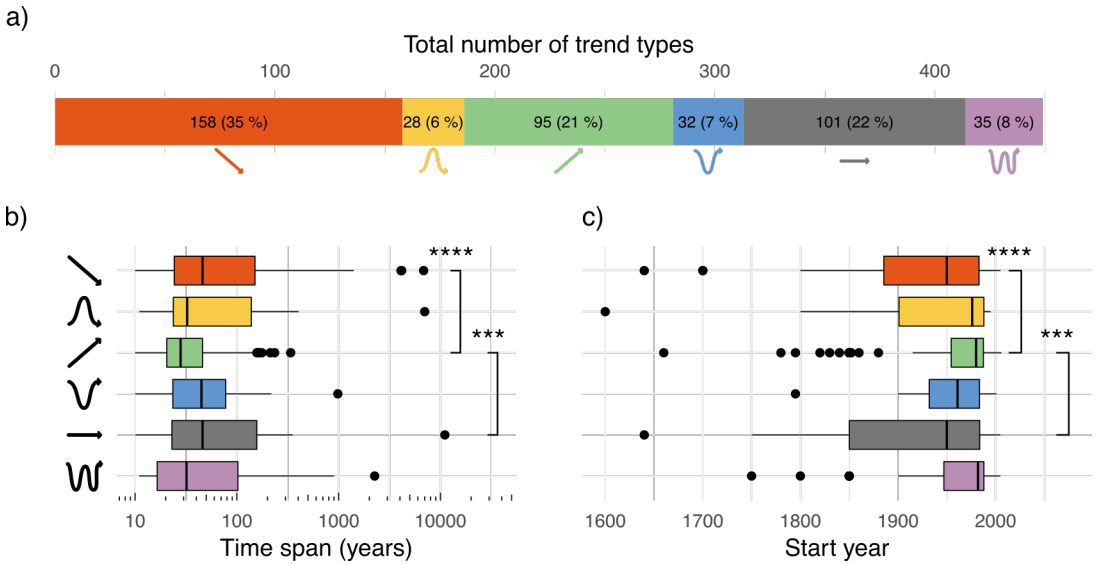

Figure 3. a) Total number of time series per trend type and their relative proportional distribution; b) length and range of time series and c) start year per trend typology. Vertical bars within boxes indicate median value, box boundaries represent 25th and 75th percentile and whiskers range from 10th to 90th percentiles. *** $p < 0.001$, **** $p < 0.0001$

SAV time series were also not uniformly distributed in space (Figure 4). Only two lakes where trends could be compiled were from South America and seven from Africa, while the remaining lakes were mostly from OECD (Organization for Economic Co-operation and Development) countries, including those from Europe, Oceania, and the USA. Within these general areas, sampled lakes were also clustered into specific countries or states. In Europe, lakes were particularly abundant in Italy, Great Britain, Germany, Denmark and the Netherlands, whereas in North America, lakes were mostly from the temperate lake regions of Wisconsin, Minnesota, New York (USA) and southern Quebec (CA). In Oceania, lakes were mostly from the northern New Zealand island, while lakes from Australia were all along the Murray-Darling river. Lakes in Asia were predominantly from the China Changjiang (Yangtze) river basin or the southern Yunnan province. In addition to the clustered spatial distribution, the trend types were associated with specific geographic regions ($X^2(df=15, n=449) = 36.9$, $p = 0.001$, Figure S2). In particular, Asia had two times more declining trends (68%) than expected compared to other continents and had no stable or oscillating trends recorded, exceptionally contributing to the X^2 score (51%). In contrast, North America had more stable (30%) and unimodal trends (10%) that were counterbalanced by a reduced number of decreasing trends (27%). Recoveries were overrepresented only in Europe (9%) and were compensated by fewer unimodal trends in that region.

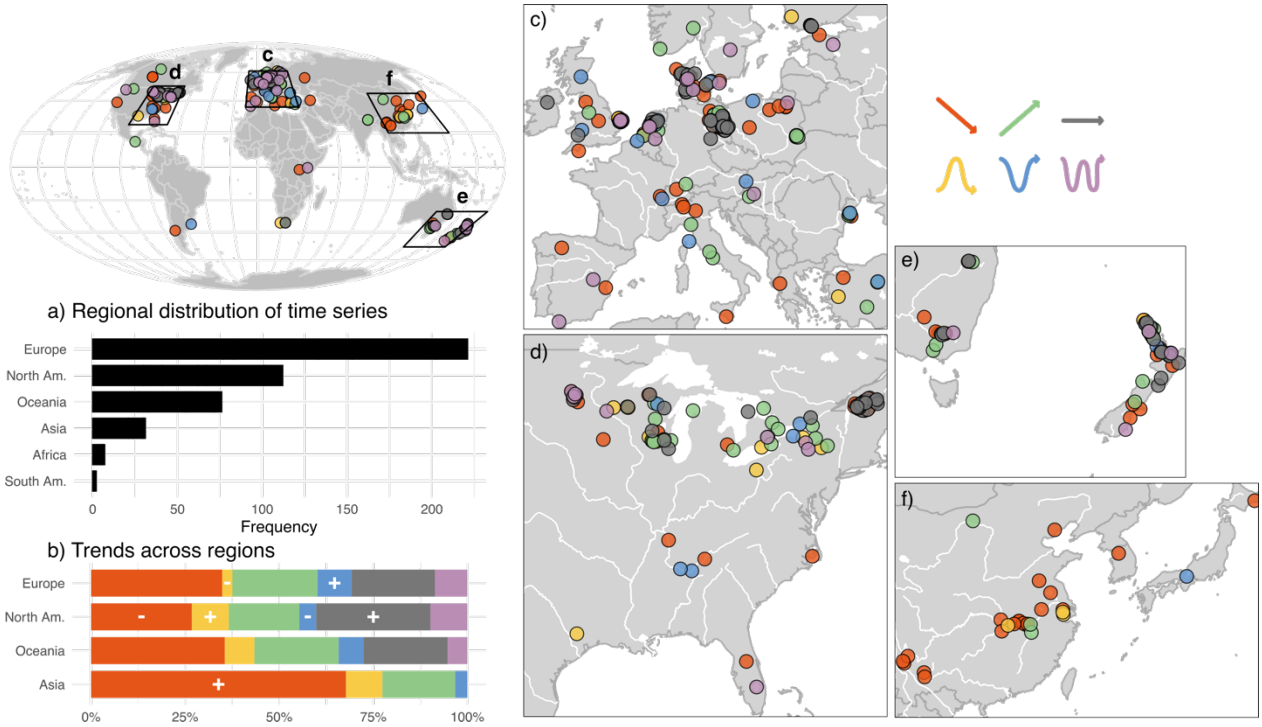

Figure 4. Geographic distribution of SAV time series showing a) regional distribution of time series, b) comparison of trend types across regions and c)-f) location of time series and their associated trend types. + and – indicate if proportion of trend type is more or less than expected compared to other continental regions and is shown for X^2 residual < -1 and >1.

Comparability of SAV trends

As methods to measure SAV were disparate, we compared the different methods and metrics used and how they were associated to various trend characteristics. The majority of time series were extracted from surveys (54%, 241), while 28% (126) were from paleolimnology and paleo+ combined. The remaining 18% (82) were from either remote sensing, combined direct observations, historical knowledge or unknown methods. Unsurprisingly, the use of either direct observational methods or paleolimnology created distinctions in the studied time scale, with paleo studies starting earlier (median = 1850) and lasting longer (median = 153-157 years) than direct observations ($median_{start}$ = 1966-1983, $median_{span}$ = 10-25 years, Figure S3). Only paleo+ studies had a higher number of observations compared to direct observations ($median_{paleo+}$ = 16, $median_{direct}$ = 2-8) given that studies using paleolimnology had a median of two observations as one reference had many lakes with two observations per lake. Methods also differed in space ($X^2(df = 18, n = 449) = 132.3$, $p < 0.0001$, SI Figure S4), with overall higher use of direct observations in Europe, Asia, and Oceania and higher use of paleolimnology in North America. In Oceania, methods were regionally distinct with time series from Australia measured using solely paleolimnology, while in New Zealand a majority were from surveys. Methods were also associated with specific trends ($X^2(df = 30, n = 449) = 131.9$, $p < 0.0001$, SI Figure S5), with direct observational methods detecting more increasing and recovery trends while paleolimnology and paleo+ detected more of the other trend types.

SAV changes were most often measured at the scale of the entire lake (78%, Figure S6), but 14% of time series were only measured within specific littoral areas. When considering those at the lake scale only, change in SAV areal cover was the most common metric used (51%), followed by abundance (28%), and fossil proxies (20%). These created differences in the detections of trends ($X^2(df = 10, n = 399) = 56.8$, $p < 0.0001$). Cover metrics were more sensitive and detected more diverse trend types, with noticeably more increasing (including recoveries), and fewer decreasing and stable trends than expected. Abundance metrics were less sensitive and tended to detect simpler decreasing and stable trends. Similar to cover, fossil metrics were also sensitive, but also tended to detect more the complex trends with inflection points (unimodal, oscillation).

Drivers of SAV trends

Time series for which SAV drivers could be identified had a similar spatial distribution to the trend dataset (Figure 5, SI Figure S7), except for Oceania where associated drivers were rarely reported. Over the complete dataset, land use was the dominant driver in SAV change (41%), followed by management (25%), biotic (13%), climate (12%) and geomorphology (9%, Figure 5a). These drivers of SAV changes differed in space with regionally specific associations ($X^2(df = 12, n = 323) = 56.9$, $p < 0.0001$, Figure 5b). In Europe, impacts of management were observed more frequently than expected (33%), and were counterbalanced by fewer changes associated with biotic drivers. The latter was overrepresented in North America that had almost three times more changes related to biotic drivers than expected (31%), contributing the most to the X^2 score (35%). This more dominant regional effect resulted in a reduced impact from the influence of land use and climate on SAV trends. In Oceania, land use was the dominant driver, while in Asia, climate and geomorphology were more important as compared to other regions. Within regions there seemed to be coherent patterns in which drivers most influenced SAV changes (SI Figure S8). In Europe, management was mostly in central Europe while climate drivers occurred with greater frequency in the Northern and Southern range of sampled lakes. In North America, changes from biotic drivers were all within or close to the Great Lakes. In Asia and Oceania, land use and geomorphology were observed across individual river basins, while climate impacts were observed in lakes sampled toward the East.

In addition to differences in space, drivers emerged over different time scales. Land use and geomorphology had a longer time span (~69-56 years) because of an earlier start in tracking (~1925-1959) and presumed influence on SAV. Management, biotic, and climate started later, around 1972-1980, and spanned ~ 30-36 years (SI Figure S9). Given these temporal and spatially uneven distributions, specific trend types were more associated with particular drivers ($X^2(df = 16, n = 323) = 83.5$, $p < 0.0001$, Figure 5c). About half of decreasing trends were associated with land use change and 15% with geomorphological alteration, contributing strongly to the X^2 score (21%). Decreases were also rarely explained by management and climate. Unimodal trends had similar associations than decreasing trends but with a larger number of trends explained by drivers other than land use or geomorphology. In contrast, increasing trends were explained by management, biotic and climate, which were not associated to decreases. However, the more complex trends of recovery and oscillation were associated with management.

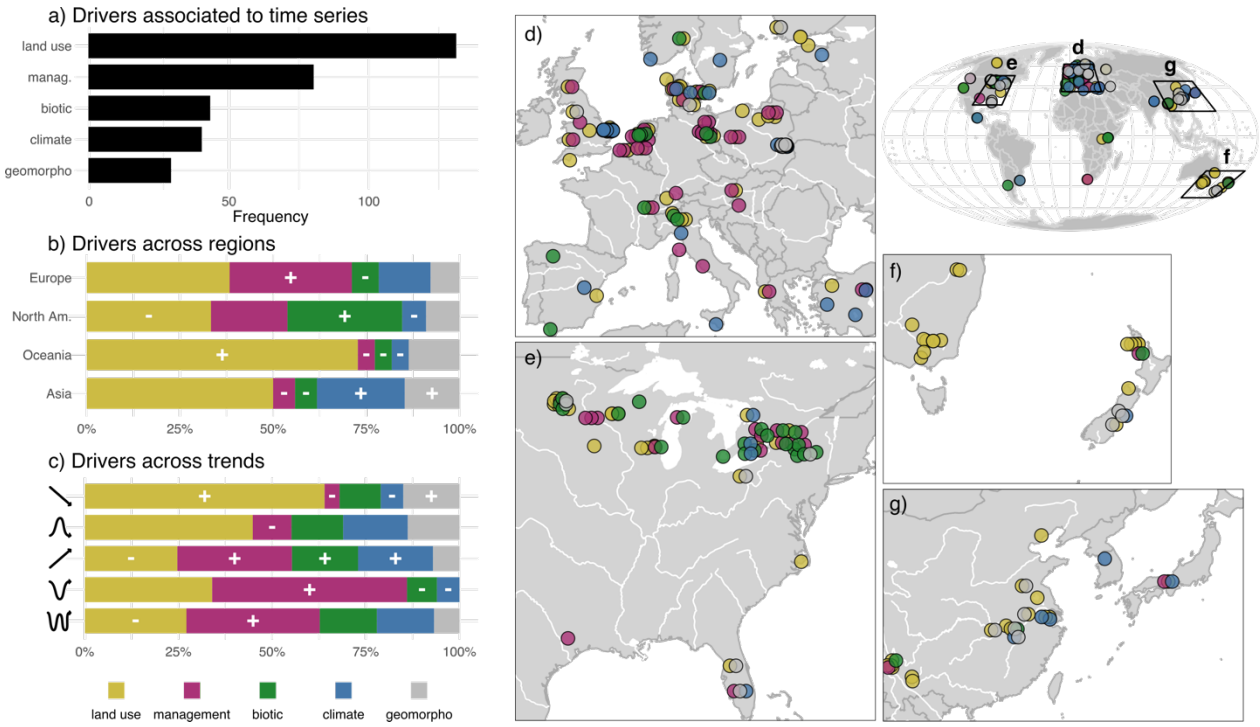

Figure 5. Geographic distribution of SAV drivers represented as a) frequency of occurrence, b) comparison across regions, c) comparison of drivers across trends and d)-g) location of time series and their associated drivers. For each time series, up to three drivers could be identified. When this was the case, points were jittered longitudinally to visualize the multiple causes. Manag. management, geomorpho. Geomorphology, North Am. North America.

By looking at more details within driver subcategories, we observed that some had a more consistent trend influence, while for others, consequences on SAV trends were diverse depending on the variable at play. Land use and geomorphological changes generally were associated with declines, mostly through eutrophication (SI Figure S10). In contrast, management from reduction of nutrient inputs to lakes (external restoration) was associated with clear SAV expansion (increasing, recovery) as compared to restoration actions within lakes that lead to more oscillating trends (Figure 6a). The effect of biotic drivers depended on the organism associated with the change, with those promoting water clarity improving SAV (Figure 6b, SI Table S2). Among facilitating species were zebra and quagga mussels (*Dreissena*) that directly increased water transparency through filter feeding, but also piscivorous fish that reduced phytoplankton through

a trophic cascade effect. In contrast, benthivores associated with SAV decline directly decreased transparency through sediment resuspension, while planktivores increased phytoplankton abundance, also through a trophic cascade. Increases in bird droppings (guano) were also associated with a SAV decline related to animal mediated eutrophication and reduction in light availability. Arrival of invasive plant species (*Egeria densia*, *Elodea canadensis*, *Hydrilla verticillata*) were associated with increasing SAV, while decreases sometimes co-occurred with arrival of various herbivores (birds, insects, crayfish, fish) directly removing SAV.

Changes brought by climate depended on the specific environmental variable at play (Figure 6c). Increases in temperature were associated with an increase in SAV, where warmer conditions and a longer growing season favored SAV range expansion (e.g. of *Ranunculus trichophyllus* Chaix. in the Himalayas above 4000 m.a.s.l., (Lacoul & Freedman, 2006). Storm events were more associated to SAV decreases through increasing water levels and turbidity. Indeed, the most frequent climate effect was water level change, where outcome in SAV directionality varied depending on whether water level was increasing or decreasing. Generally, decreasing levels were associated with increasing SAV, although this was not always the case. Changes were also often the result of broad climate patterns, like the North Atlantic oscillation (NAO), that resulted in SAV trends following these cycles through the influence of a variety of associated variables. For example, in Swedish lake Tåkern, SAV had a three-year lag with negative phase NAO causing harsh winter conditions that induced major fish kills that subsequently increased SAV biomass (Hargeby et al., 2006). In the English Broad lakes, increases in temperature and the number of sunny days were related to higher SAV coverage (Phillips et al., 2015), while in a Spanish karst lake (Lagunillo del Tejo), positive NAO phase where associated with drought and drying up of the outer ring of SAV (López-Blanco et al., 2012). Finally, the effect of browning seemed to depend on initial trophic state and was positive in an oligotrophic lake through increasing nutrient inputs associated with colored dissolved organic matter or negative in cases where there was an increased loss of light (Ejankowski & Lenard, 2015; Spierenburg et al., 2010).

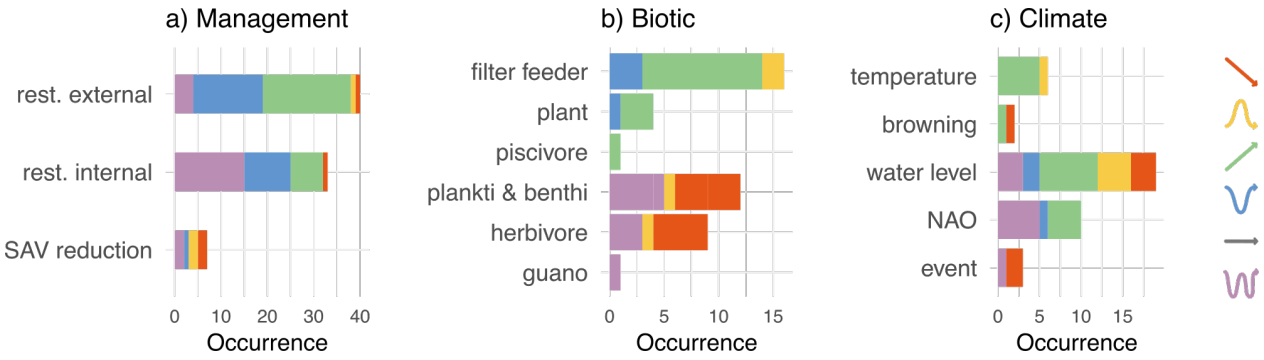

Figure 6. Drivers and associated trends showed by detailed subcategories. Rest. restoration, SAV submerged aquatic vegetation, plankti & benthi planktivore and benthivore, NAO North Atlantic Oscillation.

Discussion

In this study, we synthesized information on SAV quantities time series and their worldwide distribution. Compiling time series was a challenge given the diversity of methods and metrics used to measure SAV, but we successfully compared these different accounts by creating a simple SAV trend typology. Consistent with studies on other wetland types, SAV decline was found to be prominent globally, and in the case of SAV, were mostly due to eutrophication from anthropogenic activities, occurring either in the lake, its catchment or in both. However, we found that SAV changes were dynamic both through time and across space, where some regions exhibited consistent declines (Asia) while others (Europe) showed occasional increases in recent decades. In the last forty years, the more frequent reporting of increasing trends was associated with management actions and changes in community structure, but the factors influencing these trends varied regionally. We also found that the metric and methods adopted to report SAV quantities influenced the detection of trends, but for methods, it was more a function of the time scale they evaluated. Given the patchy and limited distribution of SAV time series across the globe, current knowledge on SAV change is biased towards temperate areas in Europe and North America, with more recent reports from China and New Zealand. As trends and driving factors vary regionally, existing information provides guidance where to fill knowledge gaps and insights on possible outcomes. This includes how positive trends related to management actions, changes in community structure, and the synergistic influence of climate, can be used to better inform restoration efforts where information is limited.

Geographic bias of SAV time series

Our compilation of SAV time series included lakes from six of the seven aquatic plant biogeographical regions, broadly corresponding to continents, with Europe, North America, South-East Asia, and Oceania being more represented than others (Chambers et al., 2008). Within these four regions, lakes tended to be concentrated in subregions (Figure 4). As more than half of time series were derived from field surveys, mostly prior to the 1980s and as early as the 17th century, this patchy distribution represents in part the development of limnology as a discipline. For example, many lakes surveyed were located in Minnesota or Wisconsin in North America or Germany, Denmark and the United Kingdom in Europe where limnological research was pioneered (Kalff, 2002). The geographic distribution of SAV time series also matched the one for combined aquatic plants (Zhang et al. 2017), albeit our approach allowed for a better overall representation, especially in Oceania. The same geographic bias was also found in a review of global distribution and diversity of aquatic plants (Alahuhta et al. 2021). We were not able to consider SAV compositional changes with our trends in quantities, as this information was highly fragmented. When comparing these SAV time series with the global distribution of lakes (Messager et al., 2016), the sample is not representative of lake population with large information gaps in the most lake-rich regions and a near absence of information in saline lakes that constitute half of global lake volume. This likely reflects where lakes are used by human populations and the presence of specific problems (e.g. eutrophication and economic interests of recreation) that can justify monitoring, while low populated areas without clear problems are not monitoring priorities. In particular, very few lakes were monitored in the richest lake region, the boreal zones (Canadian Boreal Shield, Scandinavia, and Siberia). Information was also very limited in the lake-rich mountainous regions of the Andes, Rockies, Himalaya, in the African rift lakes, and in some major tropical river floodplains like the Amazon basin. Although the accepted distribution range of SAV is said to be between 80°N and 60°S (Chambers et al. 2008), some information gaps might be due to the limited presence of SAV at higher altitudes and latitudes as well as in most tropical systems (Short et al., 2016), which remain poorly studied. In colder regions like the Arctic, lake littoral zones are typically colonized by microbial mats and reported to be devoid of vascular plants (Rautio et al., 2011). However, climate change and prolonged growing season might widen SAV distribution, as observed in the Himalayas, and may warrant monitoring at the northern and altitudinal edge of species range. In the tropics, SAV may be less dominant given the typical turbid state at lower nutrient levels and the presence of floating leaves macrophytes that can outcompete SAV for light (Feuchtmayr et al., 2009; Kosten

et al., 2009; Netten et al., 2010). Overall, these gaps highlight our poor understanding of inland SAV geographic distribution, including potential compositional changes, with most current knowledge concentrated in temperate regions of the northern hemisphere.

Methodological challenges and opportunities

Although our trend typology enabled the comparison of SAV trajectories across methods, future monitoring of SAV should aim for more consistent reporting of changing quantities, and where possible, report species compositional changes. The latter may be more sensitive to subtle environmental changes (e.g. Blindow 1992, Sand-Jensen et al. 2000), and where plant traits could influence ecosystem functions and services (Lavorel & Garnier 2004). We suggest that SAV extent as areal coverage within lakes be more systematically reported given its higher sensitivity to detect changes. This metric would allow tracking of SAV areas lost and set reasonable restoration targets. However, compiling SAV areas was challenging as often only maximum colonization depth (Z_C) was reported, but the requisite bathymetric information to estimate SAV area was not (e.g. Eigemann et al., 2016; Lachavanne et al., 1992; May & Carvalho, 2010). With bathymetric information, this depth limit could be converted into potential SAV area, where changes mitigated by light availability can be estimated from secchi measurements (Chambers & Kalff, 1985; Middelboe & Markager, 1997). Since secchi depth is a measurement often used in citizen science or monitoring programs, it could be used to predict Z_C and track changes in potential SAV area. It should be noted, however, that Z_C only represents potential SAV colonization areas as it relies primarily on light availability and does not consider the areas unsuitable for SAV development within a lake due to steep slopes or coarse substrate among others (Barko et al., 1991; Duarte & Kalff, 1990). Furthermore, plant associated epiphytes can limit SAV growth even in cases where other conditions may appear suitable for their colonization (Sand-Jensen & Søndergaard, 1981). As Z_C and secchi are standard and simple measurements of SAV and are informative when taken with caution, we do recommend their continued reporting, especially when accompanied with information on areal extents and perhaps, the presence of associated epiphytes.

Optical remote sensing techniques to detect changes in SAV areal extent is also a promising approach, at least in the 'optically shallow' areas of lakes where light reflected by underwater canopies can be detected by airborne and satellite sensors (e.g. Bresciani et al., 2012; Brooks et al., 2015; Hargeby et al., 2006; Wang et al., 2019). Because optical techniques provide information over wide spatial scales and are often available since the 1970s (e.g. for Landsat), they were predominantly

used (n = 54) for the trends in our dataset measured from remote sensing, while hydroacoustics were only used for five trends (e.g. Depew et al., 2011; Hutorowicz et al., 2017; Zhu et al., 2006). Optical remote techniques will likely become more common in assessing SAV areas with increase in the hyperspectral capacity of new satellites, and greater accessibility of drones with improved sensor technologies that could potentially be used in smaller lakes given their higher resolution (Rowan & Kalacska, 2021). In turbid and 'optically shallow' waters, reasonable SAV detection is achieved from object-based image analysis (de Grandpré et al., 2022; Krause et al., 2021). However, optical techniques poorly perform in turbid condition, being 'optically deep' at only one or two meters where hydroacoustic techniques are best suited. Similar to optical techniques, sonar technology is also rapidly developing and will likely become more accessible. The use of unmanned boats (e.g. Goulon et al., 2021), recreational-grade sonar and automatic cloud-based post-processing (Buscombe, 2017; Helminen et al., 2019; Howell & Richardson, 2019) will allow for greater aerial coverage, faster sampling, and reduced cost. The use of remote techniques, both optic and acoustic, is growing at a rapid pace particularly for the monitoring of seagrass changes (Gumusay et al., 2019; Veettil et al., 2020), and learning from the marine practices may help fast track application to inland waters. Indeed, we suggest that inland SAV researchers adopt approaches from the marine community more broadly, who recently launched a coordinated global effort to synthesize status and trends of seagrass worldwide (Coordinated Global Research Assessment of Seagrass System, C-GRASS, under the UN Environment Programme World Conservation Monitoring Centre, UNEP-WCMC). This includes the creation and application of standard protocols necessary for the intercomparison of datasets. These protocols are well developed for seagrass studies (Phillips & McRoy, 1990; Short & Coles, 2001), and could easily be applied to inland waters. Given the often high accessibility of inland waters, these could also include citizen science initiatives.

In contrast to monitoring efforts of coastal seagrass, paleolimnological approaches provide SAV assessments over much longer time scales. Given unlimited resources, paleolimnology could provide SAV times series for lakes worldwide. However, existing paleolimnological records of SAV quantities were inconsistent, as they most commonly reported indices of SAV quantities using various fossil proxies. These proxies ranged from SAV remains or spores (e.g. Kowalewski et al., 2016; Klamt et al., 2017; Volik et al., 2018) and associated flora (benthic diatoms, e.g. Davidson et al., 2013) or fauna (benthic cladocerans, chironomids, e.g. Ventelä et al., 2016; Zhang et al., 2010), but SAV dynamics were also inferred in individual studies using SAV biomarkers (n-alcane, Das et al., 2009), sponge biogenic silica (Kenney et al., 2002) or sediment C:N ratio (Stephens et al., 2018), and these

were rarely used in combination. In contrast to direct use of fossil proxies, the use of inference models to report SAV as quantities were rare. Only four studies reported SAV as either a semi-quantitative abundance estimate (Vermaire et al., 2012; Vermaire et al., 2013) or a quantitative areal cover (Bjerring et al., 2008; Johansson et al., 2005). Inference models in paleolimnology have been criticized, mainly due to biased reconstruction of non-causal relationships and overreliance on a constant relationship through space or time, and they should be interpreted more as qualitative indicators of past conditions (Juggins 2013, Whitmore et al. 2015). However, these models are useful as they simplify the complex multivariate relationship between organisms and their environment. Very few inference models for SAV were reported, but the repeated association of benthic taxa to SAV assumed in the paleolimnological studies we collected, suggest that these indicators could be used for the development of more robust inference models with multiple proxies. The availability of reliable reconstructions could facilitate interpretation and intercomparison of inferred SAV trends across lakes. Given that faunal and floral taxa used as proxies are not always associated to SAV changes related to environmental conditions (e.g. eutrophication, predation pressure, etc.), reconstruction should focus on multiproxy approaches (Jeppesen et al., 2001). Furthermore, DNA-based methods to track SAV species composition, which are currently lacking in the literature, could also be applied providing more information related to diversity changes (Domaizon et al. 2017). A list of calibration sites for the future development of these inference models is provided through our synthesis.

SAV trends and drivers of temporal and regional dynamics

We showed that SAV trends were highly dynamic in space and associated with different drivers, with the most common trend being a decrease associated to factors resulting in eutrophication. The overall decrease in SAV observed here is in agreement with a previous global aquatic plant study, although they did not identify drivers or discern SAV from other plant types (Zhang et al. 2017). Compared to other drivers, eutrophication was detected in our earlier records. Eutrophication was largely a function of land use change, including agricultural or urban development in catchments (e.g. Bennion et al., 2015; Rosińska & Gołdyn, 2018; Zhang et al., 2010), but also to within lake aquaculture (Kraska et al., 2013; Liang & Zhang, 2011) and boating activities (Bresciani et al., 2012; Garrison & Wakeman, 2000). The earlier and longer records of eutrophication are in agreement with early 20th century accounts from Europe and broad recognition of eutrophication as a driver of SAV loss in shallow lakes (Phillips et al., 2016). However, eutrophication

can have a non-linear effect where oligo- to mesotrophic lake might experience an increase in SAV with moderate nutrient addition followed by declines at higher trophic status. Indeed, we found that land use change was also associated to either unimodal or increasing trends. In fact, paleolimnological evidence from Danish lakes indicates that intensification of human activities created lush SAV beds during the Middle Ages, that collapsed with the ongoing eutrophication of the mid-20th century, with many lakes already having reduced SAV cover in the mid 19th (Bjerring et al., 2008; Johansson et al., 2005; Rasmussen & John Anderson, 2005). It has even been suggested that prior to human expansion and the eradication of the large nutrient-redistributing grazing herds of the Pleistocene era, the pristine reference state in many shallow lakes was turbid (Moss, 2015). Our current perception of clear water state with abundant SAV as a pristine "reference" state might thus reflect a shifting baseline effect (Phillips et al., 2016). Whether this is the case or not, the prominence of SAV declines in our dataset was likely a function of a shift toward higher trophic status from the 1950s, the time when most SAV records started, to that of around 2006. SAV thus joins other wetland types in their worrying global decline (Davidson, 2014; MEA, 2005). Most importantly, SAV trends are very similar to those of seagrass whose global extent is declining mostly due to alteration of water quality, but, on a more positive note, are also increasing due to recent restoration efforts (Dunic et al., 2021). These similarities could foster interesting inter-comparison of drivers, trends, and successful restoration practices across all SAV species whether located in littoral inland waters or coastal marine.

Although we found overall that SAV are largely decreasing, the situation is not entirely negative. Indeed, we report a fair number of increasing trends associated with active lake restoration, but also with changes in climate and alterations in community structure, including recolonization by invasive SAV species (Johnson et al., 2000; Newman & Biesboer, 2000). Management actions were observed in all regions with SAV time series, but they were much more widespread across Europe where strong regional policies for water conservation and restoration were actively put in place. Indeed, the European Water Framework Directive, adopted in December 2000, had the ambitious goal of achieving a minimum "good ecological status" for all European inland waterbodies by 2015 (European Union, 2000). However, not all restoration measures were successful and those carried out within the lake only, largely through biomanipulation, were mostly associated with oscillatory SAV trends and transient colonization (e.g. Hobbs et al., 2012; Søndergaard et al., 2017). This is consistent with a synthesis on SAV restoration showing that stable clear water conditions were largely obtained when external nutrient inputs were reduced or when

combining both internal and external measures (Hilt et al., 2018). In comparison with restoration practices, SAV changes that were linked to climate were more complex and associated to all types of trends. As climate is a long-term feature of the Earth System, it is somewhat surprising that it has only been recently identified as a factor influencing changes on SAV quantities (> 1970s). This may be due to the oscillatory and cyclical nature of climate that requires longer time series to disentangle climate from other confounding signals. The fact that climate controls multiple environmental variables simultaneously might also make it harder to detect. Additionally, the more recent attention may be due to climate change as a global priority (IPCC, 2018). Regardless, change in water levels was the most notable climatic influence, with reduction in levels predominantly leading to positive outcomes for SAV. This was likely a function of modest enough levels to increase light availability to bottom sediment, as opposed to complete drawdown that can be deleterious by creating conditions of SAV dry-out (Ersoy et al., 2020). How climate and eutrophication work synergistically to influence SAV quantities and species composition remains underexplored as influences may be antagonistic albeit up to a certain point, where other primary producers could outcompete SAV (Moss et al. 2011). Future research is needed to address the complex interactions of multiple stressors including climate on SAV, and how the responses vary regionally.

The arrival of invasive species or changes in biotic community structure were also associated with multiple trend types, but the response differed with organismal traits. Our findings are in agreement with a meta-analysis on the effect of invasive species on regime shifts from either a turbid to a clear state or vice versa, where the arrival of new plants and molluscs can favor SAV expansion, while crustaceans and fishes were linked to decreases in SAV (Reynolds & Aldridge, 2021). Interactions of invasive species with SAV should be included in regional restoration plans, whether the goal is to increase SAV or control its proliferation, the potential invasive may help facilitate a desired response. For example, in decimated SAV beds, the arrival of invasive plant species that enhance water quality can facilitate recolonization of native SAV species, as was observed with *Hydrilla verticillata* in the freshwater portion of the Chesapeake Bay (Orth et al., 2017). Similarly, the invasive SAV species *Gracilaria vermiculophylla* has been shown to have a positive density-dependent effect on multiple ecosystems functions, including habitat production and sediment stabilization, in a coastal mud flat along the coast of North Carolina (Ramus et al., 2017). In the case where invasive plants are a nuisance, herbivores could be used as biocontrol agents. For example, the insects that reduced SAV quantities (*Euhrychiopsis lecontei* and *Acentria ephemerella*) were native grazers of watermilfoil (*Myriophyllum spicatum*), an invasive SAV whose proliferation is

perceived as a nuisance in North American temperate lakes (Johnson et al., 2000; Newman & Biesboer, 2000). The geographic range of these native herbivores is also similar to that of registered declines in watermilfoil before the 2000s (Creed, 1998). Thus, in newly invaded areas within their range distribution, the efficiency of these herbivores to reduce milfoil quantities could be tested. We caution, however, that these manipulations must always be conducted within the natural or existing invasive species distribution range to avoid unintended consequences. This is exemplified by the Great Lakes that has been invaded by more than 145 alien species mostly from ballast water discharge from transoceanic ships. Among these species are dreissenid mussels that dramatically modified the lakes functioning through a shift in energy production from the open pelagic to the benthos, advantaging SAV at the same time (Li et al., 2021; Ricciardi & MacIsaac, 2000). This also explained why SAV time series associated with biotic drivers were primarily located in North America, around the Great Lakes, one of the world's major invasion corridors due to global trade.

Conclusion

We have successfully synthesized information on SAV time series and provided a quantitative portrait of their trends, methods and metrics as well as drivers of change. Similar to other inland wetland types and coastal seagrasses, we found that SAV are globally declining due to human activities, primarily through catchment changes that influence water quality. We argue that vegetated littoral zones of lakes should be considered separately from pelagic areas in current wetland classification schemes as these essential wetlands are highly sensitive to anthropogenic change. We have also shown that both SAV quantities and associated drivers are very dynamic both in space and time. Recent increases in SAV quantities are associated with restoration, climate and changes in biotic communities that were relatively widespread in Europe and North America. By assessing the influence of different drivers, we have also provided information that could be used for SAV management to anticipate future change. Future work should consider including information on SAV species composition together in quantitative assessments. Alterations in SAV species can point to earlier signs of environmental change. For example, characeans, mosses and slow-growing vascular rosette species (i.e. isoetids) are the first to disappear with eutrophication (Blindow 1992, Sand-Jensen et al. 2000). Furthermore, with the recent global effort to compile functional traits of aquatic plants (Iversen 2022), understanding SAV compositional changes together with quantities would provide a more robust understanding of the influence on ecosystem functions and services.

Through this work we identified major knowledge gaps in SAV research. We found that SAV studies are biased toward North temperate regions with many unknowns about their quantities and trends in higher latitudes and altitudes, as well as in the tropics. It is possible that SAV is simply not dominant or present in these regions. Therefore, a basic biogeography of SAV is required to determine whether or not this is the case, which would also inform on their potential range expansion or reduction with climate change. Recent literature reports suggest this work is emerging with an increasing understanding of aquatic plant species distributions (Alahuhta et al, 2021), but information on quantities is lacking. Standard protocols for a better understanding of SAV status and trends are needed. These developments include more systematic reporting of SAV areal coverage, but should also consider the collection of bathymetric information that is crucial in determining SAV colonization areas. The use of sedimentary archives should also be better exploited as they register lake histories and could reconstruct SAV long-term development. Finally, we recommend that global approaches adopted in coastal seagrass research could serve as a template in developing a more robust global program to tracking inland SAV. As the shoreline of lakes is four time the length of the ocean's coast (Messager et al. 2016), inland SAV also needs to be considered in global restoration and conservation efforts.

Acknowledgement

We thank Sophie Bédard, Orianne Besset and Pauline Mouche, for preliminary literature research and analysis as well as Lisa Galantini for help on data entry. We also thank Sabine Hilt, Lars Iversen and two anonymous reviewers for insightful comments that improved the manuscript. This work was supported by a Fonds de recherche du Québec – Nature et technologie (FRQNT) and Natural Sciences and Engineering Research Council of Canada (NSERC) scholarships to MB and an NSERC Discovery to RM.

Supporting information

Text S1

The following list of references have been identified as containing SAV abundance time series. However, SAV quantities for individual time series was generally not available and only a summary statistic for multiple lakes was reported.

- Bayley, S. E., I. F. Creed, G. Z. Sass, and A. S. Wong. 2007. Frequent regime shifts in trophic states in shallow lakes on the Boreal Plain: Alternative "unstable" states? Limnology and Oceanography **52:** 2002-2012.
- Cassani, J. R., E. L. De La Vega, and H. Allaire. 1995. An Assessment of Triploid Grass Carp Stocking Rates in Small Warmwater Impoundments. North American Journal of Fisheries Management **15:** 400-407.
- Cobbaert, D., A. S. Wong, and S. E. Bayley. 2015. Resistance to drought affects persistence of alternative regimes in shallow lakes of the Boreal Plains (Alberta, Canada). Freshwater Biology **60:** 2084-2099.
- de Backer, S., S. Teissier, and L. Triest. 2012. Stabilizing the clear-water state in eutrophic ponds after biomanipulation: Submerged vegetation versus fish recolonization. Hydrobiologia **689:** 161-176.
- Florida Lake Watch. Plant reports. https://lakewatch.ifas.ufl.edu/datareports/
- Helsel, D. R., S. A. Nichols, and R. S. Wakeman. 1999. Impact of aquatic plant management methodologies on eurasian watermilfoil populations in Southeast Wisconsin. Lake and Reservoir Management **15:** 159-167.
- Jones, A. R., J. A. Johnson, and R. M. Newman. 2012. Effects of repeated, early season, herbicide treatments of curlyleaf pondweed on native macrophyte assemblages in Minnesota lakes. Lake and Reservoir Management **28:** 364-374.
- Laita, M., I. Sammalkorpi, A. Mäkelä, E. Kemppainen, and A. Tarvainen. 2007. The excessive growth of submerged aquatic vegetation in the early 2000s. Terra **119:** 231-241.
- Namdev, G. R., A. Bajpai, and S. Malik. 2011. Agriculture runoff and its impact on water quality of a potable water resource, Bhopal (M.P.). Pollution Research **30:** 353-356.

- Nyström, P., J. Hansson, J. Månsson, M. Sundstedt, C. Reslow, and A. Broström. 2007. A documented amphibian decline over 40 years: Possible causes and implications for species recovery. Biological Conservation **138:** 399-411.
- Peretyatko, A., S. Teissier, S. de Backer, and L. Triest. 2009. Restoration potential of biomanipulation for eutrophic peri-urban ponds: The role of zooplankton size and submerged macrophyte cover. Hydrobiologia **634:** 125-135.
- Van Geest, G. J., H. Coops, M. Scheffer, and E. H. Van Nes. 2007. Long transients near the ghost of a stable state in eutrophic shallow lakes with fluctuating water levels. Ecosystems **10:** 36-46.
- Vanacker, M., A. Wezel, F. Arthaud, M. Guérin, and J. Robin. 2016. Determination of tipping points for aquatic plants and water quality parameters in fish pond systems: A multi-year approach. Ecological Indicators **64:** 39-48.
- Vermaire, J. C., and I. Gregory-Eaves. 2008. Reconstructing changes in macrophyte cover in lakes across the northeastern United States based on sedimentary diatom assemblages. Journal of Paleolimnology **39:** 477-490.

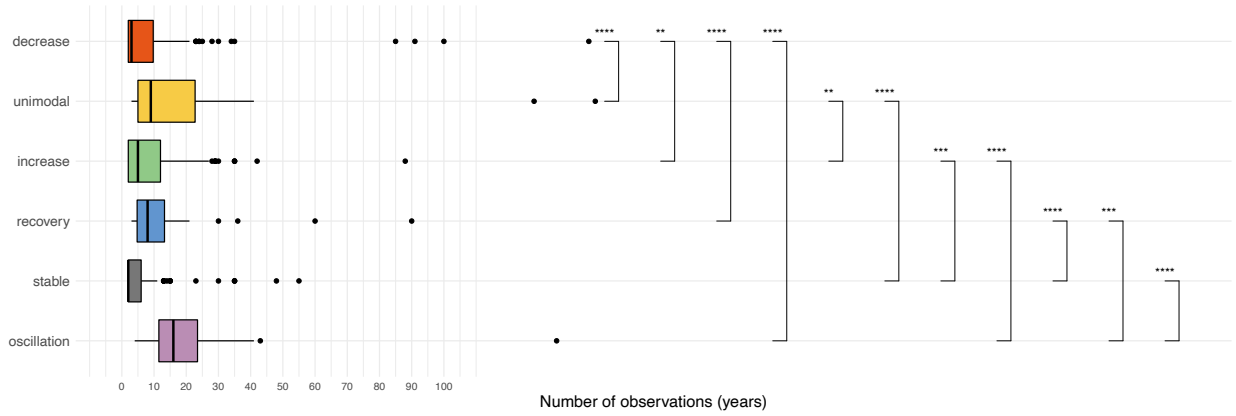

Figure S1. Number of observational years per trend types. Vertical bars within boxes indicate median value, box boundaries represent 25th and 75th percentile and whiskers range from 10th to 90th percentiles. ** $p < 0.01$, *** $p < 0.001$, **** $p < 0.0001$

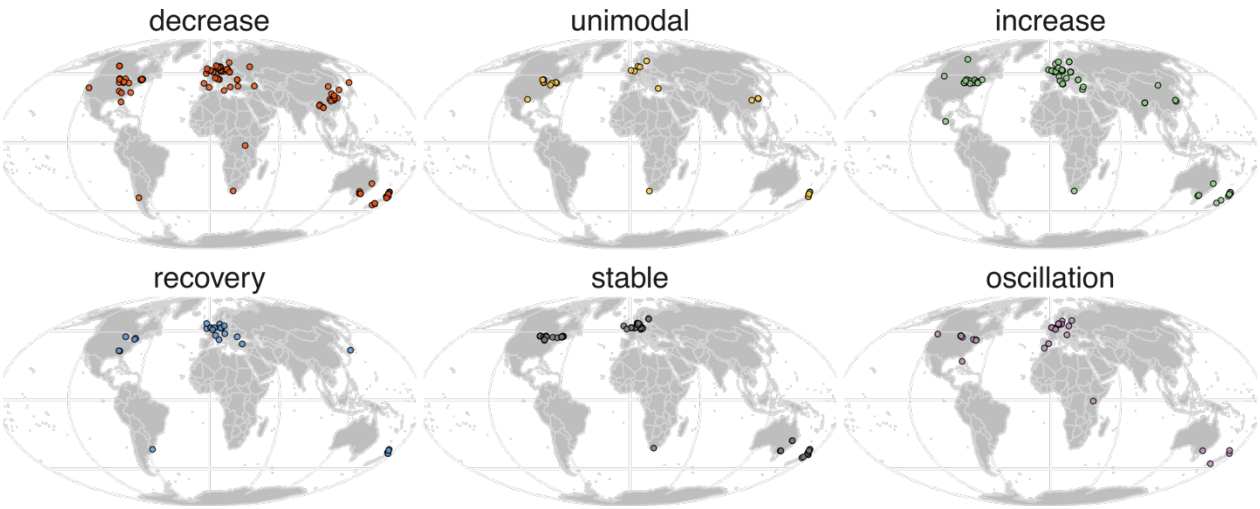

Figure S2. Geographic distribution of time series per trend type.

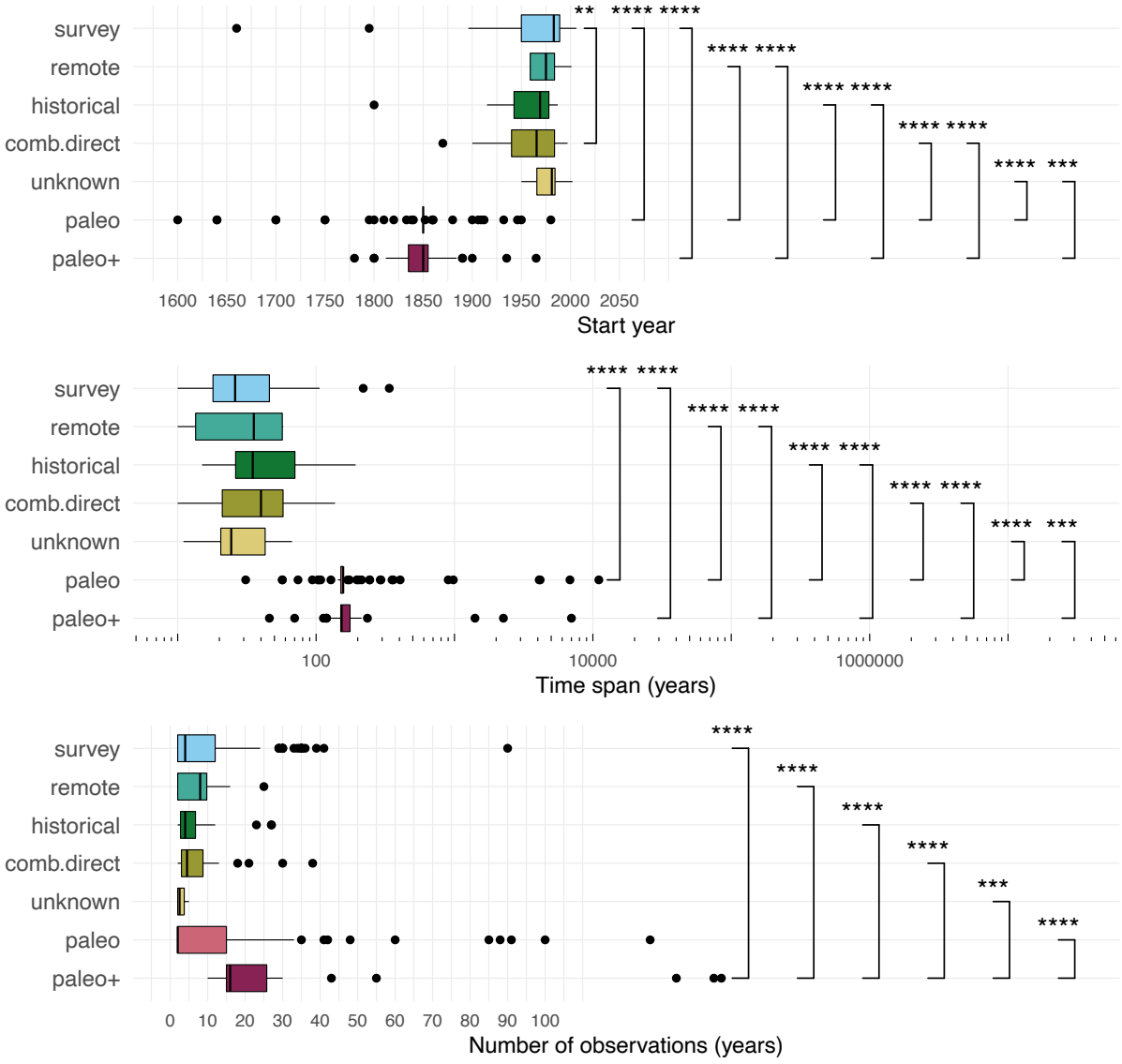

Figure S3. Method types and distributions through time. Remote remote sensing, comb. combine, paleo paleolimnology. Vertical bars within boxes indicate median value, box boundaries represent 25th and 75th percentile and whiskers range from 10th to 90th percentiles. ** $p < 0.01$, *** $p < 0.001$, **** $p < 0.0001$

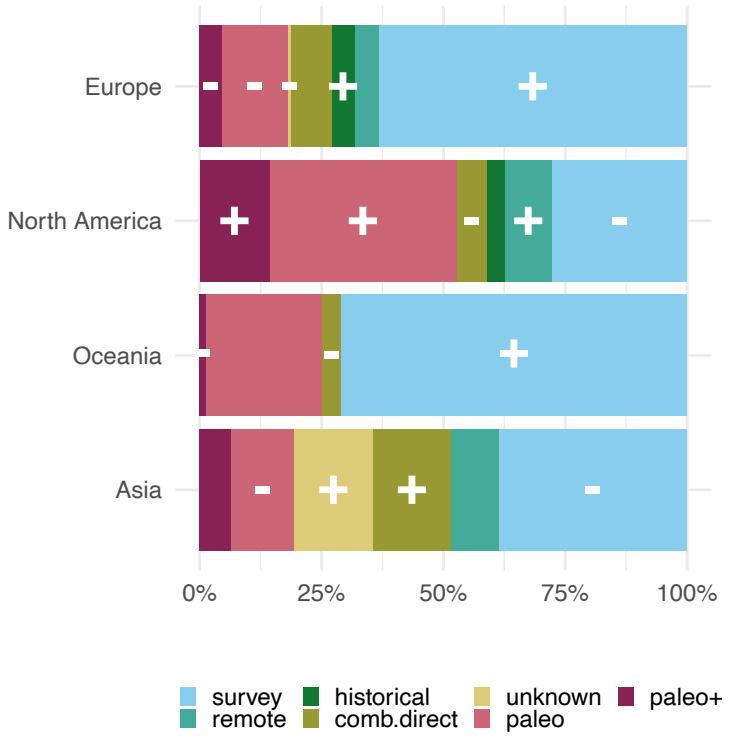

Figure S4. Method types as a function of geographic regions. + and – indicate if proportion of method type is more or less than expected and is shown for X^2 residual < -1 and > 1.

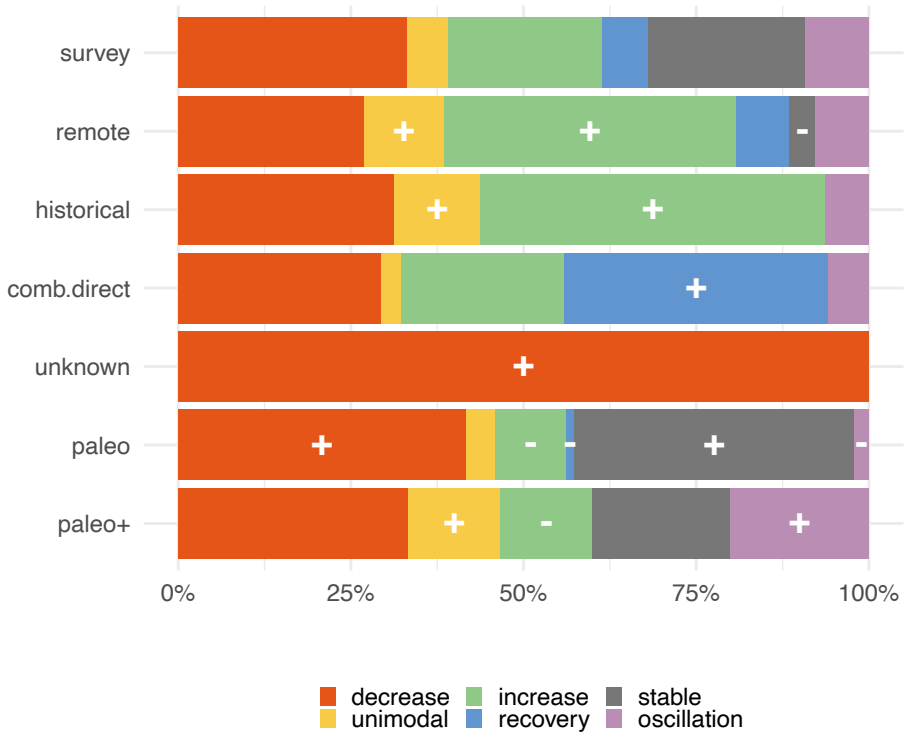

Figure S5. Methods as a function of trend types. + and – indicate if proportion of trend type is more or less than expected and is shown for X^2 residual < -1 and > 1.

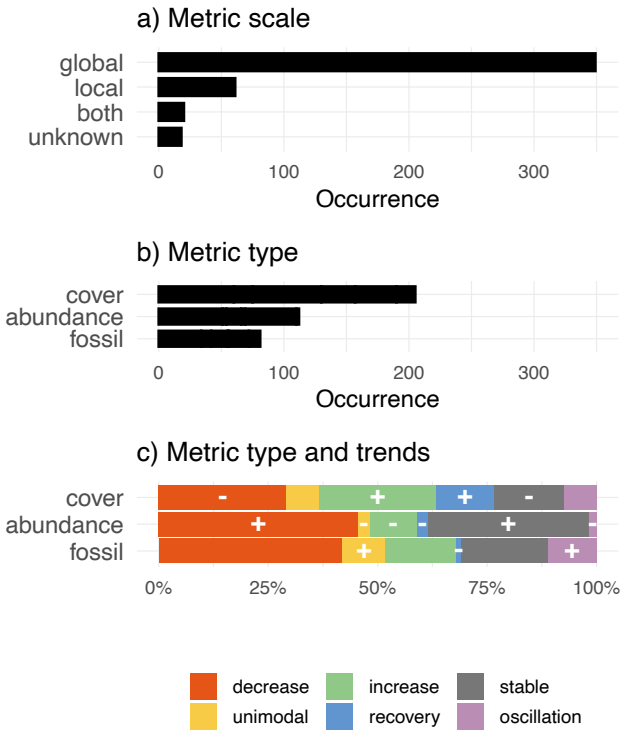

Figure S6. Metrics used in SAV studies and their occurrence by scale and by types with the associated trends. Global scale implies that SAV was measured overall within the lake, while local scale is when SAV was measured only within the littoral zone. Metric types are shown for the global scale (78% of trends). + and – indicate if proportion of trend type is more or less than expected and is shown for X^2 residual < -1 and >1.

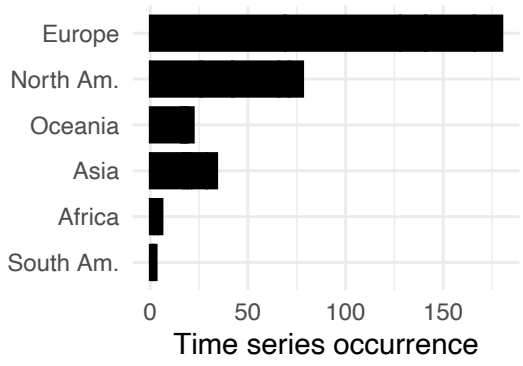

Figure S7. Number of time series with drivers per continent.

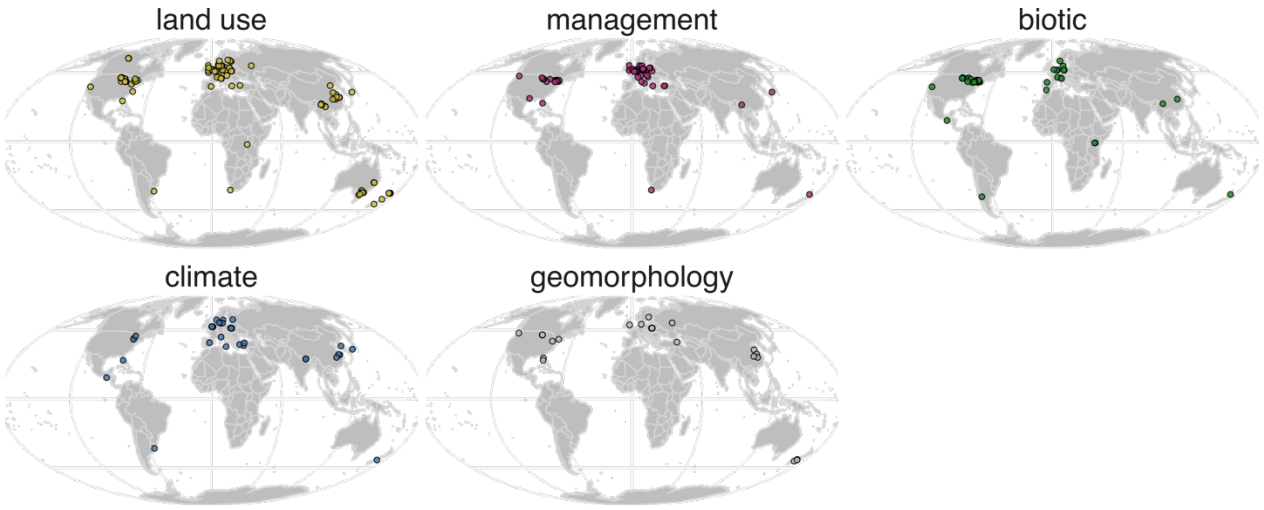

Figure S8. Geographic distribution of individual time series drivers.

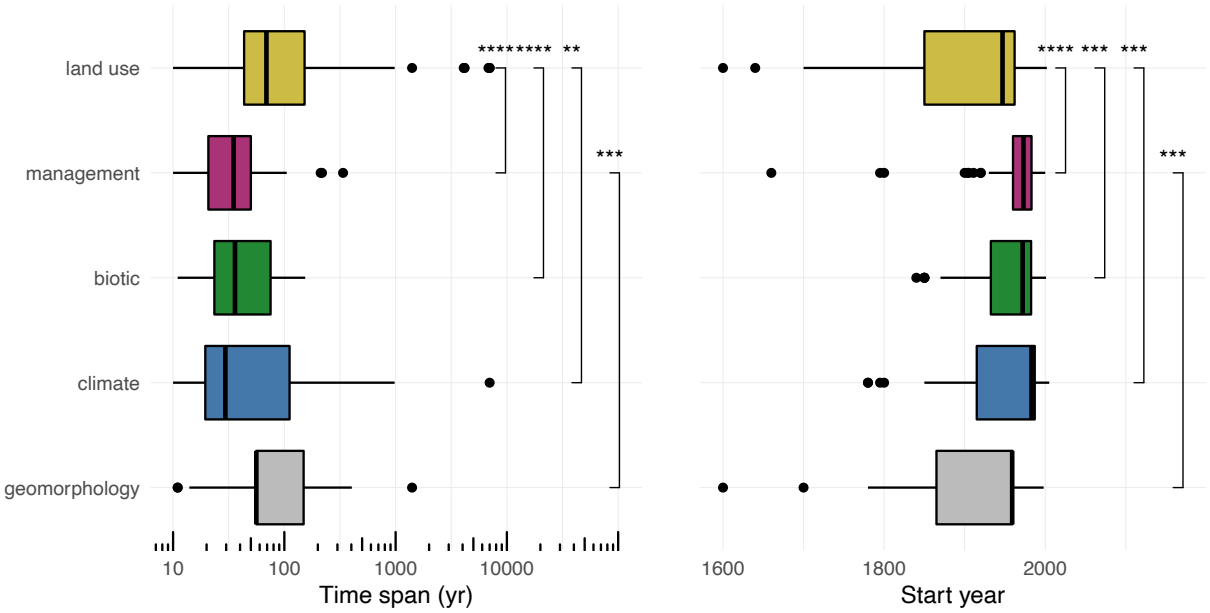

Figure S9. Distribution through time of identified SAV drivers.

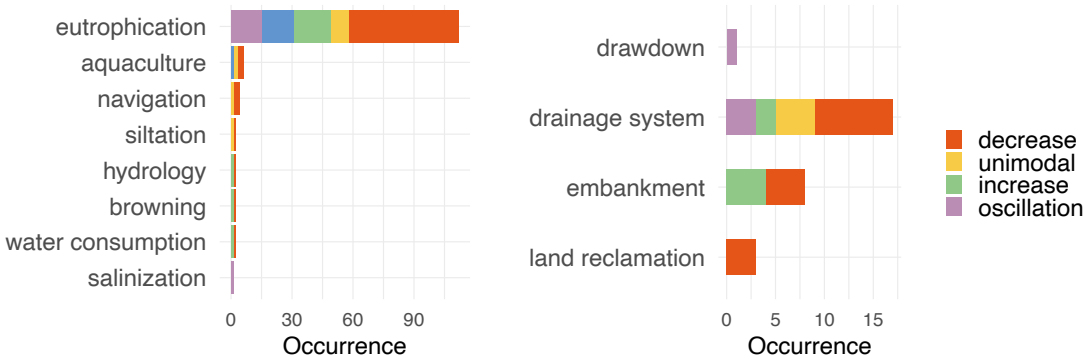

Figure S10. Occurrence of time series and associated trends with land use and geomorphology drivers.

Table S1. Summary statistics of lake morphometry. Total decadal dataset included 431 lakes, *n* indicate the number of lake for which variable could be identified.

Variable	Median	Mean	Minimum	Maximum	*n*
Lake area (km^2)	0.61	98.82	0.001	3752.7	328
Watershed area (km^2)	12.27	2875.40	0.171	162000	127
Drainage ratio	12	39	0.4	933	126
Maximum depth (m)	5.0	16.9	1.1	501	264
Mean depth (m)	2.6	7.9	0.4	305	225

Table S2. List of taxa represented in the sub-categories of biotic drivers.

Biotic sub-category	Taxa
Filter feeder	Dreissena mussel (*Dreissena polymorpha*, *Dreissena rostriformis bugensis*)
Plants	*Egeria densia*, Canadian waterweed - *Elodea canadensis*, *Hydrilla verticillata*
Piscivores	Largemouth bass (*Micropterus salmoides*) and smallmouth bass (*Micropterus dolomieu*)
Benthivores	Fish (bream, common bream - *Abramis brama*, common carp - *Cyprinus carpio*, largemouth perch - *Percichthys colhuapiensis*, *Percichthys trucha*)
Planktivores	Fathead minnow - *Pimephales promelas*
Herbivores	Insects (watermilfoil moth - *Acentria ephemerella*, milfoil weevil - *Euhrychiopsis lecontei*) Birds (coots) Crayfish (signal crayfish - *Pacifastacus leniusculus*, Louisiana crayfish - *Proclambarus clarkii*, rusty crayfish - *Orconectes rusticus*). Fish (grass carp - *Ctenopharyngodon idella*)
Guanotrophication	Birds (black-headed gull - Larus ridibundus L.)

Conclusion

Dans cette thèse, j'ai exploré comment mieux comprendre la réponse des quantités de VAS aux changements environnementaux et ses conséquences sur le fonctionnement des écosystèmes. Premièrement, j'ai développé une méthode qui profite des synergies de techniques existantes afin de mesurer sous l'eau la densité de plante, soit la biomasse. L'utilisation de deux calibrations permet de limiter l'utilisation fastidieuse du quadrat, mais qui est la plus exacte dans son estimation de la biomasse. L'application de ces calibrations permet de corriger le biais du râteau et de transformer l'indice d'échosondage en biomasse et ainsi d'utiliser ses deux techniques en combinaison. L'union du râteau et de l'échosondage permet ainsi de mesurer la biomasse à plus faible coût, peu importe les profondeurs, de couvrir de plus grandes étendues spatiales ou d'avoir une meilleure résolution temporelle. Ces développements permettront de mesurer la biomasse de la VAS dans les eaux continentales à des échelles qui demeurent inexplorées et ainsi répondre à de nouvelles questions sur la réponse et l'effet de la VAS sur les écosystèmes, ou sur l'évaluation de leur gestion.

Ensuite et en utilisant les informations sur la biomasse développé au premier chapitre, j'ai montré comment les variations climatiques affectent la rétention de l'azote dans un herbier aquatique d'une grande rivière. Ce faisant, j'ai fourni une des rares mesures empiriques sur la dynamique de l'azote et contribué à une meilleure compréhension du cycle des nutriments dans ces écosystèmes où il demeure sous étudié. Dans les grandes rivières, les difficultés principales pour mesurer la rétention de l'azote sont l'inapplicabilité des méthodes existantes, développées originellement en ruisseau, et la détermination de l'écoulement de l'eau permettant d'estimer les budgets. J'ai soulevé ces défis en calculant des budgets d'azote à l'aide d'une sonde de nitrate à haute fréquence à laquelle j'ai adapté une nouvelle technique utilisant la variation diurne pour estimer l'assimilation autotrophe. Pour enlever les effets de dispersion hydraulique ou d'événements ponctuels de pluie, j'ai appliqué une technique de décomposition spectrale pour extraire le signal diurne de nitrate, idée qui a même inspiré une publication savante à ce sujet (Chamberlin et al., 2021). Cette innovation m'a permis de non seulement estimer la consommation totale de nitrate, mais aussi de partitionner la consommation entre assimilation et dénitrification. Également, ces mesures ont été possibles parce que j'ai su utiliser un modèle hydrodynamique pour obtenir des vitesses d'écoulement et la conductivité pour déterminer la provenance de l'eau. De plus, j'ai confronté à ces budgets un indice de biomasse, la pente de la surface du niveau de l'eau, qui a été

calibré pour la première fois à des données terrain et a révélé un portrait détaillé de l'évolution de la biomasse au cours de la saison de croissance. Toutes ces étapes montrent le casse-tête que j'ai dû résoudre et l'apport méthodologique du chapitre deux à la compréhension de la rétention de l'azote et sa médiation par la VAS en grande rivière. Ce chapitre est également une contribution conceptuelle puisque, pour la première fois, nous avons montré le dynamisme et pointé des facteurs climatiques contrôlant la rétention de l'azote dans un herbier aquatique riverain, des facteurs qui agissent à la fois sur les apports en nitrate et sur la biomasse des plantes. Ce chapitre fournit des indices afin de mieux comprendre comment les changements climatiques vont modifier les services écosystémiques riverains. En ce sens, ce chapitre traite de l'état de perpétuel de changement des rivières et est une démonstration de la célèbre phrase d'Héraclite : « On ne se baigne jamais deux fois dans le même fleuve. »

Troisièmement, j'ai synthétisé les changements spatiotemporels de la quantité de VAS dans les lacs et comment elles ont été mesurées. Ce chapitre est la plus grande compilation de série temporelles sur la VAS lacustre menée à ce jour. Encore une fois, ce chapitre a une contribution méthodologique, puisque j'ai résumé des informations à travers plusieurs méthodes, recommandé quelles informations devraient être rapportées lors de la mesure de la VAS et quels seraient les futurs développements méthodologiques souhaitables. Tout comme le chapitre précédent, le condensé a montré le dynamisme de la VAS en réponse aux activités humaines, autant dans le temps que dans l'espace. La synthèse dresse un portrait d'un déclin généralisé et donc d'un besoin de restauration des herbiers aquatiques lacustres, mais pointe aussi à des rétablissements plus récents avec de grandes disparités régionales. En montrant les facteurs expliquant les tendances de VAS, j'ai fourni des informations qui pourraient permettre à des gestionnaires d'anticiper les changements futurs. La synthèse a aussi permis de montrer le biais des informations sur la VAS qui vient principalement des régions tempérées et le grand manque de connaissances sur sa distribution géographique surtout en région boréale et tropicale, soulignant ainsi de futures avenues de recherche. Enfin, la base de données qui a été assemblée et qui sera librement accessible pourra servir pour des études plus fines sur chacune des activités humaines recensées ou pour tester différents aspects méthodologiques.

À partir de la présente thèse, plusieurs nouveaux projets pourraient être construits. J'ai montré comment combiner des techniques existantes pour estimer la biomasse, mais la principale lacune de la technique est le manque de définition des espèces qui constituent cette biomasse. Un

futur développement serait donc de tester la méthode suggérée en estimant les espèces à partir du râteau. De plus, la technique a été appliquée dans un lac fluvial peu profond et il serait souhaitable de tester la technique dans d'autres types d'écosystèmes, notamment dans des lacs plus profonds où d'autres types d'engins sont nécessaires pour récolter les plantes. Je pense également que la méthode pourrait être mise à profit dans un programme de science citoyenne. Dans ce programme, des habitants riverains pourraient être équipés d'échosondeurs génériques, du type utilisé par les pêcheurs. Les échogrammes enregistrés lors de leurs déplacements nautiques permettraient de suivre le développement saisonnier et interannuel de l'aire et, avec les calibrations développées, de la biomasse de la VAS. Conjugué avec des études de terrain ciblées, notamment en déployant des sondes à haute fréquence, ce suivi permettrait de répondre à plusieurs questions sur le fonctionnement des herbiers.

Dans le chapitre 2, j'ai montré comment dans une zone de confluence, un grand herbier aquatique pouvait retenir jusqu'à 87 % des apports de bassins versants agricoles. Il s'agit d'un important service écologique et les herbiers ont un potentiel d'agir comme une solution fondée sur la nature pour résoudre des enjeux environnementaux, dans cet exemple pour atténuer l'eutrophisation. J'ai montré que le site étudié devrait être une priorité de conservation, mais pour déterminer d'autres sites de conservation et le potentiel de rétention de la VAS en rivière, il faudrait d'abord connaître où sont les herbiers le long de la rivière par rapport aux sources de pollution. Pour comprendre leur capacité à épurer les nutriments, il faudrait également déterminer à partir de quelle taille d'herbier le service de rétention est soutenu. En effet, il n'est pas clair si les rétroactions qui permettent la rétention sont entretenues dans de plus petits herbiers. Ici, la méthode présentée au chapitre 1 serait très utile pour cartographier la biomasse de la VAS en rivières. Ces données pourraient servir à prédire la localisation, la taille et la densité des herbiers. Par ailleurs, l'effet de ce grand herbier a été symbolisé dans le chapitre deux par la rétention de l'azote. Cependant, plusieurs autres fonctions et services sont soutenus par la VAS. De futures recherches pourraient s'intéresser à plusieurs fonctions simultanément, comme la rétention d'autres éléments (carbone, phosphore) ou le soutient de refuges pour la faune, afin de déterminer s'il y a des synergies entre les fonctions et s'il y a des effets de saturation. La capacité phénoménale des herbiers marins à stocker le carbone, appelé «carbone bleu», a d'ailleurs grandement propulsé leur conservation et restauration. Très peu d'information existe pour ce service chez la VAS continentale. Une autre grande frontière pour l'écologie de la VAS en rivière est de mieux comprendre l'impact de l'hiver. En lac, l'occurrence d'une saison froide et d'un couvert de glace a été montrée comme favorisant la dominance par la VAS par

rapport au phytoplancton (Hargeby et al., 2006; Kosten et al., 2009; Rabaey et al., 2021). En rivière, on en sait très peu sur l'effet de l'hiver et du type de couvert de glace sur l'écologie et notamment sur la croissance des plantes l'été suivant (Thellman et al. 2021). Ainsi, il pourrait y avoir avec les changements climatiques, une diminution de la VAS avec de potentielles conséquences sur les services soutenus.

Finalement, dans le chapitre 3, plusieurs avenues de recherche ont été soulevées. Toutes ces orientations sont pertinentes, mais à mon sens les importantes à adresser devraient tendre vers une quantification de l'aire totale de la VAS continentale. Est-ce que cette aire est importante ? Cet exercice a été réalisé pour les herbiers marins (McKenzie et al., 2020), mais à ce jour aucune estimation existe pour la VAS continentale. Les approches adoptées en milieu marin, modélisant l'aire potentiellement colonisable à partir de la disponibilité de la lumière ou de la distribution connue des espèces, pourraient être développées pour la VAS continentale. Ces approches pourraient être additionnées avec les séries temporelles mesurant l'aire couverte par la VAS qui ont été compilées dans cette thèse. En considérant que la VAS se retrouve dans la zone littorale, que le rivage des lacs est environs quatre fois plus longs que le rivage de l'océan et est dominé par les plus petits lacs (< 10 km^2) (Messager et al., 2016), il est fort probable que l'aire qu'occupe la VAS est non négligeable. Il s'agit d'un potentiel qui pourrait permettre de savoir où les efforts de restauration sont nécessaires. Une puissante combinaison serait d'allier la vision proposée ici pour estimer la répartition globale de la VAS avec les développements récents de l'écologie fonctionnelle appliquée aux plantes aquatiques (Iversen et al., 2022) pour cibler les endroits à restaurer et les espèces à implanter. De façon générale, les travaux sur la VAS continentale devraient s'inspirer de ce qui se fait en milieu marin. L'effort international pour quantifier l'aire des herbiers marins, la reconnaissance de leur perte, la quantification de leurs fonctions écosystémiques a permis d'entamer leur restauration et le retour des services qu'ils fournissent (Duarte et al. 2020, Orth et al. 2020). Une vision globale qui apporte des solutions locales.

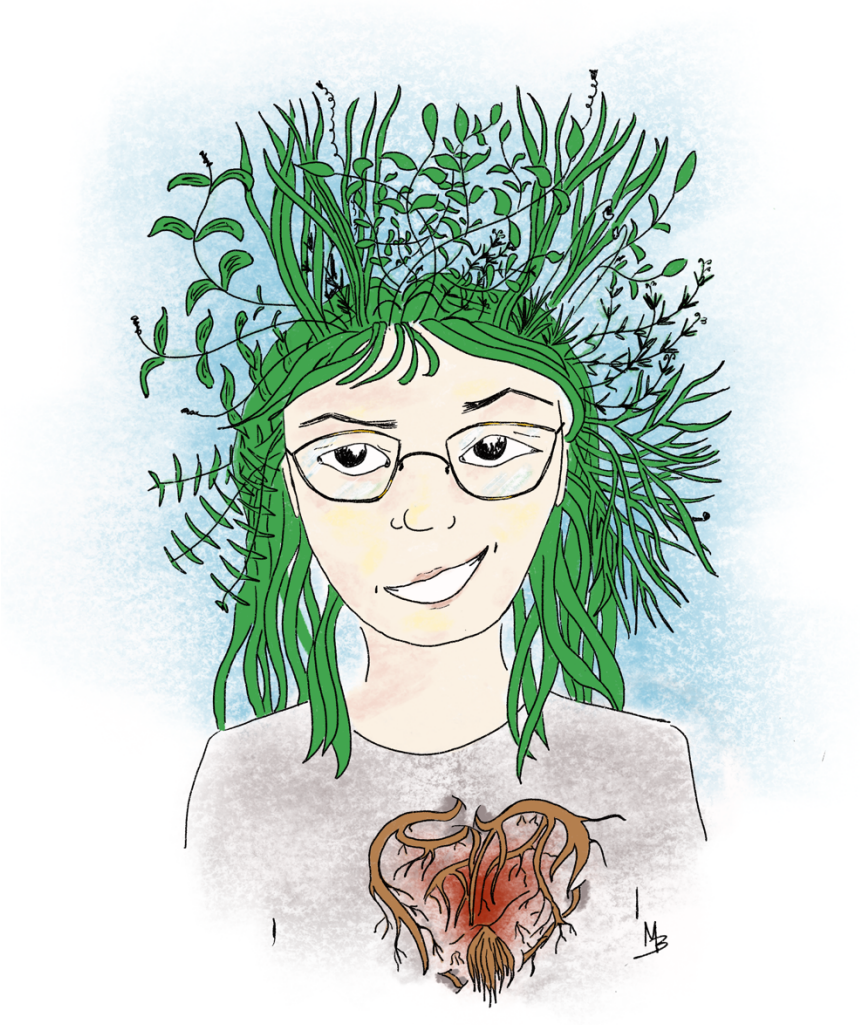

Références bibliographiques

Alahuhta, J., Lindholm, M., Baastrup-Spohr, L., García-Girón, J., Toivanen, M., Heino, J., & Murphy, K. (2021). Macroecology of macrophytes in the freshwater realm: Patterns, mechanisms and implications. *Aquatic Botany*, 168. https://doi.org/10.1016/j.aquat.2020.103325.

Alboukadel, K. (2020). ggpubr: 'ggplot2 based publication ready plots. R package version 0.4.0. https://CRAN.R-project.org/package=ggpubr

Alexander, R. B., Smith, R. A., & Schwarz, G. E. (2000). Effect of stream channel size on the delivery of nitrogen to the Gulf of Mexico. *Nature*, *403*(6771), 758-761.

Anderson, M. R., & Kalff, J. (1986). Nutrient limitation of Myriophyllum spicatum growth in situ. *Freshwater Biology*, *16*(6), 735-743.

Appling, A. P., Leon, M. C., & McDowell, W. H. (2015). Reducing bias and quantifying uncertainty in watershed flux estimates: the R package loadflex. *Ecosphere*, *6*(12), 1-25.

Armstrong, N., Planas, D., & Prepas, E. (2003). Potential for estimating macrophyte surface area from biomass. *Aquatic Botany*, *75*(2), 173-179.

Appling, A. P., & Heffernan, J. B. (2014). Nutrient limitation and physiology mediate the fine-scale (de)coupling of biogeochemical cycles. *The American Naturalist, 184*(3), 384-406. https://doi.org/10.1086/677282

Audet, J., Olsen, T. M., Elsborg, T., Baattrup-Pedersen, A., & Riis, T. (2021). Influence of plant habitats on denitrification in lowland agricultural streams. *Journal of Environmental Management*, *286*, Article 112193. https://doi.org/10.1016/j.jenvman.2021.112193

Ayres, K. R., Sayer, C. D., Skeate, E. R., & Perrow, M. R. (2008). Palaeolimnology as a tool to inform shallow lake management: an example from Upton Great Broad, Norfolk, UK. *Biodiversity and Conservation*, *17*(9), 2153-2168.

Bakker, E. S., Wood, K. A., Pagès, J. F., Veen, G. F., Christianen, M. J. A., Santamaría, L., . . . Hilt, S. (2016). Herbivory on freshwater and marine macrophytes: A review and perspective. *Aquatic Botany*, *135*, 18-36.

Ballard, T. C., Sinha, E., & Michalak, A. M. (2019). Long-Term Changes in Precipitation and Temperature Have Already Impacted Nitrogen Loading. *Environmental Science & Technology*, *53*(9), 5080-5090.

Barko, J. W., Gunnison, D., & Carpenter, S. R. (1991). Sediment interactions with submersed macrophyte growth and community dynamics. *Aquatic Botany*, *41*(1-3), 41-65.

Barko, J. W., Hardin, D. G., & Matthews, M. S. (1982). Growth and morphology of submersed freshwater macrophytes in relation to light and temperature. *Canadian Journal of Botany*, *60*(6), 877-887.

Barko, J. W., & James, W. F. (1998). Effects of Submerged Aquatic Macrophytes on Nutrient Dynamics, Sedimentation, and Resuspension. In E. Jeppesen, M. Sondergaard, M. Sondergaard, & K. Christofferson (Eds.), *The structuring role of submerged macrophytes in lakes* (Vol. 131, pp. 197-214). Springer.

Barko, J. W., Smart, R. M., McFarland, D. G., & Chen, R. L. (1988). Interrelationships between the growth of Hydrilla verticillata (Lf) Royle and sediment nutrient availability. *Aquatic Botany*, *32*(3), 205-216.

Bartoń, K. (2020). MuMIn: Multi-model inference. R package version 1.43.17. https://CRAN.R-project.org/package=MuMIn

Bates, D., Maechler, M., Bolker, B., & Walker, S. (2015). Fitting linear mixed-effects models using lme4. Journal of Statistical Softwarre 67: 1-48.

Beck-Nielsen, D., & Madsen, T. V. (2001). Occurrence of vesicular–arbuscular mycorrhiza in aquatic macrophytes from lakes and streams. *Aquatic Botany*, *71*(2), 141-148.

Bekka, R. E. H., & Berrouche, Y. (2013). Improvement of ensemble empirical mode decomposition by over-sampling. *Advances in Adaptive Data Analysis*, *05*(03), 1350012. https://doi.org/10.1142/s1793536913500l2x

Beklioglu, M., & Altinayar, G. T. (2006a). Water level control over submerged macrophyte development in five shallow lakes of Mediterranean Turkey. *Archiv für Hydrobiologie*, *166*(4), 535-556.

Benda, L., Poff, N. L., Miller, D., Dunne, T., Reeves, G., Pess, G., & Pollock, M. (2004). The Network Dynamics Hypothesis: How Channel Networks Structure Riverine Habitats. *BioScience*, *54*(5), 413-427.

Bennion, H., Davidson, T. A., Sayer, C. D., Simpson, G. L., Rose, N. L., & Sadler, J. P. (2015). Harnessing the potential of the multi-indicator palaeoecological approach: An assessment of the nature and causes of ecological change in a eutrophic shallow lake. *Freshwater Biology*, *60*(7), 1423-1442.

Bernhardt, E. S., Blaszczak, J. R., Ficken, C. D., Fork, M. L., Kaiser, K. E., & Seybold, E. C. (2017). Control Points in Ecosystems: Moving Beyond the Hot Spot Hot Moment Concept. *Ecosystems*, *20*(4), 665-682.

Bjerring, R., Bradshaw, E. G., Amsinck, S. L., Johansson, L. S., Odgaard, B. V., Nielsen, A. B., & Jeppesen, E. (2008). Inferring recent changes in the ecological state of 21 Danish candidate reference lakes (EU Water Framework Directive) using palaeolimnology. *Journal of Applied Ecology*, *45*(6), 1566-1575.

Blindow, I. (1992) Decline of charophytes during eutrophication: comparison with angiosperms. *Freshwater Biology, 28*, 9-14.

Bornette, G., & Puijalon, S. (2011). Response of aquatic plants to abiotic factors: a review. *Aquatic Sciences*, *73*(1), 1-14.

Boudreau, P. A., Leclerc, M., & Fortin, G. (1994). Modélisation hydrodynamique du lac Saint-Pierre, fleuve Saint-Laurent : l'influence de la végétation aquatique. *Canadian Journal of Civil Engineering*, *21*, 471-489.

Bowman, D. C., & Lees, J. M. (2013). The Hilbert–Huang Transform: A High Resolution Spectral Method for Nonlinear and Nonstationary Time Series. *Seismological Research Letters*, *84*(6), 1074-1080.

Boyer, C., Chaumont, D., Chartier, I., & Roy, A. G. (2010). Impact of climate change on the hydrology of St. Lawrence tributaries. *Journal of Hydrology*, *384*(1–2), 65-83.

Boylen, C. W., & Sheldon, R. B. (1976). Submergent macrophytes: growth under winter ice cover. *Science*, *194*(4267), 841-842.

Botrel, M., & Maranger, R. (2022). Data on global trends and drivers of submerged aquatic vegetation quantities in lakes. Dataset. *Zenodo*. https://doi.org/ 10.5281/zenodo.6502355

Bresciani, M., Bolpagni, R., Braga, F., Oggioni, A., & Giardino, C. (2012). Retrospective assessment of macrophytic communities in southern Lake Garda (Italy) from in situ and MIVIS (Multispectral Infrared and Visible Imaging Spectrometer) data. *Journal of Limnology*, *71*(1).

Britton, C. M., & Dodd, J. D. (1976). Relationships of photosynthetically active radiation and shortwave irradiance. *Agricultural Meteorology*, *17*(1), 1-7.

Broads Authority. (2013). *Broads annual water plant monitoring report 2013*. https://www.broads-authority.gov.uk/looking-after/managing-land-and-water/conservation-publications-and-reports/water-conservation-reports

Brooks, C., Grimm, A., Shuchman, R., Sayers, M., & Jessee, N. (2015). A satellite-based multi-temporal assessment of the extent of nuisance Cladophora and related submerged aquatic vegetation for the Laurentian Great Lakes. *Remote Sensing of Environment*, *157*, 58-71.

Brown, J. H., Gillooly, J. F., Allen, A. P., Savage, V. M., & West, G. B. (2004). Toward a metabolic theory of ecology. *Ecology*, *85*(7), 1771-1789.

Bučas, M., Šaškov, A., Šiaulys, A., & Sinkevičienė, Z. (2016). Assessment of a simple hydroacoustic system for the mapping of macrophytes in extremely shallow and turbid lagoon. *Aquatic Botany*, *134*, 39-46.

Bulat, M., Biron, P. M., Lacey, J. R. W., Botrel, M., Hudon, C., & Maranger, R. (2019). A three-dimensional numerical model investigation of the impact of submerged macrophytes on flow dynamics in a large fluvial lake. *Freshwater Biology*, *64*(9), 1627-1642.

Burt, T. P., & Pinay, G. (2005). Linking hydrology and biogeochemistry in complex landscapes. *Progress in Physical Geography: Earth and Environment*, *29*(3), 297-316.

Buscombe, D. (2017). Shallow water benthic imaging and substrate characterization using recreational-grade sidescan-sonar. *Environmental Modelling & Software*, *89*, 1-18.

Canty, A., & Riplay, B. (2021). boot: Bootstrap R (S-Plus) Functions. R package version 1.3-28.

Capers, R. S., Selsky, R., & Bugbee, G. J. (2010). The relative importance of local conditions and regional processes in structuring aquatic plant communities. *Freshwater Biology*, *55*(5), 952-966.

Caraco, N., Cole, J., Findlay, S., & Wigand, C. (2006). Vascular plants as engineers of oxygen in aquatic systems. *Bioscience*, *56*(3), 219-225.

Caraco, N. F., & Cole, J. J. (1999). Human impact on nitrate export: an analysis using major world rivers. *Ambio*, *28*(2), 167-170.

Carignan, R. (1982). An empirical model to estimate the relative importance of roots in phosphorus uptake by aquatic macrophytes. *Canadian Journal of Fisheries and Aquatic Sciences*, *39*(2), 243-247.

Carignan, R., & Kalff, J. (1980). Phosphorus sources for aquatic weeds - water or sediments. *Science*, *207*(4434), 987-989.

Carpenter, S. R., Caraco, N. F., Correll, D. L., Howarth, R. W., Sharpley, A. N., & Smith, V. H. (1998). Nonpoint pollution of surface waters with phosphorus and nitrogen. *Ecological Applications*, *8*(3), 559-568.

Carpenter, S. R., & Lodge, D. M. (1986). Effects of submersed macrophytes on ecosystem processes *Aquatic Botany*, *26*(3-4), 341-370.

Cattaneo, A., Hudon, C., Vis, C., & Gagnon, P. (2013). Hydrological control of filamentous green algae in a large fluvial lake (Lake Saint-Pierre, St. Lawrence River, Canada). *Journal of Great Lakes Research*, *39*(3), 409-419.

Chamberlin, C. A., Katul, G. G., & Heffernan, J. B. (2021). A Multiscale Approach to Timescale Analysis: Isolating Diel Signals from Solute Concentration Time Series. *Environmental Science & Technology*, *55*(18), 12731-12738.

Chambers, P., Barko, J., & Smith, C. (1993). Evaluation of invasions and declines of submersed aquatic macrophytes. *Journal of Aquatic Plant Management*, *31*, 218-220.

Chambers, P. A. (1987). Nearshore occurrence of submersed aquatic macrophytes in relation to wave action. *Canadian Journal of Fisheries and Aquatic Sciences*, *44*(9), 1666-1669.

Chambers, P. A., & Kalff, J. (1985). Depth distribution and biomass of submersed aquatic macrophyte communities in relation to Secchi depth. *Canadian Journal of Fisheries and Aquatic Sciences*, *42*(4), 701-709.

Chambers, P. A., Lacoul, P., Murphy, K. J., & Thomaz, S. M. (2008). Global diversity of aquatic macrophytes in freshwater. *Hydrobiologia*, *595*, 9-26.

Chambers, P. A., Prepas, E. E., Hamilton, H. R., & Bothwell, M. L. (1991). Current Velocity and Its Effect on Aquatic Macrophytes in Flowing Waters. *Ecological Applications*, *1*(3), 249-257.

Chapin, F. S. I., Zavaleta, E. S., Eviner, V. T., Naylor, R. L., Vitousek, P. M., Reynolds, H. L., . . . Diaz, S. (2000). Consequences of changing biodiversity. *Nature*, *405*(6783), 234-242.

Cheng, F. Y., Van Meter, K. J., Byrnes, D. K., & Basu, N. B. (2020). Maximizing US nitrate removal through wetland protection and restoration. *Nature*, *588*(7839), 625-630.

Chezik, K. A., Anderson, S. C., & Moore, J. W. (2017). River networks dampen long-term hydrological signals of climate change. *Geophysical Research Letters*, *44*(14), 7256-7264.

Cole, J. J., & Caraco, N. F. (1998). Atmospheric exchange of carbon dioxide in a low-wind oligotrophic lake measured by the addition of SF6. *Limnology and Oceanography*, *43*(4), 647-656.

Cornwell, J. C., Kemp, W. M., & Kana, T. M. (1999). Denitrification in coastal ecosystems: methods, environmental controls, and ecosystem level controls, a review. *Aquatic Ecology*, *33*(1), 41-54.

Creed, R. (1998). A biogeographic perspective on Eurasian watermilfoil declines: additional evidence for the role of herbivorous weevils in promoting declines? *Journal of Aquatic Plant Management*, *36*, 16-22.

Cyr, H., & Downing, J. A. (1988). The abundance of phytophilous invertebrates on different species of submerged macrophytes*. *Freshwater Biology*, *20*(3), 365-374.

Das, S. K., Routh, J., & Roychoudhury, A. N. (2009). Biomarker evidence of macrophyte and plankton community changes in Zeekoevlei, a shallow lake in South Africa. *Journal of Paleolimnology*, *41*(3), 507-521.

Davidson, T. A., Sayer, C. D., Bennion, H., David, C., Rose, N., & Wade, M. P. (2005). A 250 year comparison of historical, macrofossil and pollen records of aquatic plants in a shallow lake. *Freshwater Biology, 20*, 1671-1686.

Davidson, N. C. (2014). How much wetland has the world lost? Long-term and recent trends in global wetland area. *Marine and Freshwater Research*, *65*(10), 934-941.

Davidson, T. A., Reid, M. A., Sayer, C. D., & Chilcott, S. (2013). Palaeolimnological records of shallow lake biodiversity change: Exploring the merits of single versus multi-proxy approaches. *Journal of Paleolimnology*, *49*(3), 431-446.

de Grandpré, A., Kinnard, C., & Bertolo, A. (2022). Open-Source Analysis of Submerged Aquatic Vegetation Cover in Complex Waters Using High-Resolution Satellite Remote Sensing: An Adaptable Framework. *Remote Sensing*, *14*(2).

de Winton, M. (2018). *Macrophyte Lake Data. Version 1.4. The National Institute of Water and Atmospheric Research (NIWA). Occurrence dataset*. https://doi.org/https://doi.org/10.15468/bpswec

Depew, D. C., Houben, A. J., Ozersky, T., Hecky, R. E., & Guildford, S. J. (2011). Submerged aquatic vegetation in Cook's Bay, Lake Simcoe: Assessment of changes in response to increased water transparency. *Journal of Great Lakes Research*, *37*(SUPPL. 3), 72-82.

Depew, D. C., Stevens, A. W., Smith, R. E. H., & Hecky, R. E. (2009). Detection and characterization of benthic filamentous algal stands (Cladophora sp.) on rocky substrata using a high-frequency echosounder. *Limnology and Oceanography-Methods*, *7*, 693-705.

Desmet, N. J. S., Van Belleghem, S., Seuntjens, P., Bouma, T. J., Buis, K., & Meire, P. (2011). Quantification of the impact of macrophytes on oxygen dynamics and nitrogen retention in a vegetated lowland river. *Physics and Chemistry of the Earth*, *36*(12), 479-489.

Diamond, J. S., Moatar, F., Cohen, M. J., Poirel, A., Martinet, C., Maire, A., & Pinay, G. (2021). Metabolic regime shifts and ecosystem state changes are decoupled in a large river. *Limnology and Oceanography*, *n/a*(n/a).

Domaizon, I., Winegardner, A., Capo, E., Gauthier, J., & Gregory-Eaves, I. (2017). DNA-based methods in paleolimnology: new opportunities for investigating long-term dynamics of lacustrine biodiversity. *Journal of Paleolimnology*, 58, 1-21.

Downing, J. A., & Anderson, M. R. (1985). Estimating the standing biomass of aquatic macrophytes. *Canadian Journal of Fisheries and Aquatic Sciences*, *42*(12), 1860-1869.

Duarte, C. M. (1987). Use of echosounder tracings to estimate aboveground biomass of submerged plants in lakes. *Canadian Journal of Fisheries and Aquatic Sciences*, *44*(4), 732-735. https://doi.org/10.1139/f87-088

Duarte, C. M., & Kalff, J. (1987). Latitudinal influences on the depths of maximum colonization and maximum biomass of submerged angiosperms in lakes *Canadian Journal of Fisheries and Aquatic Sciences*, *44*(10), 1759-1764.

Duarte, C. M., Agusti, S., Barbier, E., Britten, G. L., Castilla, J. C., Gattuso, J.-P., . . . Worm, B. (2020). Rebuilding marine life. *Nature, 580*, 39-51.

Duarte, C. M., & Kalff, J. (1990). Patterns in the submerged macrophyte biomass of lakes and the importance of the scale of analysis in the interpretation *Canadian Journal of Fisheries and Aquatic Sciences*, *47*(2), 357-363.

Dunic, J. C., Brown, C. J., Connolly, R. M., Turschwell, M. P., & Côté, I. M. (2021). Long-term declines and recovery of meadow area across the world's seagrass bioregions. *Global Change Biology*, *27*(17), 4096-4109.

Eigemann, F., Mischke, U., Hupfer, M., Schaumburg, J., & Hilt, S. (2016). Biological indicators track differential responses of pelagic and littoral areas to nutrient load reductions in German lakes. *Ecological Indicators*, *61*, 905-910.

Ejankowski, W., & Lenard, T. (2015). Climate driven changes in the submerged macrophyte and phytoplankton community in a hard water lake [Article]. *Limnologica*, *52*, 59-66.

Ensign, S. H., & Doyle, M. W. (2006). Nutrient spiraling in streams and river networks. *Journal of Geophysical Research: Biogeosciences*, *111*(G4). https://doi.org/https://doi.org/10.1029/2005JG000114

Eriksson, P., & Weisner, S. (1996). Functional differences in epiphytic microbial communities in nutrient-rich freshwater ecosystems: an assay of denitrifying capacity. *Freshwater Biology*, *36*(3), 555-562.

Ersoy, Z., Scharfenberger, U., Baho, D. L., Bucak, T., Feldmann, T., Hejzlar, J., . . . Beklioğlu, M. (2020). Impact of nutrients and water level changes on submerged macrophytes along a temperature gradient: A pan-European mesocosm experiment. *Global Change Biology*, *26*(12), 6831-6851.

European Union. (2000). Directive 2000/60/EC of the European Parliament and of the Council of 23 October 2000 establishing a framework for Community action in the field of water policy. *Official Journal of the European Communities*, L327/321-368.

Ezer, T., & Corlett, W. B. (2012). Is sea level rise accelerating in the Chesapeake Bay? A demonstration of a novel new approach for analyzing sea level data. *Geophysical Research Letters*, *39*(19).

Farquhar, G. D., von Caemmerer, S., & Berry, J. A. (1980). A biochemical model of photosynthetic CO2 assimilation in leaves of C3 species. *Planta*, *149*(1), 78-90.

Farrés, M., Platikanov, S., Tsakovski, S., & Tauler, R. (2015). Comparison of the variable importance in projection (VIP) and of the selectivity ratio (SR) methods for variable selection and interpretation. *Journal of Chemometrics*, *29*(10), 528-536.

Feuchtmayr, H., Moran, R., Hatton, K., Connor, L., Heyes, T., Moss, B., Harvey, I., & Atkinson, D. (2009). Global warming and eutrophication: effects on water chemistry and autotrophic communities in experimental hypertrophic shallow lake mesocosms. *Journal of Applied Ecology*, *46*(3), 713-723.

FGDC (Federal Geographical Data Committee) (2013). *Classification of wetlands and deepwater habitats of the United States. FGDC-STD-004-2013. Second Edition.* Washington, DC.

Galloway, J. N., Aber, J. D., Erisman, J. W., Seitzinger, S. P., Howarth, R. W., Cowling, E. B., & Cosby, B. J. (2003). The Nitrogen Cascade. *BioScience*, *53*(4), 341-356.

Garrison, P. J., & Wakeman, R. S. (2000). Use of paleolimnology to document the effect of lake shoreland development on water quality [Article]. *Journal of Paleolimnology*, *24*(4), 369-393.

Giacomazzo, M., Bertolo, A., Brodeur, P., Massicotte, P., Goyette, J.-O., & Magnan, P. (2020). Linking fisheries to land use: How anthropogenic inputs from the watershed shape fish habitat quality. *Science of The Total Environment*, *717*, 135377.

Gilbert, D., Sundby, B., Gobeil, C., Mucci, A., & Tremblay, G. H. (2005). A seventy-two-year record of diminishing deep-water oxygen in the St. Lawrence estuary: The northwest Atlantic connection. *Limnology and Oceanography*, *50*(5), 1654-1666.

Gombin, J., Vaidyanathan, R., & Agafonkib, V. (2020). concaveman: A Very Fast 2D Concave Hull Algorithm. R package version 1.1.0. https://CRAN.R-project.org/package=concaveman

Gopal, B. (2016). Should 'wetlands' cover all aquatic ecosystems and do macrophytes make a difference to their ecosystem services? *Folia Geobotanica*, *51*(3), 209-226.

Goulon, C., Le Meaux, O., Vincent-Falquet, R., & Guillard, J. (2021). Hydroacoustic Autonomous boat for Remote fish detection in LakE (HARLE), an unmanned autonomous surface vehicle to monitor fish populations in lakes. *Limnology and Oceanography: Methods*, *19*(4), 280-292.

Goyette, J.-O., Bennett, E. M., Howarth, R. W., & Maranger, R. (2016). Changes in anthropogenic nitrogen and phosphorus inputs to the St. Lawrence sub-basin over 110 years and impacts on riverine export. *Global Biogeochemical Cycles*, *30*(7), 1000-1014.

Goyette, J.-O., Bennett, E. M., & Maranger, R. (2019). Differential influence of landscape features and climate on nitrogen and phosphorus transport throughout the watershed. *Biogeochemistry*, *142*(1), 155-174.

Gudmundsson, L., Boulange, J., Do, H. X., Gosling, S. N., Grillakis, M. G., Koutroulis, A. G., . . . Papadimitriou, L. (2021). Globally observed trends in mean and extreme river flow attributed to climate change. *Science*, *371*(6534), 1159-1162.

Gumusay, M. U., Bakirman, T., Tuney Kizilkaya, I., & Aykut, N. O. (2019). A review of seagrass detection, mapping and monitoring applications using acoustic systems. *European Journal of Remote Sensing*, *52*(1), 1-29.

Hall, R. O., Baker, M. A., Rosi-Marshall, E. J., Tank, J. L., & Newbold, J. D. (2013). Solute-specific scaling of inorganic nitrogen and phosphorus uptake in streams. *Biogeosciences*, *10*(11), 7323-7331.

Hall, R. O., & Tank, J. L. (2003). Ecosystem metabolism controls nitrogen uptake in streams in Grand Teton National Park, Wyoming. *Limnology and Oceanography*, *48*, 1120-1128.

Hall, R. O., Tank, J. L., Sobota, D. J., Mulholland, P. J., O'Brien, J. M., Dodds, W. K., . . . Arangob, C. P. (2009). Nitrate removal in stream ecosystems measured by 15N addition experiments: Total uptake. *Limnology and Oceanography*, *54*(3), 653-665.

Hanlon, S. G., Hoyer, M. V., Cichra, C. E., & Canfield, D. E. (2000). Evaluation of macrophyte control in 38 Florida lakes using triploid grass carp. *Journal of Aquatic Plant Management*, *38*(2), 48-54.

Hargeby, A., Jonzén, N., & Blindow, I. (2006). Does a long-term oscillation in nitrogen concentration reflect climate impact on submerged vegetation and vulnerability to state shifts in a shallow lake? *Oikos*, *115*(2), 334-348.

He, J., Poder, T., Dupras, J., & Enomana, H. J. (2016). *La valeur économique de la pêche blanche et des services écosystémiques au Lac Saint-Pierre: analyse coûts-avantages des stratégies d'adaptation aux changements climatiques*. Rapport présenté à la Division des impacts et de l'adaptation liés aux changements climatiques de Ressources naturelles Canada, au Gouvernement du Québec et à Ouranos. Montréal : Université du Québec à Montréal . 162 p.

Heffernan, J. B., & Cohen, M. J. (2010). Direct and indirect coupling of primary production and diel nitrate dynamics in a subtropical spring-fed river. *Limnology and Oceanography*, *55*(2), 677-688.

Helminen, J., Linnansaari, T., Bruce, M., Dolson-Edge, R., & Curry, R. A. (2019). Accuracy and Precision of Low-Cost Echosounder and Automated Data Processing Software for Habitat Mapping in a Large River. *Diversity*, *11*(7), 116.

Hensley, R. T., & Cohen, M. J. (2016). On the emergence of diel solute signals in flowing waters. *Water Resources Research, 52*, 759-772.

Hijmans, R. J. (2020). raster: Geographic Data Analysis and Modeling. R package version 3.4-5. https://CRAN.R-project.org/package=raster

Hilt, S. (2015). Regime shifts between macrophytes and phytoplankton–concepts beyond shallow lakes, unravelling stabilizing mechanisms and practical consequences. *Limnetica*, *34*(2), 467-480.

Hilt, S., Alirangues Nuñez, M. M., Bakker, E. S., Blindow, I., Davidson, T. A., Gillefalk, M., Hansson, L.-A., Janse, J. H., Janssen, A. B. G., Jeppesen, E., Kabus, T., Kelly, A., Köhler, J., Lauridsen, T. L., Mooij, W. M., Noordhuis, R., Phillips, G., Rücker, J., Schuster, H.-H., Søndergaard, M., Teurlincx, S., van de Weyer, K., van Donk, E., Waterstraat, A., Willby, N., & Sayer, C. D. (2018). Response of submerged macrophyte communities to external and internal restoration measures in north temperate shallow lakes. *Frontiers in Plant Science*, *9*, Article 194. https://doi.org/10.3389/fpls.2018.00194

Hilt, S., Brothers, S., Jeppesen, E., Veraart, A. J., & Kosten, S. (2017). Translating Regime Shifts in Shallow Lakes into Changes in Ecosystem Functions and Services. *BioScience*, *67*(10), 928-936. https://doi.org/10.1093/biosci/bix106

Hobbs, W. O., Hobbs, J. M. R., Ois, T. L., Zimmer, K. D., Theissen, K. M., Edlund, M. B., . . . Carlson, T. J. (2012). A 200-year perspective on alternative stable state theory and lake management from a biomanipulated shallow lake. *Ecological Applications*, *22*(5), 1483-1496.

Howarth, R., Swaney, D., Billen, G., Garnier, J., Hong, B., Humborg, C., . . . Marino, R. (2012). Nitrogen fluxes from the landscape are controlled by net anthropogenic nitrogen inputs and by climate. *Frontiers in Ecology and the Environment*, *10*(1), 37-43.

Howarth, R. W., Billen, G., Swaney, D., Townsend, A., Jaworski, N., Lajtha, K., . . . Zhao-Liang, Z. (1996). Regional nitrogen budgets and riverine N & P fluxes for the drainages to the North Atlantic Ocean: Natural and human influences. *Biogeochemistry*, *35*(1), 75-139.

Howell, A. W., & Richardson, R. J. (2019). Correlation of consumer grade hydroacoustic signature to submersed plant biomass. *Aquatic Botany*, *155*, 45-51.

Hu, S., Niu, Z., Chen, Y., Li, L., & Zhang, H. (2017). Global wetlands: Potential distribution, wetland loss, and status. *Science of the Total Environment*, *586*, 319-327.

Huang, N. E., Shen, Z., Long, S. R., Wu, M. C., Shih, H. H., Zheng, Q., . . . Liu, H. H. (1998). The empirical mode decomposition and the Hilbert spectrum for nonlinear and non-stationary time series analysis. *Proceedings of the Royal Society of London. Series A: Mathematical, Physical and Engineering Sciences*, *454*(1971), 903-995.

Hudon, C. (1997). Impact of water level fluctuations on St. Lawrence River aquatic vegetation. *Canadian Journal of Fisheries and Aquatic Sciences*, *54*(12), 2853-2865.

Hudon, C., Armellin, A., Gagnon, P., & Patoine, A. (2010). Variations in water temperatures and levels in the St. Lawrence River (Québec, Canada) and potential implications for three common fish species. *Hydrobiologia*, *647*(1), 145-161.

Hudon, C., & Carignan, R. (2008). Cumulative impacts of hydrology and human activities on water quality in the St. Lawrence River (Lake Saint-Pierre, Quebec, Canada) [Article]. *Canadian Journal of Fisheries and Aquatic Sciences*, *65*(6), 1165-1180.

Hudon, C., Cattaneo, A., Poirier, A.-M. T., Brodeur, P., Dumont, P., Mailhot, Y., . . . de Lafontaine, Y. (2012). Oligotrophication from wetland epuration alters the riverine trophic network and carrying capacity for fish. *Aquatic Sciences*, *74*(3), 495-511.

Hudon, C., De Sève, M., & Cattaneo, A. (2014). Increasing occurrence of the benthic filamentous cyanobacterium Lyngbya wollei: a symptom of freshwater ecosystem degradation. *Freshwater Science*, *33*(2), 606-618.

Hudon, C., Gagnon, P., Rondeau, M., Hébert, S., Gilbert, D., Hill, B., . . . Starr, M. (2017). Hydrological and biological processes modulate carbon, nitrogen and phosphorus flux from the St. Lawrence River to its estuary (Quebec, Canada). *Biogeochemistry*, *135*(3), 251-276.

Hudon, C., Jean, M., & Létourneau, G. (2018). Temporal (1970–2016) changes in human pressures and wetland response in the St. Lawrence River (Québec, Canada). *Science of The Total Environment*, *643*, 1137-1151.

Hudon, C., Lalonde, S., & Gagnon, P. (2000). Ranking the effects of site exposure, plant growth form, water depth, and transparency on aquatic plant biomass. *Canadian Journal of Fisheries and Aquatic Sciences*, *57*(S1), 31-42.

Hudon, C., Wilcox, D., & Ingram, J. (2006). Modeling wetland plant community response to assess water-level regulation scenarios in the Lake Ontario-St. Lawrence River basin. *Environmental Monitoring and Assessment*, *113*(1-3), 303-328.

Hussner, A., Stiers, I., Verhofstad, M. J. J. M., Bakker, E. S., Grutters, B. M. C., Haury, J., . . . Hofstra, D. (2017). Management and control methods of invasive alien freshwater aquatic plants: A review. *Aquatic Botany*, *136*, 112-137. https://doi.org/https://doi.org/10.1016/j.aquabot.2016.08.002

Hutorowicz, A., Białowąs, M., Długoszewski, B., & Doroszczyk, L. (2017). An attempt to assess the ecological status of a lake based on historical and current maps of submerged vegetation. *Archives of Polish Fisheries*, *25*(1), 33-42.

IPCC. (2018). Summary for Policymakers. In V. Masson-Delmotte, P. Zhai, H.-O. Pörtner, D. Roberts, J. Skea, P. R. Shukla, A. Pirani, W. Moufouma-Okia, C. Péan, R. Pidcock, S. Connors, J. B. R. Matthews, Y. Chen, X. Zhou, M. I. Gomis, E. Lonnoy, T. Maycock, M. Tignor, & T. Waterfield (Eds.), *Global Warming of 1.5°C. An IPCC Special Report on the impacts of global warming of 1.5°C above pre-industrial levels and related global greenhouse gas emission pathways, in the context of strengthening the global response to the threat of climate change, sustainable development, and efforts to eradicate poverty*.

Iversen, L. L., Girón, J. G., & Pan, Y. (2022). Towards linking freshwater plants and ecosystems via functional biogeography. *Aquatic Botany*, *176*, 103454. https://doi.org/https://doi.org/10.1016/j.aquabot.2021.103454

James, W. F. (2010). Nitrogen retention in a floodplain backwater of the upper Mississippi River (USA). *Aquatic Sciences*, *72*(1), 61-69.

Janssen, A. B. G., Hilt, S., Kosten, S., de Klein, J. J. M., Paerl, H. W., & Van de Waal, D. B. (2021). Shifting states, shifting services: Linking regime shifts to changes in ecosystem services of shallow lakes. *Freshwater Biology*, *66*(1), 1-12.

Jean, M., Létourneau, G., & Savage, C. (2002). Freshwater wetland and exotic plant species 2nd edition. In S. a. T. B. Environment Canada, Water Quality Monitoring (Ed.), *Monitoring sheet in the "Monitoring of the State of the St. Lawrence" series.*

Jeppesen, E., Leavitt, P., De Meester, L., & Jensen, J. P. (2001). Functional ecology and palaeolimnology: using cladoceran remains to reconstruct anthropogenic impact. *Trends in Ecology & Evolution*, *16*(4), 191-198.

Jeppesen, E., Sondergaard, M., Sondergaard, M., & Christofferson, K. (1998). *The structuring role of submerged macrophytes in lakes* (Vol. 131). Springer Science & Business Media.

Johansson, L. S., Amsinck, S. L., Bjerring, R., & Jeppesen, E. (2005). Mid- to late-Holocene land-use change and lake development at Dallund Sø, Denmark: Trophic structure inferred from cladoceran subfossils . *Holocene*, *15*(8), 1143-1151.

Johnson, J. A., & Newman, R. M. (2011). A comparison of two methods for sampling biomass of aquatic plants. *Journal of Aquatic Plant Management*, *49*, 1-8.

Johnson, J. B., & Omland, K. S. (2004). Model selection in ecology and evolution. *Trends in Ecology & Evolution*, *19*(2), 101-108.

Johnson, M. P. (2020). Estimating intertidal seaweed biomass at larger scales from quadrat surveys. *Marine Environmental Research*, *156*, Article 104906. https://doi.org/10.1016/j.marenvres.2020.104906

Johnson, R. L., Van Dusen, P. J., Toner, J. A., & Hairston Jr, N. G. (2000). Eurasian watermilfoil biomass associated with insect herbivores in New York. *Journal of Aquatic Plant Management*, *38*(2), 82-88.

Juggins, S. (2013). Quantitative reconstruction in palaeolimnology: new paradigm or sick science? *Quaternary Science Reviews, 64*, 20-32.

Kalff, J. (2001). *Limnology: Inland water ecosystems*. Prentice Hall, Upper Saddle River.

Karjalainen, H., Stefansdottir, G., Tuominen, L., & Kairesalo, T. (2001). Do submersed plants enhance microbial activity in sediment? *Aquatic Botany*, *69*(1), 1-13.

Keddy, P. A. (2010). *Wetland ecology: principles and conservation* (2nd ed.). Cambridge University Press.

Kenney, W. F., Waters, M. N., Schelske, C. L., & Brenner, M. (2002). Sediment records of phosphorus-driven shifts to phytoplankton dominance in shallow Florida lakes. *Journal of Paleolimnology*, *27*(3), 367-377.

Kenow, K. P., Lyon, J. E., Hines, R. K., & Elfessi, A. (2007). Estimating biomass of submersed vegetation using a simple rake sampling technique. *Hydrobiologia*, *575*, 447-454.

Kim, K., & Oh, H.-S. (2018). EMD: Empirical Mode Decomposition and Hilbert Spectral Analysis. R package version 1.5.8.

Kimber, A., Valk, A. G. v. d., & Korschgen, C. E. (1995). The distribution of Vallisneria americana seeds and seedling light requirements in the Upper Mississippi River. *Canadian Journal of Botany*, *73*(12), 1966-1973.

Klamt, A.-M, Jensen, H. S., Mortensen, M. F., Schreiber, N., Reitzel, K. (2017). The importance of catchment vegetation for alkalinity, phosphorus burial and macrophytes as revealed by a recent paleolimnological study in a soft water lake. *Science of the Total Environment, 580*, 1097-1107

Körner, S. (2002). Loss of submerged macrophytes in shallow lakes in North-Eastern Germany. *International Review of Hydrobiology*, *87*(4), 375-384.

Kornijów, R., Kowalewski, G., Sugier, P., Kaczorowska, A.,. Gasiorowski, M., & Woszczyk, M. (2016). Towards a more precisely defined macrophyte-dominated regime: the recent history of a shallow lake in Eastern Poland. *Hydrobiologia, 772*, 45–62.

Kosten, S., Kamarainen, A., Jeppesen, E., van Nes, E. H., Peeters, E. T., Mazzeo, N., . . . Lauridsen, T. L. (2009). Climate-related differences in the dominance of submerged macrophytes in shallow lakes. *Global Change Biology*, *15*(10), 2503-2517.

Kowalewski, G. A., Kornijów, R., McGowan, S., Kaczorowska, A., Bałaga, K., Namiotko, T., . . . Wasiłowska, A. (2016). Disentangling natural and anthropogenic drivers of changes in a shallow lake using palaeolimnology and historical archives. *Hydrobiologia*, *767*(1), 301-320.

Kraska, M., Klimaszyk, P., & Piotrowicz, R. (2013). Anthropogenic changes in properties of the water and spatial structure of the vegetation of the lobelia lake Lake Modre in the Bytów Lakeland. *Oceanological and Hydrobiological Studies*, *43*(3), 302-313.

Krause, J. R., Hinojosa-Corona, A., Gray, A. B., & Watson, E. B. (2021). Emerging Sensor Platforms Allow for Seagrass Extent Mapping in a Turbid Estuary and from the Meadow to Ecosystem Scale. *Remote Sensing*, *13*(18), Article 3681.

Lachavanne, J. B., Perfetta, J., & Juge, R. (1992). Influence of water eutrophication on the macrophytic vegetation of Lake Lugano. *Aquatic Sciences*, *54*(3-4), 351-363.

Lacoul, P., & Freedman, B. (2006). Environmental influences on aquatic plants in freshwater ecosystems. *Environmental Reviews*, *14*(2), 89-136.

Lacoul, P., & Freedman, B. (2006). Recent observation of a proliferation of Ranunculus trichophyllus Chaix. in high-altitude of the Mount Everest region. *Arctic, Antarctic, and Alpine Research*, *38*(3), 394-398.

Laursen, A. E., & Seitzinger, S. P. (2004). Diurnal patterns of denitrification, oxygen consumption and nitrous oxide production in rivers measured at the whole-reach scale. *Freshwater Biology, 46*, 1448-1458.

Lavorel, S. & Garnier, E. (2002). Predicting changes in community composition and ecosystem functioning from plant traits: revisiting the Holy Grail. *Functional Ecology, 16*, 545-556.

Lehmann, M. F., Barnett, B., Gélinas, Y., Gilbert, D., Maranger, R. J., Mucci, A., . . . Thibodeau, B. (2009). Aerobic respiration and hypoxia in the Lower St. Lawrence Estuary: Stable isotope ratios of dissolved oxygen constrain oxygen sink partitioning. *Limnology and Oceanography*, *54*(6), 2157-2169.

Lehner, B., & Döll, P. (2004). Development and validation of a global database of lakes, reservoirs and wetlands. *Journal of Hydrology*, *296*(1), 1-22.

Les, D. H., Crawford, D. J., Kimball, R. T., Moody, M. L., & Landolt, E. (2003). Biogeography of discontinuously distributed hydrophytes: a molecular appraisal of intercontinental disjunctions. *International Journal of Plant Sciences*, *164*(6), 917-932.

Li, J., Ianaiev, V., Huff, A., Zalusky, J., Ozersky, T., & Katsev, S. (2021). Benthic invaders control the phosphorus cycle in the world's largest freshwater ecosystem. *Proceedings of the national academy of sciences*, *118*(6).

Liang, C., & Zhang, Z. (2011). Vegetation dynamic changes of Lake Nansi wetland in Shandong of China. *Procedia Environmental Sciences, 11*, 983-988.

Lloyd, C. E. M., Freer, J. E., Collins, A. L., Johnes, P. J., & Jones, J. I. (2014). Methods for detecting change in hydrochemical time series in response to targeted pollutant mitigation in river catchments. *Journal of Hydrology*, *514*, 297-312.

Lodge, D. M. (1991). Herbivory on freshwater macrophytes. *Aquatic Botany*, *41*(1), 195-224.

López-Blanco, C., Vicente, E., & Miracle, M. R. (2012). Cladocera sub-fossils and plant macrofossils as indicators of droughts in Lagunillo del Tejo (Spain) - Implications for climatic studies. *Fundamental and Applied Limnology*, *180*(3), 207-220.

Lu, C., Zhang, J., Tian, H., Crumpton, W. G., Helmers, M. J., Cai, W.-J., . . . Lohrenz, S. E. (2020). Increased extreme precipitation challenges nitrogen load management to the Gulf of Mexico. *Communications Earth & Environment*, *1*(1), 21.

Maceina, M. J., Shireman, J. V., Langeland, K. A., & Canfield, D. E. (1984). Prediction of submersed plant biomass by use of a recording fathometer. *Journal of Aquatic Plant Management*, *22*(JAN), 35-38.

Madgwick, G., Emson, D., Sayer, C. D., Willby, N. J., Rose. N. L., Jackson, M. J., & Kelly, K. (2011). Centennial-scale changes to the aquatic vegetation structure of a shallow eutrophic lake and implications for restoration. *Freshwater Biology, 56*, 2620–2636.

Madsen, J. D. (1993). Biomass Techniques for Monitoring and Assessing Control of Aquatic Vegetation. *Lake and Reservoir Management*, *7*(2), 141-154.

Madsen, J. D., Chambers, P. A., James, W. F., Koch, E. W., & Westlake, D. F. (2001). The interaction between water movement, sediment dynamics and submersed macrophytes. *Hydrobiologia*, *444*(1-3), 71-84.

Madsen, J. D., & Wersal, R. M. (2017). A review of aquatic plant monitoring and assessment methods. *Journal of Aquatic Plant Management*, *55*(1), 1-12.

Magnuson, J. J., Carpenter, S. R., & Stanley, E. H. (2016a). *North Temperate Lakes LTER: Macrophyte Biomass - Madison Lakes Area 1995 - current* (24; Version 4) LTER. https://lter.limnology.wisc.edu/dataset/north-temperate-lakes-lter-macrophyte-biomass-madison-lakes-area-1995-current

Magnuson, J. J., Carpenter, S. R., & Stanley, E. H. (2016b). *North Temperate Lakes LTER: Macrophyte Biomass - Trout Lake 1983 - current* (21; Version 4) LTER. https://lter.limnology.wisc.edu/dataset/north-temperate-lakes-lter-macrophyte-biomass-trout-lake-1983-current

Marine Environmental Data Section. (2017). Canadian Tides and Water Levels Data Archives. Retrieved 2017/11/27. https://climate.weather.gc.ca

Masto, N. M., Bauer, B. A., Kaminski, R. M., Sharpe, C., Leland, R. C., Wiggers, E., & Gerard, P. D. (2020). Rake Sampling to Estimate Biomass of Submersed Aquatic Vegetation in Coastal Wetlands. *Wetlands*. https://doi.org/10.1007/s13157-020-01296-3

May, L., & Carvalho, L. (2010). Maximum growing depth of macrophytes in Loch Leven, Scotland, United Kingdom, in relation to historical changes in estimated phosphorus loading. *Hydrobiologia*, *646*(1), 123-131.

McKenzie, L. J., Nordlund, L. M., Jones, B. L., Cullen-Unsworth, L. C., Roelfsema, C., & Unsworth, R. K. F. (2020). The global distribution of seagrass meadows. *Environmental Research Letters*, *15*(7), 074041. https://doi.org/10.1088/1748-9326/ab7d06

MEA (Millenium Ecosystem Assessment). (2005). *Ecosystems and human well-being: wetlands and water.* World Resource Institute. Washington, DC.

Mehmood, T., Liland, K. H., Snipen, L., & Sæbø, S. (2012). A review of variable selection methods in Partial Least Squares Regression. *Chemometrics and Intelligent Laboratory Systems*, *118*, 62-69.

Messager, M. L., Lehner, B., Grill, G., Nedeva, I., & Schmitt, O. (2016). Estimating the volume and age of water stored in global lakes using a geo-statistical approach. *Nature Communications*, *7*(1), 13603. https://doi.org/10.1038/ncomms13603

Meteorological Service of Canada. (2017). Historical Climate Data. Environment and Climate Change Canada.https://climate.weather.gc.ca

Mevik, B.-H., & Wehrens, R. (2007). The pls Package: Principal Component and Partial Least Squares Regression in R. *Journal of Statistical Software*, *18*(2), 23. https://doi.org/10.18637/jss.v018.i02

Mevik, B.-H., Wehrens, R., & Liland, K. H. (2020). pls: Partial Least Squares and Principal Component Regression. R package version 2.7-3. https://CRAN.R-project.org/package=pls

Middelboe, A. L., & Markager, S. (1997). Depth limits and minimum light requirements of freshwater macrophytes. *Freshwater Biology*, *37*(3), 553-568.

Mitsch, W. J., Day, J. W., Wendell Gilliam, J., Groffman, P. M., Hey, D. L., Randall, G. W., & Wang, N. (2001). Reducing nitrogen loading to the Gulf of Mexico from the Mississippi River Basin: strategies to counter a persistent ecological problem. *BioScience*, *51*(5), 373-388.

Morin, J., & Côté, J.-P. (2003). Modifications anthropiques sur 150 ans au lac Saint-Pierre: une fenêtre sur les transformations de l'écosystème du Saint-Laurent. *VertigO*, *4*(3). https://doi.org/10.4000/vertigo.3867

Morse, B. (1990). *St. Lawrence River water levels study: Application ot the One-D hydrodynamic model*. Transport Canada, Waterways Development Division, Canadian Coast Guard.

Moss, B. (2015). Mammals, freshwater reference states, and the mitigation of climate change. *Freshwater Biology*, *60*(9), 1964-1976. https://doi.org/https://doi.org/10.1111/fwb.12614

Mulholland, P. J., Tank, J. L., Webster, J. R., Bowden, W. B., Dodds, W. K., Gregory, S. V., . . . Wollheim, W. M. (2002). Can uptake length in streams be determined by nutrient addition experiments? Results from an interbiome comparison study. *Journal of the North American Benthological Society*, *21*(4), 544-560.

Munday, E., Moore, B., & Burczynski, J. (2013, 23-27 Sept. 2013). Hydroacoustic mapping system for quantitative identification of aquatic macrophytes, substrate composition, and shallow water bathymetric surveying. 2013 OCEANS - San Diego,

Netten, J. J., Arts, G. H., Gylstra, R., van Nes, E. H., Scheffer, M., & Roijackers, R. M. (2010). Effect of temperature and nutrients on the competition between free-floating Salvinia natans and submerged Elodea nuttallii in mesocosms. *Fundamental and Applied Limnology*, *177*(2), 125.

Newbold, J. D., Elwood, J. W., O'Neill, R. V., & Winkle, W. V. (1981). Measuring nutrient spiralling in streams. *Canadian Journal of Fisheries and Aquatic Sciences*, *38*(7), 860-863.

Newman, R. M., & Biesboer, D. D. (2000). A decline of Eurasian watermilfoil in Minnesota associated with the milfoil weevil, Euhrychiopsis lecontei. *Journal of Aquatic Plant Management*, *38*(2), 105-111.

Nichols, S. (2021). *Wisconsin Lake Plants - multi source database of lake plant abundance 1930 - 2004 ver 4*. Dataset. https://doi.org/https://doi.org/10.6073/pasta/11c4066914f4cbb75d3ca5381e891453

Nijssen, B., O'Donnell, G. M., Hamlet, A. F., & Lettenmaier, D. P. (2001). Hydrologic Sensitivity of Global Rivers to Climate Change. *Climatic Change*, *50*(1), 143-175.

O'Hare, M. T., Baattrup-Pedersen, A., Baumgarte, I., Freeman, A., Gunn, I. D. M., Lázár, A. N., . . . Bowes, M. J. (2018). Responses of Aquatic Plants to Eutrophication in Rivers: A Revised Conceptual Model. *Frontiers in Plant Science*, *9*.

Oksanen, J., Blanchet, F. G., Friendly, M., Kindt, R., Legendre, P., McGlinn, D., . . . H, W. (2020). vegan: Community Ecology Package. R package version 2.5-7. https://CRAN.R-project.org/package=vegan

Orth, R. J., Dennison, W. C., Lefcheck, J. S., Gurbisz, C., Hannam, M., Keisman, J., . . . Wilcox, D. J. (2017). Submersed Aquatic Vegetation in Chesapeake Bay: Sentinel Species in a Changing World. *BioScience*, *67*(8), 698-712.

Orth, R. J., Lefcheck, J. S., McGlathery, K. S., Aoki, L., Luckenbact, M., Moore, . . . Lusks, B. (2020). Restoration of seagrass habitat leads to rapid recovery of coastal ecosystem services. *Science Advances, 6,* eabcd6434.

Ouranos. (2015). *Vers l'adaptation. Synthèse des connaissances sur les changements climatiques au Québec. Édition 2015*. Montréal, Québec: Ouranos.

Pebesma, E. J. (2004). Multivariable geostatistics in S: the gstat package. *Computers & Geoscience*, *30*, 683-691.

Pebesma, E. J. (2018). Simple Features for R: Standardized Support for Spatial Vector Data. *The R Journal*, *10*(1), 439-446.

Pebesma, E. J., & Bivand, R. S. (2005). Classes and methods for spatial data in R. R News 5 (2). https://cran.r-project.org/doc/Rnews/

Peterson, B. J., Wollheim, W. M., Mulholland, P. J., Webster, J. R., Meyer, J. L., Tank, J. L., . . . Hershey, A. E. (2001). Control of nitrogen export from watersheds by headwater streams. *Science*, *292*(5514), 86-90.

Philbrick, C. T., & Les, D. H. (1996). Evolution of Aquatic Angiosperm Reproductive Systems: What is the balance between sexual and asexual reproduction in aquatic angiosperms? *BioScience*, *46*(11), 813-826. h

Phillips, D. L., & Gregg, J. W. (2001). Uncertainty in source partitioning using stable isotopes. *Oecologia*, *127*(2), 171-179.

Phillips, G., Bennion, H., Perrow, M., Sayer, C. D., Spears, B., & Willby, N. (2015). *A Review of Lake Restoration Practices and their Performance in the Broads National Park, 1980-2013.* https://www.broads-authority.gov.uk/looking-after/managing-land-and-water/conservation-publications-and-reports/water-conservation-reports

Phillips, G., Willby, N., & Moss, B. (2016). Submerged macrophyte decline in shallow lakes: What have we learnt in the last forty years? *Aquatic Botany*, *135*, 37-45.

Phillips, R. C., & McRoy, C. P. (1990). Seagrass research methods. Monographs on oceanographic methodology. UNESCO.

Piña-Ochoa, E., & Álvarez-Cobelas, M. (2006). Denitrification in Aquatic Environments: A Cross-system Analysis. *Biogeochemistry*, *81*(1), 111-130.

Pinardi, M., Bartoli, M., Longhi, D., Marzocchi, U., Laini, A., Ribaudo, C., & Viaroli, P. (2009). Benthic metabolism and denitrification in a river reach: a comparison between vegetated and bare sediments. *Journal of Limnology*, *68*(1), 133-145.

Pinheiro, J., Bates, D., DebRoy, S., Sarkar, D., & RCoreTeam. (2020). nlme: Linear and nonlinear mixed effects models. R package version 3.1-144. https://CRAN.R-project.org/package=nlme

Preiner, S., Dai, Y., Pucher, M., Reitsema, R. E., Schoelynck, J., Meire, P., & Hein, T. (2020). Effects of macrophytes on ecosystem metabolism and net nutrient uptake in a groundwater fed lowland river. *Science of The Total Environment*, *721*, Article 137620. https://doi.org/10.1016/j.scitotenv.2020.137620

QGIS Development Team. (2014). QGIS Geographic Information System, version 2.14.2. Open Source Geospatial Foundation Project. http://qgis.org

QGIS.org. (2019). QGIS Geographic Information System 3.10. http://www.qgis.org

R Core Team. (2020). R: A language and environment for statistical computing. R Foundation for Statistical Computing, Vienna, Austria. https://www.R-project.org/

Rabaey, J. S., Domine, L. M., Zimmer, K. D., & Cotner, J. B. (2021). Winter Oxygen Regimes in Clear and Turbid Shallow Lakes. *Journal of Geophysical Research: Biogeosciences*, *126*(3), e2020JG006065. https://doi.org/https://doi.org/10.1029/2020JG006065

Ramsar Convention. (2012). Resolution XI.8 Annex 2: strategic framework and guidelines for the future development of the List of Wetlands of International Importance of the Convention on Wetlands (Ramsar, Iran, 1971) – 2012 revision.

Ramus, A. P., Silliman, B. R., Thomsen, M. S., & Long, Z. T. (2017). An invasive foundation species enhances multifunctionality in a coastal ecosystem. *Proceedings of the National Academy of Sciences of the United States of America*, *114*(32), 8580-8585.

Rascio, N. (2002). The underwater life of secondarily aquatic plants: some problems and solutions. *Critical Reviews in Plant Sciences*, *21*(4), 401-427.

Rasmussen, P., & John Anderson, N. (2005). Natural and anthropogenic forcing of aquatic macrophyte development in a shallow Danish lake during the last 7000 years. *Journal of Biogeography*, *32*(11), 1993-2005.

Rattan, R., Sharma, B., Kumar, R., Saigal, V., & Shukla, S. (2021). Ramsar Convention. In Sharma, S. & S. Singh (Eds), *Wetlands Conservation: Current Challenges and Future Stategies* (pp. 17-39). https://doi.org/https://doi.org/10.1002/9781119692621.ch2

Rautio, M., Dufresne, F., Laurion, I., Bonilla, S., Vincent, W. F., & Christoffersen, K. S. (2011). Shallow freshwater ecosystems of the circumpolar Arctic. *Écoscience*, *18*(3), 204-222.

Reddy, K. R., Patrick, W. H., & Lindau, C. W. (1989). Nitrification-denitrification at the plant root-sediment interface in wetland *Limnology and Oceanography*, *34*(6), 1004-1013.

Reynolds, S. A., & Aldridge, D. C. (2021). Global impacts of invasive species on the tipping points of shallow lakes. *Global Change Biology*, *27*(23), 6129-6138.

Ricciardi, A., & MacIsaac, H. J. (2000). Recent mass invasion of the North American Great Lakes by Ponto–Caspian species. *Trends in Ecology & Evolution*, *15*(2), 62-65.

Rice, S. P., Kiffney, P., Greene, C., & Pess, G. R. (2008). The ecological importance of tributaries and confluences. *River confluences, tributaries and the fluvial network*, 209-242.

Riis, T., Olesen, B., Clayton, J. S., Lambertini, C., Brix, H., & Sorrell, B. K. (2012). Growth and morphology in relation to temperature and light availability during the establishment of three invasive aquatic plant species. *Aquatic Botany*, *102*, 56-64.

Risgaard-Petersen, N., & Jensen, K. (1997). Nitrification and denitrification in the rhizosphere of the aquatic macrophyte Lobelia dortmanna L. *Limnology and Oceanography*, *42*(3), 529-537.

Rodusky, A. J., Sharfstein, B., East, T. L., & Maki, R. P. (2005). A comparison of three methods to collect submerged aquatic vegetation in a shallow lake. *Environmental Monitoring and Assessment*, *110*(1-3), 87-97.

Rogers, S., McFarland, D., & Barko, J. (1995). Evaluation of the growth of Vallisneria americana Michx. in relation to sediment nutrient availability. *Lake and Reservoir Management*, *11*(1), 57-66.

Rooney, N., & Kalff, J. (2000). Inter-annual variation in submerged macrophyte community biomass and distribution: the influence of temperature and lake morphometry. *Aquatic Botany*, *68*(4), 321-335.

Rooney, N., Kalff, J., & Habel, C. (2003). The role of submerged macrophyte beds in phosphorus and sediment accumulation in Lake Memphremagog, Quebec, Canada. *Limnology and Oceanography*, *48*(5), 1927-1937.

Rosińska, J., & Gołdyn, R. (2018). Response of vegetation to growing recreational pressure in the shallow Raczyńskie Lake. *Knowledge and Management of Aquatic Ecosystems*, *186*(419), 1-8.

Rowan, G. S. L., & Kalacska, M. (2021). A Review of Remote Sensing of Submerged Aquatic Vegetation for Non-Specialists. *Remote Sensing*, *13*(4), 623.

Runkel, R., & De Cicco, L. (2017). Rloadest: River Load Estimation. R package version 0.4.5.

Sabol, B. M., Melton, R. E., Chamberlain, R., Doering, P., & Haunert, K. (2002). Evaluation of a digital echo sounder system for detection of submersed aquatic vegetation. *Estuaries*, *25*(1), 133-141.

Sala, O. E., Chapin, F. S., Armesto, J. J., Berlow, E., Bloomfield, J., Dirzo, R., . . . Kinzig, A. (2000). Global biodiversity scenarios for the year 2100. *Science*, *287*(5459), 1770-1774.

Sand-Jensen, K., Riis, T., Vestergaard, O., & Larsen, S. E. (2000). Macrophyte decline in Danish lakes and streams over the past 100 years. *Journal of Ecology*, *88*(6), 1030-1040.

Sand-Jensen, K., & Søndergaard, M. (1981). Phytoplankton and Epiphyte Development and Their Shading Effect on Submerged Macrophytes in Lakes of Different Nutrient Status. *Internationale Revue der gesamten Hydrobiologie und Hydrographie*, *66*(4), 529-552.

Santamaría, L. (2002). Why are most aquatic plants widely distributed? Dispersal, clonal growth and small-scale heterogeneity in a stressful environment. *Acta Oecologica*, *23*(3), 137-154.

Scheffer, M. (2004). The story of some shallow lakes In M. Scheffer (Ed.), *Ecology of shallow lakes* (pp. 1-18). Springer.

Scheffer, M., Carpenter, S., Foley, J. A., Folke, C., & Walker, B. (2001). Catastrophic shifts in ecosystems. *Nature*, *413*(6856), 591-596.

Scheffer, M., Hosper, S. H., Meijer, M. L., Moss, B., & Jeppesen, E. (1993). Alternatives equilibria in shallow lakes *Trends in Ecology & Evolution*, *8*(8), 275-279.

Schramski, J. R., Dell, A. I., Grady, J. M., Sibly, R. M., & Brown, J. H. (2015). Metabolic theory predicts whole-ecosystem properties. *Proceedings of the National Academy of Sciences*, *112*(8), 2617-2622.

Schutten, J., Dainty, J., & Davy, A. J. (2005). Root anchorage and its significance for submerged plants in shallow lakes. *Journal of Ecology*, *93*(3), 556-571.

Seitzinger, S., Harrison, J. A., Böhlke, J. K., Bouwman, A. F., Lowrance, R., Peterson, B., . . . Drecht, G. V. (2006). Denitrification across landscapes and waterscapes: a synthesis. *Ecological Applications*, *16*(6), 2064-2090.

Seitzinger, S. P., Styles, R. V., Boyer, E. W., Alexander, R. B., Billen, G., Howarth, R. W., . . . van Breemen, N. (2002). Nitrogen retention in rivers: model development and application to watersheds in the northeastern U.S.A. *Biogeochemistry*, *57*(1), 199-237.

Short, F. T., & Coles, R. G. (2001). *Global Seagrass Research Methods*. Elsevier Science. https://doi.org/https://doi.org/10.1016/B978-044450891-1/50000-1

Short, F. T., Kosten, S., Morgan, P. A., Malone, S., & Moore, G. E. (2016). Impacts of climate change on submerged and emergent wetland plants. *Aquatic Botany*, *135*, 3-17.

Smol. J. P. (1992). Paleolimnology: an important tool for effective ecosystem management. *Journal of Aquatic Ecosystem Health, 1,* 49-58.

Søndergaard, M., Johansson, L. S., Lauridsen, T. L., Jørgensen, T. B., Liboriussen, L., & Jeppesen, E. (2010). Submerged macrophytes as indicators of the ecological quality of lakes. *Freshwater Biology*, *55*(4), 893-908.

Søndergaard, M., Lauridsen, T. L., Johansson, L. S., & Jeppesen, E. (2017). Repeated fish removal to restore lakes: Case study of Lake Væng, Denmark—Two Biomanipulations during 30 years of monitoring. *Water*, *9*(1), 43.

Spencer, D. F., Ksander, G. G., Madsen, J. D., & Owens, C. S. (2000). Emergence of vegetative propagules of Potamogeton nodosus, Potamogeton pectinatus, Vallisneria americana, and Hydrilla verticillata based on accumulated degree-days. *Aquatic Botany*, *67*(3), 237-249.

Spierenburg, P., Roelofs, J. G. M., Andersen, T. J., & Lotter, A. F. (2010). Historical changes in the macrophyte community of a Norwegian softwater lake. *Journal of Paleolimnology*, *44*(3), 841-853.

Stallone, A., Cicone, A., & Materassi, M. (2020). New insights and best practices for the successful use of Empirical Mode Decomposition, Iterative Filtering and derived algorithms. *Scientific Reports*, *10*(1), 15161.

Steffen, K., Becker, T., Herr, W., & Leuschner, C. (2013). Diversity loss in the macrophyte vegetation of northwest German streams and rivers between the 1950s and 2010. *Hydrobiologia*, *713*(1), 1-17.

Steffen, W., Broadgate, W., Deutsch, L., Gaffney, O., & Ludwig, C. (2015). The trajectory of the Anthropocene: The Great Acceleration. *The Anthropocene Review*, *2*(1), 81-98.

Steffen, W., Crutzen, P. J., & McNeill, J. R. (2007). The Anthropocene: Are Humans Now Overwhelming the Great Forces of Nature. *AMBIO: A Journal of the Human Environment*, *36*(8), 614-621.

Stephens, T., Augustinus, P., Rip, B., Gadd, P., & Zawadski, A. (2018). Managing land-use effects on Northland dune lakes: lessons from the past. *New Zealand Journal of Marine and Freshwater Research*, *52*(3), 409-429.

Stevenson, J. C. (1988). Comparative ecology of submersed grass beds in freshwater, estuarine, and marine environments1. *Limnology and Oceanography*, *33*(4part2), 867-893.

Stream Solute Workshop. (1990). Concepts and Methods for Assessing Solute Dynamics in Stream Ecosystems. *Journal of the North American Benthological Society*, *9*(2), 95-119.

Tall, L., Caraco, N., & Maranger, R. (2011). Denitrification hot spots: dominant role of invasive macrophyte Trapa natans in removing nitrogen from a tidal river. *Ecological Applications*, *21*(8), 3104-3114.

Tank, J. L., Rosi-Marshall, E. J., Baker, M. A., & Hall, R. O. (2008). Are Rivers Just Big Streams? A Pulse Method to Quantify Nitrogen Demand in a Large River. *Ecology*, *89*(10), 2935-2945.

Teng, W., Rui, H., Strub, R., & Vollmer, B. (2016). Optimal Reorganization of NASA Earth Science Data for Enhanced Accessibility and Usability for the Hydrology Community. *JAWRA Journal of the American Water Resources Association*, *52*(4), 825-835.

Thellman, A., Jankowski, K. J., Hayden, B., Yang, X., Dolan, W., Smits, A. P., & O'Sullivan, A. M. (2021). The ecology of river ice. *JGR Biogeosciences, 126*, e2021JG006275.

Thieurmel, B., & Elmarhraoui, A. (2019). Suncalc: Compute sun position, sunlight phase and Lunar Phase. R package version 0.0.5.https://CRAN.R-project.org/package=suncalc

Thomas, G. L., Thiesfeld, S. L., Bonar, S. A., Crittenden, R. N., & Pauley, G. B. (1990). Estimation of submergent plant bed biovolume using acoustic range information. *Canadian Journal of Fisheries and Aquatic Sciences*, *47*(4), 805-812.

Thomaz, S. M., & Cunha, E. R. d. (2010). The role of macrophytes in habitat structuring in aquatic ecosystems: methods of measurement, causes and consequences on animal assemblages' composition and biodiversity. *Acta Limnologica Brasiliensia*, *22*(2), 218-236.

Tomlinson, M., Devaney, G., Cook, J., Short, V., & Stephenson, S. (2019). *The Broads annual water plant monitoring 2014-2018*. https://www.broads-authority.gov.uk/looking-after/managing-land-and-water/conservation-publications-and-reports/water-conservation-reports

Vadeboncoeur, Y., Jeppesen, E., Zanden, M. J. V., Schierup, H. H., Christoffersen, K. S., & Lodge, D. M. (2003). From Greenland to green lakes: Cultural eutrophication and the loss of benthic pathways in lakes. *Limnology and Oceanography*, *48(4), 1408-1418*.

Van Meter, K. J., Chowdhury, S., Byrnes, D. K., & Basu, N. B. (2020). Biogeochemical asynchrony: Ecosystem drivers of seasonal concentration regimes across the Great Lakes Basin. *Limnology and Oceanography*, *65*(4), 848-862.

Vander Zanden, M. J., & Vadeboncoeur, Y. (2020). Putting the lake back together 20 years later: what in the benthos have we learned about habitat linkages in lakes? *Inland Waters*, *10*(3), 305-321.

Veettil, B. K., Ward, R. D., Lima, M. D. A. C., Stankovic, M., Hoai, P. N., & Quang, N. X. (2020). Opportunities for seagrass research derived from remote sensing: A review of current methods. *Ecological Indicators*, *117*, 106560.

Venables, W. N., & Ripley, B. D. (2002). *Modern Applied Statistics with S. Fourth Edition*. Springer.

Ventelä, A. M., Amsinck, S. L., Kauppila, T., Johansson, L. S., Jeppesen, E., Kirkkala, T., . . . Sarvala, J. (2016). Ecosystem change in the large and shallow Lake Säkylän Pyhäjärvi, Finland, during the past ~400 years: implications for management. *Hydrobiologia*, *778*(1), 273-294.

Vermaire, J. C., Greffard, M. H., Saulnier-Talbot, É., & Gregory-Eaves, I. (2013). Changes in submerged macrophyte abundance altered diatom and chironomid assemblages in a shallow lake. *Journal of Paleolimnology*, *50*(4), 447-456.

Vermaire, J. C., & Gregory-Eaves, I. (2008). Reconstructing changes in macrophyte cover in lakes across the northeastern United States based on sedimentary diatom assemblages. *Journal of Paleolimnology*, *39*(4), 477-490.

Vermaire, J. C., Prairie, Y. T., & Gregory-Eaves, I. (2012). Diatom-inferred decline of macrophyte abundance in lakes of southern Quebec, Canada. *Canadian Journal of Fisheries and Aquatic Sciences*, *69*(3), 511-524.

Vijayaraj, V., Laviale, M., Allen, J., Amoussou, N., Hilt, S., Hölker, F., Kipferler, N., Leflaive, J., Lóper Moreira, G. A., Polst, B. H., Schmitt-Jansen, M., Stibor, H., & Gross, E. M. (2022). Multiple-stressor exposure of aquatic food webs: Nitrate and warming modulate the effect of pesticides. *Water Research*, *216*, 118325.

Vis, C. (2004). *Importance relative des producteurs primaires sur la production globale du lac Saint-Pierre, un grand lac fluvial du Saint-Laurent*. Thèse de doctorat, Université de Montréal, Montréal.

Vis, C., Hudon, C., & Carignan, R. (2003). An evaluation of approaches used to determine the distribution and biomass of emergent and submerged aquatic macrophytes over large spatial scales. *Aquatic Botany*, *77*(3), 187-201.

Vis, C., Hudon, C., Carignan, R., & Gagnon, P. (2007). Spatial analysis of production by macrophytes, phytoplankton and epiphyton in a large river system under different water-level conditions. *Ecosystems*, *10*(2), 293-310.

Vitousek, P. M., Mooney, H. A., Lubchenco, J., & Melillo, J. M. (1997). Human domination of Earth's ecosystems. *Science*, *277*(5325), 494-499.

Volik, O., Petrone, R. M., Hall, R. I., Macrae, M. L., Wells, C. M., & Price, J. S. (2018). Organic matter accumulation and salinity change in open water areas within a saline boreal fen in the Athabasca Oil Sands Region, Canada. *Catena*, *165*, 425-433.

von Schiller, D., Bernal, S., & Martí, E. (2011). Technical Note: A comparison of two empirical approaches to estimate in-stream net nutrient uptake. *Biogeosciences*, *8*(4), 875-882.

Wang, S., Gao, Y., Li, Q., Gao, J., Zhai, S., Zhou, Y., & Cheng, Y. (2019). Long-term and inter-monthly dynamics of aquatic vegetation and its relation with environmental factors in Taihu Lake, China. *Science of the Total Environment*, *651*, 367-380.

Waycott, M., Duarte, C. M., Carruthers, T. J., Orth, R. J., Dennison, W. C., Olyarnik, S., . . . Hughes, A. R. (2009). Accelerating loss of seagrasses across the globe threatens coastal ecosystems. *Proceedings of the national academy of sciences*, *106*(30), 12377-12381.

Wetzel, R. G. (1990). Land-water interfaces: Metabolic and limnological regulators. *SIL Proceedings, 1922-2010*, *24*(1), 6-24.

Wetzel, R. G., & Søndergaard, M. (1998). Role of Submerged Macrophytes for the Microbial Community and Dynamics of Dissolved Organic Carbon in Aquatic Ecosystem. In E. Jeppesen, M. Sondergaard, M. Sondergaard, & K. Christofferson (Eds.), *The structuring role of submerged macrophytes in lakes* (Vol. 131, pp. 197-214). Springer.

Whitmore, T. J., Lauterman, F. M., Smith, K. E., & Riedinger-Whitmore, M. A. (2015). Limnetical total phosphorus transfer functions for lake management: considerations about their design, use, and effectiveness. *Frontiers in Ecology and Evolutions*, 3, doi: 10.3389/fevo.2015.00107

Wigand, C., & Stevenson, J. C. (1997). Facilitation of phosphate assimilation by aquatic mycorrhizae of Vallisneria americana Michx. *Hydrobiologia*, *342*(0), 35-41.

Wigand, C., Stevenson, J. C., & Cornwell, J. C. (1997). Effects of different submersed macrophytes on sediment biogeochemistry. *Aquatic Botany*, *56*(3–4), 233-244.

Winfield, I. J., Onoufriou, C., O'Connell, M. J., Godlewska, M., Ward, R. M., Brown, A. F., & Yallop, M. L. (2007). Assessment in two shallow lakes of a hydroacoustic system for surveying aquatic macrophytes. *Hydrobiologia*, *584*(1), 111-119.

Winslow, L. A., Zwart, J. A., Batt, R. D., Dugan, H. A., Woolway, R. I., Corman, J. R., . . . Read, J. S. (2016). LakeMetabolizer: an R package for estimating lake metabolism from free-water oxygen using diverse statistical models. *Inland Waters*, *6*(4), 622-636.

Wollheim, W. M., Voosmarty, C. J., Peterson, B. J., Seitzinger, S. P., & Hopkinson, C. S. (2006). Relationship between river size and nutrient removal. *Geophysical Research Letters*, *33*(6), Article L06410. https://doi.org/10.1029/2006gl025845

Wu, Z., & Huang, N. E. (2009). Ensemble empirical mode decomposition: a noise-assisted data analysis method. *Advances in Adaptive Data Analysis*, *01*(01), 1-41.

Wu, Z., Huang, N. E., Long, S. R., & Peng, C.-K. (2007). On the trend, detrending, and variability of nonlinear and nonstationary time series. *Proceedings of the National Academy of Sciences*, *104*(38), 14889-14894.

Xiao, C., & Liu, G. H. (2013). The relationship of seed banks to historical dynamics and reestablishment of standing vegetation in an aquaculture lake. *Aquatic Botany*, *108*, 48-54.

Ye, S., Reisinger, A. J., Tank, J. L., Baker, M. A., Hall, R. O., Rosi, E. J., & Sivapalan, M. (2017). Scaling Dissolved Nutrient Removal in River Networks: A Comparative Modeling Investigation. *Water Resources Research*, *53*(11), 9623-9641.

Yin, Y., & Kreiling, R. M. (2011). The evaluation of a rake method to quantify submersed vegetation in the Upper Mississippi River. *Hydrobiologia*, *675*(1), 187-195.

Yvon-Durocher, G., & Allen, A. P. (2012). Linking community size structure and ecosystem functioning using metabolic theory. *Philosophical Transactions of the Royal Society B-Biological Sciences*, *367*(1605), 2998-3007.

Zhang, E. L., Liu, E. F., Jones, R., Langdon, P., Yang, X. D., & Shen, J. (2010). A 150-year record of recent changes in human activity and eutrophication of Lake Wushan from the middle reach of the Yangze River, China. *Journal of Limnology*, *69*(2), 235-241.

Zhang, Y., Jeppesen, E., Liu, X., Qin, B., Shi, K., Zhou, Y., Thomaz, S. M., & Deng, J. (2017). Global loss of aquatic vegetation in lakes. *Earth-Science Reviews*, *173*, 259-265.

Zhu, B., Fitzgerald, D. G., Mayer, C. M., Rudstam, L. G., & Mills, E. L. (2006). Alteration of ecosystem function by zebra mussels in Oneida Lake: Impacts on submerged macrophytes. *Ecosystems*, *9*(6), 1017-1028.

Zuur, A. F., Ieno, E. N., Walker, N. J., Saveliev, A. A., & Smith, G. M. (2009). *Mixed Effects Models and Extensions in Ecology with R*. Springer Science+Business Media.

Annexe I : Articles comme co-autrice

La liste ci-dessous indique les publications dans des revues révisés par les pairs qui ont été réalisées à titre de co-autrice durant la thèse. Pour chaque article, la contribution est également mentionnée.

1. Massé, S., **M. Botrel***, D. A. Walsh, R. Maranger. 2019. Annual nitrification dynamics in a seasonally ice-covered lake. *PLoS ONE*. https://doi.org/10.1371/journal.pone.0213748

   Compilation de résultats, réalisation d'analyses statistiques et interprétation. Révision de l'article et *autrice de correspondance

2. Bulat, M., P. M. Biron, J. R. W. Lacey, **M. Botrel**, C. Hudon, R. Maranger. 2018. A three-dimensional numerical model investigation of the impact of submerged macrophytes on flow dynamics in a large fluvial lake. Freshwater Biology. https://doi.org/10.1111/fwb.13359

   Contribution à la récolte et au traitement des données, révision de l'ébauche

3. Charrier Tremblay, C., **M. Botrel**, J.-F. Lapointe, R. Maranger. 2020. Relative influence of watershed and geomorphic features on nutrient and carbon fluxes in a pristine and moderately urbanized stream. *Science of the Total Environment*. https://doi.org/10.1016/j.scitotenv.2019.136411

   Supervision de l'étudiant à la maîtrise qui a réalisé l'article. Interprétation des résultats, révision des ébauches.

4. Goyette, J.-O., **M. Botrel**, G. Billen., J. Garnier, R. Maranger. 2020. Agriculture specialization influences nutrient use efficiency and fluxes in the St. Lawrence Basin over the 20th century. *Science of the Total Environment*. https://doi.org/10.1016/j.scitotenv.2022.159018

   Contribution à l'analyse et interprétation des résultats, révision des ébauches d'article

5. Dupont, A., **M. Botrel**, N. Fortin St-Gelais, T. Poisot, R. Maranger. A social-ecological biogeography of Canadian lakes. En revision à *Facet*

   Supervision de l'étudiante à la maîtrise, contribution à l'analyse et l'interprétation des résultats, révision de l'ébauche d'article